

January 2012

# Development and Optimization of Kinetic Target-Guided Synthesis Approaches Targeting Protein-Protein Interactions of the Bcl-2 Family

Sameer Shamrao Kulkarni

University of South Florida, sam.dyes@gmail.com

Follow this and additional works at: <http://scholarcommons.usf.edu/etd>



Part of the [Organic Chemistry Commons](#)

## Scholar Commons Citation

Kulkarni, Sameer Shamrao, "Development and Optimization of Kinetic Target-Guided Synthesis Approaches Targeting Protein-Protein Interactions of the Bcl-2 Family" (2012). *Graduate Theses and Dissertations*.  
<http://scholarcommons.usf.edu/etd/4351>

This Dissertation is brought to you for free and open access by the Graduate School at Scholar Commons. It has been accepted for inclusion in Graduate Theses and Dissertations by an authorized administrator of Scholar Commons. For more information, please contact [scholarcommons@usf.edu](mailto:scholarcommons@usf.edu).

Development and Optimization of Kinetic Target-Guided Synthesis Approaches  
Targeting Protein-Protein Interactions of the Bcl-2 Family

by

Sameer S. Kulkarni

A dissertation submitted in partial fulfillment  
of the requirements for the degree of  
Doctor of Philosophy  
Department of Chemistry  
College of Arts and Sciences  
University of South Florida

Major Professor: Roman Manetsch, Ph.D.  
Mark McLaughlin, Ph.D.  
Wayne Guida, Ph.D.  
Jianfeng Cai, Ph.D.

Date of Approval:  
November 09, 2012

Keywords: Fragment-based lead discovery, Sulfo-click chemistry, Acylsulfonamides,  
Protein-protein interaction modulators, Amidomethylarenes, Amidation

Copyright © 2012, Sameer S. Kulkarni

### **Note to Reader**

The entire work described in Chapter 2 has been published in the ACS Chemical Biology in 2011. It was adapted with permission from *ACS Chem. Biol.* **2011**, 6 (7), 724-732. Copyright 2011 American Chemical Society. In addition, the entire work presented in Chapter 4 has been recommended for publication subject to the revisions suggested by the reviewers in the Chemical Communications in 2012. Kulkarni, S. S.; Hu, X.; Manetsch, R., A Simple Base-Mediated Amidation of Aldehydes with Azides. *Chem. Commun.* **2012**, accepted.

## **Dedication**

I would like to dedicate this dissertation to my entire family. Without their unwavering support and faith in me, I would not have been able to stay in a foreign country to pursue my education. My parents have always been inspirational for me. I started enjoying science from an early age mainly due to my father, who is a doctor by profession. He always emphasized on understanding the fundamental concepts which has immensely helped me during my work here. Without this foundation, I would not have been able to resolve the problems encountered in the research projects. My mother has always been very supportive and made sure that the atmosphere at home was conducive to study. My parents have worked extremely hard and made a lot of sacrifices to ensure that I get high quality education. I am extremely indebted to them and I will continue to work hard with the sole intention to make them proud.

## **Acknowledgments**

First and foremost, I would like to sincerely thank Dr. Roman Manetsch for allowing me to be a part of his research group and providing me an opportunity to work on some exciting projects. Over the years, he has produced some high quality research ideas. He has always been approachable and supportive all these years. He has worked extremely hard to establish the research group here at USF and it has been a wonderful journey that we all shared with him. His exceptional work ethic has been a huge motivation for me. He has not only encouraged us to maintain high research standards but also emphasized on presenting the work in a meaningful way. Due to his persuasion, I have been able to present my work in various conferences and national meetings. He has also been kind enough to provide me with RA enabling me to exclusively work on my research. I am thankful to him for having confidence and faith in me without which I would not have been able to make any progress. I honestly hope that I have been able to contribute something constructive to this lab, however small as it may be. Altogether, this experience has made me a competitive researcher and I will never stop improving myself to attain greater heights in the field of chemistry. It is truly an honor and privilege to have him as my mentor and I am extremely grateful to him for everything.

I take this opportunity to thank my committee members, Dr. Mark McLaughlin, Dr. Wayne Guida, and Dr. Jianfeng Cai. They have always provided some insightful suggestions during the meetings and their expertise and experience has been proved to be

valuable during my graduate studies. I also thank Dr. Priyesh Jain for agreeing to be the chairperson for my dissertation defense. He is a great person and has always been helpful.

I would especially like to thank my wife, Ketki for being there for me. Although, she has been a part of my life for just over a year, she has shown remarkable level of maturity during tough times and has been my strength. Even though she is not physically present, her emotional support has made it possible for me to complete my research work.

I would also like to thank my colleagues in the Manetsch lab. I have been lucky to have worked with some wonderful post-docs, Dr. Xiangdong Hu, Dr. Niranjan Kumar Namelikonda, Dr. David Flanigan, and Dr. Raghupathi Neelarapu. They always had great suggestions and were ready to help whenever I approached them. Working with them has certainly made me a better chemist. Also, I had a chance to work with graduate students who accommodated me in the lab and I share a great camaraderie with all of them. I have had some useful research discussions with most of them and it was very exciting to get a different perspective about my research from them. So, I like to thank Dr. Arun Babu Kumar, Dr. R. Matthew Cross, Dr. Shikha Mahajan, Jordany Maignan, Andrii Monastyrskiy, Iredia Iyamu, Katya Nacheva, Kurt Van Horn, and Cynthia Lichorowic. I am pleased to thank the undergraduate students, Matthew Sarnowski, Megan Barber, Petoria Gayle, and Maylene Quiroga for their contributions to some of the research projects.

I also thank my friends from other labs on the third floor of NES, Dr. Ryan Cormier, Gajendra Ingle, Sri Krishna Nimmagadda, and Pankaj Jain for making this journey memorable.

## Table of Contents

List of Tables .....	iv
List of Figures .....	v
List of Schemes .....	viii
Abstract .....	ix
Chapter 1: Various drug discovery approaches and protein-protein interaction targets .....	1
1.1 Drug discovery approaches .....	1
1.2 Combinatorial chemistry and high-throughput screening (HTS) .....	2
1.3 Fragment-based lead discovery .....	3
1.4 Target-guided synthesis (TGS) .....	4
1.4.1 Dynamic combinatorial chemistry (DCC) and its variants .....	4
1.4.2 Catalyst/reagent-accelerated target-guided synthesis .....	8
1.4.3 Kinetic target-guided synthesis .....	9
1.4.3.1 <i>In situ</i> click chemistry .....	11
1.4.3.2 Sulfo-click reaction .....	14
1.4.3.3 Other reactions used for kinetic TGS .....	16
1.5 Targeting protein-protein interactions .....	17
1.5.1 Protein-protein interactions of the Bcl-2 family .....	19
1.6 Development of novel reactions suitable for kinetic TGS .....	21
1.7 Research aims .....	22
1.7.1 Identification of protein-protein interaction modulators (PPIMs) targeting Bcl-X <sub>L</sub> .....	22
1.7.2 Identification of PPIMs targeting Mcl-1 .....	22
1.7.3 Development of an amidation reaction .....	23
1.8 References cited .....	24
Chapter 2: Screening of protein-protein interaction modulators <i>via</i> sulfo-click kinetic target-guided synthesis .....	41
2.1 Introduction .....	41
2.2 Results and discussion .....	46
2.2.1 Screening of an extended reactive fragment library .....	46
2.2.2 Kinetic TGS with mutant Bcl-X <sub>L</sub> .....	50
2.2.3 PPIM activity of kinetic TGS hits and additional acylsulfonamides .....	54

2.2.4	Discussion.....	57
2.3	Conclusions.....	59
2.4	Experimental section.....	60
2.4.1	General information.....	60
2.4.2	Expression and purification of wildtype and mutant Bcl-X <sub>L</sub> fusion proteins.....	62
2.4.3	General protocol for incubations of Bcl-X <sub>L</sub> with reactive fragments.....	62
2.4.4	General protocol for the control incubations of Bcl-X <sub>L</sub> with reactive fragments and Bim BH3 peptides.....	63
2.4.5	General protocol for the control incubations of mutants of Bcl-X <sub>L</sub> with reactive fragments.....	63
2.4.6	Fluorescence polarization-based competitive binding assay.....	64
2.4.7	Synthesis of building blocks.....	64
2.4.8	General procedure A for the synthesis of acylsulfonamides.....	71
2.4.9	General procedure B for the synthesis of acylsulfonamides.....	71
2.4.10	Synthesis of kinetic TGS hits.....	72
2.4.11	Synthesis of additional acylsulfonamides.....	75
2.4.12	Mutant Bcl-X <sub>L</sub> ( <sup>R139A</sup> Bcl-X <sub>L</sub> ) experiments: LC/MS-SIM analysis.....	93
2.4.13	Peptide control experiments: LC/MS-SIM analysis.....	96
2.5	References cited.....	98
Chapter 3:	Identification of protein-protein interaction modulators targeting Mcl-1 <i>via</i> sulfo-click kinetic target-guided synthesis.....	106
3.1	Introduction.....	106
3.2	Results and discussion.....	111
3.2.1	Expansion of fragment library.....	111
3.2.2	Kinetic TGS screening against Mcl-1.....	113
3.2.3	Biological activity of the kinetic TGS hits.....	116
3.2.4	Discussion.....	118
3.3	Conclusions.....	119
3.4	Experimental section.....	120
3.4.1	General information.....	120
3.4.2	General protocol for incubations of Mcl-1 with reactive fragments.....	121
3.4.3	General protocol for the control incubations of Mcl-1 with reactive fragments and Bim BH3 peptide.....	122
3.4.4	General procedure A for the synthesis of sulfonyl azides.....	122
3.4.5	General procedure B for the synthesis of sulfonyl azides.....	123
3.4.6	General procedure C for the synthesis of sulfonyl azides.....	123
3.4.7	Synthesis of fragments.....	124
3.4.8	Synthesis of 9-fluorenylmethyl thioesters.....	133
3.4.9	General procedure A for the synthesis of acylsulfonamides.....	135
3.4.10	General procedure B for the synthesis of acylsulfonamides.....	135
3.4.11	Synthesis of acylsulfonamides.....	136

	3.4.12 Peptide control experiments: LC/MS-SIM analysis .....	142
3.5	References cited .....	152
Chapter 4:	A simple base-mediated amidation of aldehydes with azides .....	160
4.1	Introduction.....	160
4.2	Results and discussion .....	162
	4.2.1 Optimization of the reaction conditions.....	162
	4.2.2 Scope of the reaction regarding the aldehydes .....	163
	4.2.3 Scope of the reaction regarding the azides .....	165
	4.2.4 Control experiments and the plausible mechanism .....	165
	4.2.5 Discussion .....	168
4.3	Conclusion .....	169
4.4	Experimental section.....	170
	4.4.1 General information .....	170
	4.4.2 Synthesis of azides.....	170
	4.4.3 General procedure for the synthesis of amides .....	172
	4.4.4 Synthesis of amides.....	172
4.5	References cited.....	183
Appendices.....		190
	Appendix 1 .....	191

## List of Tables

Table 2.1.	Kinetic TGS incubations.....	54
Table 2.2.	PPIM activity of kinetic TGS hit compounds.....	55
Table 2.3.	Percentage inhibition displayed by an acylsulfonamide at 50 $\mu$ M concentration.....	56
Table 2.4.	Elution gradient system 1 employed for the LC/MS-SIM analysis.....	61
Table 2.5.	Elution gradient system 2 employed for the LC/MS-SIM analysis.....	61
Table 3.1.	Biological activity of acylsulfonamides against Mcl-1 and Bcl-X <sub>L</sub> .....	117
Table 3.2.	Elution gradient system employed for the LC/MS-SIM analysis.....	121
Table 4.1.	Optimization of the reaction conditions.....	163
Table 4.2.	Reaction of benzyl azide with various aromatic aldehydes.....	164
Table 4.3.	Reaction of various azides with benzaldehyde.....	166

## List of Figures

Figure 1.1.	Schematic representation of the dynamic combinatorial chemistry (DCC) approach.....	5
Figure 1.2.	Schematic representation of tethering.....	6
Figure 1.3.	Dynamic combinatorial resolution using nitroaldol reaction.....	7
Figure 1.4.	Pseudo-dynamic combinatorial chemistry .....	8
Figure 1.5.	Schematic representation of the kinetic TGS approach.....	10
Figure 1.6.	Reactions suitable for click chemistry .....	10
Figure 1.7.	<i>In situ</i> click chemistry approach using eel AchE as a template.....	13
Figure 1.8.	Screening of sulfonyl azides and thio acids against Bcl-X <sub>L</sub> .....	15
Figure 1.9.	Other reactions explored for kinetic TGS application .....	17
Figure 1.10.	Small-molecular inhibitors of Bcl-2/Bcl-X <sub>L</sub> .....	20
Figure 2.1.	Kinetic TGS approach targeting PPIs.....	43
Figure 2.2.	Kinetic TGS screening of Bcl-X <sub>L</sub> <i>via</i> sulfo-click chemistry .....	48
Figure 2.3.	LC/MS-SIM analysis of kinetic TGS incubations with fragments <b>SZ7</b> and <b>TA2</b> targeting Bcl-X <sub>L</sub> .....	49
Figure 2.4.	LC/MS-SIM analysis of kinetic TGS incubations with fragments <b>SZ4</b> and <b>TA2</b> targeting the wildtype and mutant of Bcl-X <sub>L</sub> .....	52
Figure 2.5.	LC/MS-SIM analysis of kinetic TGS incubations with fragments <b>SZ4</b> and <b>TA2</b> targeting the wildtype and double mutant of Bcl-X <sub>L</sub> .....	53
Figure 2.6.	Bcl-X <sub>L</sub> and mutant Bcl-X <sub>L</sub> templated incubations with <b>SZ7</b> and <b>TA2</b> .....	93

Figure 2.7.	Bcl-X <sub>L</sub> and mutant Bcl-X <sub>L</sub> templated incubations with <b>SZ9</b> and <b>TA1</b> .....	94
Figure 2.8.	Bcl-X <sub>L</sub> and mutant Bcl-X <sub>L</sub> templated incubations with <b>SZ9</b> and <b>TA5</b> .....	95
Figure 2.9.	Incubation of <b>SZ9</b> and <b>TA1</b> and suppressing Bcl-X <sub>L</sub> -templated incubations with Bim and mutant Bim .....	96
Figure 2.10.	Incubation of <b>SZ9</b> and <b>TA5</b> and suppressing Bcl-X <sub>L</sub> -templated incubations with Bim and mutant Bim .....	97
Figure 3.1.	Inhibitors targeting multiple Bcl-2 family members or Mcl-1 selectively .....	108
Figure 3.2.	Comparison of SAR by NMR and SAR by ILOEs approaches .....	109
Figure 3.3.	Kinetic TGS screening <i>via</i> sulfo-click chemistry against Bcl-X <sub>L</sub> .....	110
Figure 3.4.	Library of sulfonyl azides and thioesters utilized for kinetic TGS screening against Mcl-1 .....	114
Figure 3.5.	LC/MS-SIM analysis of kinetic TGS incubations with fragments <b>SZ15</b> and <b>TA8</b> targeting Mcl-1 .....	115
Figure 3.6.	Acylsulfonamides confirmed as kinetic TGS hits against Mcl-1 .....	116
Figure 3.7.	Incubation of <b>SZ15</b> and <b>TA1</b> and suppressing Mcl-1-templated incubations with Bim BH3 peptide.....	142
Figure 3.8.	Incubation of <b>SZ15</b> and <b>TA3</b> and suppressing Mcl-1-templated incubations with Bim BH3 peptide.....	143
Figure 3.9.	Incubation of <b>SZ15</b> and <b>TA5</b> and suppressing Mcl-1-templated incubations with Bim BH3 peptide.....	144
Figure 3.10.	Incubation of <b>SZ15</b> and <b>TA6</b> and suppressing Mcl-1-templated incubations with Bim BH3 peptide.....	145
Figure 3.11.	Incubation of <b>SZ17</b> and <b>TA3</b> and suppressing Mcl-1-templated incubations with Bim BH3 peptide.....	146
Figure 3.12.	Incubation of <b>SZ17</b> and <b>TA8</b> and suppressing Mcl-1-templated incubations with Bim BH3 peptide.....	147

Figure 3.13.	Incubation of <b>SZ31</b> and <b>TA3</b> and suppressing Mcl-1-templated incubations with Bim BH3 peptide.....	148
Figure 3.14.	Incubation of <b>SZ31</b> and <b>TA6</b> and suppressing Mcl-1-templated incubations with Bim BH3 peptide.....	149
Figure 3.15.	Incubation of <b>SZ31</b> and <b>TA7</b> and suppressing Mcl-1-templated incubations with Bim BH3 peptide.....	150
Figure 3.16.	Incubation of <b>SZ31</b> and <b>TA8</b> and suppressing Mcl-1-templated incubations with Bim BH3 peptide.....	151

## List of Schemes

Scheme 1.1.	Synthesis of disubstituted 1,2,3-triazoles <i>via</i> Huisgen cycloaddition.....	12
Scheme 1.2.	Mechanism of the amidation reaction between azides and thio acids .....	14
Scheme 2.1.	Synthesis of sulfonyl azides, thio acids and acylsulfonamides.....	47
Scheme 3.1.	Synthesis of sulfonyl azides, thio acids, thioesters, and acylsulfonamides.....	112
Scheme 4.1.	Synthesis of amidomethylarenes.....	161
Scheme 4.2.	Reaction between azides and aromatic aldehydes yielding amides.....	162
Scheme 4.3.	Control experiments to investigate the reaction mechanism .....	167
Scheme 4.4.	Plausible reaction mechanism of amidation .....	168

## Abstract

Kinetic target-guided synthesis (TGS) and *in situ* click chemistry are among unconventional discovery strategies having the potential to streamline the development of protein-protein interaction modulators (PPIMs). In kinetic TGS and *in situ* click chemistry, the target is directly involved in the assembly of its own potent, bidentate ligand from a pool of reactive fragments. Herein, we report the use and validation of kinetic TGS based on the sulfo-click reaction between thio acids and sulfonyl azides as a screening and synthesis platform for the identification of high-quality PPIMs. Starting from a randomly designed library consisting of nine thio acids and nine sulfonyl azides leading to eighty one potential acylsulfonamides, the target protein, Bcl-X<sub>L</sub> selectively assembled four PPIMs, acylsulfonamides **SZ4TA2**, **SZ7TA2**, **SZ9TA1**, and **SZ9TA5**, which have been shown to modulate Bcl-X<sub>L</sub>/BH3 interactions. To further investigate the Bcl-X<sub>L</sub> templation effect, control experiments were carried out using two mutants of Bcl-X<sub>L</sub>. In one mutant, phenylalanine Phe131 and aspartic acid Asp133, which are critical for the BH3 domain binding, have been substituted by alanines, while arginine Arg139, a residue identified to play a crucial role in the binding of **ABT-737**, a BH3 mimetic, has been replaced by an alanine in the other mutant. Incubation of these mutants with the reactive fragments and subsequent LC/MS-SIM analysis confirmed that these building block combinations yield the corresponding acylsulfonamides at the BH3 binding site, the actual “hot spot” of Bcl-X<sub>L</sub>. These results validate kinetic TGS using the sulfo-click reaction as a valuable tool for the straightforward identification of high-quality PPIMs.

Protein-protein interactions of the Bcl-2 family have been extensively investigated and the anti-apoptotic proteins (Bcl-2, Bcl-X<sub>L</sub>, and Mcl-1) have been validated as crucial targets for the discovery of potential anti-cancer agents. At the outset, Bcl-2 and Bcl-X<sub>L</sub> were considered to play an important role in the regulation of apoptosis. Accordingly, several small molecule inhibitors targeting Bcl-2 and/or Bcl-X<sub>L</sub> proteins were primarily designed. A series of acylsulfonamides targeting these proteins were reported by Abbott laboratories, **ABT-737** and **ABT-263** being the most potent candidates. Remarkably, these molecules were found to exhibit weaker binding affinities against Mcl-1, another anti-apoptotic protein. Further experimental evidence suggests that, inhibitors targeting Mcl-1 selectively or in combination with other anti-apoptotic proteins would lead to desired therapeutic effect. As a result, numerous small molecules displaying activity against Mcl-1 have been identified so far. Specifically, acylsulfonamides derived from structure activity relationship by interligand nuclear overhauser effect (SAR by ILOEs), a fragment-based approach, have been recently reported with binding affinities in the nanomolar range. In the meantime, we have reported that the kinetic TGS approach can also be applied to identify acylsulfonamides as PPIMs targeting Bcl-X<sub>L</sub>. Taken together, structurally novel acylsulfonamides can be potentially discovered as Mcl-1 inhibitors using the kinetic TGS approach. Thus, a library of thirty one sulfonyl azides and ten thio acids providing three hundred and ten potential products was screened against Mcl-1 and the kinetic TGS hits were identified. Subsequently, control experiments involving Bim BH3 peptide were conducted to confirm that the fragments are assembled at the binding site of the protein. The kinetic TGS hits were then synthesized and subjected to the fluorescence polarization assay.

Gratifyingly, activities in single digit micromolar range were detected, demonstrating that the sulfo-click kinetic TGS approach can also be used for screening and identification of acylsulfonamides as PPIMs targeting Mcl-1.

The amide bond serves as one of nature's most fundamental functional group and is observed in a large number of organic and biological molecules. Traditionally, the amide functionality is introduced in a molecule through coupling of an amine and an activated carboxylic acid. Recently, various alternative methods have been reported wherein, the aldehydes or alcohols are oxidized using transition metal catalysts and are treated with amines to transform into the corresponding amides. These transformations however, require specially designed catalysts, long reaction times and high temperatures. We herein describe a practical and efficient amidation reaction involving aromatic aldehydes and various azides under mild basic conditions. A broad spectrum of functional groups was tolerated, demonstrating the scope of the reaction. Consequently, the amides were synthesized in moderate to excellent yields, presenting an attractive alternative to the currently available synthetic methods.

## Chapter 1

### Various Drug Discovery Approaches and Protein-Protein Interaction Targets

#### 1.1 Drug discovery approaches

Advances in the field of molecular biology have resulted in a better understanding of various biochemical pathways. Consequently, a large number of proteins have been recognized and validated as therapeutic targets creating an urgent need for generation of novel drug-like molecules. Over the last two decades, conventional drug discovery approaches such as combinatorial chemistry and high-throughput screening (HTS) have been extensively explored in the quest of biologically active molecules. These approaches demand generation of a large library of compounds and data analysis making it expensive and cumbersome. Moreover, the false positives obtained during the library screening presents additional drawbacks thereby impeding the drug discovery and development process. Alternatively, a wide range of fragment-based approaches have emerged as promising tools towards lead discovery. These approaches can be divided into two categories. In the first category, the fragments with weak binding affinities are identified using various biophysical techniques and are subsequently converted into the drug-like molecules using traditional synthetic procedures. In the second category, the target serves as a template assembling the fragments together to yield the inhibitor of that target itself. These approaches are termed as template-assisted strategies or target-guided synthesis

(TGS). TGS can be further classified into three subcategories: (a) dynamic combinatorial chemistry (DCC), (b) catalyst/reagent-accelerated TGS and (c) kinetic TGS.

## 1.2 Combinatorial chemistry and high-throughput screening (HTS)

Combinatorial chemistry was developed by Merrifield in 1960s to rapidly generate a large number of compounds, utilizing a solid phase synthesis methodology.<sup>1</sup> Since then this approach has been widely used for drug discovery and development.<sup>2</sup> Hundreds to thousands of compounds can be synthesized and tested in much shorter time compared to the conventional synthetic procedures thereby increasing the chances of finding molecules with biological activity. Especially, mixtures of compounds are obtained in a mix and split method. These mixtures are directly subjected to the biological assays and if found active, the exact compound displaying the activity can then be identified via a specialized deconvolution procedure. In the HTS approach, libraries of compounds ( $> 10^6$ ), primarily generated through combinatorial chemistry, are tested in an automated fashion against a wide range of targets to identify potential hits. Various types of HTS assays have been developed to detect binding of the compound to a desired target. Some of the commonly used assays include the fluorescence polarization (FP) assay<sup>3</sup> and the amplified luminescent proximity homogeneous assay (Alpha).<sup>4</sup> Importantly, these strategies require huge investments since a large set of molecules needs to be synthesized and analyzed using automated liquid handling tools. Also, a high rate of false positives is observed during HTS screening especially for difficult targets considered to belong to the class of “undruggable” targets. This could be attributed to the presence of chemically reactive members in the library and/or inhibitory activity arising from formation of molecular aggregates, known as promiscuous inhibitors. Moreover,

approximately  $10^{63}$  drug-like molecules consisting of up to 30 heavy atoms have been estimated to exist.<sup>5</sup> Screening all of these molecules is practically impossible, presenting limitations in exploring the chemical space efficiently.<sup>6</sup> As a result, although the pharmaceutical industry has heavily relied on combinatorial chemistry and HTS approaches, they have met with limited success. In order to find alternatives, modern approaches such as fragment-based lead discovery (FBLD) have been extensively exploited.

### 1.3 Fragment-based lead discovery

Recently, several fragment-based lead discovery (FBLD) approaches have been established as an attractive alternative to the conventional drug discovery methods.<sup>7</sup> This approach involves synthesis of libraries of small molecules or fragments (molecular weight in the range of 150-300 Da).<sup>8</sup> As opposed to the drug-like molecules, only  $10^7$  fragments consisting of up to 12 heavy atoms have been estimated to exist.<sup>9</sup> Consequently, the fragments possess higher ligand efficiency compared to the molecules arising from the combinatorial libraries and HTS. Initially, the fragments exhibiting weak affinity (binding constants in the milli- to micromolar ranges) are identified and subsequently combined using synthetic procedures to develop ligands with high affinity (binding constants in the micro- to nanomolar ranges).<sup>8, 10</sup> Various techniques employed to detect fragments with weak binding affinities include surface plasmon resonance (SPR),<sup>11</sup> X-ray crystallography,<sup>12</sup> isothermal titration calorimetry (ITC),<sup>13</sup> nuclear magnetic resonance (NMR) spectroscopy<sup>14</sup> and mass spectrometry.<sup>15</sup> Some of the disadvantages of the aforementioned methods are the relatively low throughput, the requirement of sensitive and expensive instrumentation for the detection of small

molecular weight compounds, and the necessity of large amount of protein. Importantly, these techniques fail to provide the most critical piece of information: what is the best way to combine identified fragments with weak binding affinities leading to high-affinity ligands?<sup>16</sup> Thus, extensive synthetic efforts have to be implemented in order to obtain potent inhibitors immediately after the fragments are detected. For example, Fesik *et al.* utilized a SAR by NMR approach to develop dual inhibitors of anti-apoptotic proteins, Bcl-2 and Bcl-X<sub>L</sub>.<sup>17</sup> Starting from the initial fragments, more than 2300 compounds had to be synthesized,<sup>18</sup> leading to **ABT-737**, one of the most potent inhibitor of Bcl-2 and Bcl-X<sub>L</sub>.<sup>19</sup> To overcome these shortcomings, several template-assisted strategies, known as target-guided synthesis (TGS), have been recently established.

#### 1.4 Target-guided synthesis (TGS)

In a target-guided synthesis (TGS) approach, the biological target, a protein or an enzyme plays a significant role in the synthesis of its own bidentate ligand from a library of various building blocks derivatized with complementary reacting functional groups. The TGS can be broadly divided into three sets: (a) dynamic combinatorial chemistry (DCC) (b) catalyst/reagent-accelerated TGS and (c) kinetic TGS.

##### 1.4.1 Dynamic combinatorial chemistry (DCC) and its variants

The dynamic combinatorial chemistry (DCC) approach was first applied by Huc *et al.* in 1997 to discover inhibitors of carbonic anhydrase.<sup>20</sup> In a DCC approach, the reaction combining sublibraries of building blocks into a larger library of larger compounds is reversible (Figure 1.1). When the biological target is added to this library, also known as the dynamic combinatorial library (DCL), the equilibrium is shifted

towards the formation of compounds possessing the strongest affinities towards the target, thereby enabling the identification of the most potent compounds from the DCC library.<sup>21</sup>

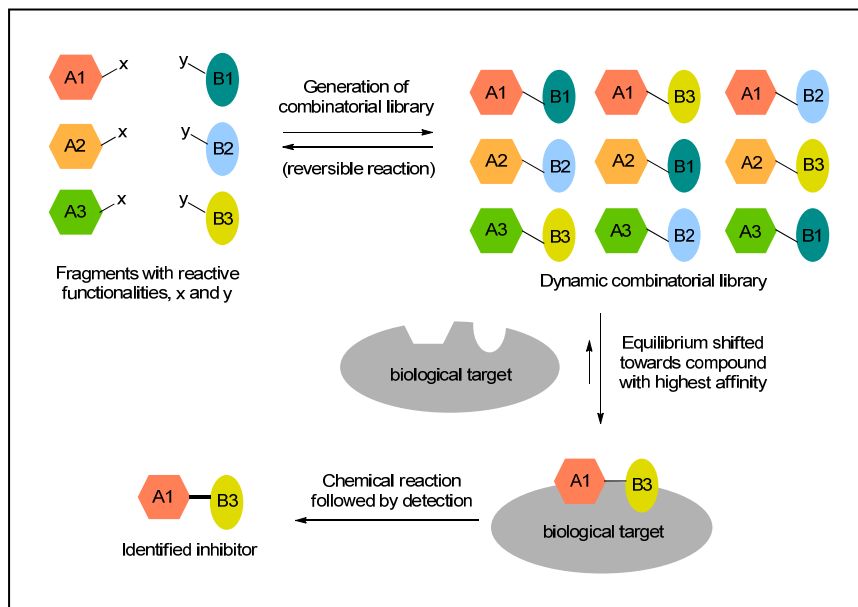


**Figure 1.1.** Schematic representation of the dynamic combinatorial chemistry (DCC) approach

Hence, the generation and isolation of the desired compound can be combined in a single step making the entire process simple and rapid. Especially, the DCC approach has been proved useful in case of library of building blocks possessing a variety of functional groups, which are not compatible and cannot be handled conveniently using the conventional combinatorial chemistry methods. For example, Hochgurtel *et al.* designed the DCL of imines derived from a highly functionalized diamine and 41 diverse ketones, which was screened against an influenza virus enzyme, neuraminidase.<sup>22</sup> Reduction of imines using  $\text{NaCNBH}_3$  yielded corresponding amines, which were subjected to HPLC/MS analysis for the identification of hits. Other examples of the reactions utilized in developing the DCLs include, the trans-esterification, the olefin

metathesis, the peptide-bond exchange, the boronic ester formation, the Diels-Alder reaction and the disulfide formation.<sup>23</sup> The variants of DCC consist of tethering, pseudo-dynamic combinatorial chemistry (pDCC) and dynamic combinatorial resolution (DCR).

Tethering, a DCC variant has been proved to be highly successful in the identification of inhibitors for numerous challenging targets such as interleukin-2 (IL-2),<sup>24</sup> protein tyrosine phosphatase 1B (PTP-1B),<sup>25</sup> caspases<sup>26</sup> and others.<sup>27</sup> A specific segment of the protein template is exploited, wherein a cysteine residue in the proximity of the binding site actively takes part in the thiol-disulfide exchange reaction (Figure 1.2).<sup>24, 27b</sup>

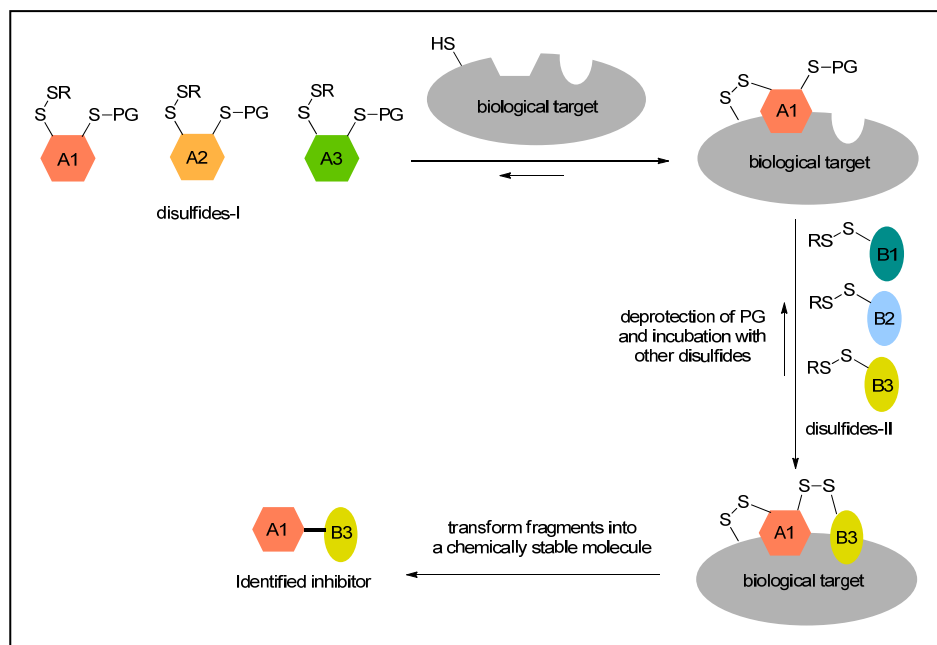


**Figure 1.2.** Schematic representation of tethering

Alternatively, a cysteine residue can be either incorporated through site-directed mutagenesis<sup>27a, 28</sup> or extended by a thiol bearing linker.<sup>26</sup> For example, the caspase-3

enzyme was modified by attaching a thiol bearing aspartate analogue and subsequently screened against a library of 7000 disulfides.<sup>26</sup> The disulfides binding near the thiol-bearing linker would thus be exchanged through the reaction with the thiol. The enzyme-disulfide complex can be subsequently identified using mass spectrometry. Although the disulfide needs to be transformed into a chemically stable entity and large amounts of the biological template (close to stoichiometric amounts) are required, this tethering approach can be applied to various enzymes/proteins due to the readily available cysteine residue.<sup>6</sup> In case of dynamic combinatorial resolution (DCR),<sup>29</sup> an enzyme, when treated with the DCL, selectively transforms certain members of the library into structurally different products through an irreversible reaction. Ramstrom and co-workers have demonstrated the utility of this approach using a nitroaldol in a Henry reaction (Figure 1.3).<sup>29a</sup>

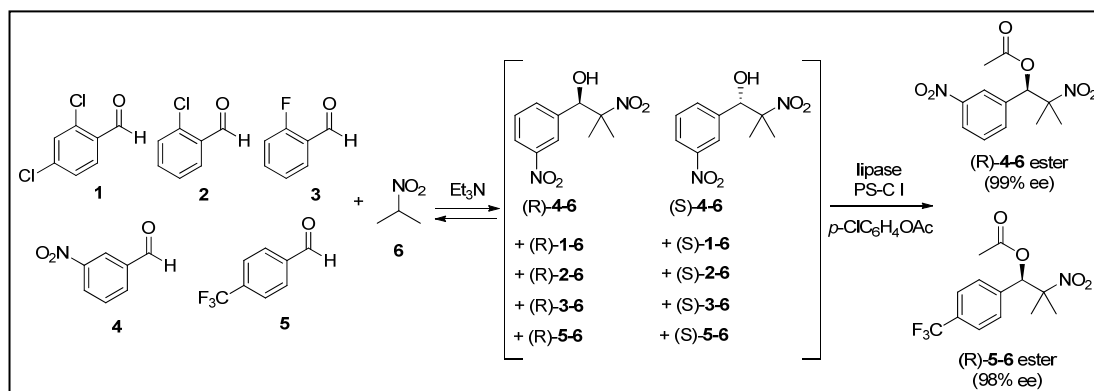


**Figure 1.3.** Dynamic combinatorial resolution using nitroaldol reaction

The DCL consisting of five different aromatic aldehydes along with 2-nitropropane leading to ten corresponding nitroaldol products (including all the enantiomers) was designed and treated with lipase PS-C I in the presence of 4-chlorophenyl acetate serving as the acyl donor. Only two  $\beta$ -nitroalcohols (as single

enantiomers) were found by  $^1\text{H}$  NMR spectroscopy to be predominantly acylated by the lipase after 14 days of incubation.<sup>29a</sup> On the contrary, pseudo-dynamic combinatorial chemistry (pDCC)<sup>30</sup> strategy relies on an enzymatic bond cleavage reaction (Figure 1.4). This strategy was successfully employed by Corbett *et al.* utilizing pronase, a nonspecific protease, facilitating the hydrolysis of dipeptides. Eight dipeptides were synthesized and incubated with carbonic anhydrase and subsequently treated with pronase. Consequently, the dipeptide with highest binding affinity towards carbonic anhydrase was protected, whereas other dipeptides, being more susceptible to hydrolysis by pronase, were eliminated.<sup>30a</sup> Although the applicability of this approach is restrained by the cleavage reaction, requirement of the template in only catalytic amounts makes it advantageous over conventional DCC methods.

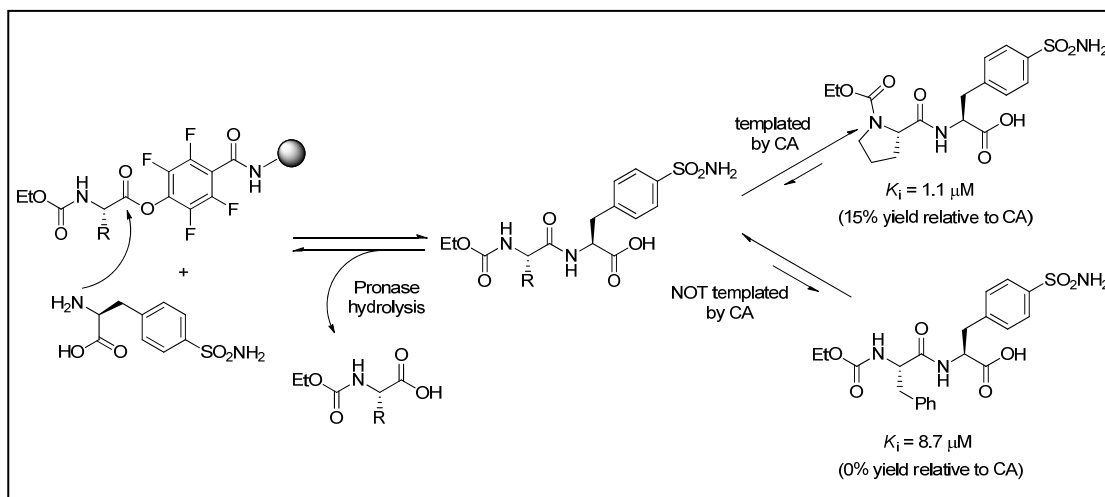


**Figure 1.4.** Pseudo-dynamic combinatorial chemistry

#### 1.4.2 Catalyst/reagent-accelerated target-guided synthesis

In this two-step approach, the templated combination of two fragments with highest binding affinities by the protein target constitutes the first step. The second step

entails the addition of a catalyst or a reagent resulting in the covalent bond formation between the binding fragments. This approach has been successfully applied to develop various Vancomycin dimers,<sup>31</sup> trimers<sup>32</sup> or oligomers<sup>33</sup> as inhibitors of vancomycin-resistant bacterial strains. Nicolaou and co-workers employed the disulfide bond forming reaction and/or the olefin metathesis reaction to link two Vancomycin units together in a back-to-back fashion generating disulfide or alkene linkages, respectively.<sup>34</sup> The reaction conditions for the disulfide bond formation were comprised of a saponification using NaOH followed by the dimerization *via* air oxidation, whereas the Grubb's catalyst ( $[(PCy_3)_2Ru(CHPh)Cl_2]$ ) along with a phase-transfer catalyst ( $C_{12}H_{25}NMe_3Br$ ) were required for the olefin metathesis reaction. Several analogues with varied linker lengths and/or different amino acid sequences at the N-terminus were designed and subjected to the aforementioned reaction conditions in the presence and absence of the targets Ac-D-Ala-D-Ala or Ac<sub>2</sub>-L-Lys-D-Ala-D-Ala. The rate of dimerization was found to be accelerated by the target for selective Vancomycin derivatives. In accordance, these dimers displayed higher potency compared to other dimers against the Vancomycin-resistant bacterial strains, demonstrating the utility of this approach.

#### 1.4.3 Kinetic target-guided synthesis

In this particular approach, the used building blocks or fragments are decorated with complementary reacting functional groups. Thus, when a biological target (a protein or an enzyme) is introduced, it selectively templates the irreversible bond formation between specific building blocks with high affinity. As a result, the target-facilitated covalent bond formation between two building blocks yields a potent inhibitor through an

irreversible reaction, which ideally has characteristics of a click chemistry reaction (Figure 1.5).<sup>35</sup>

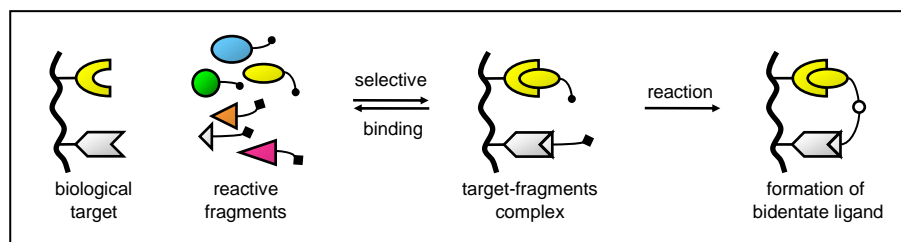


**Figure 1.5.** Schematic representation of the kinetic TGS approach

A set of criteria that must be met for a reaction to be used as a click reaction includes: (a) high yield, (b) sluggish reactivity profile, (c) wide scope, and (d) generate no or minimal amounts of byproducts.<sup>36</sup> In addition, the reaction needs to stereospecifically proceed smoothly in organic as well as aqueous solvents, along with a simple isolation of the product.<sup>36</sup>

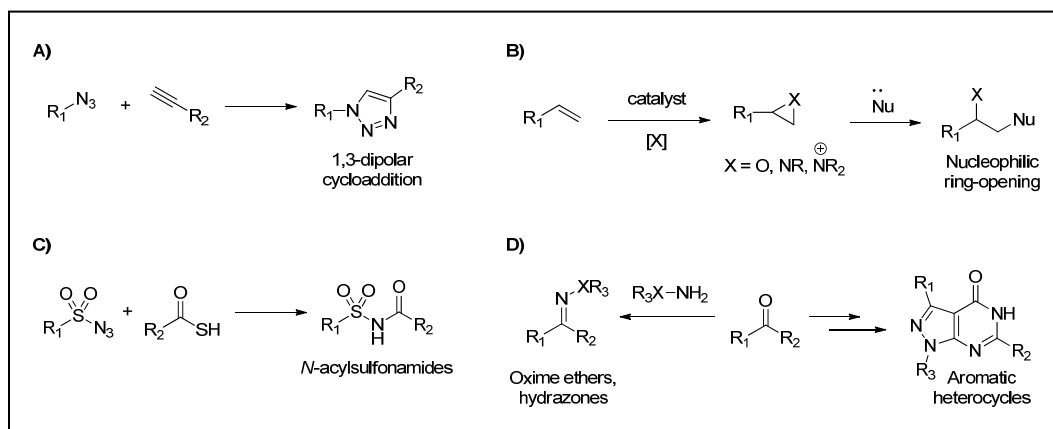


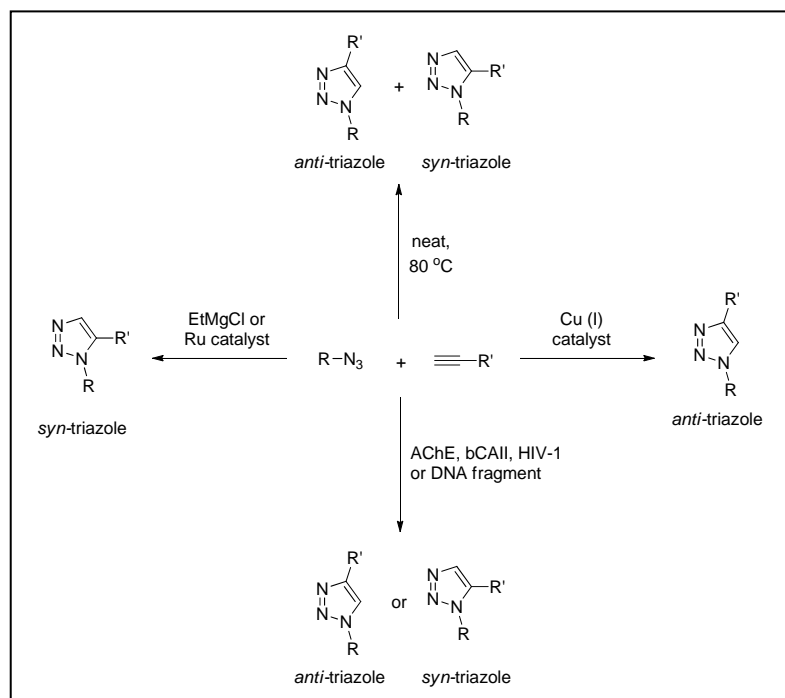
**Figure 1.6.** Reactions suitable for click chemistry

Typically, reactions leading to a carbon-heteroatom bond formation are found to be suitable as click reactions. Some well-known reactions used for the click chemistry are: (a) the 1,3-dipolar cycloaddition, (b) the hetero-Diels-Alder reaction, (c) the

nucleophilic ring-opening reactions of aziridines and epoxides, (d) the non-aldol reactions of carbonyl moiety generating oxime ethers, the formation of hydrazones and aromatic heterocycles, (e) the oxidative additions to olefins such as dihydroxylations and epoxidations, and (f) the recently developed sulfo-click reaction between azides or sulfonyl azides and thio acids yielding amides or acylsulfonamides (Figure 1.6 A-D).<sup>36-37</sup>

#### 1.4.3.1 *In situ* click chemistry

Amongst the reactions mentioned above, the Huisgen 1,3-dipolar cycloaddition reaction between azides and alkynes resulting in 1,2,3-triazoles, termed as *in situ* click chemistry, has been instrumental in the validation of kinetic TGS approaches due to its desirable reactivity profile. Conveniently, the triazoles display favorable physicochemical properties, take part in hydrogen-bonding, and are stable towards hydrolytic cleavage as well as oxidative or reductive reaction conditions.<sup>36b</sup> Various reaction conditions have been established to synthesize the disubstituted 1,2,3-triazoles (Scheme 1.1). For example, copper(I) catalysts are generally employed to regioselectively obtain 1,4-disubstituted triazoles (*anti*-triazoles),<sup>38</sup> whereas 1,5-disubstituted triazoles (*syn*-triazoles) can be synthesized using magnesium acetylides or ruthenium catalysts.<sup>39</sup> On the contrary, when an azide and an alkyne are heated in the absence of solvent, equimolar mixture of *syn*- and *anti*-triazoles is obtained.<sup>36a, 40</sup> Interestingly, only one of the regioisomers is preferentially formed in the templated reaction.<sup>41</sup>



**Scheme 1.1.** Synthesis of disubstituted 1,2,3-triazoles *via* Huisgen cycloaddition

The sluggish rate of this reaction has actually been proved to be advantageous for its application in the kinetic TGS approach.<sup>42</sup> Mock and co-workers investigated the reaction of an azide and an alkyne, each attached to an alkyl ammonium moiety. They reported that the rate of triazole formation was radically accelerated (by a factor of  $5.5 \times 10^4$ ) in the presence of catalytic amounts of cucurbituril, a nonadecacyclic cage-like structure comprised of substituted urea subunits.<sup>43</sup> Based on the NMR studies and other experiments, the ammonium moiety ( $\text{RNH}_3^+$ ) was found to be involved in the hydrogen bonding with the urea carbonyls, placing the azide and alkyne functionalities in proximity within the cavity of the cucurbituril cage, thereby accelerating the triazole formation.<sup>43a</sup> Inspired by these results, Sharpless and co-workers extended this approach to acetylcholinesterase (AChE),<sup>41, 44</sup> an enzyme which a crucial role in the functioning of central and peripheral nervous system by catalyzing hydrolysis of acetylcholine.<sup>45</sup> A set

of azides and alkynes leading to ninety eight potential triazoles (arising from forty nine combinations, considering *syn*- and *anti*- regioisomers) were incubated as binary mixtures in the presence of an eel AChE at room temperature for 6 days (Figure 1.7).<sup>44a</sup>

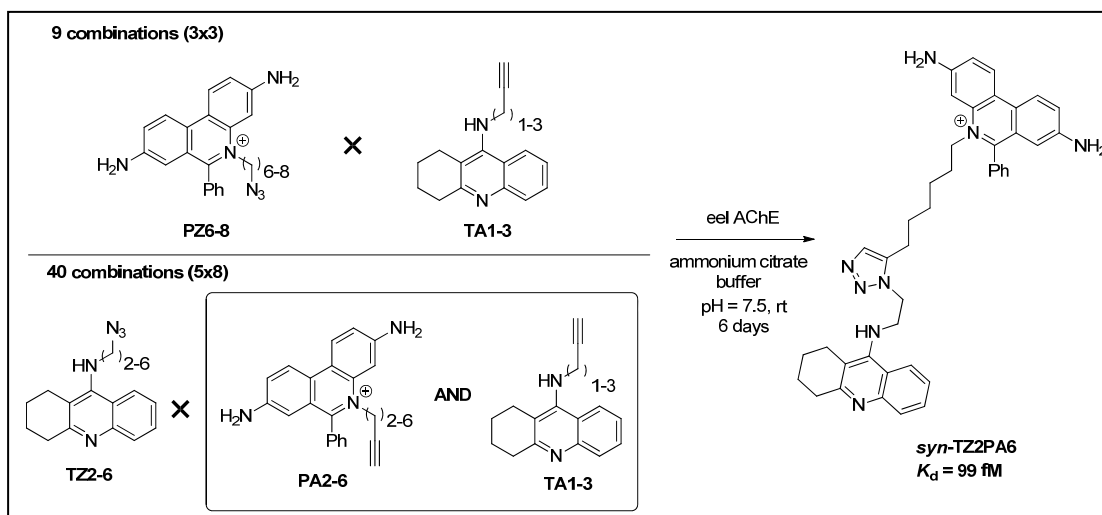


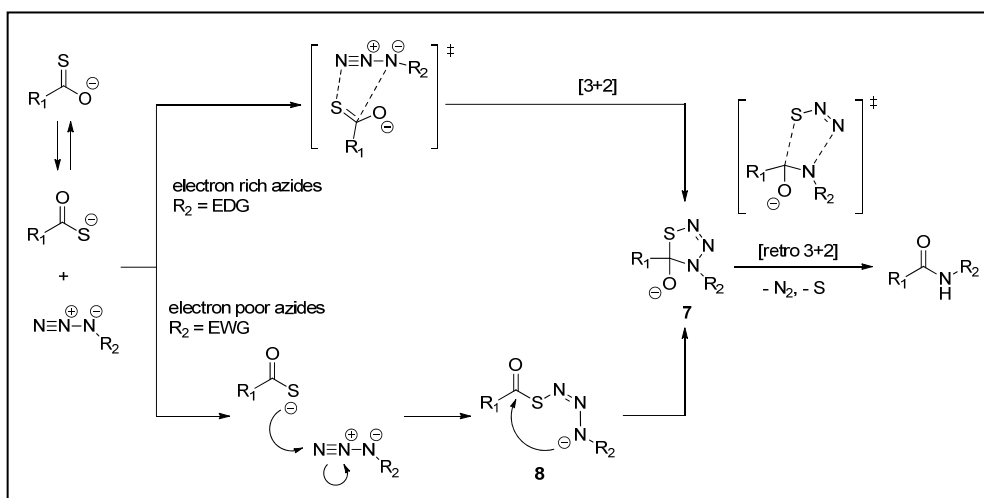
**Figure 1.7.** *In situ* click chemistry approach using eel AChE as a template

Out of ninety eight potential triazoles, only one triazole, *syn*-**TZ2PA6**, was generated in detectable amounts in the presence of the eel AChE. It is important to note that, the sluggish rate of this reaction would make it impossible to generate detectable amount of triazole in the absence of the target, underlining the role of the templation in accelerating the triazole formation by bringing the azide and alkyne functionalities together. The dissociation constants for *syn*- and *anti*-**TZ2PA6** were found to be 99 fM and 14 pM respectively.<sup>44a</sup> These results clearly indicate that the triazole *syn*-**TZ2PA6** with its significantly higher potency was preferentially assembled by the enzyme. Due to its versatility and reliability, the *in situ* click chemistry approach has been successfully employed to discover potent inhibitors of the enzymes such as bovine carbonic anhydrase (bCAII),<sup>46</sup> HIV-1 protease<sup>47</sup> and chitinase.<sup>48</sup> Other noteworthy examples include,

DNA-templated triazole formation starting from hairpin polyamide azides and alkynes,<sup>49</sup> and polypeptide-based antibody-like capture agents for bCAII.<sup>50</sup>

### 1.4.3.2 Sulfo-click reaction

Williams and co-workers recently developed a reaction, wherein electron-deficient azides (sulfonyl azides) or electron-rich azides (alkyl/aryl azides) react with thio acids leading to the corresponding amides.<sup>37a, b</sup> Detailed mechanistic studies have revealed that this reaction follows two distinct pathways depending upon the electronic nature of the azide used. The electron-rich azides favor the formation of thiatriazoline intermediate **7** directly whereas the electron-deficient azides primarily generate the linear intermediate **8** eventually leading to thiatriazoline **7** (Scheme 1.2).<sup>37b</sup> This reaction requires mild conditions, is high yielding and can be carried out in various organic as well as aqueous solvents. Importantly, the byproducts generated are not detrimental to the biological systems.



**Scheme 1.2.** Mechanism of the amidation reaction between azides and thio acids

These features qualify this amidation reaction, involving sulfonyl azides (termed as sulfo-click reaction<sup>37c</sup>) to be applied for the kinetic TGS approach. For example, Hu *et al.* designed a proof-of-concept experiment wherein, a set of six sulfonyl azides (**SZ1-SZ6**) and three thio acids (**TA1-TA3**) (eighteen possible combinations) was incubated as binary mixtures at 37 °C for six hours with the target protein Bcl-X<sub>L</sub>, an anti-apoptotic protein of the Bcl-2 family (Figure 1.8).<sup>51</sup> As a control, all eighteen combinations were incubated in the phosphate buffer without Bcl-X<sub>L</sub>. The samples were then analyzed by liquid chromatography combined with mass spectrometry using selected ion mode (LC/MS-SIM). Of all eighteen possible *N*-acylsulfonamide products, **SZ4TA2**, an inhibitor of Bcl-X<sub>L</sub> reported by Abbott laboratories,<sup>52</sup> was identified as a kinetic TGS hit.

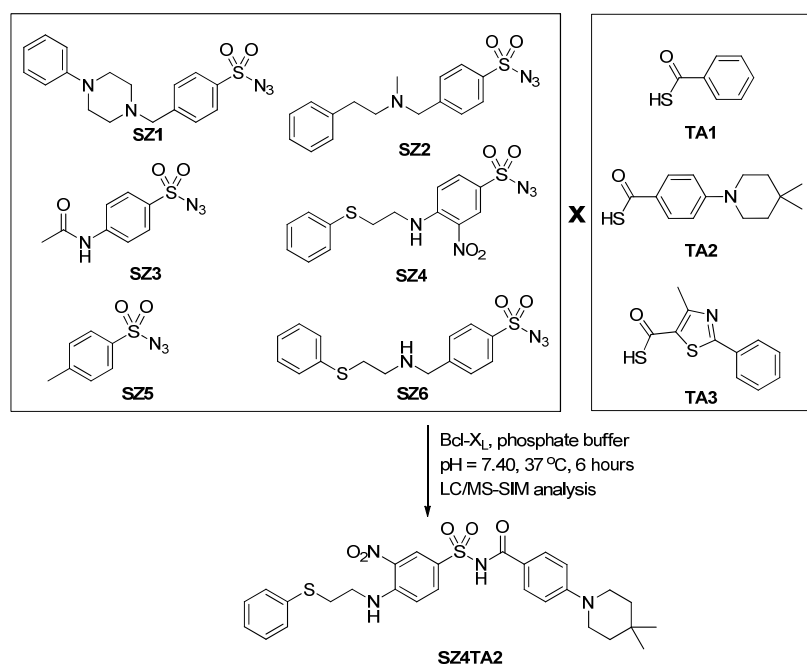


**Figure 1.8.** Screening of sulfonyl azides and thio acids against Bcl-X<sub>L</sub>

Additional control experiments incorporating wildtype (WT) and mutant versions of pro-apoptotic BH3 peptides (Bak and Bim) were carried out to probe whether the fragments are being templated at the binding site of Bcl-X<sub>L</sub> or through non-specific binding. The WT BH3 peptides were found to compete with the fragments resulting in the suppression of the templated product formation, whereas the mutant BH3 peptides did not affect the templated reaction owing to the weaker binding affinities.<sup>51</sup> These findings have suggested that the kinetic TGS approach utilizing an amidation reaction could also be applied to protein-protein interaction targets.

#### 1.4.3.3 Other reactions used for kinetic TGS

Apart from the reactions described above, additional reactions have also been found suitable for the kinetic TGS approach due to their favorable characteristics (Figure 1.9 A-D). Inspired from the serendipitous discovery by Chase and Tubbs involving carnitine acetyltransferase templated C-S bond forming reaction between bromoacetyl-carnitine and coenzyme-A,<sup>53</sup> Nguyen and Huc extended this approach against bovine carbonic anhydrase II (CA II).<sup>54</sup> A set of five alkyl chlorides and a thiol consisting of a sulfonamide moiety were used for this purpose. It is important to note that the fragments leading to more potent sulfides were preferably templated by CA II when two alkyl chlorides and one thiol were simultaneously incubated. Other reactions utilized as click reactions include a C-N bond formation templated by glycinamide ribonucleotide transformylase (GAR Tfase),<sup>55</sup> a C-C bond formation with sirtuin as a template<sup>56</sup> and a multi-component Ugi reaction templated by thrombin.<sup>57</sup>

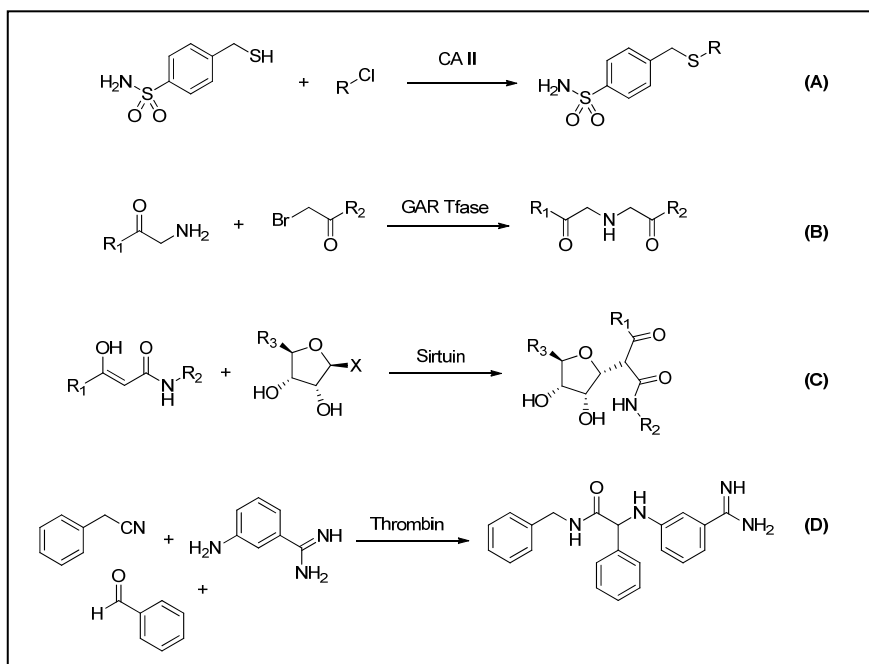


**Figure 1.9.** Other reactions explored for kinetic TGS application

### 1.5 Targeting protein-protein interactions

Protein-protein interactions constitute an integral part of the biological system and are involved in the regulation of many key processes ranging from signal transduction to apoptosis, a programmed cell death mechanism. Therefore, targeting specific protein-protein interactions has been of great therapeutic interest.<sup>58</sup> Despite enormous potential, identification of small molecules disrupting these interactions remains a challenging task.<sup>58c, 58l, 59</sup> The challenges are mainly associated with the nature of binding interfaces involved during these interactions. Typically, these interfaces are large (1500-3000 Å<sup>2</sup>),<sup>60</sup> flat and do not provide well-defined binding pockets or grooves.<sup>58a, b</sup> Additionally, the binding regions involved are noncontiguous, which complicates the design of synthetic peptides.<sup>58b, 58d</sup> Moreover, unlike enzymatic targets, natural small molecules or ligands binding to the protein-protein interfaces are hardly available posing difficulties during the inception.<sup>58a-c</sup> Proteins are also known to undergo significant

conformational changes. As a result, X-ray crystal structures may not be able to reveal deep cavities.<sup>58a, 58e</sup> In fact, a particular crystal structure can possibly represent merely one out of various conformations. It is quite possible that the conformation of the protein suitable for small molecule binding may not be obtained in one crystal structure.<sup>58a, 61</sup> Due to these hurdles, protein-protein interaction targets were thought to be ‘undruggable’. However, Clackson and Wells demonstrated through the pioneering work, that only a small region of the interface composed of few amino acids in the binding interface heavily contribute to the free energy of binding.<sup>62</sup> It was then envisioned that the small molecules targeting these small regions, termed as ‘hot spots’, would serve as initial drug candidates displaying reasonable binding affinities. Generally, the ‘hot spots’ are identified by alanine scanning<sup>62b, 63</sup> (wherein amino acid residues are replaced by alanine methodically and the change in the binding free energy for each mutation is determined) and are mainly comprised of aromatic as well as positively charged residues.<sup>62b</sup> Wells and co-workers used this technique to analyze the binding interactions between human growth hormone (hGH) and the extracellular domain of its receptor (hGHbp).<sup>64</sup> During the alanine screening, they discovered that out of thirty one side chains constituting the binding interface of hGH, only eight make up for approximately 85% of the binding free energy, while eleven of the side chains did not contribute towards the binding affinity at all.<sup>64b</sup> These findings have tremendously triggered the drug discovery process towards identification of various small molecules as protein-protein interaction modulators. Some noteworthy examples of protein-protein interactions include Bcl-X<sub>L</sub> / Bak, IL-2 / IL-2R $\alpha$ , MDM2 / p53, LFA-1 / ICAM-1, Mcl-1 / Bim and TNF / TNFRc1.<sup>58a, b, 65</sup>

### 1.5.1 Protein-protein interactions of the Bcl-2 family

The Bcl-2 family of proteins has been validated as a central regulator of apoptosis through an intrinsic pathway (also known as mitochondrial pathway) and can be divided into two categories, namely pro-apoptotic proteins and anti-apoptotic proteins.<sup>66</sup> The pro-apoptotic proteins, which can be further divided into two sub-categories, include Bak, Bax, Bok (multidomain proteins) and Bid, Bim, Bad and Noxa (BH3-only proteins). On the other hand, anti-apoptotic proteins mainly include Bcl-2, Bcl-X<sub>L</sub>, Mcl-1, Bcl-w and A1.<sup>66c</sup> Almost all the Bcl-2 family proteins consist of a dimerization domain, known as BH3 domain, represented by a 16 amino acid amphipathic  $\alpha$  helix. The NMR structure of Bcl-X<sub>L</sub> bound to Bak has revealed that the latter, in the  $\alpha$ -helical structure, binds to the hydrophobic groove of Bcl-X<sub>L</sub>.<sup>67</sup> The ability of the anti-apoptotic proteins to heterodimerize with pro-apoptotic proteins (both, multidomain and BH3 only) through the BH3 domain can be correlated with their role in the suppression of cell death mechanism resulting in tumor progression.<sup>66a</sup> In accordance, the majority of human cancers display overexpression of anti-apoptotic Bcl-2 family proteins. For example, high levels of Bcl-2 and Bcl-X<sub>L</sub> are observed in prostate, breast and colorectal cancers.<sup>68</sup> Some BH3-only proteins (e.g. Bad) antagonize the anti-apoptotic proteins making the multidomain pro-apoptotic proteins available during apoptosis and are known as sensitizers or de-repressors. Alternatively, other BH3-only proteins (such as Bid or Bim) can directly activate the Bak or Bax and hence are termed as activators.<sup>66c</sup> Therefore, small molecules mimicking the BH3 domain can be developed to induce apoptosis and hence have the potential as anti-cancer therapeutics.<sup>69</sup>

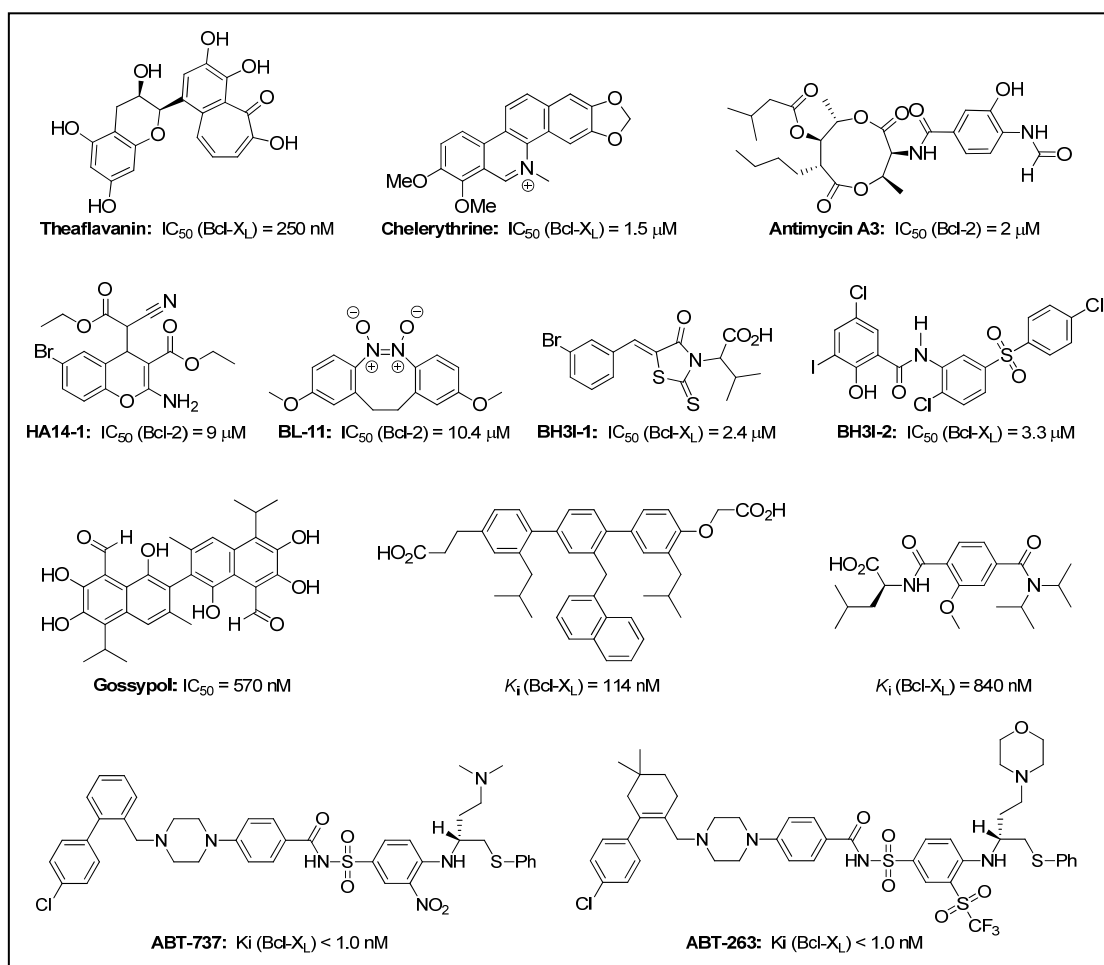


**Figure 1.10.** Small-molecular inhibitors of Bcl-2/Bcl-X<sub>L</sub>

Several combinations of drug discovery methods have been employed for developing potent inhibitors of the Bcl-2 and/or Bcl-X<sub>L</sub> (Figure 1.10).<sup>19, 52, 70</sup> In particular, small molecules mimicking the  $\alpha$ -helix involved in the binding interactions have displayed high affinities ( $K_i \sim 5\text{-}100 \text{ nM}$ ).<sup>71</sup> During the last decade, Fesik and co-workers at Abbott laboratories designed highly potent small molecular dual inhibitors of Bcl-2 and Bcl-X<sub>L</sub> utilizing a fragment-based approach known as SAR-by-NMR.<sup>17, 19, 52, 72</sup> In this approach, small fragments were screened against <sup>15</sup>N-labeled Bcl-X<sub>L</sub> using <sup>15</sup>N HSQC analysis. First, ligands with weak binding affinities targeting first and second site within the hydrophobic groove of Bcl-X<sub>L</sub> were identified. These fragments were then

optimized using NMR analysis in combination with parallel synthesis to generate high-affinity ligands. Moreover, these compounds retained the activity in cell-based assays as well as in animals (tumor xenograft models).<sup>58b</sup> The most potent compound, **ABT-737** obtained after extensive efforts exhibited a  $K_i$  of 0.6 nM against Bcl-2, Bcl-X<sub>L</sub> and Bcl-w.<sup>19</sup> **ABT-263**, an analogue of **ABT-737** has entered in phase I/II clinical trials for cancer treatment.<sup>73</sup> Interestingly, these compounds were found to be selective and showed lower binding affinity ( $K_i = 0.46 \mu\text{M}$ ) against other anti-apoptotic proteins such as Mcl-1, Bcl-B and A1.<sup>19</sup> Analysis of various peptides derived from Bak through alanine scanning has revealed that the amino acid residues Val 74, Leu 78, Ile 81, Asp 83 and Ile 85 are responsible for the key binding interactions with Bcl-X<sub>L</sub>.<sup>67, 71b</sup> Although **ABT-737** binds to Bcl-X<sub>L</sub> in the same domain as observed for Bak-analogous peptides, it captures Bcl-X<sub>L</sub> in a different conformation, exposing deeper cavities in the binding site.<sup>58b</sup> Remarkably, these findings have highlighted the significance of ‘hot spots’ in targeting protein-protein interactions.

## 1.6 Development of novel reactions suitable for kinetic TGS

As described earlier, the kinetic TGS approach has the potential to streamline the drug discovery process and has been successfully applied to various enzymatic as well as protein-protein interaction targets. Various reactions suitable for kinetic TGS have been identified so far. Most prominent examples include, (a) the Huisgen 1,3-dipolar cycloaddition reaction between azides and alkynes resulting in 1,2,3-triazoles, and (b) the sulfo-click reaction between sulfonyl azides and thio acids yielding amides. Importantly, using these reactions, biologically valuable functional moieties such as triazoles and amides could be incorporated generating drug-like molecules. Therefore, the

development of novel reactions with the potential to be applied for a kinetic TGS approach would be of great importance.

## 1.7 Research aims

### 1.7.1 Identification of protein-protein interaction modulators (PPIMs) targeting Bcl-X<sub>L</sub>

Although protein-protein interactions possess significant biological importance, identification of small molecules modulating specific protein-protein interactions remains challenging due to the flexible nature of proteins. Several fragment based approaches have been established to identify fragments with good ligand efficiencies, but fail to provide insights into efficient fragment linkage, making the drug discovery process complicated. In another type of fragment-based approach, termed as kinetic target-guided synthesis (TGS), the target serves as a template assembling the fragments together to yield the inhibitor of that target itself. This approach was recently shown to be suitable for the identification of PPIMs. Our research efforts were focused on utilizing the kinetic TGS approach based on the sulfo-click reaction between thio acids and sulfonyl azides for the identification of high-quality PPIMs targeting an anti-apoptotic protein, Bcl-X<sub>L</sub>.

### 1.7.2 Identification of PPIMs targeting Mcl-1

Recently, Mcl-1, another anti-apoptotic protein of the Bcl-2 family has been established to be actively involved in controlling the apoptotic pathway. As a result, several small molecules targeting Mcl-1 selectively or in combination with other anti-apoptotic proteins have been reported in the past few years. After obtaining encouraging results with Bcl-X<sub>L</sub>, our aim was to extend the kinetic TGS approach to Mcl-1 utilizing the sulfo-click reaction. The key features of this research endeavor

involved (a) the expansion of sulfonyl azide and thio acid libraries, (b) the *in situ* generation of thio acids starting from thio esters to address the issues associated with the stability of thio acids, (c) the screening of the expanded libraries of sulfonyl azides and thio acids against Mcl-1, (d) the confirmation of the kinetic TGS hits identified using control experiments followed by synthesis of the same, and (e) the determination of biological activities ( $IC_{50}$  values) of these kinetic TGS hits against Mcl-1 and Bcl-X<sub>L</sub> using fluorescence polarization assay.

### 1.7.3 Development of an amidation reaction

Although, the kinetic TGS has been well established as a highly reliable and efficient approach for the identification of novel inhibitors of various biological targets with therapeutic interest, only a limited set of reactions have been found to be suitable for this method. We identified that a set of alkyl azides (substituted benzyl azides and  $\alpha$ -azido amides) can undergo a reaction with aromatic aldehydes under mild basic conditions generating corresponding amides. First, the reaction conditions were optimized and *t*-BuOK alone was found to be suitable for this transformation, while best results were obtained when DMF was used as a solvent. The potential of this reaction to be used for kinetic TGS approach was then probed. Unfortunately, this reaction turned out to be sensitive to moisture and thus cannot be applied for the TGS. Nevertheless, biologically relevant amidomethylarenes could be easily generated using this method. As a result, our efforts entailed (a) expanding the scope of the reaction with respect to both azides and aldehydes, and (b) designing control experiments to investigate the mechanistic details.

## 1.8 References cited

1. (a) Merrifield, R. B., Solid Phase Peptide Synthesis .1. Synthesis of a Tetrapeptide. *J. Am. Chem. Soc.* **1963**, 85 (14), 2149-&; (b) Merrifield, B., Solid-Phase Synthesis. *Science* **1986**, 232 (4748), 341-347.
2. (a) Golebiowski, A.; Klopfenstein, S. R.; Portlock, D. E., Lead compounds discovered from libraries. *Curr. Opin. Chem. Biol.* **2001**, 5 (3), 273-284; (b) Golebiowski, A.; Klopfenstein, S. R.; Portlock, D. E., Lead compounds discovered from libraries: Part 2. *Curr. Opin. Chem. Biol.* **2003**, 7 (3), 308-325.
3. Zhang, H. C.; Nimmer, P.; Rosenberg, S. H.; Ng, S. C.; Joseph, M., Development of a high-throughput fluorescence polarization assay for Bcl-x(L). *Anal. Biochem.* **2002**, 307 (1), 70-75.
4. (a) Ullman, E. F.; Kirakossian, H.; Singh, S.; Wu, Z. P.; Irvin, B. R.; Pease, J. S.; Switchenko, A. C.; Irvine, J. D.; Dafforn, A.; Skold, C. N.; Wagner, D. B., Luminescent Oxygen Channeling Immunoassay - Measurement of Particle Binding-Kinetics by Chemiluminescence. *Proc. Natl. Acad. Sci. U.S.A.* **1994**, 91 (12), 5426-5430; (b) Ullman, E. F.; Kirakossian, H.; Switchenko, A. C.; Ishkanian, J.; Ericson, M.; Wartchow, C. A.; Pirio, M.; Pease, J.; Irvin, B. R.; Singh, S.; Singh, R.; Patel, R.; Dafforn, A.; Davalian, D.; Skold, C.; Kurn, N.; Wagner, D. B., Luminescent oxygen channeling assay (LOCI(TM)): Sensitive, broadly applicable homogeneous immunoassay method. *Clin. Chem.* **1996**, 42 (9), 1518-1526.
5. Bohacek, R. S.; McMartin, C.; Guida, W. C., The art and practice of structure-based drug design: A molecular modeling perspective. *Med. Res. Rev.* **1996**, 16 (1), 3-50.

6. Schmidt, M. F.; Rademann, J., Dynamic template-assisted strategies in fragment-based drug discovery. *Trends Biotechnol.* **2009**, *27* (9), 512-521.
7. (a) Carr, R. A. E.; Congreve, M.; Murray, C. W.; Rees, D. C., Fragment-based lead discovery: leads by design. *Drug Discov. Today* **2005**, *10* (14), 987-992; (b) Erlanson, D. A., Fragment-based lead discovery: a chemical update. *Curr. Opin. Biotechnol.* **2006**, *17* (6), 643-652; (c) Albert, J. S.; Blomberg, N.; Breeze, A. L.; Brown, A. J. H.; Burrows, J. N.; Edwards, P. D.; Folmer, R. H. A.; Geschwindner, S.; Griffen, E. J.; Kenny, P. W.; Nowak, T.; Olsson, L. L.; Sanganee, H.; Shapiro, A. B., An integrated approach to fragment-based lead generation: Philosophy, strategy and case studies from AstraZeneca's drug discovery programmes. *Curr. Top. Med. Chem.* **2007**, *7* (16), 1600-1629; (d) Congreve, M.; Chessari, G.; Tisi, D.; Woodhead, A. J., Recent developments in fragment-based drug discovery. *J. Med. Chem.* **2008**, *51* (13), 3661-3680.
8. Rees, D. C.; Congreve, M.; Murray, C. W.; Carr, R., Fragment-based lead discovery. *Nat. Rev. Drug Discov.* **2004**, *3* (8), 660-672.
9. Fink, T.; Bruggesser, H.; Reymond, J. L., Virtual exploration of the small-molecule chemical universe below 160 daltons. *Angew. Chem., Int. Ed.* **2005**, *44* (10), 1504-1508.
10. Erlanson, D. A.; Hansen, S. K., Making drugs on proteins: site-directed ligand discovery for fragment-based lead assembly. *Curr. Opin. Chem. Biol.* **2004**, *8* (4), 399-406.
11. Neumann, T.; Junker, H. D.; Schmidt, K.; Sekul, R., SPR-based fragment screening: Advantages and applications. *Curr. Top. Med. Chem.* **2007**, *7* (16), 1630-1642.

12. (a) Nienaber, V. L.; Richardson, P. L.; Klighofer, V.; Bouska, J. J.; Giranda, V. L.; Greer, J., Discovering novel ligands for macromolecules using X-ray crystallographic screening. *Nat. Biotechnol.* **2000**, *18* (10), 1105-1108; (b) Blundell, T. L.; Jhoti, H.; Abell, C., High-throughput crystallography for lead discovery in drug design. *Nat. Rev. Drug Discov.* **2002**, *1* (1), 45-54; (c) Blundell, T. L.; Patel, S., High-throughput X-ray crystallography for drug discovery. *Curr. Opin. Pharmacol.* **2004**, *4* (5), 490-496.
13. (a) Freire, E., Isothermal titration calorimetry: controlling binding forces in lead optimization. *Drug Discovery Today Technol.* **2004**, *1* (3), 295-299; (b) Ciulli, A.; Scott, D. E.; Ando, M.; Reyes, F.; Saldanha, S. A.; Tuck, K. L.; Chirgadze, D. Y.; Blundell, T. L.; Abell, C., Inhibition of Mycobacterium tuberculosis Pantothenate Synthetase by Analogues of the Reaction Intermediate. *Chembiochem* **2008**, *9* (16), 2606-2611.
14. Shuker, S. B.; Hajduk, P. J.; Meadows, R. P.; Fesik, S. W., Discovering high-affinity ligands for proteins: SAR by NMR. *Science* **1996**, *274* (5292), 1531-1534.
15. Swayze, E. E.; Jefferson, E. A.; Sannes-Lowery, K. A.; Blyn, L. B.; Risen, L. M.; Arakawa, S.; Osgood, S. A.; Hofstadler, S. A.; Griffey, R. H., SAR by MS: A ligand based technique for drug lead discovery against structured RNA targets. *J. Med. Chem.* **2002**, *45* (18), 3816-3819.
16. Whitty, A., Cooperativity and biological complexity. *Nat. Chem. Biol.* **2008**, *4* (8), 435-439.
17. Bruncko, M.; Oost, T. K.; Belli, B. A.; Ding, H.; Joseph, M. K.; Kunzer, A.; Martineau, D.; McClellan, W. J.; Mitten, M.; Ng, S. C.; Nimmer, P. M.; Oltersdorf, T.; Park, C. M.; Petros, A. M.; Shoemaker, A. R.; Song, X. H.; Wang, X. L.; Wendt, M. D.;

Zhang, H. C.; Fesik, S. W.; Rosenberg, S. H.; Elmore, S. W., Studies leading to potent, dual inhibitors of bcl-2 and Bcl-xL. *J. Med. Chem.* **2007**, *50* (4), 641-662.

18. Hajduk, P. J., Fragment-based drug design: How big is too big? *J. Med. Chem.* **2006**, *49* (24), 6972-6976.

19. Oltersdorf, T.; Elmore, S. W.; Shoemaker, A. R.; Armstrong, R. C.; Augeri, D. J.; Belli, B. A.; Bruncko, M.; Deckwerth, T. L.; Dinges, J.; Hajduk, P. J.; Joseph, M. K.; Kitada, S.; Korsmeyer, S. J.; Kunzer, A. R.; Letai, A.; Li, C.; Mitten, M. J.; Nettlesheim, D. G.; Ng, S.; Nimmer, P. M.; O'Connor, J. M.; Oleksijew, A.; Petros, A. M.; Reed, J. C.; Shen, W.; Tahir, S. K.; Thompson, C. B.; Tomaselli, K. J.; Wang, B. L.; Wendt, M. D.; Zhang, H. C.; Fesik, S. W.; Rosenberg, S. H., An inhibitor of Bcl-2 family proteins induces regression of solid tumours. *Nature* **2005**, *435* (7042), 677-681.

20. Huc, I.; Lehn, J. M., Virtual combinatorial libraries: Dynamic generation of molecular and supramolecular diversity by self-assembly (vol 94, pg 2106, 1997). *Proc. Natl. Acad. Sci. U.S.A.* **1997**, *94* (15), 8272-8272.

21. Corbett, P. T.; Leclaire, J.; Vial, L.; West, K. R.; Wietor, J. L.; Sanders, J. K. M.; Otto, S., Dynamic combinatorial chemistry. *Chem. Rev.* **2006**, *106* (9), 3652-3711.

22. Hochgurtel, M.; Biesinger, R.; Kroth, H.; Piecha, D.; Hofmann, M. W.; Krause, S.; Schaaf, O.; Nicolau, C.; Eliseev, A. V., Ketones as building blocks for dynamic combinatorial libraries: Highly active neuraminidase inhibitors generated via selection pressure of the biological target. *J. Med. Chem.* **2003**, *46* (3), 356-358.

23. (a) Ramstrom, O.; Lehn, J. M., Drug discovery by dynamic combinatorial libraries. *Nat. Rev. Drug Discov.* **2002**, *1* (1), 26-36; (b) Otto, S.; Furlan, R. L. E.;

- Sanders, J. K. M., Dynamic combinatorial chemistry. *Drug Discov. Today* **2002**, 7 (2), 117-125.
24. Erlanson, D. A.; Wells, J. A.; Braisted, A. C., Tethering: Fragment-based drug discovery. *Annu. Rev. Biophys. Biomol. Struct.* **2004**, 33, 199-223.
25. Erlanson, D. A.; McDowell, R. S.; He, M. M.; Randal, M.; Simmons, R. L.; Kung, J.; Waight, A.; Hansen, S. K., Discovery of a new phosphotyrosine mimetic for PTP1B using breakaway tethering. *J. Am. Chem. Soc.* **2003**, 125 (19), 5602-5603.
26. Erlanson, D. A.; Lam, J. W.; Wiesmann, C.; Luong, T. N.; Simmons, R. L.; DeLano, W. L.; Choong, I. C.; Burdett, M. T.; Flanagan, W. M.; Lee, D.; Gordon, E. M.; O'Brien, T., In situ assembly of enzyme inhibitors using extended tethering. *Nat. Biotechnol.* **2003**, 21 (3), 308-314.
27. (a) Erlanson, D. A.; Braisted, A. C.; Raphael, D. R.; Randal, M.; Stroud, R. M.; Gordon, E. M.; Wells, J. A., Site-directed ligand discovery. *Proc. Natl. Acad. Sci. U.S.A.* **2000**, 97 (17), 9367-9372; (b) Ramstrom, O.; Lehn, J. M., In situ generation and screening of a dynamic combinatorial carbohydrate library against concanavalin A. *Chembiochem* **2000**, 1 (1), 41-48.
28. Cancilla, M. T.; He, M. M.; Viswanathan, N.; Simmons, R. L.; Taylor, M.; Fung, A. D.; Cao, K.; Erlanson, D. A., Discovery of an Aurora kinase inhibitor through site-specific dynamic combinatorial chemistry. *Bioorg. Med. Chem. Lett.* **2008**, 18 (14), 3978-3981.
29. (a) Vongvilai, P.; Angelin, M.; Larsson, R.; Ramstrom, O., Dynamic combinatorial resolution: Direct asymmetric lipase-mediated screening of a dynamic nitroaldol library. *Angew. Chem., Int. Ed.* **2007**, 46 (6), 948-950; (b) Angelin, M.;

- Vongvilai, P.; Fischer, A.; Ramstrom, O., Tandem driven dynamic combinatorial resolution via Henry-iminolactone rearrangement. *Chem. Commun.* **2008**, (6), 768-770;
- (c) Maly, D. J.; Choong, I. C.; Ellman, J. A., Combinatorial target-guided ligand assembly: Identification of potent subtype-selective c-Src inhibitors. *Proc. Natl. Acad. Sci. U.S.A.* **2000**, 97 (6), 2419-2424.
30. (a) Corbett, A. R.; Cheeseman, J. D.; Kazlauskas, R. J.; Gleason, J. L., Pseudodynamic combinatorial libraries: A receptor-assisted approach for drug discovery. *Angew. Chem., Int. Ed.* **2004**, 43 (18), 2432-2436; (b) Corbett, A. D.; Gleason, J. L., Preparation of active esters on solid support for aqueous-phase peptide couplings. *Tetrahedron Lett.* **2002**, 43 (8), 1369-1372.
31. (a) Sundram, U. N.; Griffin, J. H.; Nicas, T. I., Novel vancomycin dimers with activity against vancomycin-resistant enterococci. *J. Am. Chem. Soc.* **1996**, 118 (51), 13107-13108; (b) Rao, J. H.; Whitesides, G. M., Tight binding of a dimeric derivative of vancomycin with dimeric L-Lys-D-Ala-D-Ala. *J. Am. Chem. Soc.* **1997**, 119 (43), 10286-10290; (c) Staroske, T.; Williams, D. H., Synthesis of covalent head-to-tail dimers of vancomycin. *Tetrahedron Lett.* **1998**, 39 (27), 4917-4920; (d) Adameczyk, M.; Moore, J. A.; Rege, S. D.; Yu, Z. G., Investigations into self-association of vancomycin covalent dimers using surface plasmon resonance technology. *Bioorg. Med. Chem. Lett.* **1999**, 9 (16), 2437-2440.
32. (a) Rao, J. H.; Lahiri, J.; Weis, R. M.; Whitesides, G. M., Design, synthesis, and characterization of a high-affinity trivalent system derived from vancomycin and L-Lys-D-Ala-D-Ala. *J. Am. Chem. Soc.* **2000**, 122 (12), 2698-2710; (b) Rao, J. H.; Lahiri, J.; Isaacs, L.; Weis, R. M.; Whitesides, G. M., A trivalent system from vancomycin center

dot D-Ala-D-Ala with higher affinity than avidin center dot biotin. *Science* **1998**, 280 (5364), 708-711.

33. Arimoto, H.; Nishimura, K.; Kinumi, T.; Hayakawa, I.; Uemura, D., Multi-valent polymer of vancomycin: enhanced antibacterial activity against VRE. *Chem. Commun.* **1999**, (15), 1361-1362.

34. (a) Nicolaou, K. C.; Hughes, R.; Cho, S. Y.; Winssinger, N.; Smethurst, C.; Labischinski, H.; Endermann, R., Target-accelerated combinatorial synthesis and discovery of highly potent antibiotics effective against vancomycin-resistant bacteria. *Angew. Chem., Int. Ed.* **2000**, 39 (21), 3823-+; (b) Nicolaou, K. C.; Hughes, R.; Cho, S. Y.; Winssinger, N.; Labischinski, H.; Endermann, R., Synthesis and biological evaluation of vancomycin dimers with potent activity against vancomycin-resistant bacteria: target-accelerated combinatorial synthesis. *Chem.-Eur. J.* **2001**, 7 (17), 3824-3843.

35. (a) Hu, X. D.; Manetsch, R., Kinetic target-guided synthesis. *Chem. Soc. Rev.* **2010**, 39 (4), 1316-1324; (b) Sharpless, K. B.; Manetsch, R., In situ click chemistry: a powerful means for lead discovery. *Expert Opin. Drug Discovery* **2006**, 1 (6), 525-538.

36. (a) Kolb, H. C.; Finn, M. G.; Sharpless, K. B., Click chemistry: Diverse chemical function from a few good reactions. *Angew. Chem., Int. Ed.* **2001**, 40 (11), 2004-+; (b) Kolb, H. C.; Sharpless, K. B., The growing impact of click chemistry on drug discovery. *Drug Discov. Today* **2003**, 8 (24), 1128-1137.

37. (a) Shangguan, N.; Katukojvala, S.; Greenburg, R.; Williams, L. J., The reaction of thio acids with azides: A new mechanism and new synthetic applications. *J. Am. Chem. Soc.* **2003**, 125 (26), 7754-7755; (b) Kolakowski, R. V.; Shangguan, N.; Sauers, R. R.; Williams, L. J., Mechanism of thio acid/azide amidation. *J. Am. Chem. Soc.* **2006**,

- 128 (17), 5695-5702; (c) Rijkers, D. T. S.; Merkx, R.; Yim, C. B.; Brouwer, A. J.; Liskamp, R. M. J., 'Sulfo-click' for ligation as well as for site-specific conjugation with peptides, fluorophores, and metal chelators. *J. Pept. Sci.* **2010**, *16* (1), 1-5.
38. (a) Rostovtsev, V. V.; Green, L. G.; Fokin, V. V.; Sharpless, K. B., A stepwise Huisgen cycloaddition process: Copper(I)-catalyzed regioselective "ligation" of azides and terminal alkynes. *Angew. Chem., Int. Ed.* **2002**, *41* (14), 2596-+; (b) Tornøe, C. W.; Christensen, C.; Meldal, M., Peptidotriazoles on solid phase: [1,2,3]-triazoles by regiospecific copper(I)-catalyzed 1,3-dipolar cycloadditions of terminal alkynes to azides. *J. Org. Chem.* **2002**, *67* (9), 3057-3064.
39. (a) Krasinski, A.; Fokin, V. V.; Sharpless, K. B., Direct synthesis of 1,5-disubstituted-4-magnesio-1,2,3-triazoles, revisited. *Org. Lett.* **2004**, *6* (8), 1237-1240; (b) Zhang, L.; Chen, X. G.; Xue, P.; Sun, H. H. Y.; Williams, I. D.; Sharpless, K. B.; Fokin, V. V.; Jia, G. C., Ruthenium-catalyzed cycloaddition of alkynes and organic azides. *J. Am. Chem. Soc.* **2005**, *127* (46), 15998-15999; (c) Boren, B. C.; Narayan, S.; Rasmussen, L. K.; Zhang, L.; Zhao, H. T.; Lin, Z. Y.; Jia, G. C.; Fokin, V. V., Ruthenium-catalyzed azide-alkyne cycloaddition: Scope and mechanism. *J. Am. Chem. Soc.* **2008**, *130* (28), 8923-8930.
40. Huisgen, R.; Szeimies, G.; Mobius, L., 1,3-Dipolare Cycloadditionen .32. Kinetik Der Additionen Organischer Azide an Cc-Mehrfachbindungen. *Chem Ber-Recl* **1967**, *100* (8), 2494-&.
41. Manetsch, R.; Krasinski, A.; Radic, Z.; Raushel, J.; Taylor, P.; Sharpless, K. B.; Kolb, H. C., In situ click chemistry: Enzyme inhibitors made to their own specifications. *J. Am. Chem. Soc.* **2004**, *126* (40), 12809-12818.

42. Mamidyala, S. K.; Finn, M. G., In situ click chemistry: probing the binding landscapes of biological molecules. *Chem. Soc. Rev.* **2010**, *39* (4), 1252-1261.
43. (a) Mock, W. L.; Shih, N. Y., Host Guest Binding-Capacity of Cucurbituril. *J. Org. Chem.* **1983**, *48* (20), 3618-3619; (b) Mock, W. L.; Irra, T. A.; Wepsiec, J. P.; Manimaran, T. L., Cycloaddition Induced by Cucurbituril - a Case of Pauling Principle Catalysis. *J. Org. Chem.* **1983**, *48* (20), 3619-3620; (c) Mock, W. L.; Irra, T. A.; Wepsiec, J. P.; Adhya, M., Catalysis by Cucurbituril - the Significance of Bound-Substrate Destabilization for Induced Triazole Formation. *J. Org. Chem.* **1989**, *54* (22), 5302-5308.
44. (a) Lewis, W. G.; Green, L. G.; Grynszpan, F.; Radic, Z.; Carlier, P. R.; Taylor, P.; Finn, M. G.; Sharpless, K. B., Click chemistry in situ: Acetylcholinesterase as a reaction vessel for the selective assembly of a femtomolar inhibitor from an array of building blocks. *Angew. Chem., Int. Ed.* **2002**, *41* (6), 1053-+; (b) Krasinski, A.; Radic, Z.; Manetsch, R.; Raushel, J.; Taylor, P.; Sharpless, K. B.; Kolb, H. C., In situ selection of lead compounds by click chemistry: Target-guided optimization of acetylcholinesterase inhibitors. *J. Am. Chem. Soc.* **2005**, *127* (18), 6686-6692.
45. (a) Quinn, D. M., Acetylcholinesterase - Enzyme Structure, Reaction Dynamics, and Virtual Transition-States. *Chem. Rev.* **1987**, *87* (5), 955-979; (b) Taylor, P.; Radic, Z., The Cholinesterases - from Genes to Proteins. *Annu. Rev. Pharmacol. Toxicol.* **1994**, *34*, 281-320.
46. Mocharla, V. P.; Colasson, B.; Lee, L. V.; Roper, S.; Sharpless, K. B.; Wong, C. H.; Kolb, H. C., In situ click chemistry: Enzyme-generated inhibitors of carbonic anhydrase II. *Angew. Chem., Int. Ed.* **2005**, *44* (1), 116-120.

47. Whiting, M.; Muldoon, J.; Lin, Y. C.; Silverman, S. M.; Lindstrom, W.; Olson, A. J.; Kolb, H. C.; Finn, M. G.; Sharpless, K. B.; Elder, J. H.; Fokin, V. V., Inhibitors of HIV-1 protease by using in situ click chemistry. *Angew. Chem., Int. Ed.* **2006**, *45* (9), 1435-1439.
48. Hirose, T.; Sunazuka, T.; Sugawara, A.; Endo, A.; Iguchi, K.; Yamamoto, T.; Ui, H.; Shiomi, K.; Watanabe, T.; Sharpless, K. B.; Omura, S., Chitinase inhibitors: extraction of the active framework from natural argifin and use of in situ click chemistry. *J. Antibiot.* **2009**, *62* (5), 277-282.
49. Poulin-Kerstien, A. T.; Dervan, P. B., DNA-templated dimerization of hairpin polyamides. *J. Am. Chem. Soc.* **2003**, *125* (51), 15811-15821.
50. Agnew, H. D.; Rohde, R. D.; Millward, S. W.; Nag, A.; Yeo, W. S.; Hein, J. E.; Pitram, S. M.; Tariq, A. A.; Burns, V. M.; Krom, R. J.; Fokin, V. V.; Sharpless, K. B.; Heath, J. R., Iterative In Situ Click Chemistry Creates Antibody-like Protein-Capture Agents. *Angew. Chem., Int. Ed.* **2009**, *48* (27), 4944-4948.
51. Hu, X. D.; Sun, J. Z.; Wang, H. G.; Manetsch, R., Bcl-X-L-templated assembly of its own protein-protein interaction modulator from fragments decorated with thio acids and sulfonyl azides. *J. Am. Chem. Soc.* **2008**, *130* (42), 13820-13821.
52. Wendt, M. D.; Shen, W.; Kunzer, A.; McClellan, W. J.; Bruncko, M.; Oost, T. K.; Ding, H.; Joseph, M. K.; Zhang, H. C.; Nimmer, P. M.; Ng, S. C.; Shoemaker, A. R.; Petros, A. M.; Oleksijew, A.; Marsh, K.; Bauch, J.; Oltersdorf, T.; Belli, B. A.; Martineau, D.; Fesik, S. W.; Rosenberg, S. H.; Elmore, S. W., Discovery and structure-activity relationship of antagonists of B-cell lymphoma 2 family proteins with chemopotential activity in vitro and in vivo. *J. Med. Chem.* **2006**, *49* (3), 1165-1181.

53. Chase, J. F. A.; Tubbs, P. K., Conditions for Self-Catalysed Inactivation of Carnitine Acetyltransferase - a Novel Form of Enzyme Inhibition. *Biochem. J.* **1969**, *111* (2), 225-&.
54. Nguyen, R.; Huc, I., Using an enzyme's active site to template inhibitors. *Angew. Chem., Int. Ed.* **2001**, *40* (9), 1774-1776.
55. (a) Inglese, J.; Benkovic, S. J., Multisubstrate Adduct Inhibitors of Glycinamide Ribonucleotide Transformylase - Synthetic and Enzyme-Assembled. *Tetrahedron* **1991**, *47* (14-15), 2351-2364; (b) Boger, D. L.; Haynes, N. E.; Warren, M. S.; Ramcharan, J.; Kitos, P. A.; Benkovic, S. J., Multisubstrate analogue based on 5,8,10-trideazafolate. *Bioorg. Med. Chem.* **1997**, *5* (9), 1853-1857; (c) Greasley, S. E.; Marsilje, T. H.; Cai, H.; Baker, S.; Benkovic, S. J.; Boger, D. L.; Wilson, I. A., Unexpected formation of an epoxide-derived multisubstrate adduct inhibitor on the active site of GAR transformylase. *Biochemistry* **2001**, *40* (45), 13538-13547.
56. Asaba, T.; Suzuki, T.; Ueda, R.; Tsumoto, H.; Nakagawa, H.; Miyata, N., Inhibition of Human Sirtuins by in Situ Generation of an Acetylated Lysine-ADP-Ribose Conjugate. *J. Am. Chem. Soc.* **2009**, *131* (20), 6989-6996.
57. Weber, L., In vitro combinatorial chemistry to create drug candidates. *Drug Discovery Today Technol.* **2004**, *1* (3), 261-267.
58. (a) Arkin, M. R.; Wells, J. A., Small-molecule inhibitors of protein-protein interactions: Progressing towards the dream. *Nat. Rev. Drug Discov.* **2004**, *3* (4), 301-317; (b) Wells, J. A.; McClendon, C. L., Reaching for high-hanging fruit in drug discovery at protein-protein interfaces. *Nature* **2007**, *450* (7172), 1001-1009; (c) Berg, T., Modulation of protein-protein interactions with small organic molecules. *Angew. Chem.,*

*Int. Ed.* **2003**, *42* (22), 2462-2481; (d) Yin, H.; Hamilton, A. D., Strategies for targeting protein-protein interactions with synthetic agents. *Angew. Chem., Int. Ed.* **2005**, *44* (27), 4130-4163; (e) Eyrisch, S.; Helms, V., Transient pockets on protein surfaces involved in protein-protein interaction. *J. Med. Chem.* **2007**, *50* (15), 3457-3464; (f) Saraogi, I.; Hamilton, A. D., alpha-Helix mimetics as inhibitors of protein-protein interactions. *Biochem. Soc. Trans.* **2008**, *36*, 1414-1417; (g) Block, P.; Weskamp, N.; Wolf, A.; Klebe, G., Strategies to search and design stabilizers of protein-protein interactions: A feasibility study. *Proteins* **2007**, *68* (1), 170-186; (h) Fry, D. C., Protein-protein interactions as targets for small molecule drug discovery. *Biopolymers* **2006**, *84* (6), 535-552; (i) Blazer, L. L.; Neubig, R. R., Small Molecule Protein-Protein Interaction Inhibitors as CNS Therapeutic Agents: Current Progress and Future Hurdles. *Neuropsychopharmacol.* **2009**, *34* (1), 126-141; (j) Domling, A., Small molecular weight protein-protein interaction antagonists - an insurmountable challenge? *Curr. Opin. Chem. Biol.* **2008**, *12* (3), 281-291; (k) Chene, P., Drugs targeting protein-protein interactions. *Chemmedchem* **2006**, *1* (4), 400-411; (l) Sharma, S. K.; Ramsey, T. M.; Bair, K. W., Protein-protein interactions: lessons learned. *Curr. Med. Chem. Anti-Cancer Agents* **2002**, *2* (2), 311-330; (m) Stites, W. E., Protein-protein interactions: Interface structure, binding thermodynamics, and mutational analysis. *Chem. Rev.* **1997**, *97* (5), 1233-1250.

59. (a) Cochran, A. G., Protein-protein interfaces: mimics and inhibitors. *Curr. Opin. Chem. Biol.* **2001**, *5* (6), 654-659; (b) Gadek, T. R.; Nicholas, J. B., Small molecule antagonists of proteins. *Biochem. Pharmacol.* **2003**, *65* (1), 1-8; (c) Ockey, D. A.; Gadek, T. R., Inhibitors of protein-protein interactions. *Expert Opin. Ther. Pat.* **2002**, *12* (3),

393-400; (d) Toogood, P. L., Inhibition of protein-protein association by small molecules: Approaches and progress. *J. Med. Chem.* **2002**, *45* (8), 1543-1558.

60. (a) Jones, S.; Thornton, J. M., Principles of protein-protein interactions. *Proc. Natl. Acad. Sci. U.S.A.* **1996**, *93* (1), 13-20; (b) Lo Conte, L.; Chothia, C.; Janin, J., The atomic structure of protein-protein recognition sites. *J. Mol. Biol.* **1999**, *285* (5), 2177-2198.

61. (a) Teague, S. J., Implications of protein flexibility for drug discovery. *Nat. Rev. Drug Discov.* **2003**, *2* (7), 527-541; (b) Luque, I.; Freire, E., Structural stability of binding sites: Consequences for binding affinity and allosteric effects. *Proteins-Structure Function and Genetics* **2000**, 63-71; (c) Ma, B. Y.; Shatsky, M.; Wolfson, H. J.; Nussinov, R., Multiple diverse ligands binding at a single protein site: A matter of pre-existing populations. *Protein Sci.* **2002**, *11* (2), 184-197.

62. (a) Clackson, T.; Wells, J. A., A Hot-Spot of Binding-Energy in a Hormone-Receptor Interface. *Science* **1995**, *267* (5196), 383-386; (b) Bogan, A. A.; Thorn, K. S., Anatomy of hot spots in protein interfaces. *J. Mol. Biol.* **1998**, *280* (1), 1-9; (c) Clackson, T.; Ultsch, M. H.; Wells, J. A.; de Vos, A. M., Structural and functional analysis of the 1 : 1 growth hormone : receptor complex reveals the molecular basis for receptor affinity. *J. Mol. Biol.* **1998**, *277* (5), 1111-1128; (d) DeLano, W. L., Unraveling hot spots in binding interfaces: progress and challenges. *Curr. Opin. Struct. Biol.* **2002**, *12* (1), 14-20; (e) Ma, B. Y.; Elkayam, T.; Wolfson, H.; Nussinov, R., Protein-protein interactions: Structurally conserved residues distinguish between binding sites and exposed protein surfaces. *Proc. Natl. Acad. Sci. U.S.A.* **2003**, *100* (10), 5772-5777; (f) Thanos, C. D.; DeLano, W. L.; Wells, J. A., Hot-spot mimicry of a cytokine receptor by a small

- molecule. *Proc. Natl. Acad. Sci. U.S.A.* **2006**, *103* (42), 15422-15427; (g) Moreira, I. S.; Fernandes, P. A.; Ramos, M. J., Hot spots-A review of the protein-protein interface determinant amino-acid residues. *Proteins* **2007**, *68* (4), 803-812.
63. Wells, J. A., Systematic Mutational Analyses of Protein Protein Interfaces. *Methods Enzymol.* **1991**, *202*, 390-411.
64. (a) Bass, S. H.; Mulkerrin, M. G.; Wells, J. A., A Systematic Mutational Analysis of Hormone-Binding Determinants in the Human Growth-Hormone Receptor. *Proc. Natl. Acad. Sci. U.S.A.* **1991**, *88* (10), 4498-4502; (b) Cunningham, B. C.; Wells, J. A., Comparison of a Structural and a Functional Epitope. *J. Mol. Biol.* **1993**, *234* (3), 554-563.
65. Stewart, M. L.; Fire, E.; Keating, A. E.; Walensky, L. D., The MCL-1 BH3 helix is an exclusive MCL-1 inhibitor and apoptosis sensitizer. *Nat. Chem. Biol.* **2010**, *6* (8), 595-601.
66. (a) Reed, J. C., Apoptosis-regulating proteins as targets for drug discovery. *Trends Mol. Med.* **2001**, *7* (7), 314-319; (b) Green, D. R.; Evan, G. I., A matter of life and death. *Cancer Cell* **2002**, *1* (1), 19-30; (c) Walensky, L. D., BCL-2 in the crosshairs: tipping the balance of life and death. *Cell Death Differ.* **2006**, *13* (8), 1339-1350; (d) Youle, R. J.; Strasser, A., The BCL-2 protein family: opposing activities that mediate cell death. *Nat. Rev. Mol. Cell Biol.* **2008**, *9* (1), 47-59.
67. Sattler, M.; Liang, H.; Nettlesheim, D.; Meadows, R. P.; Harlan, J. E.; Eberstadt, M.; Yoon, H. S.; Shuker, S. B.; Chang, B. S.; Minn, A. J.; Thompson, C. B.; Fesik, S. W., Structure of Bcl-x(L)-Bak peptide complex: Recognition between regulators of apoptosis. *Science* **1997**, *275* (5302), 983-986.

68. Wang, S. M.; Yang, D. J.; Lippman, M. E., Targeting Bcl-2 and Bcl-X-L with nonpeptidic small-molecule antagonists. *Semin. Oncol.* **2003**, *30* (5), 133-142.
69. Willis, S. N.; Chen, L.; Dewson, G.; Wei, A.; Naik, E.; Fletcher, J. I.; Adams, J. M.; Huang, D. C. S., Proapoptotic Bak is sequestered by Mcl-1 and Bcl-x(L), but not Bcl-2, until displaced by BH3-only proteins. *Gene Dev* **2005**, *19* (11), 1294-1305.
70. (a) Wang, J. L.; Liu, D. X.; Zhang, Z. J.; Shan, S. M.; Han, X. B.; Srinivasula, S. M.; Croce, C. M.; Alnemri, E. S.; Huang, Z. W., Structure-based discovery of an organic compound that binds Bcl-2 protein and induces apoptosis of tumor cells. *Proc. Natl. Acad. Sci. U.S.A.* **2000**, *97* (13), 7124-7129; (b) Degterev, A.; Lugovskoy, A.; Cardone, M.; Mulley, B.; Wagner, G.; Mitchison, T.; Yuan, J. Y., Identification of small-molecule inhibitors of interaction between the BH3 domain and Bcl-x(L). *Nat. Cell Biol.* **2001**, *3* (2), 173-182; (c) Tzung, S. P.; Kim, K. M.; Basanez, G.; Giedt, C. D.; Simon, J.; Zimmerberg, J.; Zhang, K. Y. J.; Hockenbery, D. M., Antimycin A mimics a cell-death-inducing Bcl-2 homology domain 3. *Nat. Cell Biol.* **2001**, *3* (2), 183-191; (d) Enyedy, I. J.; Ling, Y.; Nacro, K.; Tomita, Y.; Wu, X. H.; Cao, Y. Y.; Guo, R. B.; Li, B. H.; Zhu, X. F.; Huang, Y.; Long, Y. Q.; Roller, P. P.; Yang, D. J.; Wang, S. M., Discovery of small-molecule inhibitors of bcl-2 through structure-based computer screening. *J. Med. Chem.* **2001**, *44* (25), 4313-4324; (e) Kutzki, O.; Park, H. S.; Ernst, J. T.; Orner, B. P.; Yin, H.; Hamilton, A. D., Development of a potent Bcl-x(L) antagonist based on alpha-helix mimicry. *J. Am. Chem. Soc.* **2002**, *124* (40), 11838-11839; (f) Chan, S. L.; Lee, M. C.; Tan, K. O.; Yang, L. K.; Lee, A. S. Y.; Flotow, H.; Fu, N. Y.; Butler, M. S.; Soejarto, D. D.; Buss, A. D.; Yu, V. C., Identification of chelerythrine as an inhibitor of BclXL function. *J. Biol. Chem.* **2003**, *278* (23), 20453-20456; (g) Kitada, S.; Leone, M.; Sareth,

S.; Zhai, D. Y.; Reed, J. C.; Pellecchia, M., Discovery, characterization, and structure - Activity relationships studies of proapoptotic polyphenols targeting B-cell lymphocyte/leukemia-2 proteins. *J. Med. Chem.* **2003**, *46* (20), 4259-4264; (h) Becattini, B.; Kitada, S.; Leone, M.; Monosov, E.; Chandler, S.; Zhai, D. Y.; Kipps, T. J.; Reed, J. C.; Pellecchia, M., Rational design and real time, in-cell detection of the proapoptotic activity of a novel compound targeting Bcl-X-L. *Chem. Biol.* **2004**, *11* (3), 389-395; (i) Leone, M.; Zhai, D. Y.; Sareth, S.; Kitada, S.; Reed, J. C.; Pellecchia, M., Cancer prevention by tea polyphenols is linked to their direct inhibition of antiapoptotic Bcl-2-family proteins. *Cancer Res.* **2003**, *63* (23), 8118-8121.

71. (a) Sadowsky, J. D.; Murray, J. K.; Tomita, Y.; Gellman, S. H., Exploration of backbone space in foldamers containing alpha- and beta-amino acid residues: Developing protease-resistant oligomers that bind tightly to the BH3-recognition cleft of Bcl-x(L). *Chembiochem* **2007**, *8* (8), 903-916; (b) Sadowsky, J. D.; Fairlie, W. D.; Hadley, E. B.; Lee, H. S.; Umezawa, N.; Nikolovska-Coleska, Z.; Wang, S. M.; Huang, D. C. S.; Tomita, Y.; Gellman, S. H., (alpha/beta+alpha)-Peptide antagonists of BH3 Domain/Bcl-x(L) recognition: Toward general strategies for foldamer-based inhibition of protein-protein interactions. *J. Am. Chem. Soc.* **2007**, *129* (1), 139-154; (c) Yin, H.; Lee, G. I.; Sedey, K. A.; Kutzki, O.; Park, H. S.; Orner, B. P.; Ernst, J. T.; Wang, H. G.; Sebt, S. M.; Hamilton, A. D., Terphenyl-based bak BH3 alpha-helical proteomimetics as low-molecular-weight antagonists of Bcl-X-L. *J. Am. Chem. Soc.* **2005**, *127* (29), 10191-10196; (d) Walensky, L. D.; Kung, A. L.; Escher, I.; Malia, T. J.; Barbuto, S.; Wright, R. D.; Wagner, G.; Verdine, G. L.; Korsmeyer, S. J., Activation of apoptosis in vivo by a hydrocarbon-stapled BH3 helix. *Science* **2004**, *305* (5689), 1466-1470.

72. (a) Petros, A. M.; Dinges, J.; Augeri, D. J.; Baumeister, S. A.; Betebenner, D. A.; Bures, M. G.; Elmore, S. W.; Hajduk, P. J.; Joseph, M. K.; Landis, S. K.; Nettlesheim, D. G.; Rosenberg, S. H.; Shen, W.; Thomas, S.; Wang, X. L.; Zanze, I.; Zhang, H. C.; Fesik, S. W., Discovery of a potent inhibitor of the antiapoptotic protein Bcl-x(L) from NMR and parallel synthesis. *J. Med. Chem.* **2006**, *49* (2), 656-663; (b) Hajduk, P. J., SAR by NMR: Putting the pieces together. *Mol. Interv.* **2006**, *6* (5), 266-+.
73. Yip, K. W.; Reed, J. C., Bcl-2 family proteins and cancer. *Oncogene* **2008**, *27* (50), 6398-6406.

## Chapter 2

### Screening of Protein-Protein Interaction Modulators *via* Sulfo-Click Kinetic Target-Guided Synthesis

#### 2.1 Introduction

Protein-protein interactions (PPIs) are central to a large number of vital biological processes and thus represent attractive targets for the development of novel therapies for a variety of diseases.<sup>1</sup> Although scientists recognized the tremendous potential in targeting PPIs over the last two decades, the development of small molecules, which specifically modulate or disrupt a particular PPI, remains a challenging and risky undertaking.<sup>1a</sup> Commonly, protein-protein interfaces are large and flat, and they lack deep cavities that might serve as good binding sites for small molecules.<sup>2</sup> Moreover, amino acids at the interfaces of PPIs are flexible and thus pose challenges at conducting computer-guided compound design.<sup>3</sup>

Although protein-protein interfaces bury 500–3000 Å<sup>2</sup> of total surface area, which exceeds the potential binding area of low-molecular-weight compounds,<sup>4</sup> Wells and co-workers demonstrated that only a fraction of the amino acid residues at the protein-protein interface contributes to the major portion of the binding free energy.<sup>5</sup> These key amino acids, defined as recognition patches or hot spots, therefore provide the theoretical and experimental evidence that PPIs can be disrupted or modulated by

low-molecular-weight compounds. In the last 15 years, numerous approaches have been developed for the discovery of small molecules modulating or disrupting PPIs. Often, small molecule design is aimed at mimicking a peptide or a protein secondary structure in a truncated form.<sup>6</sup> Alternatively, fragment-based drug discovery strategies using biomolecular NMR, X-ray crystallography, or surface plasmon resonance (SPR) lead to the identification of fragments with good ligand efficiencies, which are further developed into potent protein-protein interaction modulators (PPIMs). Herein we report the expansion and utilization of kinetic target-guided synthesis (TGS) as a screening platform for the identification of PPIMs.

In the last two decades, several TGS approaches have been described, in which the target biomolecule assembles its inhibitory ligand from a collection of reactive fragments. Depending on the nature of the assembly step, TGS approaches can be classified into (a) dynamic combinatorial chemistry (DCC), (b) reagent-accelerated TGS, and (c) kinetic TGS.<sup>7</sup> In dynamic combinatorial chemistry, the assembly process is reversible, whereas reagent-accelerated TGS uses building blocks, which combine in an irreversible fashion only in presence of an external reagent or a catalyst upon binding to the biological target. In kinetic TGS, a biological target accelerates the irreversible covalent bond formation only between complementary reacting fragments binding to adjacent binding sites of the target (Figure 2.1A). Kinetic TGS<sup>6b</sup> and *in situ* click chemistry<sup>7a, b</sup> have been exclusively applied for the identification of inhibitors of enzymatic targets with well defined binding pockets. In a recent proof-of-concept study with the anti-apoptotic protein Bcl-X<sub>L</sub> as the biological target, we demonstrated that kinetic TGS can also be used for the “rediscovery” of a PPIM previously reported

by the Abbott Laboratories starting from smaller fragments bearing a thio acid or a sulfonyl azide functional group.<sup>7d</sup> Williams and coworkers described that the amidation reaction between thio acids and sulfonyl azides,<sup>8</sup> which in the meantime has been named as the sulfo-click reaction,<sup>9</sup> proceeds in aqueous media.

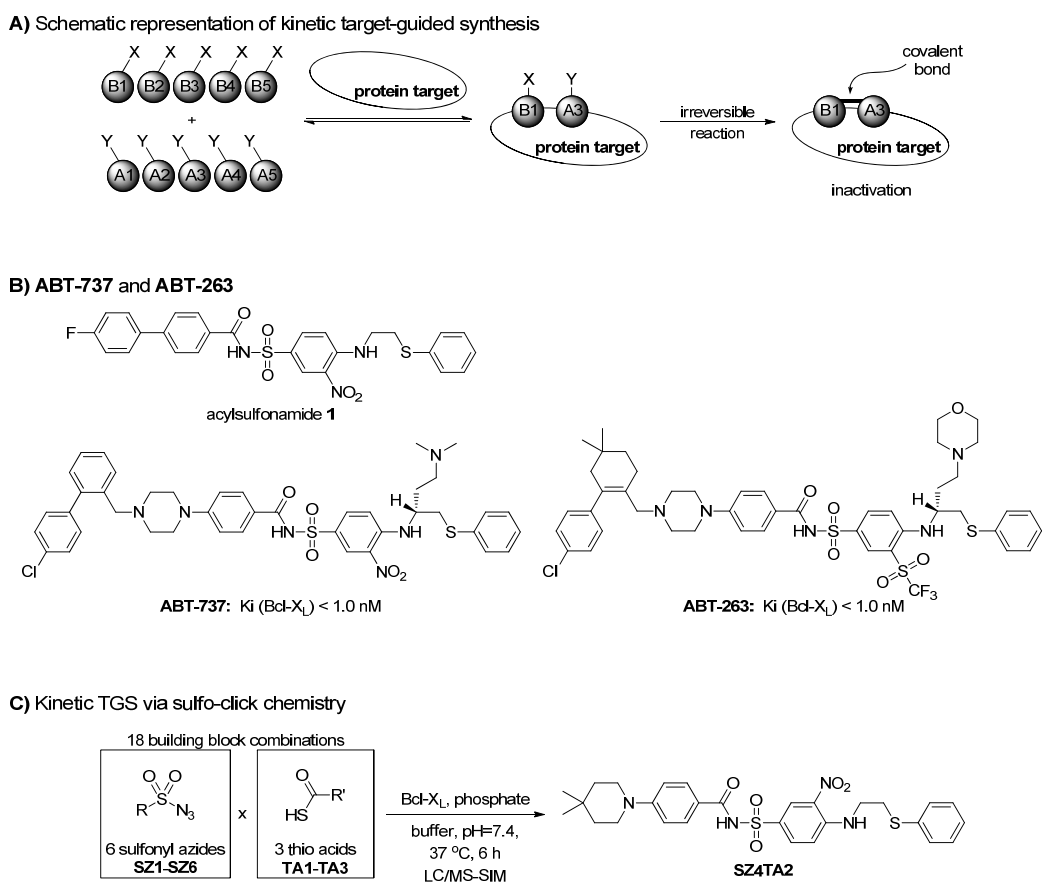


**Figure 2.1.** Kinetic TGS approach targeting PPIs. A) TGS approaches are based on the principle that multidentate interactions between a ligand and a biological target are collectively much stronger than the corresponding monovalent interactions of each of the fragments.<sup>10</sup> Thus, target-assembled compound most likely will have a stronger interaction with the biological target as compared to the individual building blocks.<sup>10</sup> In kinetic TGS, fragments decorated with complementary reactive groups

are incubated with the target biomolecule. If two fragments reside simultaneously in close proximity in binding pockets of the target, the two reactive functionalities react with each other forming a covalent linkage between the two fragments. B) Acylsulfonamide **1**, **ABT-737** and **ABT-263** compounds targeting Bcl-X<sub>L</sub>. C) Proof-of-concept study to demonstrate that the amidation between thio acids and sulfonyl azides is suited for kinetic TGS targeting PPIs.

The proteins of the Bcl-2 family have been validated as attractive PPI targets for cancer therapy.<sup>11</sup> The Bcl-2 family of proteins, which consists of both anti- and pro-apoptotic molecules, plays a pivotal role in the regulation of the intrinsic pathway of apoptosis. The anti-apoptotic Bcl-2 family proteins Bcl-2, Bcl-X<sub>L</sub>, and Mcl-1 inhibit the release of certain pro-apoptotic factors from mitochondria. In contrast, pro-apoptotic Bcl-2 family members, which can be further separated into two subgroups, the multidomain BH1-3 proteins (i.e., Bax and Bak) and the BH3-only proteins (e.g., Bad, Bim, and Noxa), induce the release of mitochondrial apoptogenic molecules into the cytosol.<sup>12</sup> Evidence has been accumulated that the majority of human cancers overexpress the pro-survival Bcl-2 family proteins, which not only contribute to cancer progression by preventing normal cell turnover, but also render cancer cells resistant to current cancer treatments.<sup>13</sup> Although there is a controversy over how anti-apoptotic Bcl-2 family proteins function,<sup>14</sup> it is generally accepted that apoptosis is initiated by the binding of pro-apoptotic BH3-only proteins to anti-apoptotic Bcl-2 family molecules in cancer cells. These interactions are mediated by the insertion of the BH3 domain of pro-death proteins into the hydrophobic groove on the surface of anti-apoptotic proteins Bcl-2, Bcl-X<sub>L</sub>, or Mcl-1.<sup>15</sup> Therefore, small

molecules that mimic the BH3 domains of pro-apoptotic Bcl-2 family proteins have potential as anti-cancer therapeutics.

Previously, Abbott Laboratories developed acylsulfonamide **1**, **ABT-737**, **ABT-263**, and other structurally related acylsulfonamides, which efficiently disrupt Bcl-X<sub>L</sub>-Bad interaction (Figure 2.1B).<sup>16</sup> On the basis of these reports, we designed reactive fragments structurally related to **ABT-737** and **ABT-263** (**SZ1-SZ6** and **TA1-TA3**), and incubated these as binary fragment mixtures in presence of Bcl-X<sub>L</sub> (Figure 2.1C). Analysis of each incubation sample by liquid chromatography combined with mass spectrometry detection in the Selected Ion Mode (LC/MS-SIM) showed that of all 18 possible products only compound **SZ4TA2**, which was developed by Abbott Laboratories, has been detected. In comparison, incubations of fragments in the absence of Bcl-X<sub>L</sub> or in presence of Bcl-X<sub>L</sub> and various BH3-containing peptides failed to yield detectable amounts of acylsulfonamide products. In addition, IC<sub>50</sub> inhibitory constants in the nM range have been determined for **SZ4TA2**, while their corresponding thio acid or sulfonyl azide fragments did not show any inhibition up to 100 μM concentrations.

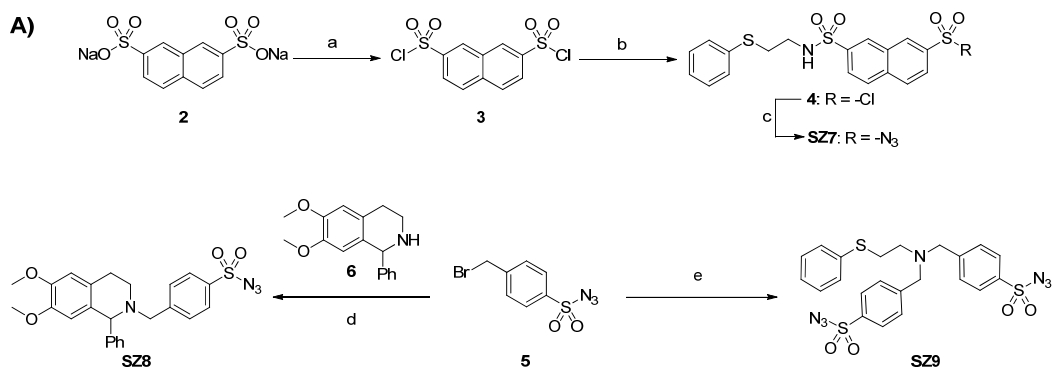
Herein, we successfully employed and validated the sulfo-click kinetic TGS approach as a straightforward yet reliable PPIM screening platform for the identification of Bcl-X<sub>L</sub>-protein modulators. The design of kinetic TGS incubations with wildtype and mutant Bcl-X<sub>L</sub> proteins provided an additional layer of confirmatory experiments for the delivery of high-quality PPIMs. Furthermore, experimental evidence has been accumulated indicating that kinetic TGS is a PPIM

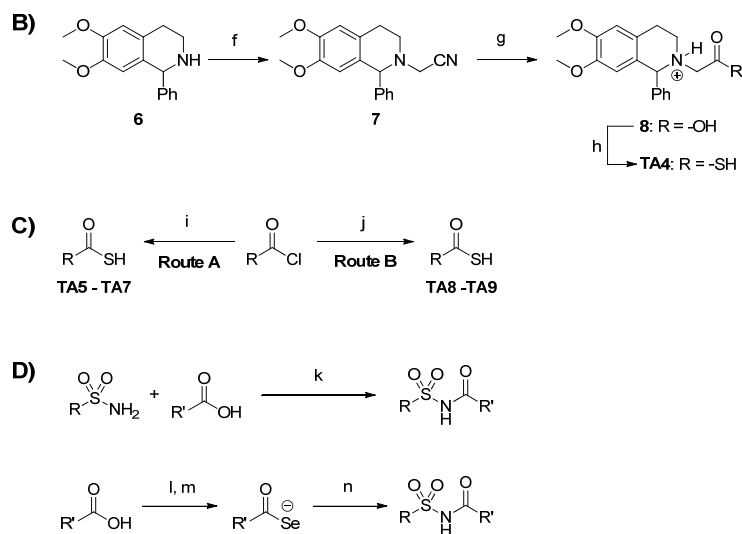
screening and synthesis method generating only active compounds.

## 2.2 Results and discussion

### 2.2.1 Screening of an extended reactive fragment library

The proof-of-concept study motivated us to investigate whether kinetic TGS is also successful at generating hit compounds which have not been previously reported. Two sublibraries of reactive fragments, one consisting of thio acids and the other of sulfonyl azides, have been synthesized. The thio acids were generated from the corresponding acid chlorides and sodium hydrosulfide, while the sulfonyl azides were prepared by alkylation of amines with 4-(bromomethyl)benzenesulfonyl azide (Scheme 2.1A-C). A selection of acylsulfonamides has been synthesized mainly by: a) EDCI coupling of corresponding carboxylic acids and sulfonamides, or b) the previously reported reaction between sulfonyl azides and selenocarboxylates which were generated from corresponding carboxylic acids and the selenating reagent,  $\text{LiAlHSeH}$  (Scheme 2.1D).<sup>17</sup>





**Scheme 2.1.** Synthesis of sulfonyl azides, thio acids and acylsulfonamides. Reaction conditions: (a)  $\text{SOCl}_2$ , DMF, reflux, 2 h (b) 2-(phenylthio)ethanamine (0.5 eq),  $\text{K}_2\text{CO}_3$ ,  $\text{CHCl}_3$ , 12 h, RT (c)  $\text{NaN}_3$ , acetone,  $\text{H}_2\text{O}$ , 0 °C, 3 h, 70% (over 3 steps) (d)  $\text{K}_2\text{CO}_3$ ,  $\text{CH}_3\text{CN}:\text{H}_2\text{O}$  (9:1), 12 h, RT, 87% (e) 2-(phenylthio)ethanamine (0.5 eq),  $\text{K}_2\text{CO}_3$ ,  $\text{CH}_3\text{CN}:\text{H}_2\text{O}$  (9:1), 12 h, RT, 60% (f)  $\text{ICH}_2\text{CN}$ ,  $\text{K}_2\text{CO}_3$ ,  $\text{CH}_3\text{CN}:\text{H}_2\text{O}$  (10:1), 2 d, 60 °C, 79% (g) 12 N HCl, 90 °C, 3 h, 66% (h) i)  $(\text{COCl})_2$ ,  $\text{CH}_2\text{Cl}_2$ , 0 °C to RT, 8 h; ii) dimethylthioformamide,  $\text{H}_2\text{S}$ , 15 min, 25% (i) NaSH, acetone,  $\text{H}_2\text{O}$ , 2 h, RT (j) NaSH, neat, 0 °C to RT, 1 h (k) EDCI, DMAP,  $\text{CH}_2\text{Cl}_2$ , RT, 24-48 h (l)  $(\text{CH}_3)_2\text{CHOCOC}$ l, *N*-methyl piperidine, THF, 0 °C, 30 min (m)  $\text{LiAlHSeH}$ , THF, 0 °C, 30 min (n)  $\text{RSO}_2\text{N}_3$ , THF, 0 °C to RT, 3 h.

The majority of the reactive fragments have been randomly selected, while a small fraction of the reactive fragments has been designed to be structurally related to **ABT-737** or **ABT-263**. Eighty one binary mixtures containing one thio acid (**TA1-TA9**) and one sulfonyl azide (**SZ1-SZ9**) were incubated with the target protein Bcl- $X_L$  for 6 hours at 37 °C (Figure 2.2).

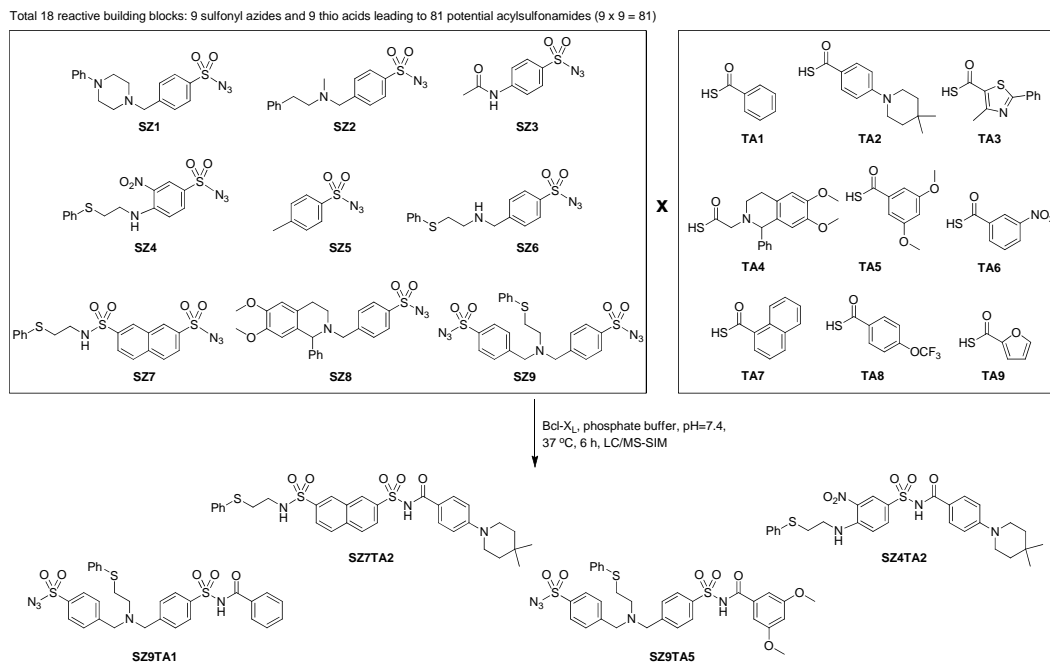


**Figure 2.2.** Kinetic TGS screening of Bcl-X<sub>L</sub> via sulfo-click chemistry

In parallel, identical binary fragment mixtures were incubated in buffer without Bcl-X<sub>L</sub>. Similar to *in situ* click chemistry,<sup>7a, b</sup> all incubations were directly subjected to HPLC analysis with acylsulfonamide product detection by electrospray ionization in the positive Selected Ion Mode (LC/MS-SIM).<sup>18</sup> Comparison of the LC/MS-SIM traces of identical fragment combinations with or without protein Bcl-X<sub>L</sub>, led to the identification of the previously reported fragment combination **SZ4TA2**<sup>7d</sup> and three new combinations **SZ7TA2**, **SZ9TA1**, and **SZ9TA5** with increased amounts of acylsulfonamide products in the incubations containing Bcl-X<sub>L</sub> (Figure 2.3A-B and experimental section).

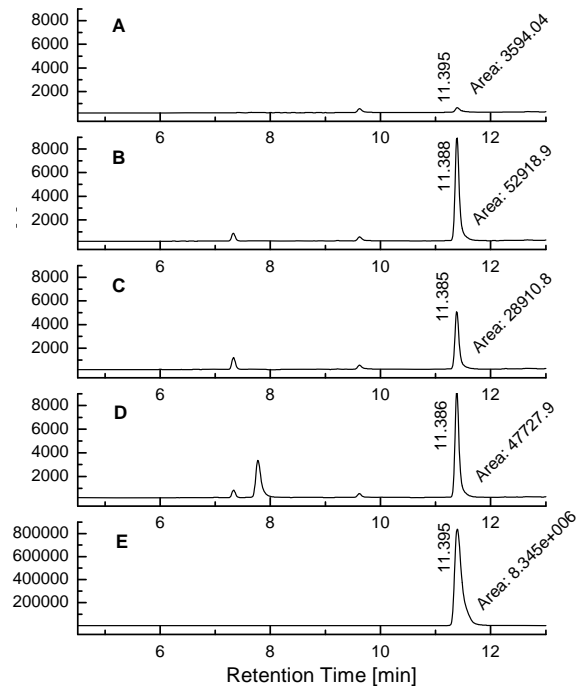


**Figure 2.3.** LC/MS-SIM analysis of kinetic TGS incubations with fragments **SZ7** and **TA2** targeting Bcl-X<sub>L</sub>. The samples were incubated at 37 °C for 6 hours and subjected to LC/MS-SIM analysis with gradient system 1 (see experimental section). A) Incubation sample containing fragments **SZ7** and **TA2** in absence of Bcl-X<sub>L</sub>; B) Incubation sample containing fragments **SZ7** and **TA2** in presence of 2 μM Bcl-X<sub>L</sub>; C) Incubation sample containing fragments **SZ7** and **TA2** in presence of 2 μM Bcl-X<sub>L</sub> and 20 μM Bim BH3 peptide; D) Incubation sample containing fragments **SZ7** and **TA2** in presence of 2 μM Bcl-X<sub>L</sub> and 20 μM mutant Bim BH3 peptide; E) Synthetic **SZ7TA2** as the reference compound.

Prior to synthesizing the new TGS hit compounds **SZ7TA2**, **SZ9TA1**, and **SZ9TA5**, control incubations with wildtype and mutant pro-apoptotic Bim BH3

peptides were conducted to assess whether the hit combinations assemble at the targeted binding sites of Bcl-X<sub>L</sub> or randomly elsewhere on the protein surface (Figure 2.3C-D and experimental section). These control experiments with Bak BH3 peptide have been previously introduced to confirm the kinetic TGS assembly of compound **SZ4TA2**.<sup>7d</sup> Wildtype Bim BH3 peptide (Bim sequence CEIWIAQELRRIGDEFNAYYAR), the natural Bcl-X<sub>L</sub> ligand, outcompetes the reactive fragments for binding at the BH3 binding site of Bcl-X<sub>L</sub> and thus suppresses the Bcl-X<sub>L</sub>-templated assembly of acylsulfonamides **SZ7TA2**, **SZ9TA1**, and **SZ9TA5**. Contrarily, mutant of the Bim BH3 peptide (mutant Bim sequence CEIWIAQEARRIGAEFNAYYAR) exhibits low affinity towards Bcl-X<sub>L</sub> and therefore does not significantly affect the Bcl-X<sub>L</sub>-templated assembly of **SZ7TA2**, **SZ9TA1**, and **SZ9TA5**. Since these co-incubations with wildtype and mutant BH3 peptides strongly suggest that the formation of acylsulfonamides **SZ7TA2**, **SZ9TA1**, and **SZ9TA5** takes place at the BH3 binding site of Bcl-X<sub>L</sub>, compounds **SZ7TA2**, **SZ9TA1**, and **SZ9TA5** have been synthesized and subjected to LC/MS-SIM analysis. Comparison of the LC/MS-SIM traces of the Bcl-X<sub>L</sub>-templated reactions with the ones of the synthetic compounds clearly confirmed that Bcl-X<sub>L</sub> templates the formation of hit compounds **SZ7TA2**, **SZ9TA1**, and **SZ9TA5** (Figure 2.3E and experimental section).

### 2.2.2 Kinetic TGS with mutant Bcl-X<sub>L</sub>

Experiments were designed, in which mutated Bcl-X<sub>L</sub> proteins are incubated with reactive fragments. Alterations of the BH3 binding site directly affect the

binding of reactive fragments **SZ4**, **SZ7**, **SZ9**, **TA1**, **TA2**, and **TA5** to the protein, which in turn will influence the rate of the protein-templated acylsulfonamide formation. The purpose of these mutant Bcl-X<sub>L</sub> proteins is to expand the repertoire of controls with Bim BH3 peptides with complementary experiments indicating whether the TGS reaction occurs with the help of the target protein Bcl-X<sub>L</sub> and specifically at the binding site of interest. The known mutant of Bcl-X<sub>L</sub>, in which phenylalanine Phe131 and aspartic acid Asp133 have been substituted by alanines, has been prepared since it fails at interacting with Bak or Bim BH3 peptides.<sup>19</sup> In addition, a second mutant Bcl-X<sub>L</sub> has been prepared, in which arginine Arg139 has been replaced by alanine. Arginine Arg139 has been identified to be a key residue interacting with **ABT-737** and analogues thereof.<sup>16a</sup> As a proof-of-concept, incubations of the mutant Bcl-X<sub>L</sub> with building blocks **SZ4** and **TA2** were first undertaken at various reactive fragment concentrations (Figures 2.4, 2.5 and experimental section). In comparison to the incubation with wildtype Bcl-X<sub>L</sub>, a reduction in the templation activity by approximately 40% or more has been observed in both mutant Bcl-X<sub>L</sub>-templated reactions (Table 2.1). This observation can be explained by closer examination of a reported NMR-structure of Bcl-X<sub>L</sub> complexed with acylsulfonamide **1**, whose structure is closely related to the kinetic TGS product **SZ4TA2**.<sup>16a</sup> Comparison of the location of Phe131 and Asp133 with the position of compound **1** in the wildtype Bcl-X<sub>L</sub> binding site reveals that the residues Phe131 and Asp133, although important for the binding to Bak or Bim BH3 peptides, are relatively distant from the acylsulfonamide **1**, while Arg139 appears to be closer to compound **1**. Surprisingly, mutant <sup>R139A</sup>Bcl-X<sub>L</sub> displays a slightly increased templation reaction in comparison to

<sup>F131A,D133A</sup>Bcl-X<sub>L</sub>. Conformational changes induced by seemingly distant amino acid residues are difficult to trace and may probably influence the templation effect observed during the incubations with wildtype and mutant Bcl-X<sub>L</sub> proteins.

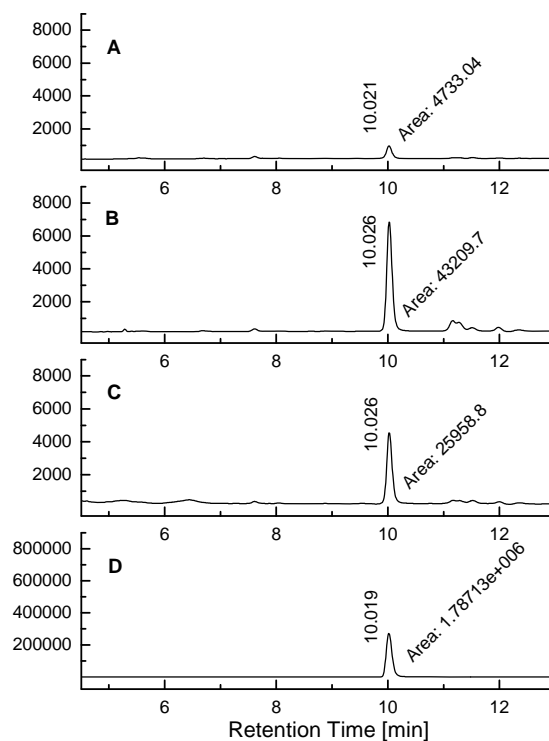


**Figure 2.4.** LC/MS-SIM analysis of kinetic TGS incubations with fragments **SZ4** and **TA2** targeting the wildtype and mutant of Bcl-X<sub>L</sub>. The samples were incubated at 37 °C for 6 hours and subjected to LC/MS-SIM analysis with gradient system 1 (see experimental section). A) Incubation sample containing fragments **SZ4** and **TA2** in absence of wildtype Bcl-X<sub>L</sub>; B) Incubation sample containing fragments **SZ4** and **TA2** in presence of 2 μM wildtype Bcl-X<sub>L</sub>; C) Incubation sample containing fragments **SZ4** and **TA2** in presence of 2 μM single mutant <sup>R139A</sup>Bcl-X<sub>L</sub>; D) Synthetic **SZ4TA2** as the reference compound.

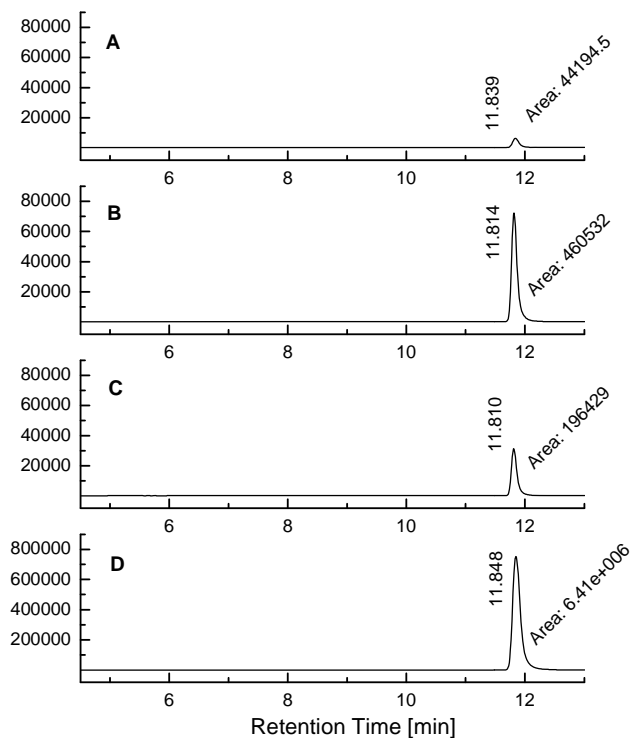


**Figure 2.5.** LC/MS-SIM analysis of kinetic TGS incubations with fragments **SZ4** and **TA2** targeting the wildtype and double mutant of Bcl-X<sub>L</sub>. The samples were incubated at 37 °C for 6 hours and subjected to LC/MS-SIM analysis with gradient system 2 (see experimental section). A) Incubation sample containing fragments **SZ4** and **TA2** in absence of wildtype Bcl-X<sub>L</sub>; B) Incubation sample containing fragments **SZ4** and **TA2** in presence of 2 μM wildtype Bcl-X<sub>L</sub>; C) Incubation sample containing fragments **SZ4** and **TA2** in presence of 2 μM double mutant <sup>F131A,D133A</sup>Bcl-X<sub>L</sub>; D) Synthetic **SZ4TA2** as the reference compound.

For TGS hit combinations **SZ7TA2**, **SZ9TA1**, and **SZ9TA5**, confirmatory

experiments have been conducted with single mutant <sup>R139A</sup>Bcl-X<sub>L</sub> only, since the preparation of double mutant <sup>F131A,D133A</sup>Bcl-X<sub>L</sub> has been cumbersome. Similar to the incubations of fragments **SZ4** and **TA2**, experiments with the mutant protein leading to acylsulfonamides **SZ7TA2**, **SZ9TA1**, and **SZ9TA5** displayed a reduction in acylsulfonamide formation compared to the incubations with wildtype Bcl-X<sub>L</sub>. These experiments suggest that the acylsulfonamide genesis occurs in proximity to key amino acid residue Arg139.

**Table 2.1.** Kinetic TGS incubations

Incubation	Fragment Combinations							
	SZ4TA2		SZ7TA2		SZ9TA1		SZ9TA5	
	Peak Area	% Signal	Peak Area	% Signal	Peak Area	% Signal	Peak Area	% Signal
Buffer alone	26,794	7.4	3,594	6.8	313	35.3	466	10.9
WT Bcl-X <sub>L</sub>	363,187	100.0	52,920	100.0	887	100.0	4,275	100.0
WT Bcl-X <sub>L</sub> and WT Bak BH3	59,437	16.3	n.d.	n.d.	n.d.	n.d.	n.d.	n.d.
WT Bcl-X <sub>L</sub> and mutant Bak BH3	181,156	49.8	n.d.	n.d.	n.d.	n.d.	n.d.	n.d.
WT Bcl-X <sub>L</sub> and WT Bim BH3	51,773	14.3	28,911	54.6	552	62.2	944	22.1
WT Bcl-X <sub>L</sub> and mutant Bim BH3	217,813	59.9	47,728	90.2	761	85.8	2,557	59.8
Buffer alone	44195	9.6	n.d.	n.d.	n.d.	n.d.	n.d.	n.d.
WT Bcl-X <sub>L</sub>	460532	100.0	n.d.	n.d.	n.d.	n.d.	n.d.	n.d.
<sup>F131A,D133A</sup> Bcl-X <sub>L</sub>	196429	42.7	n.d.	n.d.	n.d.	n.d.	n.d.	n.d.
Buffer alone	4,733	11.0	2,046	7.2	939	25.0	726	11.4
WT Bcl-X <sub>L</sub>	43,210	100.0	28,600	100.0	3,750	100.0	6,370	100.0
<sup>R139A</sup> Bcl-X <sub>L</sub>	25,959	60.1	16,965	59.3	2,637	70.3	4,406	69.2

n.d. = not determined; WT = wildtype

### 2.2.3 PPIM activity of kinetic TGS hits and additional acylsulfonamides

The kinetic TGS hits were subjected to dose–response studies to obtain IC<sub>50</sub>s and to investigate if the hit compounds are also modulating or disrupting the interaction between Bcl-X<sub>L</sub> and a native BH3 peptide ligand. Previously, Abbott Laboratories determined by their assay, that **SZ4TA2** is a good PPIM with a K<sub>i</sub> constant of 19 nM.<sup>16b, c</sup>

Abbott determined the dissociation constants by a competitive fluorescence polarization assay using a fluorescein-labeled Bad-BH3 peptide. In order to precisely compare the inhibitory properties of our kinetic TGS hits with the compounds reported by Abbott, we decided to perform binding studies by a fluorescence polarization assay implemented in our laboratories, which uses GST-Bcl-X<sub>L</sub> and fluorescein-labeled Bak-BH3 peptide. Consistently, compound **SZ4TA2** has been validated by our assay as a Bcl-X<sub>L</sub> inhibitor against Bak-BH3 with an IC<sub>50</sub> constant of 106 nM (Table 2.2). Kinetic TGS hit compounds **SZ7TA2**, **SZ9TA1**, and **SZ9TA5** showed IC<sub>50</sub>s in the low μM range (Figure 2.3 and experimental section). Taken together, these results indicate that the hit compounds **SZ4TA2**, **SZ7TA2**, **SZ9TA1**, and **SZ9TA5** identified through the kinetic TGS screening are indeed respectable ligands of the biological target, which underscores the utility of kinetic TGS as a valuable approach to PPIM discovery.

**Table 2.2.** PPIM activity of kinetic TGS hit compounds

Compound	IC <sub>50</sub>	K <sub>i</sub>
<b>SZ4TA2</b>	106 ± 12 nM	37.5 ± 5.0 nM
<b>SZ7TA2</b>	28.4 ± 3.5 μM	11.5 ± 1.4 μM
<b>SZ9TA1</b>	28.7 ± 4.1 μM	11.6 ± 1.6 μM
<b>SZ9TA5</b>	36.0 ± 2.5 μM	14.6 ± 1.0 μM

To assess whether the kinetic TGS hits are more potent than acylsulfonamides, which were not identified in the kinetic TGS screening, 33 randomly selected acylsulfonamides were synthesized. All compounds, as well as TGS hit compounds **SZ4TA2**, **SZ7TA2**, **SZ9TA1**, and **SZ9TA5** were tested at a 50 μM concentration for PPI disruption in the Bcl-X<sub>L</sub>/Bak-BH3 fluorescence polarization assay. The 37

acylsulfonamides tested corresponds to 45.7% of the 81 member library. Strikingly, the four kinetic TGS hits were the most potent compounds tested, disrupting the Bcl-X<sub>L</sub>/BH3 interaction with 60% inhibition or more, while the randomly selected acylsulfonamides demonstrated an average of 15% inhibition (Table 2.3). Only four of the 33 randomly selected acylsulfonamides demonstrated moderate inhibition (35–45%). In contrast, all reactive fragments **SZ1-SZ9** and **TA1-TA9** have been tested in the fluorescence polarization assay at 100  $\mu$ M concentration and less than 5% inhibition was detected. These measurements indicate that the dissociation constants for the corresponding reactive building blocks **SZ1-SZ9** and **TA1-TA9** have to be higher than 100  $\mu$ M. These important results suggest that the amidation reaction between thio acids and sulfonyl azides is suitable for kinetic TGS using building blocks displaying weak binding affinities. In addition, this study strongly suggests that the kinetic TGS screening identified the more active members of the library of potential acylsulfonamides arising from reactive fragments **SZ1-SZ9** and **TA1-TA9**.

**Table 2.3.** Percentage inhibition displayed by an acylsulfonamide at 50  $\mu$ M concentration. Of the 37 compounds tested, the four most potent compounds were identified by kinetic TGS

Fragments	SZ1	SZ2	SZ3	SZ4	SZ5	SZ6	SZ7	SZ8	SZ9
TA1	n.d.	2	0	14	29	n.d.	n.d.	19	80
TA2	n.d.	8	n.d.	100	28	26	76	n.d.	38
TA3	6	7	n.d.	n.d.	n.d.	n.d.	n.d.	30	22
TA4	n.d.	25	n.d.	n.d.	n.d.	n.d.	n.d.	8	n.d.
TA5	5	n.d.	n.d.	n.d.	0	n.d.	15	11	60
TA6	4	n.d.	0	n.d.	0	n.d.	20	n.d.	n.d.
TA7	n.d.	n.d.	0	n.d.	n.d.	n.d.	47	30	45
TA8	n.d.	n.d.	0	n.d.	n.d.	n.d.	n.d.	38	n.d.
TA9	3	n.d.	0	n.d.	1	n.d.	n.d.	24	n.d.

n.d. = not determined

## 2.2.4 Discussion

Generally, cell-permeable small modulators of PPIs have been considered to be desirable tools with great implications for drug discovery and development.<sup>1c, d</sup> Nevertheless, reliable yet straightforward techniques or approaches for the development of potent and effective PPIMs are currently unavailable. Over the past 15 years, a variety of fragment-based lead discovery approaches have been developed and successfully applied for the development of potent PPIMs.<sup>20</sup> These approaches are commonly based on the detection of fragments binding to the target protein followed by the study of their binding to the protein target at atomic level resolution using X-ray crystallography or NMR spectroscopy. The initial hits are further optimized via fragment growing, in which fragments are extended into identified binding sites step-by-step, or via fragment linking, in which fragments identified to bind to adjacent binding sites are covalently linked together.<sup>20c, 21</sup> Even though fragment-based lead discovery strategies have been very successful for the development of PPIMs, they are mainly limited by two constraints. Detection and quantification of fragment binding requires specially designed methodology due to the weak binding typically observed for fragments. Furthermore, the optimization of fragments into potent and selective compounds is not straightforward and not rapidly achievable, even though structural information is available.<sup>21b, 22</sup> For example, though high quality NMR structures were available, the development of Bcl-X<sub>L</sub> PPIMs by Abbott<sup>16a, b</sup> required several design iterations, and the preparation and testing of more than 1000 compounds in order to yield **ABT-737** and **ABT-263**.<sup>23</sup> Furthermore, of the very first design consisting of 21 different structures containing the structural motifs of the initial fragments identified by NMR, most compounds bound to Bcl-X<sub>L</sub> with a

dissociation constant greater than 10  $\mu\text{M}$ .<sup>16a</sup> Thus, though the hit compounds **SZ7TA2**, **SZ9TA1**, and **SZ9TA5** display  $\text{IC}_{50}$  constants of 28–37  $\mu\text{M}$  in the Bak-BH3 fluorescence polarization assay, the herein reported kinetic TGS approach suggests that the high-quality PPIMs will be identified early on in the screening process. This outcome is consistent with previously reported kinetic TGS studies, in which the enzyme carbonic anhydrase II preferably accelerates the formation of the better inhibitory compounds from a pool of reactive fragments.<sup>24</sup> Other kinetic TGS examples using exclusively *in situ* click chemistry also suggest that the triazoles generated in the protein-templated reactions are the more potent inhibitors.<sup>18, 24b, 25</sup>

Recently, fragment-based discovery strategies have been reported which involve the protein target directly to select and assemble its own inhibitory compounds from a pool of reactive fragments. These approaches, also termed as *in situ* click chemistry or kinetic TGS approaches,<sup>6b, 7b</sup> were conceptually described in the 1980s<sup>26</sup> and are still relatively unexplored compared to dynamic combinatorial chemistry. Thus far, kinetic TGS has mainly been applied to the identification of potent enzyme inhibitors. Nevertheless, the herein reported kinetic TGS offers an attractive approach to PPIM lead discovery because it allows the protein to select and combine building blocks that fit best into its binding sites, thus assembling larger compounds.<sup>6b, 7b</sup> The screening method can be as simple as determining whether or not the PPIM product has been formed in a given test mixture. This is especially advantageous over a conventional high-throughput screening of difficult targets such as protein interfaces requiring cumbersome and time-consuming experiments to confirm whether screening hits are true or false positives.

Finally, considering that the flexible nature of protein interfaces complicates the development of PPIMs by conventional means, kinetic TGS has the potential to target the protein in a conformation, which is short-lived, undetectable or easily missed with present techniques. A small number of *in situ* click chemistry approaches targeting enzymatic systems lead to the identification of triazole inhibitors stabilizing the protein in an unprecedented and less abundant conformation.<sup>27</sup> Thus, we speculate that the herein reported sulfo-click chemistry kinetic TGS approach provides medicinal chemists a straightforward search strategy to stabilize conformations of dynamic protein targets such as PPIs.

### 2.3 Conclusions

Herein, we demonstrate that the sulfo-click kinetic TGS approach exhibits great promise in fragment-based PPIM discovery since it combines synthesis and screening of libraries of low-molecular-weight PPIMs into a single step. Samples containing the protein target Bcl-X<sub>L</sub> and reacting fragments leading to 81 structurally different acylsulfonamides have been incubated and analyzed by LC/MS-SIM for acylsulfonamide formation. Of the 81 possible fragment combinations, only combinations **SZ4TA2**, **SZ7TA2**, **SZ9TA1**, and **SZ9TA5** yielded acylsulfonamides in the Bcl-X<sub>L</sub>-templated reactions. Control incubations with the four hit fragment combinations, in which the BH3 binding site of the wildtype Bcl-X<sub>L</sub> has been competitively occupied by a Bim BH3 peptide, generated decreased amounts of acylsulfonamides. Furthermore, control incubations with mutants <sup>R139A</sup>Bcl-X<sub>L</sub> or <sup>F131A,D133A</sup>Bcl-X<sub>L</sub>, in which amino acid residues at the BH3 binding site have been replaced by alanines, also failed at generating the hit

acylsulfonamides suggesting that the protein-templated assembly of **SZ4TA2**, **SZ7TA2**, **SZ9TA1**, and **SZ9TA5** occurs at the desired BH3 binding site of Bcl-X<sub>L</sub>. Subsequent testing of synthesized kinetic TGS hit acylsulfonamides in a fluorescence-based competitive binding assay demonstrated that the kinetic TGS hit compounds indeed display PPIM activity. These findings have been supported by a set of 33 additional acylsulfonamides randomly selected from the 81-member library, which have been shown to fail at demonstrating potent PPIM activity in the fluorescence-based competitive binding assay. These results provide a general test case for the sulfo-click kinetic TGS approach to generate hits targeting the proteins of the Bcl-2 family and further validate the kinetic TGS approach to be suitable for PPIM discovery. In contrast to conventional screening approaches, experimental data suggests that PPIM screening via kinetic TGS reduces the number of false positives, cutting down the number of screening hits to be validated in confirmatory assays. We speculate that the herein reported PPIM discovery strategy for the family of the Bcl-2 proteins is general and can easily be implemented to lead development targeting other PPIs such as MDM2/p53, IAP/caspase, and others.<sup>1a, 1d, 28</sup>

## 2.4 Experimental section

### 2.4.1 General information

All reagents and solvents were purchased from commercial sources and used without further purification. All reactions were run under an Argon atmosphere unless otherwise indicated. Prior to use of solvents in reactions, they were purified by passing the degassed solvents through a column of activated alumina and transferred by an oven-

dried syringe or cannula. Thin layer chromatography was performed on Merck TLC plates (silica gel 60 F<sub>254</sub>). <sup>1</sup>H NMR and <sup>13</sup>C NMR were recorded on a Varian Inova 400 (400 MHz) or a Bruker Avance DPX-250 (250 MHz) instrument. The purification of designated compounds was carried out using reverse phase HPLC system (Waters Prep LC 4000 system with Waters 996 photo-diode array detector, Agilent column Eclipse XDB-C18, 5 μm, 9.4 mm × 250 mm). Compounds were eluted using a gradient elution of A:B (80:20 to 0:100) over 40 min at a flow rate of 5.0 mL/min, where solvent A was H<sub>2</sub>O (0.05% TFA) and solvent B was CH<sub>3</sub>CN (0.05% TFA). The HRMS data were measured on an Agilent 1100 Series MSD/TOF with electrospray ionization. The LC/MS data were measured on an Agilent 1100 LC/MSD-VL with electrospray ionization.

The gradient used for LC/MS-SIM analysis is shown below:

**Table 2.4.** Elution gradient system 1 employed for the LC/MS-SIM analysis

Time	% B*	Flow rate	Time	% B*	Flow rate
0.00	10%	0.7 mL min <sup>-1</sup>	11.50	100%	1.0 mL min <sup>-1</sup>
2.00	10%	0.7 mL min <sup>-1</sup>	11.51	10%	0.7 mL min <sup>-1</sup>
10.00	100%	1.0 mL min <sup>-1</sup>	13.50	10%	0.7 mL min <sup>-1</sup>

\* eluent A: H<sub>2</sub>O (0.05% TFA); eluent B: CH<sub>3</sub>CN (0.05% TFA)

**Table 2.5.** Elution gradient system 2 employed for the LC/MS-SIM analysis

Time	% B*	Flow rate	Time	% B*	Flow rate
0.00	10%	0.7 mL min <sup>-1</sup>	13.01	100%	1.5 mL min <sup>-1</sup>
4.00	20%	0.7 mL min <sup>-1</sup>	15.00	100%	1.5 mL min <sup>-1</sup>
12.00	100%	0.7 mL min <sup>-1</sup>	15.50	20%	0.7 mL min <sup>-1</sup>
13.00	100%	0.7 mL min <sup>-1</sup>	16.50	20%	0.7 mL min <sup>-1</sup>

\* eluent A: H<sub>2</sub>O (0.05% TFA); eluent B: CH<sub>3</sub>CN (0.05% TFA)

The sulfonyl azides, **SZ1-SZ6**, thio acids, **TA1-TA3** and the acylsulfonamides **SZ2TA1**, **SZ2TA2**, **SZ2TA3**, **SZ4TA1**, **SZ4TA2**, **SZ5TA1** and **SZ5TA2** have been previously reported.<sup>7d</sup>

#### 2.4.2 Expression and purification of wildtype and mutant Bcl-X<sub>L</sub> fusion proteins

The protocols for the expression and purification of GST-tagged and His-tagged Bcl-X<sub>L</sub> ΔTM fusion proteins have been previously reported.<sup>7d</sup> The <sup>F131A,D133A</sup>Bcl-X<sub>L</sub> ΔTM and <sup>R139A</sup>Bcl-X<sub>L</sub> ΔTM mutants were generated by PCR mutagenesis using Bcl-X<sub>L</sub> ΔTM cDNA as a template as described previously.<sup>19</sup>

#### 2.4.3 General protocol for incubations of Bcl-X<sub>L</sub> with reactive fragments

In a 96-well plate, one thio acid building block (1 μL of a 2 mM solution in methanol) and one sulfonyl azide building block (1 μL of a 2 mM solution in methanol) were added to a solution of Bcl-X<sub>L</sub> (98 μL of a 2 μM Bcl-X<sub>L</sub> solution in buffer (58 mM Na<sub>2</sub>HPO<sub>4</sub>, 17 mM NaH<sub>2</sub>PO<sub>4</sub>, 68 mM NaCl, 1 mM NaN<sub>3</sub>, pH = 7.40)). The 96-well plate was sealed and incubated at 37 °C for six hours. The incubation samples were then subjected to Liquid Chromatography combined with mass spectrometry analysis in the Selected Ion Mode (LC/MS-SIM, Zorbax SB-C18 preceded by a Phenomenex C18 guard column, electrospray ionization and mass spectrometric detection in the positive SIM, tuned to the expected molecular mass of the product). The TGS hit compound was identified by the mass and the retention time. As a control, identical building block combinations were incubated in buffer without Bcl-X<sub>L</sub> and subjected to LC/MS-SIM analysis. Comparison of the LC/MS-SIM chromatograms of these control incubations

with the chromatograms of the Bcl-X<sub>L</sub> containing incubations allows us to determine whether the protein is templating the corresponding amidation reaction. Furthermore, synthetically prepared acylsulfonamide was subjected to LC/MS-SIM analysis and the retention time was compared with the one identified in the Bcl-X<sub>L</sub> containing incubation.

#### 2.4.4 General protocol for the control incubations of Bcl-X<sub>L</sub> with reactive fragments and Bim BH3 peptides

For the Bcl-X<sub>L</sub> containing incubation sample showing acylsulfonamide formation, control incubations with Bim peptides have been undertaken to demonstrate that the templation reaction occurs at the desired binding site. Thus, in a 96-well plate, one thio acid (1 μL of a 2 mM solution in methanol) and one sulfonyl azide (1 μL of a 2 mM solution in methanol) were added to a solution of Bcl-X<sub>L</sub> (97 μL of a 2 μM Bcl-X<sub>L</sub> solution in buffer). Finally, Bim BH3 peptide (1 μL of a 2 mM solution in DMSO) was added and the incubation sample in a sealed 96-well plate was incubated at 37 °C for six hours. Similar procedure was followed for the mutant Bim BH3 peptide incubation. These two incubation samples were then subjected to LC/MS-SIM analysis along with the wildtype Bcl-X<sub>L</sub> containing sample without any of the Bim BH3 peptides.

#### 2.4.5 General protocol for the control incubations of mutants of Bcl-X<sub>L</sub> with reactive fragments

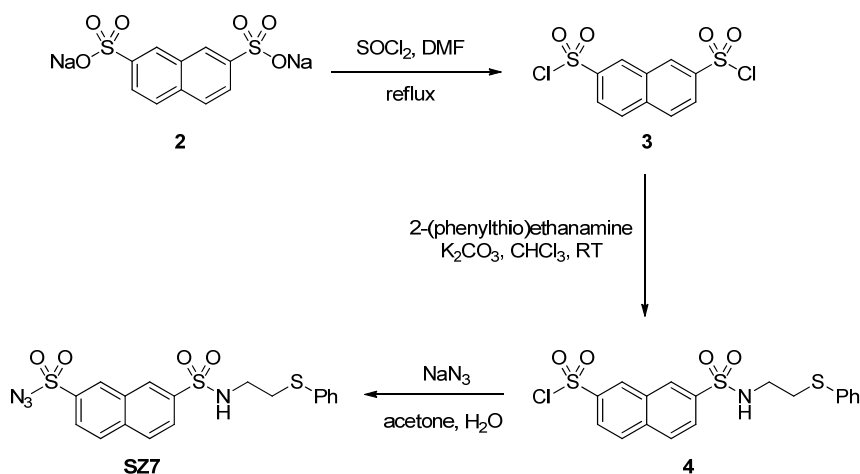
Additional control experiments were carried out using the mutants of Bcl-X<sub>L</sub>. In a 96-well plate, one thio acid (1 μL of a 2 mM solution in methanol) and one sulfonyl azide (1 μL of a 2 mM solution in methanol) were added to a solution of mutant Bcl-X<sub>L</sub> (98 μL

of a 2  $\mu$ M mutant Bcl-X<sub>L</sub> solution in buffer). This control sample was incubated along with the wildtype Bcl-X<sub>L</sub> containing sample at 37 °C for six hours and subjected to LC/MS-SIM analysis.

#### 2.4.6 Fluorescence polarization-based competitive binding assay

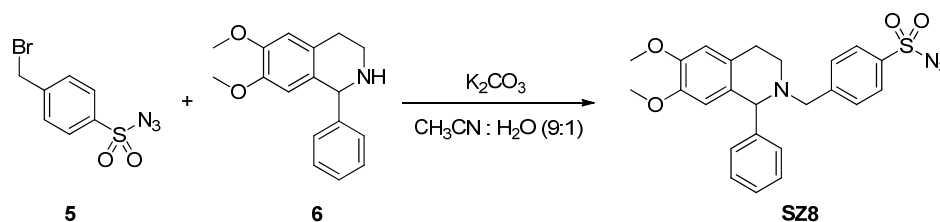
The detailed protocol to conduct fluorescence polarization-based competitive binding assays has been previously reported.<sup>7d</sup>

#### 2.4.7 Synthesis of building blocks



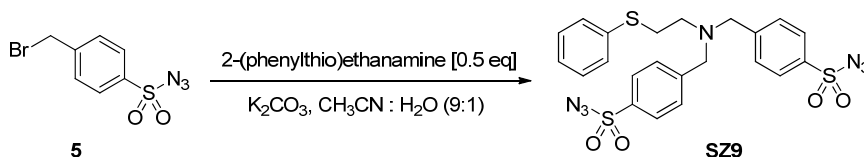
**Sulfonyl azide SZ7:** The mixture of compound **2** (664 mg, 2 mmol),  $\text{SOCl}_2$  (4 mL), and DMF (16 mL) was refluxed for 2 h. The reaction mixture was then treated with cold water (15 mL), extracted with DCM (15 mL  $\times$  3), and combined organic phases were dried over  $\text{Na}_2\text{SO}_4$ . A quick filtration through a pad of silica gel, evaporation, and vacuum drying gave the crude product **3** according to a similar procedure.<sup>29</sup> The sulfonyl chloride **3** obtained was used for the next step without further purification. A solution of sulfonyl chloride **3** (325 mg, 1 mmol), 2-(phenylthio)ethanamine (155 mg, 1 mmol) and

potassium carbonate (200 mg, 1.44 mmol) in  $\text{CHCl}_3$  (8 mL) was stirred at room temperature for 12 hours. The reaction mixture was then concentrated, treated with ethyl acetate (20 mL) and water (20 mL), and extracted with ethyl acetate (20 mL  $\times$  3). The combined organic layers were dried over  $\text{Na}_2\text{SO}_4$  and concentrated. The crude product **4** obtained was dissolved in acetone and the solution of sodium azide (70 mg, 1 mmol) in water was added dropwise at 0 °C. The mixture was stirred at 0 °C for 3 hours. Ethyl acetate (20 mL) and saturated aqueous potassium carbonate solution (20 mL) were added to the mixture and after extraction with ethyl acetate (20 mL  $\times$  3), the combined organic phases were dried over  $\text{Na}_2\text{SO}_4$  and concentrated. The sulfonyl azide **SZ7** (315 mg, 70% over 3 steps) was obtained by flash chromatography (hexane : EtOAc = 4:1;  $R_f$  = 0.6 in hexane : EtOAc = 1:1).  $^1\text{H}$  NMR (400 MHz,  $\text{CDCl}_3$ )  $\delta$ : 8.56 (s, 1H), 8.49 (s, 1H), 8.11 – 8.01 (m, 4H), 7.19 – 7.10 (m, 5H), 5.37 (t,  $J$  = 6.0 Hz, 1H), 3.21 – 3.13 (m, 2H), 2.99 (t,  $J$  = 6.4 Hz, 2H) ppm.  $^{13}\text{C}$  NMR (101 MHz,  $\text{CDCl}_3$ )  $\delta$ : 139.27, 137.05, 136.80, 133.49, 130.84, 130.25, 130.22, 130.15, 129.76, 129.44, 129.04, 126.93, 126.24, 124.59, 41.60, 33.85 ppm. HRMS (ESI) calcd for  $\text{C}_{18}\text{H}_{16}\text{N}_4\text{O}_4\text{S}_3$   $[\text{M}+\text{H}]^+$ : 449.0406, found: 449.0410

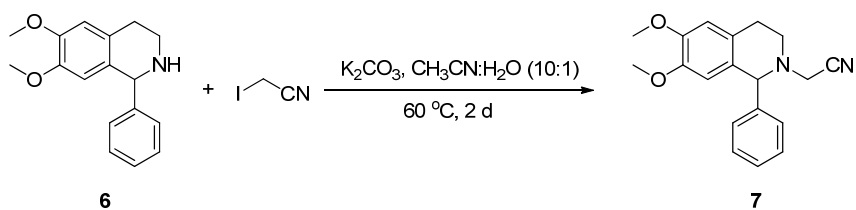


**Sulfonyl Azide SZ8:** A mixture of bromide **5**<sup>7d</sup> (276 mg, 1 mmol), amine **6**<sup>30</sup> (276 mg, 1 mmol), and potassium carbonate (200 mg, 1.44 mmol) in acetonitrile and water (9:1; 6 mL), was stirred at room temperature for 12 hours. After treating with ethyl acetate (20 mL) and water (20 mL), the system was extracted with ethyl acetate (20 mL  $\times$  3). The

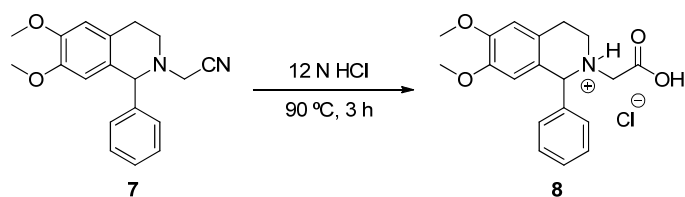
combined organic layers were dried over anhydrous sodium sulfate and concentrated. Sulfonyl azide **SZ8** (404 mg, 87%) was obtained by flash chromatography (hexane : EtOAc = 6:1 with 0.1% triethylamine;  $R_f = 0.4$  in hexane : EtOAc = 1:1).  $^1\text{H}$  NMR (400 MHz,  $\text{CDCl}_3$ )  $\delta$ : 7.82 (d,  $J = 6.8$  Hz, 2H), 7.54 (d,  $J = 7.3$  Hz, 2H), 7.38 – 7.18 (m, 5H), 6.62 (s, 1H), 6.20 (s, 1H), 4.57 (s, 1H), 3.84 (d,  $J = 10.6$  Hz, 1H), 3.80 (s, 3H), 3.56 (s, 3H), 3.39 (d,  $J = 14.5$  Hz, 1H), 3.05 – 2.95 (m, 2H), 2.71 (d,  $J = 15.4$  Hz, 1H), 2.58 – 2.48 (m, 1H) ppm.  $^{13}\text{C}$  NMR (101 MHz,  $\text{CDCl}_3$ )  $\delta$ : 147.82, 147.18, 146.78, 143.40, 136.27, 129.48, 129.15, 129.08, 128.04, 127.14, 127.03, 126.22, 111.36, 110.59, 68.05, 57.90, 55.42, 47.32, 28.21 ppm. HRMS (ESI) calcd for  $\text{C}_{24}\text{H}_{24}\text{N}_4\text{O}_4\text{S}$   $[\text{M}+\text{H}]^+$ : 465.1597, found: 465.1597



**Sulfonyl azide SZ9:** The sulfonyl azide **SZ9** was synthesized using a procedure described for the synthesis of **SZ8**, starting from 2-(phenylthio)ethanamine (72 mg, 0.47 mmol) and bromide **5** (260.4 mg, 0.94 mmol). The sulfonyl azide **SZ9** (154 mg, 60%) was obtained by flash chromatography (hexane : EtOAc = 6:1;  $R_f = 0.2$  in hexane : EtOAc = 4:1).  $^1\text{H}$  NMR (400 MHz,  $\text{CDCl}_3$ )  $\delta$ : 7.87 (d,  $J = 8.3$  Hz, 4H), 7.6 (d,  $J = 8.1$  Hz, 4H), 7.33 – 7.09 (m, 5H), 3.72 (s, 4H), 3.07 (t,  $J = 7.2$  Hz, 2H), 2.76 (t,  $J = 6.9$  Hz, 2H) ppm.  $^{13}\text{C}$  NMR (101 MHz,  $\text{CDCl}_3$ )  $\delta$ : 146.61, 137.36, 129.63, 129.22, 128.97, 127.92, 127.65, 126.35, 57.91, 52.73, 31.48 ppm. HRMS (ESI) calcd for  $\text{C}_{22}\text{H}_{21}\text{N}_7\text{O}_4\text{S}_3$   $[\text{M}+\text{H}]^+$ : 544.0890, found: 544.0887

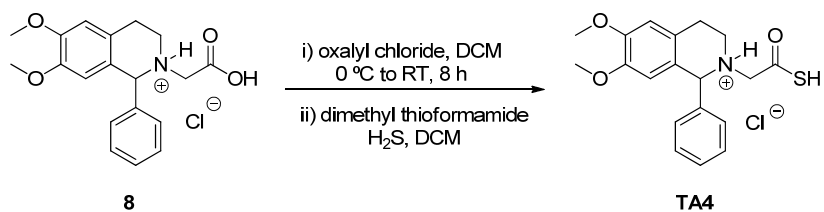


**Nitrile 7:** To a solution of amine **6**<sup>30</sup> (1 g, 3.71 mmol) and iodoacetonitrile (620 mg, 3.71 mmol) in acetonitrile (30 mL) and water (3 mL), was added potassium carbonate (1.53 g, 11.13 mmol) and the resulting reaction mixture was stirred at 60 °C for 2 days. After cooling to room temperature, the solvent was removed under reduced pressure and the crude was purified by flash chromatography (hexane : EtOAc = 6:1;  $R_f$  = 0.67 in hexane : EtOAc = 1:1) to obtain nitrile **7** with 79% yield (904 mg). <sup>1</sup>H NMR (400 MHz, CDCl<sub>3</sub>)  $\delta$ : 7.33 – 7.26 (m, 5H), 6.58 (s, 1H), 6.06 (s, 1H), 4.62 (s, 1H), 3.82 (s, 3H), 3.53 (s, 3H), 3.41 (d,  $J$  = 8.1 Hz, 2H), 3.27 – 3.16 (m, 1H), 3.09 – 2.94 (m, 2H), 2.74 (d,  $J$  = 15.7 Hz, 1H) ppm. <sup>13</sup>C NMR (101 MHz, CDCl<sub>3</sub>)  $\delta$ : 147.85, 147.47, 142.24, 129.53, 128.97, 128.38, 125.92, 115.05, 111.63, 110.89, 66.98, 56.01, 50.04, 44.00, 29.18 ppm. HRMS (ESI) calcd for C<sub>19</sub>H<sub>20</sub>N<sub>2</sub>O<sub>2</sub> [M+H]<sup>+</sup>: 309.1598, found: 309.1584

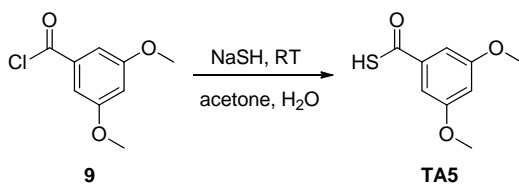


**Acid 8:** To a flask charged with nitrile **7** (100 mg, 0.32 mmol), was added 12 N HCl (1.5 mL) and the reaction mixture was stirred at 90 °C for 3 hours. The reaction mixture was then cooled to room temperature and treated with 2 N NaOH solution (pH = 5). The crashed out white solid was filtered, washed with cold MeOH and dried to obtain acid **8**

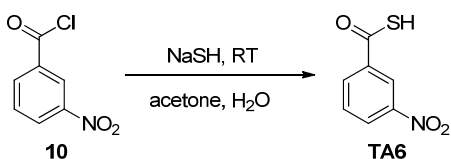
as a hydrochloride salt (66%, 78 mg). The analytical sample was obtained by flash chromatography (MeOH : EtOAc = 2:1 with 0.2% acetic acid;  $R_f$  = 0.5 in MeOH : EtOAc = 3:1).  $^1\text{H}$  NMR (400 MHz, DMSO-*d*<sub>6</sub>)  $\delta$  7.31 – 7.18 (m, 5H), 6.69 (s, 1H), 6.13 (s, 1H), 4.95 (s, 1H), 3.71 (s, 3H), 3.44 (s, 3H), 3.07 – 2.98 (m, 1H), 2.96 – 2.81 (m, 4H), 2.72 – 2.62 (m, 1H) ppm.  $^{13}\text{C}$  NMR (101 MHz, DMSO-*d*<sub>6</sub>)  $\delta$  174.02, 147.02, 146.60, 144.42, 130.23, 129.29, 127.87, 126.85, 126.83, 111.98, 111.51, 64.97, 57.17, 55.44, 55.38, 47.30, 28.31 ppm. HRMS (ESI) calcd for C<sub>19</sub>H<sub>21</sub>NO<sub>4</sub> [M+H]<sup>+</sup>: 328.1543, found: 328.1536



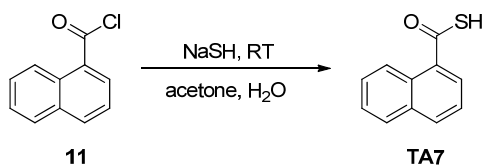
**Thio acid TA4:** The thio acid **TA4** was obtained starting from acid **8** (340 mg, 0.93 mmol) with 25% yield via the same procedure as previously reported for the thio acid **TA2**.<sup>7d</sup>  $R_f$  = 0.6 in DCM : MeOH = 10:1.  $^1\text{H}$  NMR (400 MHz, CDCl<sub>3</sub>)  $\delta$ : 7.35 – 7.23 (m, 5H), 6.66 (s, 1H), 6.27 (s, 1H), 5.57 (s, 1H), 3.83 (s, 3H), 3.63 (s, 3H), 3.50 – 3.39 (m, 2H), 3.37 (s, 2H), 3.24 – 3.01 (m, 2H) ppm.  $^{13}\text{C}$  NMR (101 MHz, CDCl<sub>3</sub>)  $\delta$ : 204.67, 149.54, 148.69, 136.42, 130.45, 129.99, 129.30, 123.44, 121.74, 111.17, 110.88, 66.16, 63.53, 56.08, 45.27, 24.46 ppm. HRMS (ESI) calcd for C<sub>19</sub>H<sub>21</sub>NO<sub>3</sub>S [M+H]<sup>+</sup>: 344.1315, found: 344.1315



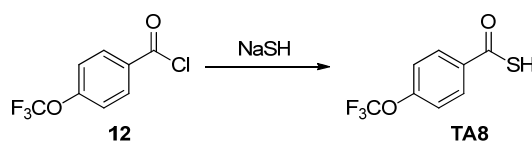
**Thio acid TA5:** The synthesis of thio acid **TA5** was accomplished starting from acid chloride **9** (400 mg, 1.99 mmol) via the same procedure as previously reported for thio acid **TA3**<sup>7d</sup> with 15% yield.  $R_f = 0.17$  in hexane : EtOAc = 2:1. <sup>1</sup>H NMR (400 MHz, CDCl<sub>3</sub>)  $\delta$ : 7.00 (d,  $J = 2.1$  Hz, 2H), 6.65 – 6.63 (m, 1H), 3.8 (s, 6H) ppm. <sup>13</sup>C NMR (101 MHz, CDCl<sub>3</sub>)  $\delta$ : 190.10, 160.97, 138.57, 106.36, 105.69, 55.73 ppm. HRMS (ESI) calcd for C<sub>9</sub>H<sub>10</sub>O<sub>3</sub>S [M-H]<sup>-</sup>: 197.0278, found: 197.0278



**Thio acid TA6:** To a solution of NaSH (90 mg, 1.6 mmol) in water (1mL) was added dropwise a solution of acid chloride **10** (200 mg, 1.07 mmol) in acetone (6 mL). The resulting mixture was stirred for 2 h. The solvent was removed under reduced pressure and resulting crude was basified using 10% NaOH solution (pH = 12). The reaction mixture was then extracted with ethyl acetate to remove organic impurities. The aqueous layer was slowly acidified using 2 N HCl solution (pH = 1). Corresponding thio acid **TA6** crashed out and was filtered, washed with deionized water and dried under vacuum to obtain pale yellow crystals of thio acid **TA6** with 25% yield.  $R_f = 0.26$  in hexane : EtOAc = 1:3. <sup>1</sup>H NMR (400 MHz, CDCl<sub>3</sub>)  $\delta$ : 8.75 – 8.72 (m, 1H), 8.50 – 8.44 (m, 1H), 8.22 (d,  $J = 7.8$  Hz, 1H), 7.70 (t,  $J = 8.0$  Hz, 1H) ppm. <sup>13</sup>C NMR (101 MHz, CDCl<sub>3</sub>)  $\delta$ : 188.19, 137.96, 133.42, 130.32, 128.32, 122.96 ppm. HRMS (ESI) calcd for C<sub>7</sub>H<sub>5</sub>NO<sub>3</sub>S [M-H]<sup>-</sup>: 181.9917, found: 181.9917

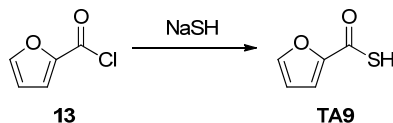


**Thio acid TA7:** To a solution of NaSH (90 mg, 1.6 mmol) in water (1mL) was added dropwise a solution of acid chloride **11** (204 mg, 1.07 mmol) in acetone (6 mL). The resulting mixture was stirred for 2 h. The solvent was removed under reduced pressure and resulting crude was basified using 10% NaOH solution (pH = 12). The reaction mixture was then extracted with ethyl acetate to remove organic impurities. The aqueous layer was slowly acidified using 2 N HCl solution and the aqueous layer was extracted using ethyl acetate at various pH values starting from 6 to 2, collecting organic fractions for every unit change in the pH. Fractions collected between pH changing from 5 to 2 were combined and were subjected to preparative HPLC to obtain thio acid **TA7** with 27% yield.  $R_f = 0.24$  in hexane : EtOAc = 1:1.  $^1\text{H NMR}$  (400 MHz,  $\text{CDCl}_3$ )  $\delta$ : 8.61 – 8.50 (m, 1H), 8.35 (d,  $J = 7.1$  Hz, 1H), 8.13 – 7.99 (m, 1H), 7.94 – 7.84 (m, 1H), 7.68 – 7.53 (m, 3H) ppm.  $^{13}\text{C NMR}$  (101 MHz,  $\text{CDCl}_3$ )  $\delta$ : 188.15, 134.29, 134.00, 133.43, 129.52, 129.09, 128.79, 128.65, 127.27, 125.41, 124.71 ppm. HRMS (ESI) calcd for  $\text{C}_{11}\text{H}_8\text{OS}$   $[\text{M-H}]^-$ : 187.0223, found: 187.0218



**Thio acid TA8:** The acid chloride **12** (500 mg, 2.22 mmol) and NaSH (149 mg, 2.66 mmol) were stirred at 0 °C under solvent free conditions for 1 h and the thio acid **TA8** obtained, after filtering the salts, was used without further purification.  $^1\text{H NMR}$  (250

MHz, CDCl<sub>3</sub>)  $\delta$ : 7.93 – 7.85 (m, 2H), 7.32 – 7.17 (m, 2H) ppm. HRMS (ESI) calcd for C<sub>8</sub>H<sub>5</sub>F<sub>3</sub>O<sub>2</sub>S [M-H]<sup>-</sup>: 220.9890, found: 220.9886



**Thio acid TA9:** The thio acid **TA9** was prepared following the same procedure as described for **TA8**. <sup>1</sup>H NMR (250 MHz, CD<sub>3</sub>OD)  $\delta$ : 7.92 (dd, *J* = 1.7, 0.8 Hz, 1H), 7.49 (dd, *J* = 3.7, 0.8 Hz, 1H), 6.73 (dd, *J* = 3.7, 1.7 Hz, 1H) ppm. HRMS (ESI) calcd for C<sub>5</sub>H<sub>4</sub>O<sub>2</sub>S [M-H]<sup>-</sup>: 126.9859, found: 126.9863

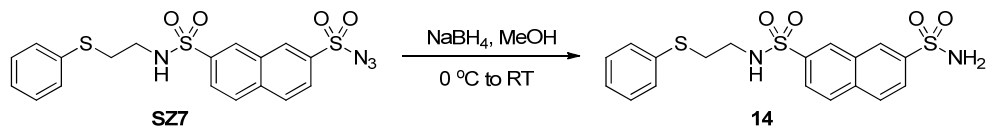
#### 2.4.8 General procedure A for the synthesis of acylsulfonamides

A solution of sulfonamide (1 eq), carboxylic acid (1 eq), EDCI (2 eq) and DMAP (0.2 eq) were stirred in dry DCM or THF, under inert atmosphere at room temperature overnight, quenched by adding water and the system was extracted with ethyl acetate. The combined organic layers were dried over anhydrous sodium sulfate and concentrated. The crude was then subjected to flash chromatography to obtain the corresponding acylsulfonamide.

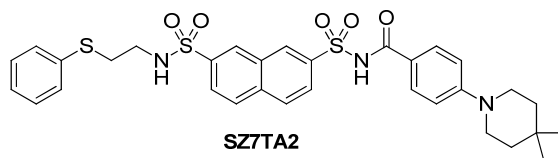
#### 2.4.9 General procedure B for the synthesis of acylsulfonamides

Synthesis of acylsulfonamide was accomplished by reacting selenocarboxylate (generated from corresponding carboxylic acid and selenating reagent, LiAlHSeH) with the sulfonyl azide according to a previously reported procedure.<sup>17</sup>

#### 2.4.10 Synthesis of kinetic TGS hits

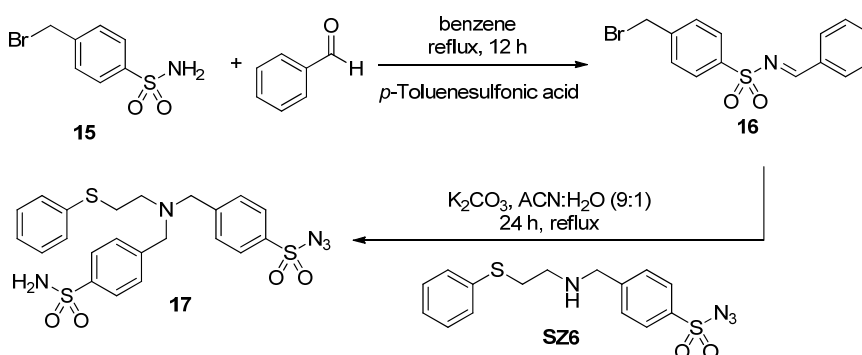


**Sulfonamide 14:** Sodium borohydride (60 mg, 1.5 mmol) was added slowly to the solution of **SZ7** (500 mg, 1.1 mmol) in methanol (6mL) at 0 °C. The reaction mixture was stirred for 30 min at room temperature, quenched using solid  $\text{NH}_4\text{Cl}$  and the solvent was removed under reduced pressure to afford the crude product. Sulfonamide **14** (418 mg, 90%) was obtained by flash chromatography.  $R_f = 0.64$  in hexane : EtOAc = 1:2.  $^1\text{H}$  NMR (250 MHz, Acetone-*d*6)  $\delta$ : 8.67 (s, 1H), 8.60 (s, 1H), 8.21 – 8.12 (m, 3H), 8.02 (dd,  $J = 8.7, 1.7$  Hz, 1H), 7.28 – 7.10 (m, 5H), 6.97 (t,  $J = 5.8$  Hz, 1H), 6.87 (bs, 2H), 3.30 – 3.18 (m, 2H), 3.15 – 3.06 (m, 2H) ppm.  $^{13}\text{C}$  NMR (63 MHz, Acetone-*d*6)  $\delta$ : 143.54, 140.22, 136.63, 135.93, 132.11, 130.57, 130.32, 130.03, 129.97, 129.74, 128.52, 127.20, 125.86, 125.83, 43.24, 33.73 ppm. HRMS (ESI) calcd for  $\text{C}_{18}\text{H}_{18}\text{N}_2\text{O}_4\text{S}_3$   $[\text{M}+\text{H}]^+$ : 423.0502, found: 423.0486



**Acylsulfonamide SZ7TA2:** The acylsulfonamide **SZ7TA2** was prepared following the general procedure **A**, starting from sulfonamide **14** and 4-(4,4-dimethylpiperidin-1-yl)benzoic acid<sup>7d</sup> with 16% yield (102 mg) after purification using preparative HPLC system.  $R_f = 0.28$  in EtOAc.  $^1\text{H}$  NMR (400 MHz,  $\text{CDCl}_3$ )  $\delta$ : 8.77 (s, 1H), 8.46 (s, 1H), 8.23 (d,  $J = 8.2$  Hz, 1H), 7.91 – 7.78 (m, 3H), 7.67 (d,  $J = 8.1$  Hz, 2H), 7.19 – 7.01 (m,

5H), 6.64 (d,  $J = 8.0$  Hz, 2H), 5.65 (bs, 1H), 3.34 – 3.15 (m, 4H), 3.12 (d,  $J = 5.7$  Hz, 2H), 2.96 (d,  $J = 5.6$  Hz, 2H), 1.46 – 1.23 (m, 4H), 0.93 (s, 6H) ppm.  $^{13}\text{C}$  NMR (101 MHz,  $\text{CDCl}_3$ )  $\delta$ : 164.05, 154.37, 138.41, 137.92, 136.46, 133.56, 131.23, 130.84, 130.17, 129.94, 129.51, 129.45, 129.02, 126.88, 126.18, 125.42, 117.85, 113.03, 43.71, 41.66, 37.76, 33.87, 28.58, 27.68 ppm. HRMS (ESI) calcd for  $\text{C}_{32}\text{H}_{35}\text{N}_3\text{O}_5\text{S}_3$   $[\text{M}+\text{H}]^+$ : 638.1812, found: 638.1810

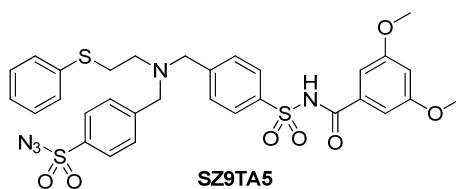


**Sulfonamide 17:** A solution of sulfonamide **15**<sup>7d</sup> (900 mg, 3.6 mmol), benzaldehyde (381 mg, 3.6 mmol) and *p*-toluenesulfonic acid (10 mg) in benzene was refluxed for 12 h using Dean-stark apparatus. The reaction mixture was cooled down to room temperature and extracted with ethyl acetate (20 mL  $\times$  3). The combined organic phases were dried over anhydrous sodium sulfate and concentrated to afford the product **16**, which was used without further purification. The mixture of **16** (1.22 g, 3.6 mmol), sulfonamide **SZ6** (1.25 g, 3.6 mmol) and potassium carbonate (1.0 g, 7.2 mmol) in acetonitrile and water (9:1, 20 mL), was refluxed for 24 hours. After cooling down to room temperature, the reaction mixture was treated with ethyl acetate (20 mL) and water (20 mL), extracted with ethyl acetate (20 mL  $\times$  3). The combined organic phases were dried over anhydrous sodium sulfate and concentrated. Interestingly, hydrolysis of the imine occurred smoothly

under this basic condition. Sulfonamide **17** (930 mg, 50% over 2 steps) was thus obtained by flash chromatography (hexane : EtOAc = 2:1;  $R_f$  = 0.2 in hexane : EtOAc = 2:1).  $^1\text{H}$  NMR (400 MHz,  $\text{CDCl}_3$ )  $\delta$ : 7.83 (d,  $J$  = 8.2 Hz, 4H), 7.56 (d,  $J$  = 8.2 Hz, 2H), 7.47 (d,  $J$  = 8.2 Hz, 2H), 7.24 – 7.14 (m, 5H), 5.00 (bs, 2H), 3.67 (d,  $J$  = 3.8 Hz, 4H), 3.06 (t,  $J$  = 6.8 Hz, 2H), 2.75 (t,  $J$  = 6.8 Hz, 2H) ppm.  $^{13}\text{C}$  NMR (101 MHz,  $\text{CDCl}_3$ )  $\delta$ : 147.00, 144.11, 140.87, 137.06, 135.81, 129.61, 129.24, 129.08, 128.94, 127.50, 126.52, 126.19, 58.11, 57.99, 53.01, 31.56 ppm. HRMS (ESI) calcd for  $\text{C}_{22}\text{H}_{23}\text{N}_5\text{O}_4\text{S}_3$   $[\text{M}+\text{H}]^+$ : 518.0985, found: 518.0999

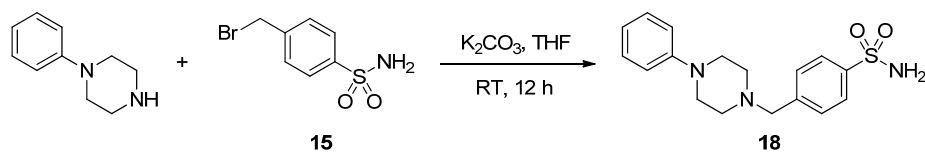


**Acylsulfonamide SZ9TA1:** The acylsulfonamide **SZ9TA1** was prepared following the general procedure **A** starting from sulfonamide **17** and benzoic acid with 54% yield (65 mg).  $R_f$  = 0.77 in EtOAc.  $^1\text{H}$  NMR (400 MHz,  $\text{CDCl}_3$ )  $\delta$ : 8.09 (d,  $J$  = 8.0 Hz, 2H), 7.78 (d,  $J$  = 8.1 Hz, 2H), 7.77 (d,  $J$  = 7.6 Hz, 2H), 7.60 – 7.51 (m, 5H), 7.47 – 7.37 (m, 3H), 7.19 (d,  $J$  = 4.3 Hz, 3H), 7.14 – 7.08 (m, 1H), 3.67 (s, 4H), 3.04 (t,  $J$  = 7.2 Hz, 2H), 2.73 (t,  $J$  = 7.2 Hz, 2H) ppm.  $^{13}\text{C}$  NMR (101 MHz,  $\text{CDCl}_3$ )  $\delta$ : 165.13, 147.07, 145.64, 137.64, 137.16, 135.85, 133.47, 131.42, 130.22, 129.70, 129.14, 129.03, 128.86, 128.73, 128.09, 127.64, 126.28, 58.00, 57.92, 52.84, 31.50 ppm. HRMS (ESI) calcd for  $\text{C}_{29}\text{H}_{27}\text{N}_5\text{O}_5\text{S}_3$   $[\text{M}+\text{H}]^+$ : 622.1247, found: 622.1240



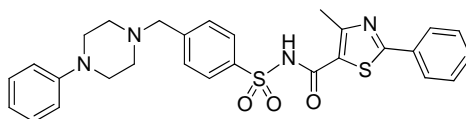
**Acylsulfonamide SZ9TA5:** was prepared following the general procedure **A** starting from sulfonamide **17** and 3,5-dimethoxybenzoic acid with 56% yield (110 mg).  $R_f = 0.28$  in hexane : EtOAc = 1:1.  $^1\text{H}$  NMR (400 MHz,  $\text{CDCl}_3$ )  $\delta$ : 7.97 (d,  $J = 6.8$  Hz, 2H), 7.78 (d,  $J = 7.8$  Hz, 2H), 7.47 (d,  $J = 7.6$  Hz, 2H), 7.33 – 6.92 (m, 10H), 6.42 (s, 1H), 3.66 – 3.48 (m, 10H), 3.04 – 2.85 (m, 2H), 2.79 – 2.50 (m, 2H) ppm.  $^{13}\text{C}$  NMR (101 MHz,  $\text{CDCl}_3$ )  $\delta$ : 160.67, 147.23, 137.21, 135.98, 129.81, 129.16, 129.00, 127.72, 126.37, 106.56, 105.27, 58.07, 57.91, 55.61, 52.89, 31.50 ppm. HRMS (ESI) calcd for  $\text{C}_{31}\text{H}_{31}\text{N}_5\text{O}_7\text{S}_3$   $[\text{M}+\text{H}]^+$ : 682.1458, found: 682.1440

#### 2.4.11 Synthesis of additional acylsulfonamides



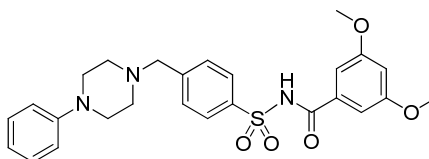
**Sulfonamide 18:** To a solution of 1-phenylpiperazine (285 mg, 1.76 mmol) and bromide **15** (400 mg, 1.59 mmol) in THF (8 mL), was added potassium carbonate (441 mg, 3.19 mmol) and the resulting solution was stirred at room temperature overnight. The reaction mixture was treated with 1N potassium carbonate solution (10 mL), extracted with ethyl acetate (20 mL  $\times$  3). The combined organic phases were dried over anhydrous sodium sulfate and concentrated. The sulfonamide **18** (461 mg, 87%) was thus obtained by flash chromatography (hexane : EtOAc = 2:1 with 0.1% triethylamine;  $R_f = 0.38$  in hexane :

EtOAc = 1:2).  $^1\text{H}$  NMR (400 MHz, DMSO-*d*6)  $\delta$  7.80 – 7.75 (m, 2H), 7.49 (d,  $J$  = 8.1 Hz, 2H), 7.31 – 7.28 (m, 2H), 7.16 (t,  $J$  = 7.7 Hz, 2H), 6.88 (d,  $J$  = 8.1 Hz, 2H), 6.73 (t,  $J$  = 7.2 Hz, 1H), 3.56 (s, 2H), 3.11 – 3.08 (m, 4H), 2.50 – 2.46 (m, 4H) ppm.  $^{13}\text{C}$  NMR (101 MHz, DMSO-*d*6)  $\delta$  151.41, 143.24, 142.77, 129.59, 129.32, 126.07, 119.23, 115.81, 61.76, 52.98, 48.64 ppm. HRMS (ESI) calcd for  $\text{C}_{17}\text{H}_{21}\text{N}_3\text{O}_2\text{S}$   $[\text{M}+\text{H}]^+$ : 332.1427, found: 332.1425



**SZ1TA3**

**Acylsulfonamide SZ1TA3:** was prepared following the general procedure **A** starting from sulfonamide **18** and 4-methyl-2-phenylthiazole-5-carboxylic acid with 58% yield (279 mg).  $R_f$  = 0.3 in EtOAc : MeOH = 20:1.  $^1\text{H}$  NMR (400 MHz,  $\text{CD}_3\text{OD}$ )  $\delta$  8.16 (d,  $J$  = 7.0 Hz, 2H), 7.76 (t,  $J$  = 10.0 Hz, 4H), 7.39 – 7.29 (m, 3H), 7.13 (t,  $J$  = 6.8 Hz, 2H), 6.84 (d,  $J$  = 7.3 Hz, 2H), 6.79 (t,  $J$  = 6.6 Hz, 1H), 5.28 – 5.10 (m, 2H), 4.42 (s, 2H), 3.45 – 3.23 (m, 6H), 2.46 (s, 3H) ppm.  $^{13}\text{C}$  NMR (101 MHz,  $\text{CD}_3\text{OD}$ )  $\delta$  169.70, 161.16, 160.43, 149.67, 141.85, 134.50, 132.22, 132.00, 131.40, 129.16, 129.12, 128.86, 126.68, 123.40, 121.18, 116.73, 59.25, 51.80, 46.63, 16.60 ppm. HRMS (ESI) calcd for  $\text{C}_{28}\text{H}_{28}\text{N}_4\text{O}_3\text{S}_2$   $[\text{M}+\text{H}]^+$ : 533.1676, found: 533.1668

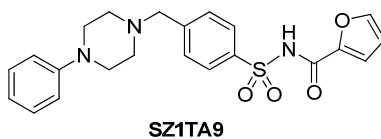


**SZ1TA5**

**Acylsulfonamide SZ1TA5:** was prepared following the general procedure **B** with 45% yield (67 mg).  $R_f = 0.44$  in EtOAc.  $^1\text{H NMR}$  (400 MHz,  $\text{CDCl}_3$ )  $\delta$  8.24 – 7.97 (m, 2H), 7.82 – 7.51 (m, 2H), 7.05 – 6.79 (m, 6H), 6.56 (s, 2H), 4.33 (s, 2H), 3.70 (s, 6H), 3.57 – 3.04 (m, 8H) ppm.  $^{13}\text{C NMR}$  (101 MHz,  $\text{CDCl}_3$ )  $\delta$  165.35, 161.11, 148.73, 140.80, 134.11, 133.02, 132.01, 129.77, 129.57, 122.78, 117.63, 106.30, 106.07, 60.10, 55.78, 51.89, 47.48 ppm. HRMS (ESI) calcd for  $\text{C}_{26}\text{H}_{29}\text{N}_3\text{O}_5\text{S}$   $[\text{M}+\text{H}]^+$ : 496.1901, found: 496.1915



**Acylsulfonamide SZ1TA6:** was prepared following the general procedure **B** with 33% yield (48 mg).  $R_f = 0.54$  in hexane : EtOAc = 1:1.  $^1\text{H NMR}$  (400 MHz,  $\text{CD}_3\text{OD}$ )  $\delta$  8.58 – 8.55 (m, 1H), 8.40 – 8.34 (m, 1H), 8.18 (d,  $J = 8.3$  Hz, 2H), 8.13 (d,  $J = 7.9$  Hz, 1H), 7.77 (d,  $J = 8.4$  Hz, 2H), 7.67 (t,  $J = 8.0$  Hz, 1H), 7.20 (t,  $J = 8.0$  Hz, 2H), 6.92 (d,  $J = 8.0$  Hz, 2H), 6.85 (t,  $J = 7.3$  Hz, 1H), 4.48 (s, 2H), 3.47 – 3.32 (m, 6H), 3.28 – 3.22 (m, 2H) ppm.  $^{13}\text{C NMR}$  (101 MHz,  $\text{CD}_3\text{OD}$ )  $\delta$  164.63, 149.76, 148.45, 141.33, 134.81, 133.89, 133.77, 132.88, 131.95, 130.19, 129.10, 127.39, 122.99, 121.22, 116.79, 59.22, 51.88, 46.74 ppm. HRMS (ESI) calcd for  $\text{C}_{24}\text{H}_{24}\text{N}_4\text{O}_5\text{S}$   $[\text{M}+\text{H}]^+$ : 481.1540, found: 481.1551



**Acylsulfonamide SZ1TA9:** was prepared following the general procedure **B** with 15% yield (19 mg).  $R_f = 0.47$  in hexane : EtOAc = 1:1.  $^1\text{H NMR}$  (400 MHz,  $\text{CDCl}_3$ )  $\delta$  8.15 (d,

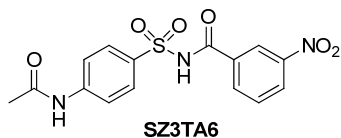
$J = 8.0$  Hz, 2H), 7.66 (d,  $J = 8.1$  Hz, 2H), 7.50 (s, 1H), 7.31 – 7.23 (m, 4H), 6.97 (t,  $J = 7.2$  Hz, 1H), 6.90 (d,  $J = 8.3$  Hz, 2H), 6.53 – 6.49 (m, 1H), 4.33 (s, 2H), 3.57 – 3.12 (m, 8H) ppm.  $^{13}\text{C}$  NMR (101 MHz,  $\text{CDCl}_3$ )  $\delta$  155.11, 149.12, 146.53, 145.08, 140.71, 134.43, 131.97, 129.74, 129.60, 122.43, 118.81, 117.51, 113.23, 59.99, 51.87, 47.32 ppm. HRMS (ESI) calcd for  $\text{C}_{22}\text{H}_{23}\text{N}_3\text{O}_4\text{S}$   $[\text{M}+\text{H}]^+$  : 426.1482, found: 426.1481



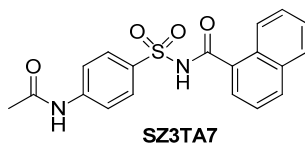
**Acylsulfonamide SZ2TA4:** was prepared following the general procedure **B** with 15% yield (55 mg).  $R_f = 0.56$  in  $\text{DCM} : \text{MeOH} = 10:1$ .  $^1\text{H}$  NMR (400 MHz,  $\text{CD}_3\text{OD}$ )  $\delta$  8.14 (d,  $J = 8.4$  Hz, 2H), 7.76 (d,  $J = 8.4$  Hz, 2H), 7.46 – 7.41 (m, 3H), 7.33 – 7.24 (m, 7H), 6.90 (s, 1H), 6.38 (s, 1H), 5.76 (s, 1H), 4.58 – 4.48 (m, 1H), 4.17 – 4.09 (m, 1H), 4.04 – 3.98 (m, 1H), 3.88 – 3.84 (m, 4H), 3.60 (s, 3H), 3.44 – 3.40 (m, 2H), 3.20 – 3.11 (m, 4H), 2.89 (s, 3H), 2.81 – 2.75 (m, 1H), 2.64 – 2.58 (m, 1H) ppm.  $^{13}\text{C}$  NMR (101 MHz,  $\text{CD}_3\text{OD}$ )  $\delta$  167.91, 151.33, 150.33, 143.97, 137.46, 136.69, 136.11, 132.85, 132.11, 131.45, 130.38, 130.18, 129.96, 129.91, 128.52, 124.76, 122.31, 112.66, 112.51, 67.06, 60.19, 58.51, 56.62, 56.56, 56.01, 46.83, 40.46, 31.50, 27.98 ppm. HRMS (ESI) calcd for  $\text{C}_{35}\text{H}_{39}\text{N}_3\text{O}_5\text{S}$   $[\text{M}+\text{H}]^+$  : 614.2683, found: 614.2675



**Acylsulfonamide SZ3TA1:** was prepared following the general procedure **B** with 11% yield (21 mg).  $R_f = 0.33$  in EtOAc : MeOH = 20:1.  $^1\text{H}$  NMR (400 MHz, DMSO-*d*6)  $\delta$  7.91 – 7.83 (m, 4H), 7.75 (d,  $J = 8.3$  Hz, 2H), 7.56 (t,  $J = 7.1$  Hz, 1H), 7.44 (t,  $J = 7.7$  Hz, 2H), 2.05 (s, 3H) ppm.  $^{13}\text{C}$  NMR (126 MHz, DMSO-*d*6)  $\delta$  169.54, 166.17, 144.03, 133.86, 133.38, 132.66, 129.45, 128.94, 128.81, 118.76, 24.61 ppm. HRMS (ESI) calcd for  $\text{C}_{15}\text{H}_{14}\text{N}_2\text{O}_4\text{S}$   $[\text{M}+\text{H}]^+$ : 319.0747, found: 319.0744

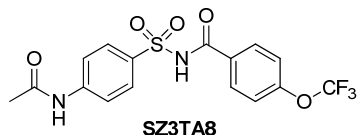


**Acylsulfonamide SZ3TA6:** was prepared following the general procedure **A** with 46 % yield (78 mg).  $R_f = 0.25$  in EtOAc : MeOH = 20:1.  $^1\text{H}$  NMR (250 MHz, Acetone-*d*6)  $\delta$ : 8.61 (s, 1H), 8.32 (dd,  $J = 8.1, 1.5$  Hz, 1H), 8.22 (d,  $J = 7.7$  Hz, 1H), 7.91 (d,  $J = 8.7$  Hz, 2H), 7.75 – 7.64 (m, 3H), 1.99 (s, 3H) ppm.  $^{13}\text{C}$  NMR (63 MHz, Acetone-*d*6)  $\delta$ : 169.69, 149.19, 145.17, 135.18, 135.04, 134.10, 131.13, 130.49, 128.09, 123.91, 119.11, 24.37 ppm. HRMS (ESI) calcd for  $\text{C}_{15}\text{H}_{13}\text{N}_3\text{O}_6\text{S}$   $[\text{M}+\text{H}]^+$ : 364.0598, found: 364.0588

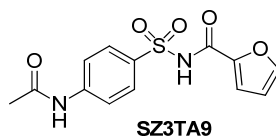


**Acylsulfonamide SZ3TA7:** was prepared following the general procedure **B** with 14% yield (31 mg).  $R_f = 0.44$  in hexane : EtOAc = 1:3.  $^1\text{H}$  NMR (400 MHz, CD<sub>3</sub>OD)  $\delta$  8.08 (d,  $J = 8.8$  Hz, 2H), 8.01 (d,  $J = 8.2$  Hz, 1H), 7.94 (d,  $J = 8.0$  Hz, 1H), 7.91 – 7.87 (m, 1H), 7.84 (d,  $J = 8.8$  Hz, 2H), 7.65 (d,  $J = 7.0$  Hz, 1H), 7.51 – 7.46 (m, 3H), 2.17 (s, 3H) ppm.  $^{13}\text{C}$  NMR (101 MHz, CD<sub>3</sub>OD)  $\delta$  170.66, 168.03, 143.78, 133.64, 133.48, 131.69,

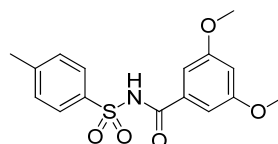
130.91, 129.74, 129.18, 128.14, 127.10, 126.25, 126.18, 124.26, 124.11, 118.72, 22.66 ppm. HRMS (ESI) calcd for C<sub>19</sub>H<sub>16</sub>N<sub>2</sub>O<sub>4</sub>S [M+H]<sup>+</sup>: 369.0904, found: 369.0904



**Acylsulfonamide SZ3TA8:** was prepared following the general procedure **B** with 26% yield (63 mg). R<sub>f</sub> = 0.63 in hexane : EtOAc = 1:3. <sup>1</sup>H NMR (400 MHz, CD<sub>3</sub>OD) δ 8.01 – 7.98 (m, 2H), 7.91 – 7.87 (m, 2H), 7.78 – 7.74 (m, 2H), 7.36 – 7.32 (m, 2H), 2.13 (s, 3H) ppm. <sup>13</sup>C NMR (101 MHz, CD<sub>3</sub>OD) δ 170.62, 164.89, 152.34, 143.69, 133.35, 130.74, 130.16, 129.22, 120.30, 118.62, 22.62 ppm. HRMS (ESI) calcd for C<sub>16</sub>H<sub>13</sub>F<sub>3</sub>N<sub>2</sub>O<sub>5</sub>S [M+H]<sup>+</sup>: 403.0570, found: 403.0566

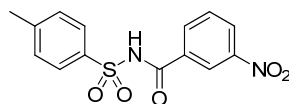


**Acylsulfonamide SZ3TA9:** was prepared following the general procedure **A** with 36% yield (52 mg). R<sub>f</sub> = 0.23 in EtOAc. <sup>1</sup>H NMR (400 MHz, CD<sub>3</sub>OD) δ: 7.97 (d, *J* = 8.8 Hz, 2H), 7.75 (d, *J* = 8.8 Hz, 2H), 7.70 (s, 1H), 7.25 (d, *J* = 3.5 Hz, 1H), 6.58 (dd, *J* = 3.4, 1.5 Hz, 1H), 2.13 (s, 3H) ppm. <sup>13</sup>C NMR (101 MHz, CD<sub>3</sub>OD) δ: 170.87, 156.36, 147.08, 145.63, 143.91, 133.74, 129.33, 118.85, 117.76, 112.34, 22.87 ppm. HRMS (ESI) calcd for C<sub>13</sub>H<sub>12</sub>N<sub>2</sub>O<sub>5</sub>S [M+H]<sup>+</sup>: 309.0540, found: 309.0547



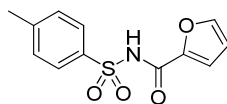
**SZ5TA5**

**Acylsulfonamide SZ5TA5:** was prepared following the general procedure **B** with 46% yield (46 mg).  $R_f = 0.72$  in EtOAc.  $^1\text{H NMR}$  (400 MHz,  $\text{CDCl}_3$ )  $\delta$  8.04 (d,  $J = 8.2$  Hz, 2H), 7.35 (d,  $J = 8.1$  Hz, 2H), 6.94 (d,  $J = 2.0$  Hz, 2H), 6.61 – 6.59 (m, 1H), 3.75 (s, 6H), 2.44 (s, 3H) ppm.  $^{13}\text{C NMR}$  (101 MHz,  $\text{CDCl}_3$ )  $\delta$  164.37, 161.20, 145.50, 135.56, 133.22, 129.85, 128.83, 106.53, 105.59, 55.85, 21.91 ppm. HRMS (ESI) calcd for  $\text{C}_{16}\text{H}_{17}\text{NO}_5\text{S}$   $[\text{M}+\text{H}]^+$ : 336.0900, found: 336.0904



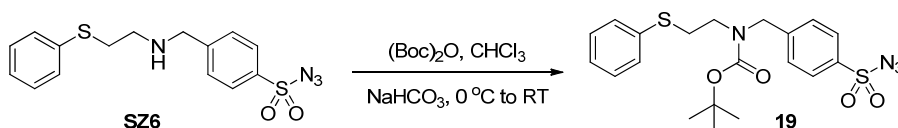
**SZ5TA6**

**Acylsulfonamide SZ5TA6:** was prepared following the general procedure **B** with 10% yield (10 mg).  $R_f = 0.29$  in EtOAc.  $^1\text{H NMR}$  (400 MHz,  $\text{CDCl}_3$ )  $\delta$  8.68 (s, 1H), 8.41 (d,  $J = 7.9$  Hz, 1H), 8.17 (d,  $J = 7.6$  Hz, 1H), 8.06 (d,  $J = 8.0$  Hz, 2H), 7.66 (t,  $J = 7.9$  Hz, 1H), 7.38 (d,  $J = 7.9$  Hz, 2H), 2.45 (s, 3H) ppm.  $^{13}\text{C NMR}$  (101 MHz,  $\text{CDCl}_3$ )  $\delta$  162.46, 148.54, 145.97, 135.11, 133.80, 133.21, 130.46, 129.96, 128.98, 127.93, 123.11, 21.95 ppm. HRMS (ESI) calcd for  $\text{C}_{14}\text{H}_{12}\text{N}_2\text{O}_5\text{S}$   $[\text{M}+\text{H}]^+$ : 321.0540, found: 321.0533

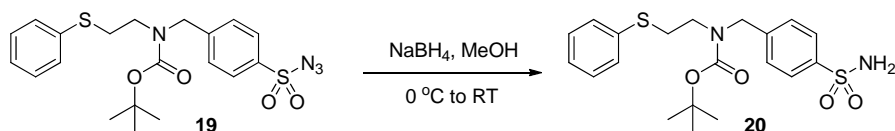


**SZ5TA9**

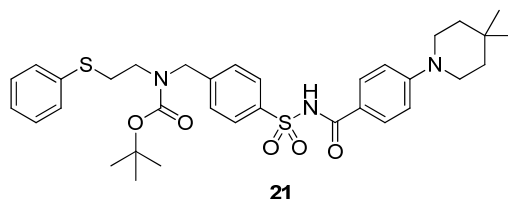
**Acylsulfonamide SZ5TA9:** was prepared following the general procedure **B** with 40% yield (32 mg).  $R_f = 0.4$  in EtOAc.  $^1\text{H NMR}$  (400 MHz,  $\text{CDCl}_3$ )  $\delta$  8.84 (s, 1H), 8.03 (d,  $J = 8.2$  Hz, 2H), 7.50 (s, 1H), 7.34 (d,  $J = 8.1$  Hz, 2H), 7.22 (d,  $J = 3.4$  Hz, 1H), 6.53 (d,  $J = 1.8$  Hz, 1H), 2.43 (s, 3H) ppm.  $^{13}\text{C NMR}$  (101 MHz,  $\text{CDCl}_3$ )  $\delta$  154.53, 145.97, 145.50, 145.40, 135.71, 129.80, 128.82, 118.30, 113.26, 21.89 ppm. HRMS (ESI) calcd for  $\text{C}_{12}\text{H}_{11}\text{NO}_4\text{S}$   $[\text{M}+\text{H}]^+$ : 266.0482, found: 266.0481



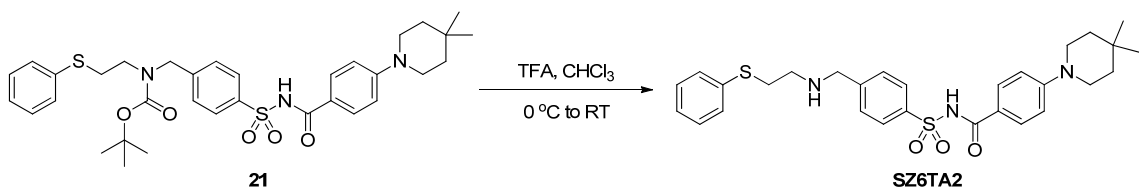
**Sulfonyl Azide 19:** To a solution of sulfonamide **SZ6**<sup>7d</sup> (600 mg, 1.72 mmol) and  $\text{NaHCO}_3$  (145 mg, 1.72 mmol) in  $\text{CHCl}_3$  (6.5 mL) was added  $(\text{Boc})_2\text{O}$  (376 mg, 1.72 mmol) at 0 °C. The reaction mixture was then slowly warmed to room temperature and monitored using TLC until **SZ6** was completely consumed. The reaction mixture was then treated with 1N  $\text{NaHCO}_3$  solution (20 mL) and extracted with  $\text{CHCl}_3$  (15 mL  $\times$  3). The combined organic phases were dried over anhydrous sodium sulfate and concentrated. The crude obtained was subjected to flash chromatography (hexane : EtOAc = 8:1;  $R_f = 0.54$  in hexane : EtOAc = 2:1) to obtain the corresponding sulfonyl azide **19** with 93% yield (717 mg).  $^1\text{H NMR}$  (400 MHz,  $\text{CDCl}_3$ )  $\delta$  7.86 (d,  $J = 8.2$  Hz, 2H), 7.38 – 7.16 (m, 7H), 4.51 (s, 2H), 3.39 – 3.29 (m, 2H), 3.01 – 2.95 (m, 2H), 1.45 (s, 9H) ppm.  $^{13}\text{C NMR}$  (101 MHz,  $\text{CDCl}_3$ )  $\delta$  155.50, 146.12, 137.21, 129.52, 129.07, 128.52, 127.99, 127.78, 126.52, 80.82, 50.48, 47.04, 31.80, 28.32 ppm. HRMS (ESI) calcd for  $\text{C}_{20}\text{H}_{24}\text{N}_4\text{O}_4\text{S}_2$   $[\text{M}+\text{Na}]^+$ : 471.1131, found: 471.1127



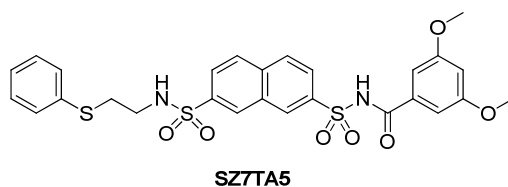
**Sulfonamide 20:** The sulfonamide **20** was prepared starting from sulfonamide **19** (600 mg, 1.54 mmol) following the procedure described for synthesis of sulfonamide **14** with 92% yield (600 mg).  $R_f = 0.42$  in hexane : EtOAc = 1:1.  $^1\text{H}$  NMR (400 MHz,  $\text{CDCl}_3$ )  $\delta$  7.81 (d,  $J = 7.3$  Hz, 2H), 7.30 – 7.13 (m, 7H), 5.16 (s, 2H), 4.45 (s, 2H), 3.34 – 3.27 (m, 2H), 3.00 – 2.89 (m, 2H), 1.43 (s, 9H) ppm.  $^{13}\text{C}$  NMR (101 MHz,  $\text{CDCl}_3$ )  $\delta$  155.57, 143.41, 140.98, 135.12, 129.44, 129.05, 128.08, 127.53, 126.68, 80.73, 50.37, 46.90, 31.66, 28.34 ppm. HRMS (ESI) calcd for  $\text{C}_{20}\text{H}_{26}\text{N}_2\text{O}_4\text{S}_2$   $[\text{M}+\text{Na}]^+$ : 445.1226, found: 445.1219



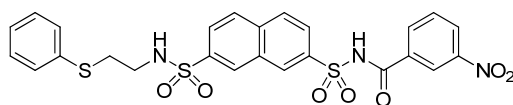
**Acylsulfonamide 21:** was prepared following the general procedure **A** with 85% yield (576 mg).  $R_f = 0.54$  in hexane : EtOAc = 1:1.  $^1\text{H}$  NMR (400 MHz,  $\text{CDCl}_3$ )  $\delta$  8.04 (d,  $J = 8.1$  Hz, 2H), 7.71 (d,  $J = 8.9$  Hz, 2H), 7.31 – 7.06 (m, 9H), 4.47 (s, 2H), 3.38 – 3.30 (m, 6H), 3.01 – 2.90 (m, 2H), 1.59 (t,  $J = 5.4$  Hz, 4H), 1.41 (s, 9H), 1.00 (s, 6H) ppm.  $^{13}\text{C}$  NMR (101 MHz,  $\text{CDCl}_3$ )  $\delta$  163.91, 155.80, 150.97, 137.88, 135.29, 130.25, 129.72, 129.26, 129.09, 127.97, 127.56, 126.68, 126.38, 116.78, 80.99, 50.62, 47.71, 47.23, 37.11, 31.93, 28.52, 28.28, 27.72 ppm. HRMS (ESI) calcd for  $\text{C}_{34}\text{H}_{43}\text{N}_3\text{O}_5\text{S}_2$   $[\text{M}+\text{H}]^+$ : 638.2717, found: 638.2693



**Acylsulfonamide SZ6TA2:** To a solution of acylsulfonamide **21** (437 mg, 0.68 mmol) in CHCl<sub>3</sub> (5 mL) cooled to 0 °C, was added TFA (1.2 mL) dropwise. The reaction mixture was then slowly warmed to room temperature and monitored using TLC until acylsulfonamide **21** was completely consumed. The reaction was then treated with saturated K<sub>2</sub>CO<sub>3</sub> solution (pH = 7) and extracted with CHCl<sub>3</sub> (20 mL × 3). The combined organic phases were dried over anhydrous sodium sulfate and concentrated. The crude obtained was purified using preparative HPLC to afford the acylsulfonamide **SZ6TA2** with 90% yield (330 mg). R<sub>f</sub> = 0.69 in EtOAc : MeOH = 20:1. <sup>1</sup>H NMR (400 MHz, CD<sub>3</sub>OD) δ 8.21 (d, *J* = 8.4 Hz, 2H), 7.77 (dd, *J* = 17.2, 8.7 Hz, 4H), 7.49 (d, *J* = 7.7 Hz, 2H), 7.40 (t, *J* = 7.5 Hz, 2H), 7.32 (t, *J* = 7.3 Hz, 1H), 7.08 (d, *J* = 9.1 Hz, 2H), 4.40 (s, 2H), 3.53 – 3.44 (m, 4H), 3.41 – 3.38 (m, 3H), 1.63 – 1.52 (m, 4H), 1.37 (s, 1H), 1.10 (s, 6H) ppm. <sup>13</sup>C NMR (101 MHz, CD<sub>3</sub>OD) δ 165.85, 154.02, 141.32, 136.66, 133.42, 130.61, 130.22, 130.07, 129.29, 128.91, 127.38, 120.11, 113.83, 50.10, 46.32, 44.57, 37.67, 29.35, 28.26, 26.87 ppm. HRMS (ESI) calcd for C<sub>29</sub>H<sub>35</sub>N<sub>3</sub>O<sub>3</sub>S<sub>2</sub> [M+H]<sup>+</sup>: 538.2193, found: 538.2180

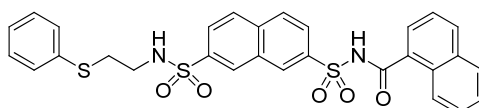


**Acylsulfonamide SZ7TA5:** was prepared following the general procedure **B** with 28% yield (49 mg).  $R_f = 0.31$  in EtOAc.  $^1\text{H}$  NMR (400 MHz,  $\text{CD}_3\text{OD}$ )  $\delta$  8.80 (s, 1H), 8.50 (s, 1H), 8.22 (d,  $J = 8.0$  Hz, 1H), 8.18 – 8.05 (m, 2H), 7.98 (d,  $J = 8.2$  Hz, 1H), 7.17 – 7.01 (m, 5H), 6.97 (s, 2H), 6.67 (s, 1H), 3.77 (s, 6H), 3.07 (t,  $J = 6.1$  Hz, 2H), 2.94 (t,  $J = 6.2$  Hz, 2H).  $^{13}\text{C}$  NMR (101 MHz,  $\text{CD}_3\text{OD}$ )  $\delta$  166.26, 161.22, 139.44, 138.34, 136.65, 134.86, 133.71, 131.15, 131.02, 129.52, 129.10, 128.74, 126.28, 125.57, 105.83, 105.28, 54.86, 41.97, 32.93 ppm. HRMS (ESI) calcd for  $\text{C}_{27}\text{H}_{26}\text{N}_2\text{O}_7\text{S}_3$   $[\text{M}+\text{H}]^+$ : 609.0794, found: 609.0772



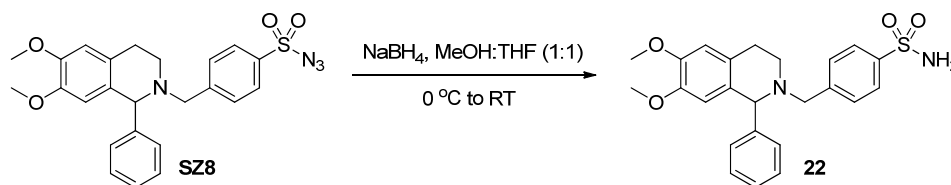
**SZ7TA6**

**Acylsulfonamide SZ7TA6:** was prepared following the general procedure **B** with 46% yield (79 mg).  $R_f = 0.5$  in EtOAc.  $^1\text{H}$  NMR (400 MHz,  $\text{CD}_3\text{OD}$ )  $\delta$  8.79 (s, 1H), 8.61 (s, 1H), 8.47 (s, 1H), 8.37 (d,  $J = 7.4$  Hz, 1H), 8.23 – 8.03 (m, 4H), 7.94 (d,  $J = 8.0$  Hz, 1H), 7.67 (t,  $J = 8.0$  Hz, 1H), 7.15 – 6.95 (m, 6H), 3.04 (t,  $J = 7.0$  Hz, 2H), 2.91 (t,  $J = 7.0$  Hz, 2H) ppm.  $^{13}\text{C}$  NMR (101 MHz,  $\text{CD}_3\text{OD}$ )  $\delta$  164.42, 148.39, 139.47, 138.06, 136.70, 134.89, 133.95, 133.63, 131.31, 131.01, 130.13, 129.54, 129.46, 129.22, 129.12, 128.74, 127.36, 126.24, 125.61, 123.00, 41.99, 32.94 ppm. HRMS (ESI) calcd for  $\text{C}_{25}\text{H}_{21}\text{N}_3\text{O}_7\text{S}_3$   $[\text{M}+\text{H}]^+$ : 572.0614, found: 572.0597

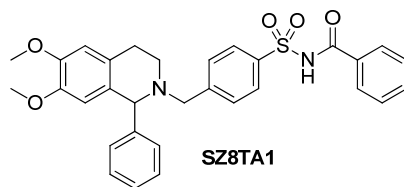


**SZ7TA7**

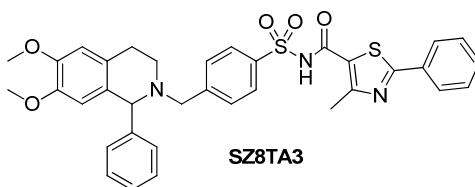
**Acylsulfonamide SZ7TA7:** was prepared following the general procedure **B** with 42% yield (145 mg).  $R_f = 0.48$  in EtOAc : MeOH = 20:1.  $^1\text{H}$  NMR (400 MHz,  $\text{CDCl}_3$ )  $\delta$  8.78 (s, 1H), 8.45 (s, 1H), 8.27 (d,  $J = 8.7$  Hz, 1H), 8.09 (d,  $J = 8.3$  Hz, 1H), 7.98 (d,  $J = 8.7$  Hz, 1H), 7.95 – 7.83 (m, 4H), 7.72 (d,  $J = 8.0$  Hz, 1H), 7.66 (d,  $J = 7.1$  Hz, 1H), 7.43 – 7.29 (m, 4H), 7.14 – 7.05 (m, 5H), 3.11 (m, 2H), 2.93 (t,  $J = 6.4$  Hz, 2H) ppm.  $^{13}\text{C}$  NMR (101 MHz,  $\text{CDCl}_3$ )  $\delta$  166.50, 138.81, 137.55, 136.87, 133.78, 133.36, 131.85, 131.09, 130.43, 130.10, 129.80, 129.53, 129.29, 128.71, 128.18, 127.25, 127.17, 127.02, 126.17, 125.88, 124.85, 124.55, 41.86, 34.12 ppm. HRMS (ESI) calcd for  $\text{C}_{29}\text{H}_{24}\text{N}_2\text{O}_5\text{S}_3$   $[\text{M}+\text{H}]^+$ : 577.0920, found: 577.0905



**Sulfonamide 22:** The sulfonamide **22** was obtained starting from sulfonamide **SZ8** (290 mg, 0.62 mmol) following the procedure described for synthesis of sulfonamide **14** with 89% yield (243 mg).  $R_f = 0.33$  in hexane : EtOAc = 1:1.  $^1\text{H}$  NMR (250 MHz,  $\text{CDCl}_3$ )  $\delta$ : 7.59 (d,  $J = 7.6$  Hz, 2H), 7.22 – 7.00 (m, 7H), 6.39 (s, 1H), 5.99 (s, 1H), 5.28 (bs, 2H), 4.34 (s, 1H), 3.62 – 3.51 (m, 4H), 3.34 (s, 3H), 3.11 (d,  $J = 13.9$  Hz, 1H), 2.85 – 2.67 (m, 2H), 2.55 – 2.42 (m, 1H), 2.36 – 2.21 (m, 1H) ppm.  $^{13}\text{C}$  NMR (63 MHz,  $\text{CDCl}_3$ )  $\delta$  147.44, 147.06, 144.95, 143.84, 140.81, 129.97, 129.51, 129.10, 128.45, 127.52, 126.78, 126.30, 111.75, 111.03, 68.20, 58.26, 55.80, 55.74, 47.26, 28.47 ppm. HRMS (ESI) calcd for  $\text{C}_{24}\text{H}_{26}\text{N}_2\text{O}_4\text{S}$   $[\text{M}+\text{H}]^+$ : 439.1686, found: 439.1682

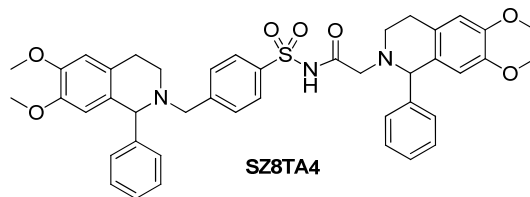


**Acylsulfonamide SZ8TA1:** was prepared following the general procedure **B** with 50% yield (163 mg).  $R_f = 0.4$  in hexane : EtOAc = 1:1.  $^1\text{H}$  NMR (400 MHz,  $\text{CD}_3\text{OD}$ )  $\delta$ : 8.17 (d,  $J = 8.3$  Hz, 2H), 7.77 (d,  $J = 7.8$  Hz, 2H), 7.67 (d,  $J = 8.3$  Hz, 2H), 7.63 – 7.55 (m, 1H), 7.51 – 7.42 (m, 5H), 7.29 (s, 2H), 6.89 (s, 1H), 6.35 (s, 1H), 5.71 (s, 1H), 4.57 (d,  $J = 12.7$  Hz, 1H), 4.35 (bs, 1H), 3.83 (s, 3H), 3.71 – 3.60 (m, 1H), 3.57 (s, 3H), 3.49 – 3.37 (m, 2H), 3.23 (d,  $J = 5.4$  Hz, 2H) ppm.  $^{13}\text{C}$  NMR (101 MHz,  $\text{CD}_3\text{OD}$ )  $\delta$  166.83, 149.85, 148.85, 141.35, 136.04, 135.70, 133.27, 132.08, 131.45, 130.70, 130.04, 129.21, 128.99, 128.62, 128.09, 123.76, 111.17, 66.85, 56.59, 55.27, 55.19, 45.22, 23.57 ppm. HRMS (ESI) calcd for  $\text{C}_{31}\text{H}_{30}\text{N}_2\text{O}_5\text{S}$   $[\text{M}+\text{H}]^+$ : 543.1948, found: 543.1936

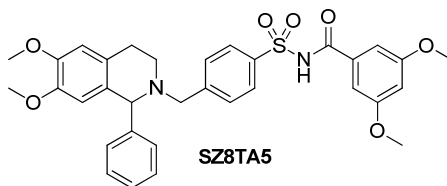


**Acylsulfonamide SZ8TA3:** was prepared following the general procedure **A** with 14% yield (20 mg).  $R_f = 0.35$  in EtOAc.  $^1\text{H}$  NMR (400 MHz,  $\text{CDCl}_3$ )  $\delta$ : 8.09 (bs, 2H), 7.82 (d,  $J = 7.2$  Hz, 2H), 7.63 (bs, 2H), 7.47 – 7.34 (m, 6H), 7.24 (bs, 2H), 6.67 (s, 1H), 6.25 (s, 1H), 4.51 (d,  $J = 10.1$  Hz, 1H), 3.82 (s, 3H), 3.65 (s, 3H), 3.58 – 3.34 (m, 3H), 3.33 – 3.06 (m, 3H), 2.60 (s, 3H) ppm.  $^{13}\text{C}$  NMR (101 MHz,  $\text{CDCl}_3$ )  $\delta$ : 169.52, 161.45, 159.66, 149.51, 148.72, 140.63, 135.02, 133.97, 132.17, 131.55, 131.41, 130.99, 130.28, 129.72,

129.22, 129.12, 126.89, 126.61, 122.50, 122.22, 110.54, 65.52, 55.88, 43.00, 23.67, 17.73 ppm. HRMS (ESI) calcd for C<sub>35</sub>H<sub>33</sub>N<sub>3</sub>O<sub>5</sub>S<sub>2</sub> [M+H]<sup>+</sup>: 640.1940, found: 640.1935

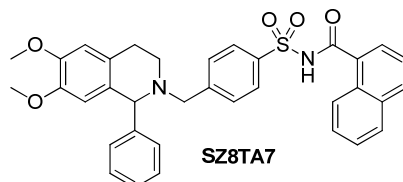


**Acylsulfonamide SZ8TA4:** was prepared following the general procedure **A** with 18% yield (31 mg). R<sub>f</sub> = 0.45 in EtOAc. <sup>1</sup>H NMR (400 MHz, CDCl<sub>3</sub>) δ: 9.58 (bs, 1H), 7.98 (bs, 2H), 7.56 (bs, 2H), 7.39 – 7.18 (m, 11H), 6.65 (s, 2H), 6.20 (s, 2H), 5.68 (s, 1H), 4.45 – 4.25 (m, 2H), 4.07 – 3.96 (m, 3H), 3.84 (s, 3H), 3.83 (s, 3H), 3.60 (s, 6H), 3.38 (bs, 3H), 3.13 – 3.03 (m, 4H) ppm. <sup>13</sup>C NMR (101 MHz, CDCl<sub>3</sub>) δ: 165.34, 149.47, 148.56, 140.50, 134.64, 131.67, 130.80, 130.16, 129.71, 129.25, 129.13, 128.63, 127.99, 122.76, 121.64, 120.84, 110.84, 110.63, 66.50, 65.95, 56.20, 55.85, 54.09, 45.50, 23.51 ppm. HRMS (ESI) calcd for C<sub>43</sub>H<sub>45</sub>N<sub>3</sub>O<sub>7</sub>S [M+H]<sup>+</sup>: 748.3057, found: 748.3062

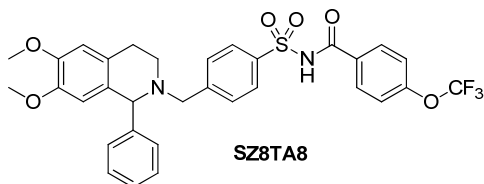


**Acylsulfonamide SZ8TA5:** was prepared following the general procedure **B** with 42% yield (152 mg). R<sub>f</sub> = 0.58 in hexane : EtOAc = 1:3. <sup>1</sup>H NMR (400 MHz, CD<sub>3</sub>OD) δ: 8.21 – 8.12 (m, 2H), 7.69 – 7.63 (m, 2H), 7.49 – 7.43 (m, 3H), 7.30 – 7.25 (m, 2H), 6.94 – 6.85 (m, 3H), 6.69 – 6.65 (m, 1H), 6.33 (s, 1H), 5.64 (s, 1H), 4.50 (d, J = 13.1 Hz, 1H), 3.83 (s, 3H), 3.76 (s, 6H), 3.67 – 3.60 (m, 1H), 3.57 (s, 3H), 3.46 – 3.34 (m, 1H), 3.31 –

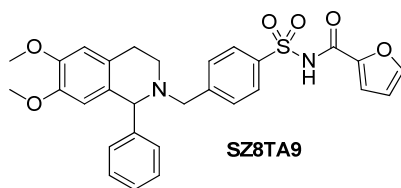
3.26 (m, 1H), 3.23 – 3.15 (m, 2H) ppm.  $^{13}\text{C}$  NMR (101 MHz,  $\text{CD}_3\text{OD}$ )  $\delta$ : 166.18, 161.04, 149.68, 148.67, 141.13, 135.56, 133.58, 131.29, 130.51, 129.89, 129.20, 129.02, 128.84, 123.41, 110.95, 110.88, 105.64, 104.85, 66.54, 56.29, 55.03, 54.95, 54.65, 23.20 ppm. HRMS (ESI) calcd for  $\text{C}_{33}\text{H}_{34}\text{N}_2\text{O}_7\text{S}$   $[\text{M}+\text{H}]^+$ : 603.2160, found: 603.2145



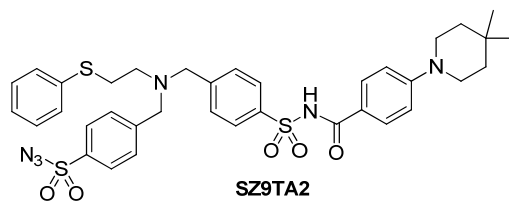
**Acylsulfonamide SZ8TA7:** was prepared following the general procedure A with 48% yield (97 mg).  $R_f = 0.41$  in hexane : EtOAc = 1:1.  $^1\text{H}$  NMR (400 MHz,  $\text{CD}_3\text{OD}$ )  $\delta$  8.24 (d,  $J = 8.1$  Hz, 2H), 8.07 – 7.86 (m, 4H), 7.77 – 7.66 (m, 4H), 7.54 – 7.45 (m, 5H), 7.32 – 7.26 (m, 1H), 6.90 (s, 1H), 6.34 (s, 1H), 5.68 (s, 1H), 4.58 (d,  $J = 12.9$  Hz, 1H), 3.84 (s, 3H), 3.70 – 3.62 (m, 1H), 3.55 (s, 3H), 3.48 – 3.40 (m, 1H), 3.35 – 3.30 (m, 1H), 3.26 – 3.19 (m, 2H) ppm.  $^{13}\text{C}$  NMR (101 MHz,  $\text{CD}_3\text{OD}$ )  $\delta$  168.17, 150.02, 148.99, 141.41, 135.69, 135.18, 133.95, 133.65, 132.18, 131.79, 130.80, 130.52, 130.26, 129.33, 129.16, 128.53, 127.42, 126.92, 126.55, 124.52, 124.28, 123.53, 121.83, 111.22, 111.08, 66.62, 56.41, 55.29, 55.19, 45.10, 23.25 ppm. HRMS (ESI) calcd for  $\text{C}_{35}\text{H}_{32}\text{N}_2\text{O}_5\text{S}$   $[\text{M}+\text{H}]^+$ : 593.2105, found: 593.2094



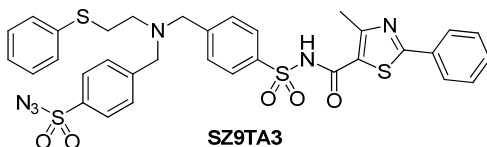
**Acylsulfonamide SZ8TA8:** was prepared following the general procedure **A** with 44% yield (50 mg).  $R_f = 0.63$  in EtOAc : MeOH = 20:1.  $^1\text{H}$  NMR (400 MHz,  $\text{CD}_3\text{OD}$ )  $\delta$  7.98 (d,  $J = 8.2$  Hz, 2H), 7.71 (d,  $J = 8.7$  Hz, 2H), 7.54 (d,  $J = 8.2$  Hz, 2H), 7.30 – 7.23 (m, 3H), 7.14 (d,  $J = 8.2$  Hz, 4H), 6.69 (s, 1H), 6.17 (s, 1H), 5.57 (s, 1H), 4.40 (d,  $J = 13.3$  Hz, 1H), 4.20 (s, 1H), 3.63 (s, 3H), 3.53 – 3.44 (m, 1H), 3.36 (s, 3H), 3.15 – 3.02 (m, 3H) ppm.  $^{13}\text{C}$  NMR (101 MHz,  $\text{CD}_3\text{OD}$ )  $\delta$  165.65, 152.66, 149.86, 148.82, 141.39, 135.45, 135.11, 131.81, 130.89, 130.55, 130.20, 129.29, 128.99, 123.64, 122.17, 120.53, 120.49 (q,  $J = 259.81$  Hz), 111.22, 111.14, 66.88, 56.53, 55.29, 55.22, 45.14, 23.42 ppm. HRMS (ESI) calcd for  $\text{C}_{32}\text{H}_{29}\text{F}_3\text{N}_2\text{O}_6\text{S}$   $[\text{M}+\text{H}]^+$ : 627.1771, found: 627.1785



**Acylsulfonamide SZ8TA9:** was prepared following the general procedure **A** with 49% yield (47 mg).  $R_f = 0.52$  in EtOAc : MeOH = 20:1.  $^1\text{H}$  NMR (400 MHz,  $\text{CD}_3\text{OD}$ )  $\delta$  8.13 (d,  $J = 7.8$  Hz, 2H), 7.73 – 7.65 (m, 3H), 7.44 (s, 3H), 7.31 (s, 2H), 7.25 (d,  $J = 3.2$  Hz, 1H), 6.88 (s, 1H), 6.58 (d,  $J = 2.0$  Hz, 1H), 6.35 (s, 1H), 5.73 (s, 1H), 4.57 (d,  $J = 12.9$  Hz, 1H), 4.36 (s, 1H), 3.82 (s, 3H), 3.70 – 3.60 (m, 1H), 3.56 (s, 3H), 3.49 – 3.40 (m, 1H), 3.23 (s, 2H) ppm.  $^{13}\text{C}$  NMR (101 MHz,  $\text{CD}_3\text{OD}$ )  $\delta$  156.66, 149.87, 148.83, 147.32, 145.55, 141.36, 135.47, 135.06, 131.77, 130.84, 130.19, 129.27, 128.89, 123.58, 122.05, 118.06, 112.46, 111.18, 111.09, 66.81, 56.51, 55.29, 55.21, 45.10, 23.34 ppm. HRMS (ESI) calcd for  $\text{C}_{29}\text{H}_{28}\text{N}_2\text{O}_6\text{S}$   $[\text{M}+\text{H}]^+$ : 533.1741, found: 533.1735



**Acylsulfonamide SZ9TA2:** was prepared following the general procedure **A** with 60% yield (169 mg).  $R_f = 0.56$  in hexane : EtOAc = 1:1.  $^1\text{H}$  NMR (400 MHz,  $\text{CDCl}_3$ )  $\delta$ : 8.08 (d,  $J = 8.4$  Hz, 2H), 7.85 (d,  $J = 8.0$  Hz, 2H), 7.63 (d,  $J = 8.6$  Hz, 2H), 7.56 (d,  $J = 8.4$  Hz, 2H), 7.51 (d,  $J = 8.0$  Hz, 2H), 7.22 – 7.12 (m, 5H), 6.86 (d,  $J = 9.2$  Hz, 2H), 3.77 (d,  $J = 4.8$  Hz, 4H), 3.32 (t,  $J = 5.8$  Hz, 4H), 3.06 (t,  $J = 7.2$  Hz, 2H), 2.79 (t,  $J = 7.2$  Hz, 2H), 1.47 (t,  $J = 5.6$  Hz, 4H), 0.98 (s, 6H) ppm.  $^{13}\text{C}$  NMR (101 MHz,  $\text{CDCl}_3$ )  $\delta$ : 154.12, 147.00, 136.96, 135.69, 130.03, 129.54, 128.96, 128.87, 128.72, 128.30, 127.46, 126.11, 113.06, 57.87, 57.69, 52.65, 43.87, 37.79, 31.29, 28.53, 27.70, 27.59 ppm. HRMS (ESI) calcd for  $\text{C}_{36}\text{H}_{40}\text{N}_6\text{O}_5\text{S}_3$   $[\text{M}+\text{H}]^+$ : 733.2295, found: 733.2297



**Acylsulfonamide SZ9TA3:** was prepared following the general procedure **A** with 45% yield (62 mg).  $R_f = 0.66$  in EtOAc : MeOH = 20:1.  $^1\text{H}$  NMR (400 MHz,  $\text{DMSO}-d_6$ )  $\delta$  8.01 – 7.95 (m, 4H), 7.95 – 7.91 (m, 2H), 7.76 (d,  $J = 8.4$ , 2H), 7.66 (d,  $J = 8.2$ , 2H), 7.53 – 7.49 (m, 3H), 7.19 – 7.15 (m, 4H), 7.09 – 7.04 (m, 1H), 3.91 (s, 4H), 3.21 (t,  $J = 7.1$  Hz, 2H), 2.73 (s, 2H), 2.55 (s, 3H) ppm.  $^{13}\text{C}$  NMR (101 MHz,  $\text{DMSO}-d_6$ )  $\delta$  168.41, 161.13, 159.47, 145.80, 143.06, 139.86, 136.90, 135.55, 132.49, 131.71, 130.99, 129.91, 129.77, 129.33, 128.55, 128.21, 127.80, 126.85, 126.15, 124.67, 57.27, 57.14, 52.14,

29.03, 17.81 ppm. HRMS (ESI) calcd for  $C_{33}H_{30}N_6O_5S_4$   $[M+H]^+$ : 719.1233, found: 719.1228



**Acylsulfonamide SZ9TA7:** was prepared following the general procedure **A** with 69% yield (45 mg).  $R_f = 0.44$  in hexane : EtOAc = 1:1.  $^1H$  NMR (400 MHz,  $CDCl_3$ )  $\delta$ : 8.44 (s, 1H), 7.96 (d,  $J = 8.0$  Hz, 2H), 7.74 – 7.68 (m, 3H), 7.60 – 7.51 (m, 3H), 7.35 (d,  $J = 8.0$  Hz, 2H), 7.18 – 6.93 (m, 10H), 3.37 (s, 2H), 3.31 (s, 2H), 2.86 (t,  $J = 6.4$  Hz, 2H), 2.50 (bs, 2H) ppm.  $^{13}C$  NMR (101 MHz,  $CDCl_3$ )  $\delta$ : 146.99, 143.43, 140.01, 136.83, 135.75, 133.39, 131.40, 130.42, 129.47, 128.86, 128.82, 128.66, 127.93, 127.66, 127.36, 127.12, 126.86, 126.06, 125.73, 124.34, 57.60, 57.39, 52.47, 31.14 ppm. HRMS (ESI) calcd for  $C_{33}H_{29}N_5O_5S_3$   $[M+H]^+$ : 672.1404, found: 672.1409

## 2.4.12 Mutant Bcl-X<sub>L</sub> (<sup>R139A</sup>Bcl-X<sub>L</sub>) experiments: LC/MS-SIM analysis

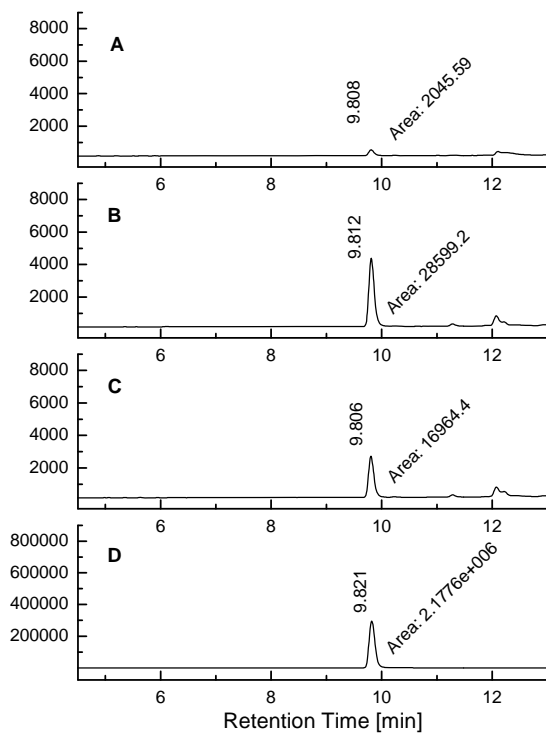


**Figure 2.6.** Bcl-X<sub>L</sub> and mutant Bcl-X<sub>L</sub> templated incubations with **SZ7** and **TA2**. The samples were incubated for six hours at 37 °C and subjected to LC/MS-SIM analysis with gradient system 1. A) Incubation of **SZ7** and **TA2** without Bcl-X<sub>L</sub> B) Incubation of **SZ7** and **TA2** with 2 μM Bcl-X<sub>L</sub> C) Incubation of **SZ7** and **TA2** with 2 μM mutant Bcl-X<sub>L</sub> D) Synthetic **SZ7TA2** as the reference.

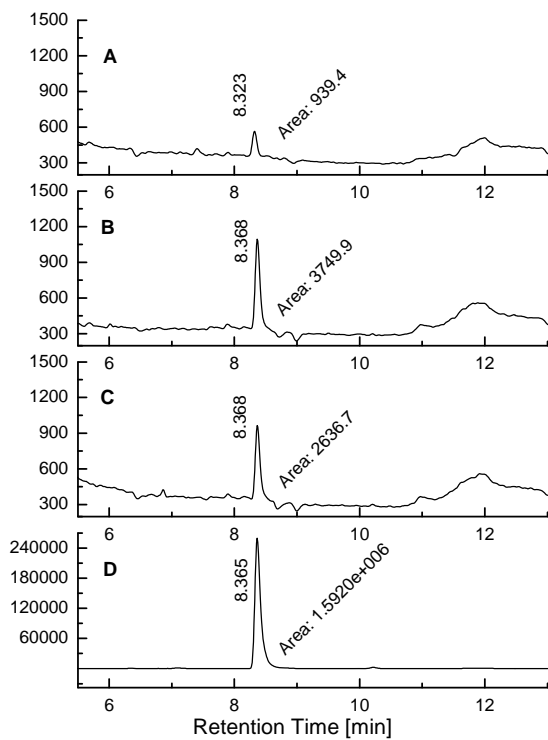


**Figure 2.7.** Bcl-X<sub>L</sub> and mutant Bcl-X<sub>L</sub> templated incubations with **SZ9** and **TA1**. The samples were incubated for six hours at 37 °C and subjected to LC/MS-SIM analysis with gradient system 1. A) Incubation of **SZ9** and **TA1** without Bcl-X<sub>L</sub> B) Incubation of **SZ9** and **TA1** with 2 μM Bcl-X<sub>L</sub> C) Incubation of **SZ9** and **TA1** with 2 μM mutant Bcl-X<sub>L</sub> D) Synthetic **SZ9TA1** as the reference.

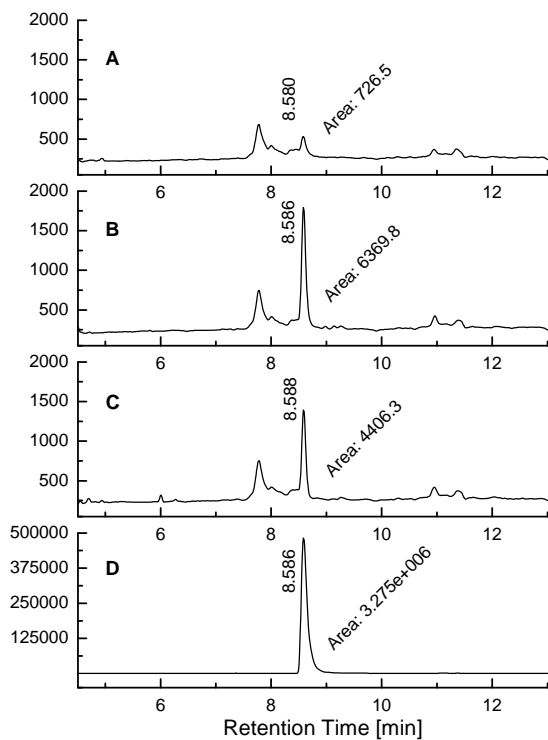


**Figure 2.8.** Bcl-X<sub>L</sub> and mutant Bcl-X<sub>L</sub> templated incubations with **SZ9** and **TA5**. The samples were incubated for six hours at 37 °C and subjected to LC/MS-SIM analysis with gradient system 1. A) Incubation of **SZ9** and **TA5** without Bcl-X<sub>L</sub> B) Incubation of **SZ9** and **TA5** with 2 μM Bcl-X<sub>L</sub> C) Incubation of **SZ9** and **TA5** with 2 μM mutant Bcl-X<sub>L</sub> D) Synthetic **SZ9TA5** as the reference.

### 2.4.13 Peptide control experiments: LC/MS-SIM analysis

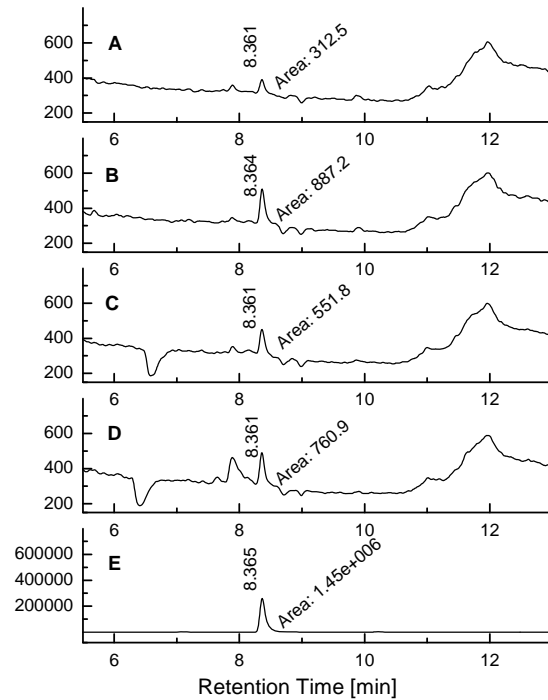


**Figure 2.9.** Incubation of **SZ9** and **TA1** and suppressing Bcl-X<sub>L</sub>-templated incubations with Bim and mutant Bim. The samples were incubated for six hours at 37 °C and subjected to LC/MS-SIM analysis with gradient system 1. A) Incubation of **SZ9** and **TA1** without Bcl-X<sub>L</sub> B) Incubation of **SZ9** and **TA1** with 2 μM Bcl-X<sub>L</sub> C) Incubation of **SZ9** and **TA1** with 2 μM Bcl-X<sub>L</sub> and 20 μM Bim D) Incubation of **SZ9** and **TA1** with 2 μM Bcl-X<sub>L</sub> and 20 μM mutant Bim E) Synthetic **SZ9TA1** as the reference.

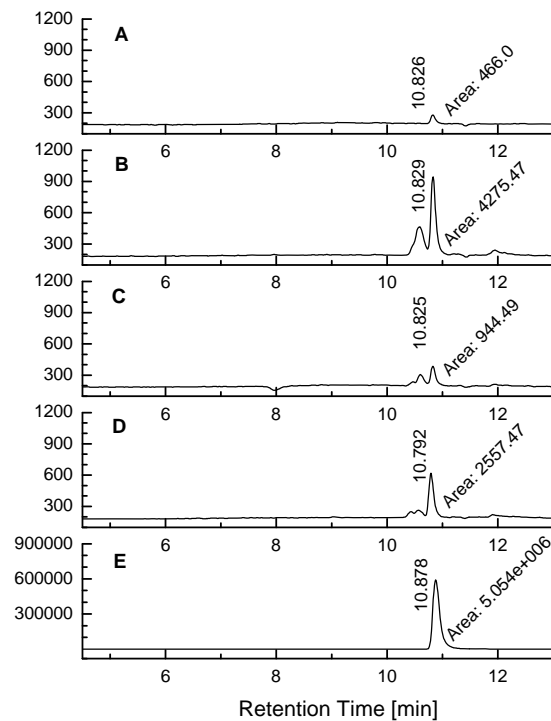


**Figure 2.10.** Incubation of **SZ9** and **TA5** and suppressing Bcl-X<sub>L</sub>-templated incubations with Bim and mutant Bim. The samples were incubated for six hours at 37 °C and subjected to LC/MS-SIM analysis with gradient system 2. A) Incubation of **SZ9** and **TA5** without Bcl-X<sub>L</sub> B) Incubation of **SZ9** and **TA5** with 2 μM Bcl-X<sub>L</sub> C) Incubation of **SZ9** and **TA5** with 2 μM Bcl-X<sub>L</sub> and 20 μM Bim D) Incubation of **SZ9** and **TA5** with 2 μM Bcl-X<sub>L</sub> and 20 μM mutant Bim E) Synthetic **SZ9TA5** as the reference.

## 2.5 References cited

1. (a) Wells, J. A.; McClendon, C. L., Reaching for high-hanging fruit in drug discovery at protein-protein interfaces. *Nature* **2007**, *450* (7172), 1001-1009; (b) Arkin, M., Protein-protein interactions and cancer: small molecules going in for the kill. *Curr. Opin. Chem. Biol.* **2005**, *9* (3), 317-324; (c) Arkin, M. R.; Wells, J. A., Small-molecule inhibitors of protein-protein interactions: Progressing towards the dream. *Nat. Rev. Drug Discov.* **2004**, *3* (4), 301-317; (d) Berg, T., Modulation of protein-protein interactions with small organic molecules. *Angew. Chem., Int. Ed.* **2003**, *42* (22), 2462-2481.
2. (a) Preissner, R.; Goede, A.; Frommel, C., Dictionary of interfaces in proteins (DIP). Data bank of complementary molecular surface patches. *J. Mol. Biol.* **1998**, *280* (3), 535-550; (b) McCoy, A. J.; Epa, V. C.; Colman, P. M., Electrostatic complementarity at protein/protein interfaces. *J. Mol. Biol.* **1997**, *268* (2), 570-584.
3. (a) DeLano, W. L.; Ultsch, M. H.; de Vos, A. M.; Wells, J. A., Convergent solutions to binding at a protein-protein interface. *Science* **2000**, *287* (5456), 1279-1283; (b) Janin, J.; Henrick, K.; Moulton, J.; Ten Eyck, L.; Sternberg, M. J. E.; Vajda, S.; Vasker, I.; Wodak, S. J., CAPRI: A Critical Assessment of PRedicted Interactions. *Proteins* **2003**, *52* (1), 2-9; (c) Nooren, I. M. A.; Thornton, J. M., Structural characterisation and functional significance of transient protein-protein interactions. *J. Mol. Biol.* **2003**, *325* (5), 991-1018.
4. (a) Lo Conte, L.; Chothia, C.; Janin, J., The atomic structure of protein-protein recognition sites. *J. Mol. Biol.* **1999**, *285* (5), 2177-2198; (b) Nooren, I. M. A.; Thornton, J. M., Diversity of protein-protein interactions. *EMBO J.* **2003**, *22* (14), 3486-3492.

5. (a) Clackson, T.; Wells, J. A., A Hot-Spot of Binding-Energy in a Hormone-Receptor Interface. *Science* **1995**, *267* (5196), 383-386; (b) Bogan, A. A.; Thorn, K. S., Anatomy of hot spots in protein interfaces. *J. Mol. Biol.* **1998**, *280* (1), 1-9; (c) DeLano, W. L., Unraveling hot spots in binding interfaces: progress and challenges. *Curr. Opin. Struc. Biol.* **2002**, *12* (1), 14-20.
6. (a) Stigers, K. D.; Soth, M. J.; Nowick, J. S., Designed molecules that fold to mimic protein secondary structures. *Curr. Opin. Chem. Biol.* **1999**, *3* (6), 714-723; (b) Hu, X. D.; Manetsch, R., Kinetic target-guided synthesis. *Chem. Soc. Rev.* **2010**, *39* (4), 1316-1324.
7. (a) Mamidyala, S. K.; Finn, M. G., In situ click chemistry: probing the binding landscapes of biological molecules. *Chem. Soc. Rev.* **2010**, *39* (4), 1252-1261; (b) Sharpless, K. B.; Manetsch, R., In situ click chemistry: a powerful means for lead discovery. *Expert Opin. Drug Discovery* **2006**, *1* (6), 525-538; (c) Corbett, P. T.; Leclaire, J.; Vial, L.; West, K. R.; Wietor, J. L.; Sanders, J. K. M.; Otto, S., Dynamic combinatorial chemistry. *Chem. Rev.* **2006**, *106* (9), 3652-3711; (d) Hu, X. D.; Sun, J. Z.; Wang, H. G.; Manetsch, R., Bcl-X-L-templated assembly of its own protein-protein interaction modulator from fragments decorated with thio acids and sulfonyl azides. *J. Am. Chem. Soc.* **2008**, *130* (42), 13820-13821.
8. (a) Shangguan, N.; Katukojvala, S.; Greenburg, R.; Williams, L. J., The reaction of thio acids with azides: A new mechanism and new synthetic applications. *J. Am. Chem. Soc.* **2003**, *125* (26), 7754-7755; (b) Kolakowski, R. V.; Shangguan, N.; Sauers, R. R.; Williams, L. J., Mechanism of thio acid/azide amidation. *J. Am. Chem. Soc.* **2006**, *128* (17), 5695-5702.

9. Rijkers, D. T. S.; Merkx, R.; Yim, C. B.; Brouwer, A. J.; Liskamp, R. M. J., 'Sulfo-click' for ligation as well as for site-specific conjugation with peptides, fluorophores, and metal chelators. *J. Pept. Sci.* **2010**, *16* (1), 1-5.
10. Mammen, M.; Choi, S. K.; Whitesides, G. M., Polyvalent interactions in biological systems: Implications for design and use of multivalent ligands and inhibitors. *Angew. Chem., Int. Ed.* **1998**, *37* (20), 2755-2794.
11. Danial, N. N.; Korsmeyer, S. J., Cell death: Critical control points. *Cell* **2004**, *116* (2), 205-219.
12. (a) Green, D. R.; Evan, G. I., A matter of life and death. *Cancer Cell* **2002**, *1* (1), 19-30; (b) Reed, J. C., Apoptosis-regulating proteins as targets for drug discovery. *Trends Mol. Med.* **2001**, *7* (7), 314-319.
13. (a) Reed, J. C.; Miyashita, T.; Takayama, S.; Wang, H. G.; Sato, T.; Krajewski, S.; AimeSempe, C.; Bodrug, S.; Kitada, S.; Hanada, M., BCL-2 family proteins: Regulators of cell death involved in the pathogenesis of cancer and resistance to therapy. *J. Cell. Biochem.* **1996**, *60* (1), 23-32; (b) Reed, J. C., Bcl-2 family proteins: strategies for overcoming chemoresistance in cancer. *Adv. Pharmacol. (San Diego)* **1997**, *41* (Apoptosis), 501-532.
14. (a) Green, D. R., At the gates of death. *Cancer Cell* **2006**, *9* (5), 328-330; (b) Youle, R. J.; Strasser, A., The BCL-2 protein family: opposing activities that mediate cell death. *Nat. Rev. Mol. Cell Biol.* **2008**, *9* (1), 47-59.
15. (a) Sattler, M.; Liang, H.; Nettlesheim, D.; Meadows, R. P.; Harlan, J. E.; Eberstadt, M.; Yoon, H. S.; Shuker, S. B.; Chang, B. S.; Minn, A. J.; Thompson, C. B.; Fesik, S. W., Structure of Bcl-x(L)-Bak peptide complex: Recognition between regulators

of apoptosis. *Science* **1997**, *275* (5302), 983-986; (b) Czabotar, P. E.; Lee, E. F.; van Delft, M. F.; Day, C. L.; Smith, B. J.; Huang, D. C. S.; Fairlie, W. D.; Hinds, M. G.; Colman, P. M., Structural insights into the degradation of Mcl-1 induced by BH3 domains. *Proc. Natl. Acad. Sci. U.S.A.* **2007**, *104* (15), 6217-6222.

16. (a) Oltersdorf, T.; Elmore, S. W.; Shoemaker, A. R.; Armstrong, R. C.; Augeri, D. J.; Belli, B. A.; Bruncko, M.; Deckwerth, T. L.; Dinges, J.; Hajduk, P. J.; Joseph, M. K.; Kitada, S.; Korsmeyer, S. J.; Kunzer, A. R.; Letai, A.; Li, C.; Mitten, M. J.; Nettesheim, D. G.; Ng, S.; Nimmer, P. M.; O'Connor, J. M.; Oleksijew, A.; Petros, A. M.; Reed, J. C.; Shen, W.; Tahir, S. K.; Thompson, C. B.; Tomaselli, K. J.; Wang, B. L.; Wendt, M. D.; Zhang, H. C.; Fesik, S. W.; Rosenberg, S. H., An inhibitor of Bcl-2 family proteins induces regression of solid tumours. *Nature* **2005**, *435* (7042), 677-681; (b) Wendt, M. D.; Shen, W.; Kunzer, A.; McClellan, W. J.; Bruncko, M.; Oost, T. K.; Ding, H.; Joseph, M. K.; Zhang, H. C.; Nimmer, P. M.; Ng, S. C.; Shoemaker, A. R.; Petros, A. M.; Oleksijew, A.; Marsh, K.; Bauch, J.; Oltersdorf, T.; Belli, B. A.; Martineau, D.; Fesik, S. W.; Rosenberg, S. H.; Elmore, S. W., Discovery and structure-activity relationship of antagonists of B-cell lymphoma 2 family proteins with chemopotential activity in vitro and in vivo. *J. Med. Chem.* **2006**, *49* (3), 1165-1181; (c) Petros, A. M.; Dinges, J.; Augeri, D. J.; Baumeister, S. A.; Betebenner, D. A.; Bures, M. G.; Elmore, S. W.; Hajduk, P. J.; Joseph, M. K.; Landis, S. K.; Nettesheim, D. G.; Rosenberg, S. H.; Shen, W.; Thomas, S.; Wang, X. L.; Zanze, I.; Zhang, H. C.; Fesik, S. W., Discovery of a potent inhibitor of the antiapoptotic protein Bcl-x(L) from NMR and parallel synthesis. *J. Med. Chem.* **2006**, *49* (2), 656-663.

17. Wu, X. H.; Hu, L. Q., Efficient amidation from carboxylic acids and azides via selenocarboxylates: Application to the coupling of amino acids and peptides with azides. *J. Org. Chem.* **2007**, *72* (3), 765-774.
18. Manetsch, R.; Krasinski, A.; Radic, Z.; Raushel, J.; Taylor, P.; Sharpless, K. B.; Kolb, H. C., In situ click chemistry: Enzyme inhibitors made to their own specifications. *J. Am. Chem. Soc.* **2004**, *126* (40), 12809-12818.
19. Yamaguchi, H.; Wang, H. G., Bcl-XL protects BimEL-induced Bax conformational change and cytochrome c release independent of interacting with Bax or BimEL. *J. Biol. Chem.* **2002**, *277* (44), 41604-41612.
20. (a) Albert, J. S.; Blomberg, N.; Breeze, A. L.; Brown, A. J. H.; Burrows, J. N.; Edwards, P. D.; Folmer, R. H. A.; Geschwindner, S.; Griffen, E. J.; Kenny, P. W.; Nowak, T.; Olsson, L. L.; Sanganee, H.; Shapiro, A. B., An integrated approach to fragment-based lead generation: Philosophy, strategy and case studies from AstraZeneca's drug discovery programmes. *Curr. Top. Med. Chem.* **2007**, *7* (16), 1600-1629; (b) Erlanson, D. A., Fragment-based lead discovery: a chemical update. *Curr. Opin. Biotechnol.* **2006**, *17* (6), 643-652; (c) Carr, R. A. E.; Congreve, M.; Murray, C. W.; Rees, D. C., Fragment-based lead discovery: leads by design. *Drug Discov. Today* **2005**, *10* (14), 987-992.
21. (a) Poulsen, S. A.; Bornaghi, L. F., Fragment-based drug discovery of carbonic anhydrase II inhibitors by dynamic combinatorial chemistry utilizing alkene cross metathesis. *Bioorg. Med. Chem.* **2006**, *14* (10), 3275-3284; (b) Schulz, M. N.; Hubbard, R. E., Recent progress in fragment-based lead discovery. *Curr. Opin. Pharmacol.* **2009**, *9* (5), 615-621; (c) Congreve, M.; Chessari, G.; Tisi, D.; Woodhead, A. J., Recent

developments in fragment-based drug discovery. *J. Med. Chem.* **2008**, *51* (13), 3661-3680.

22. Murray, C. W.; Rees, D. C., The rise of fragment-based drug discovery. *Nat. Chem.* **2009**, *1* (3), 187-192.

23. Hajduk, P. J., Fragment-based drug design: How big is too big? *J. Med. Chem.* **2006**, *49* (24), 6972-6976.

24. (a) Nguyen, R.; Huc, I., Using an enzyme's active site to template inhibitors. *Angew. Chem., Int. Ed.* **2001**, *40* (9), 1774-1776; (b) Mocharla, V. P.; Colasson, B.; Lee, L. V.; Roper, S.; Sharpless, K. B.; Wong, C. H.; Kolb, H. C., In situ click chemistry: Enzyme-generated inhibitors of carbonic anhydrase II. *Angew. Chem., Int. Ed.* **2005**, *44* (1), 116-120.

25. (a) Krasinski, A.; Radic, Z.; Manetsch, R.; Raushel, J.; Taylor, P.; Sharpless, K. B.; Kolb, H. C., In situ selection of lead compounds by click chemistry: Target-guided optimization of acetylcholinesterase inhibitors. *J. Am. Chem. Soc.* **2005**, *127* (18), 6686-6692; (b) Whiting, M.; Muldoon, J.; Lin, Y. C.; Silverman, S. M.; Lindstrom, W.; Olson, A. J.; Kolb, H. C.; Finn, M. G.; Sharpless, K. B.; Elder, J. H.; Fokin, V. V., Inhibitors of HIV-1 protease by using in situ click chemistry. *Angew. Chem., Int. Ed.* **2006**, *45* (9), 1435-1439; (c) Wang, J. Y.; Sui, G. D.; Mocharla, V. P.; Lin, R. J.; Phelps, M. E.; Kolb, H. C.; Tseng, H. R., Integrated microfluidics for parallel screening of an in situ click chemistry library. *Angew. Chem., Int. Ed.* **2006**, *45* (32), 5276-5281; (d) Hirose, T.; Sunazuka, T.; Sugawara, A.; Endo, A.; Iguchi, K.; Yamamoto, T.; Ui, H.; Shiomi, K.; Watanabe, T.; Sharpless, K. B.; Omura, S., Chitinase inhibitors: extraction of the active framework from natural argifin and use of in situ click chemistry. *J. Antibiot.* **2009**, *62*

- (5), 277-282; (e) Agnew, H. D.; Rohde, R. D.; Millward, S. W.; Nag, A.; Yeo, W. S.; Hein, J. E.; Pitram, S. M.; Tariq, A. A.; Burns, V. M.; Krom, R. J.; Fokin, V. V.; Sharpless, K. B.; Heath, J. R., Iterative In Situ Click Chemistry Creates Antibody-like Protein-Capture Agents. *Angew. Chem., Int. Ed.* **2009**, *48* (27), 4944-4948; (f) Wang, Y. J.; Lin, W. Y.; Liu, K.; Lin, R. J.; Selke, M.; Kolb, H. C.; Zhang, N. G.; Zhao, X. Z.; Phelps, M. E.; Shen, C. K. F.; Faull, K. F.; Tseng, H. R., An integrated microfluidic device for large-scale in situ click chemistry screening. *Lab Chip* **2009**, *9* (16), 2281-2285.
26. Jencks, W. P., On the Attribution and Additivity of Binding-Energies. *Proc. Natl. Acad. Sci. U.S.A.* **1981**, *78* (7), 4046-4050.
27. (a) Bourne, Y.; Kolb, H. C.; Radic, Z.; Sharpless, K. B.; Taylor, P.; Marchot, P., Freeze-frame inhibitor captures acetylcholinesterase in a unique conformation. *Proc. Natl. Acad. Sci. U.S.A.* **2004**, *101* (6), 1449-1454; (b) Bourne, Y.; Radic, Z.; Kolb, H. C.; Sharpless, K. B.; Taylor, P.; Marchot, P., Structural insights into conformational flexibility at the peripheral site and within the active center gorge of AChE. *Chem.-Biol. Interact.* **2005**, *157*, 159-165; (c) Willand, N.; Desroses, M.; Toto, P.; Dirie, B.; Lens, Z.; Villeret, V.; Rucktooa, P.; Loch, C.; Baulard, A.; Deprez, B., Exploring Drug Target Flexibility Using in Situ Click Chemistry: Application to a Mycobacterial Transcriptional Regulator. *ACS Chem. Biol.* **2010**, *5* (11), 1007-1013.
28. Bohacek, R. S.; McMartin, C.; Guida, W. C., The art and practice of structure-based drug design: A molecular modeling perspective. *Med. Res. Rev.* **1996**, *16* (1), 3-50.
29. Paruch, K.; Vyklicky, L.; Katz, T. J.; Incarvito, C. D.; Rheingold, A. L., Expedient procedure to synthesize ethers and esters of tri- and

tetrahydroxy[6]helicenebisquinones from the dye-intermediates disodium 4-hydroxy- and 4,5-dihydroxynaphthalene-2,7-disulfonates. *J. Org. Chem.* **2000**, *65* (25), 8774-8782.

30. Aubry, S.; Pellet-Rostaing, S.; Faure, R.; Lemaire, M., Racemic and diastereoselective synthesis of aryl and heteroaryl tetrahydroisoquinolines via the Pictet-Spengler reaction. *J. Heterocycl. Chem.* **2006**, *43* (1), 139-148.

## Chapter 3

### Identification of Protein-Protein Interaction Modulators Targeting Mcl-1 *via* Sulfo-Click Kinetic Target-Guided Synthesis

#### 3.1 Introduction

The discovery of B-cell lymphoma-2 (Bcl-2) almost three decades ago has been considered as a major breakthrough in understanding the development of cancer, thus providing channels to deliver potential anti-cancer agents.<sup>1</sup> This Bcl-2 family can be classified into two categories: pro-apoptotic and anti-apoptotic proteins. Although the complete mechanism through which these two types of proteins interact remains controversial, the anti-apoptotic proteins in the Bcl-2 family (e.g. Bcl-2, Bcl-X<sub>L</sub>, Mcl-1) have been established as the promising targets for drug discovery and development.<sup>2</sup> Initially, Bcl-2 and Bcl-X<sub>L</sub> were identified as the key players in regulation of apoptosis. As a result, majority of the research endeavors were aimed at development of small-molecules disrupting the interactions between pro-apoptotic proteins and Bcl-2/Bcl-X<sub>L</sub>.<sup>3</sup> Remarkably, a few of these candidates have made it to the clinical trials.<sup>4</sup> For example, **ABT-263**, an analogue of **ABT-737**, was developed by Abbott laboratories and is currently in phase I/II clinical trials.<sup>4c</sup> Despite being highly potent against Bcl-2 and Bcl-X<sub>L</sub> ( $K_i < 1$  nM), these molecules exhibited weaker binding affinities against Mcl-1 ( $K_i = 550$  nM for **ABT-263**;  $K_i > 1000$  nM for **ABT-737**).<sup>4c</sup> Moreover, cancer cells have been reported to develop resistance against **ABT-737** through up-regulation of Mcl-1.<sup>5</sup>

Accordingly, down-regulation of Mcl-1 has resulted in restoring the sensitivity of cancer cells towards **ABT-263** and **ABT-737**.<sup>4c, 6</sup> Meanwhile, Willis *et al.*<sup>7</sup> and Warr *et al.*<sup>8</sup> have recently demonstrated that Mcl-1 also plays a crucial role in regulating the apoptotic pathway. For instance, the pro-apoptotic Bak interacts with Bcl-X<sub>L</sub> and Mcl-1 through BH3 domain, which is also essential for dimerization of Bak, eventually leading to apoptosis.<sup>7</sup> Besides, Bak does not bind to the other members of the anti-apoptotic family, Bcl-2, Bcl-w and A1. In other words, antagonism of both, Bcl-X<sub>L</sub> and Mcl-1 by BH3-only proteins is required for the Bak-assisted cell death.<sup>7</sup> Strikingly, certain BH3-only proteins are known to heterodimerize with anti-apoptotic members with high selectivity. For example, Noxa binds strongly to Mcl-1 (but not Bcl-2 and Bcl-X<sub>L</sub>) and also triggers its destruction. Whereas, Bad binds to Bcl-X<sub>L</sub> and Bcl-2 but not Mcl-1.<sup>9</sup> Collectively, these findings suggest that the small molecule inhibitors either targeting Mcl-1 selectively or multiple members of the Bcl-2 family (Bcl-2, Bcl-X<sub>L</sub> and Mcl-1) simultaneously, hold great therapeutic potential. Consequently, several research groups have reported structurally diverse molecules as pan-active antagonists of the Bcl-2 family (Figure 3.1A),<sup>10</sup> although a few Mcl-1-selective candidates are also available (Figure 3.1B).<sup>9, 11</sup>

Recently, Pellecchia and co-workers identified acylsulfonamides as potent inhibitors displaying nanomolar binding affinities against both, Bcl-X<sub>L</sub> and Mcl-1 using a fragment-based approach, termed as SAR by ILOE (structure activity relationship by interligand nuclear overhauser effect).<sup>10d</sup> Contrary to SAR by NMR, SAR by ILOE<sup>12</sup>

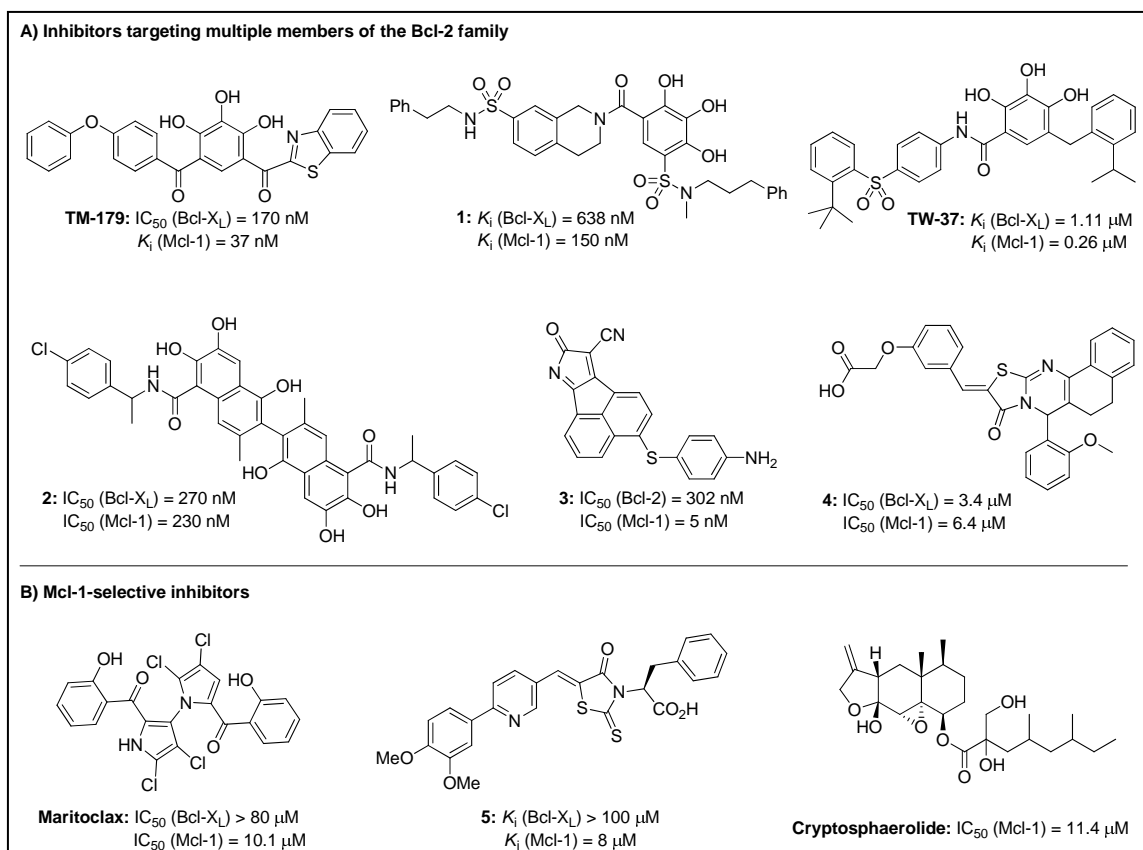


**Figure 3.1.** Inhibitors targeting multiple Bcl-2 family members or Mcl-1 selectively

relies on identifying protein-assisted ligand-ligand NOEs (ILOEs) between two adjacently binding fragments at the binding site of the protein, which can be covalently linked, guided by molecular modeling studies along with appropriate synthetic methods to obtain a bidentate ligand (Figure 3.2B).<sup>10d</sup> Importantly, <sup>15</sup>N labeled protein is not required for ILOE-based screening. Moreover, tedious HSQC experiments need not be performed, presenting advantages over the SAR by NMR approach.

Initially, fragments binding to Bcl-X<sub>L</sub>, identified by Petros *et al.*<sup>13</sup> through SAR by NMR screening, were chosen as model substrates. As anticipated, Bcl-X<sub>L</sub>-assisted ILOEs between hydrogens on the aromatic rings of acid **6** and methylene hydrogens of naphthalenol **7** were clearly recognized (Figure 3.2). Additionally, the majority of the

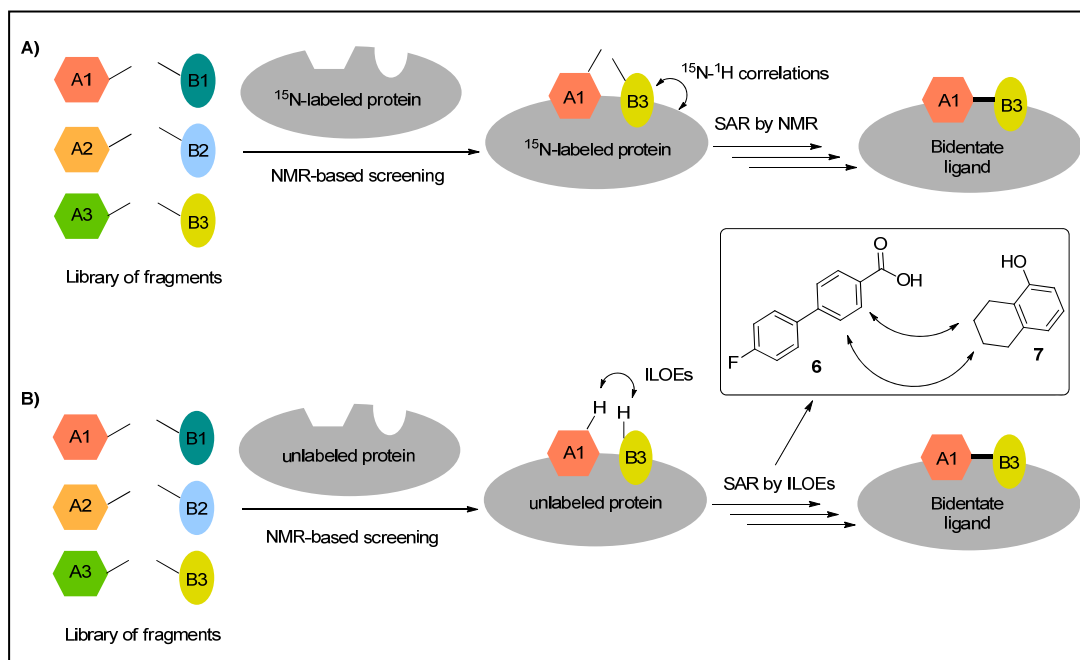


**Figure 3.2.** Comparison of SAR by NMR and SAR by ILOEs approaches

ILOE signals were abolished when Bak BH3 peptide was added to the NMR sample, indicating that the fragments were targeting the binding site of Bcl-X<sub>L</sub>.<sup>10d</sup> ILOEs arising from nonspecific binding interactions can thus be clearly distinguished and corresponding fragments may not be considered useful. After establishing these experiments, Pellecchia *et al.* utilized this approach with diverse set of fragments to identify several acylsulfonamides as potent inhibitors of Bcl-X<sub>L</sub> and Mcl-1. Strikingly, this is the only example in the literature wherein acylsulfonamides were found to be active against Mcl-1, since the Abbott candidates (**ABT-737** and **ABT-263**) exhibited poor binding affinities against this target. Meanwhile, Manetsch and co-workers have established another fragment-based approach, kinetic target-guided synthesis (TGS) for the identification of protein-protein interaction modulators (PPIMs). They reported that the sulfo-click reaction, wherein sulfonyl azides react with thio acids generating acylsulfonamides, can be successfully employed to disrupt Bcl-X<sub>L</sub>-protein interactions.<sup>14</sup>

Total 18 reactive building blocks: 9 sulfonyl azides and 9 thio acids leading to 81 potential acylsulfonamides (9 x 9 = 81)

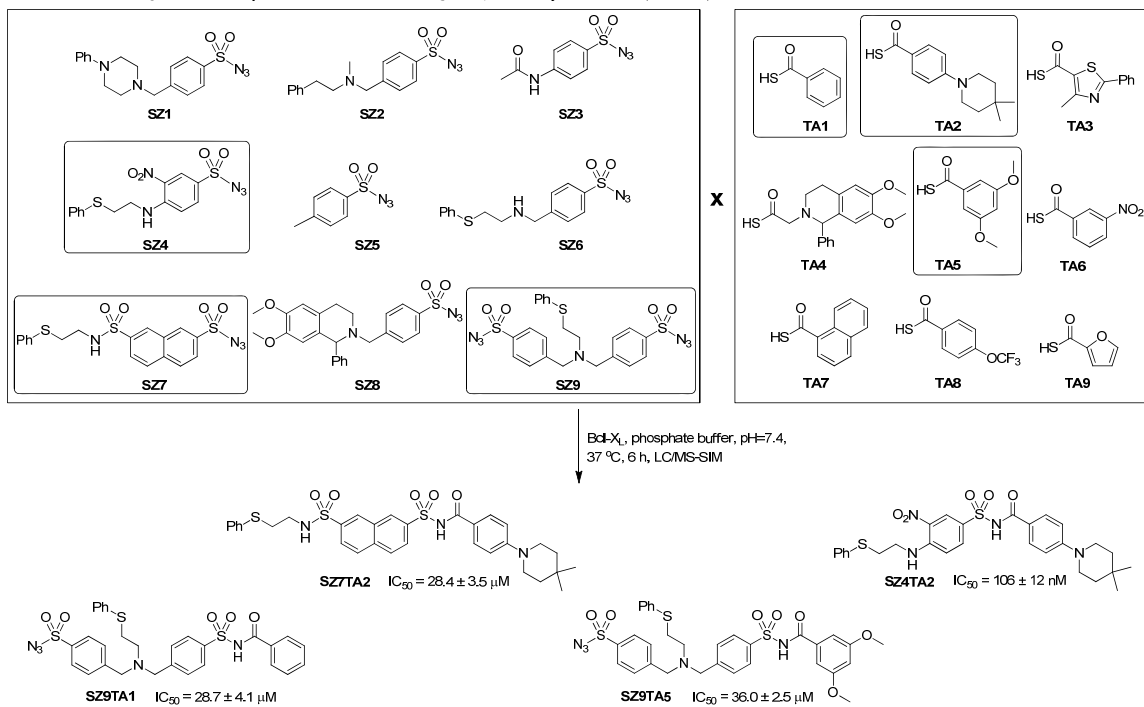


**Figure 3.3.** Kinetic TGS screening *via* sulfo-click chemistry against Bcl-X<sub>L</sub>

A library of nine sulfonyl azides and nine thio acids (eighty one potential products), was incubated as binary mixtures at 37 °C for six hours in presence and absence of Bcl-X<sub>L</sub> and the samples were analyzed by liquid chromatography combined with mass spectrometry detection in the selected ion mode (LC/MS-SIM) for the product formation (Figure 3.3). Comparison of samples with and without Bcl-X<sub>L</sub> revealed that, of all eighteen fragments, only **SZ4**, **SZ7**, **SZ9**, **TA1**, **TA2**, and **TA5** were selectively templated by Bcl-X<sub>L</sub> thereby yielding acylsulfonamides **SZ4TA2**, **SZ7TA2**, **SZ9TA1**, and **SZ9TA5** in amplified amounts. Furthermore, these compounds showed IC<sub>50</sub>s in the low micromolar range, which underscores the utility of kinetic TGS as a valuable approach to PPIM discovery.<sup>14b</sup> Based on the reports from Pellecchia and Manetsch, the kinetic TGS approach can also be envisioned to be applied to Mcl-1 to discover

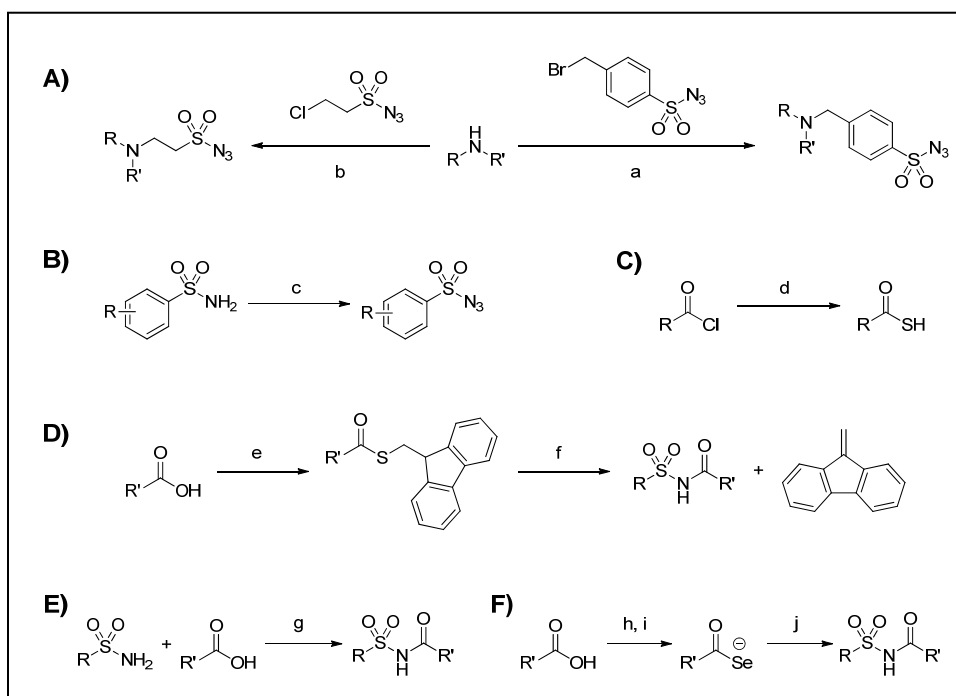
structurally diverse acylsulfonamides. Herein, we disclose our findings towards screening and identification of acylsulfonamides as PPIMs targeting Mcl-1 *via* sulfo-click kinetic TGS.

## 3.2 Results and discussion

### 3.2.1 Expansion of fragment library

Inspired by the results obtained for Bcl-X<sub>L</sub>, the libraries of sulfonyl azides and thio acids were first expanded in order to explore a wider chemical space. Majority of the sulfonyl azides were synthesized using one of the following three reactions conditions: (a) alkylation of amines with 4-(bromomethyl)benzenesulfonyl azide,<sup>14b</sup> (b) treating the corresponding sulfonamides with triflyl azide (TfN<sub>3</sub>), a diazo transfer reagent,<sup>15</sup> or (c) alkylation of amines with *in situ* generated 2-chloroethanesulfonyl azide (Scheme 3.1 A-B).<sup>16</sup> Thus, a set of twenty two sulfonyl azides were added to the previous library bringing up the total number of fragments to thirty one.

The thio acids were derived from corresponding acid chlorides using sodium hydrosulfide (Scheme 3.1C). Although the synthetic procedure seems fairly straightforward, purification of the thio acids is problematic at times. Moreover, they are not stable over a reasonable period of time due to formation of by-products such as anhydride of thio acid. As a result, handling and storage of thio acids becomes difficult and they have to be freshly prepared before the kinetic TGS screening to obtain reproducible results. A method deprived of these limitations was recently reported, wherein the carboxylic acids were first coupled with 9-fluorenylmethanethiol providing



**Scheme 3.1.** Synthesis of sulfonyl azides, thio acids, thioesters and acylsulfonamides.

Reaction conditions: (a)  $\text{K}_2\text{CO}_3$ ,  $\text{CH}_3\text{CN}:\text{H}_2\text{O}$  (9:1), 12 h, rt (b)  $\text{K}_2\text{CO}_3$ , KI (cat.),  $\text{CH}_3\text{CN}:\text{H}_2\text{O}$  (9:1), 3 h, rt (c)  $\text{TfN}_3$ ,  $\text{CuSO}_4$ ,  $\text{NaHCO}_3$ ,  $\text{H}_2\text{O}$ , toluene, *t*-BuOH, 24 to 48 h, rt (d) NaSH, acetone,  $\text{H}_2\text{O}$ , 2 h, rt or NaSH, neat, 1 h, 0 °C to rt (e) EDCI, DMAP, DCM, 2 h, rt (f) 3.5% DBU, DMF, 1 min, rt;  $\text{RSO}_2\text{N}_3$ , 1 min, rt (g) EDCI, DMAP,  $\text{CH}_2\text{Cl}_2$ , rt, 24 to 48 h (h)  $(\text{CH}_3)_2\text{CHOCOCl}$ , *N*-methyl piperidine, THF, 0 °C, 30 min (i)  $\text{LiAlHSeH}$ , THF, 0 °C, 30 min (j)  $\text{RSO}_2\text{N}_3$ , THF, 0 °C to rt, 3 h

corresponding thioesters, which upon deprotection quantitatively yield the thio acids.<sup>16</sup>

Hence, the corresponding thioesters of the thio acids **TA1-TA10** were synthesized as described above. The deprotection can be accomplished by treating the thioesters with (a) 5% piperidine in DMF, or (b) 3.5% 1,8-Diazabicycloundec-7-ene (DBU) in DMF, or (c) 5 equivalents of  $\text{Cs}_2\text{CO}_3$ . The reaction is completed in about an hour with  $\text{Cs}_2\text{CO}_3$ , whereas it takes two minutes when DBU or piperidine is used, making it highly efficient.<sup>16</sup> After deprotection with piperidine, the thio acid generated can be diluted to a

stock solution in methanol and used for kinetic TGS experiments without further purification. Importantly, this process has been tailored towards synthesis of acylsulfonamides (Scheme 3.1D). In a one-pot approach, deprotection of thio ester with DBU or  $\text{Cs}_2\text{CO}_3$  followed by addition of sulfonyl azide results in formation of corresponding acylsulfonamide in good to excellent yields.<sup>16</sup> Alternatively, the acylsulfonamides can be synthesized by (a) reaction between sulfonamides and carboxylic acids using EDCI coupling conditions, or (b) the previously reported reaction between sulfonyl azides and selenocarboxylates which were produced from corresponding carboxylic acids and the selenating reagent  $\text{LiAlHSeH}$  (Scheme 3.1 E-F).<sup>17</sup>

### 3.2.2 Kinetic TGS screening against Mcl-1

The entire library of fragments was incubated as binary mixtures (31 sulfonyl azides and 10 thio acids; 310 possible combinations) against Mcl-1 at 37 °C for six hours (Figure 3.4). As previously described, the thio acids **TA1-TA10** were generated *in situ* from corresponding thio esters using 5% piperidine in DMF prior to the kinetic TGS screening. Based on previously optimized conditions for Bcl-X<sub>L</sub>, initially the screening was carried out at 2 μM concentration of Mcl-1. Unfortunately, no TGS hits were obtained under these conditions, while increasing the concentration by five-fold to 10 μM provided consistent results. Furthermore, these 310 binary mixtures were incubated in the phosphate buffer in the absence of Mcl-1. Subsequently, all the samples were analyzed using liquid chromatography in combination with mass spectrometry equipped with electrospray ionization in the positive selected ion mode (LC/MS-SIM) to detect corresponding acylsulfonamides.

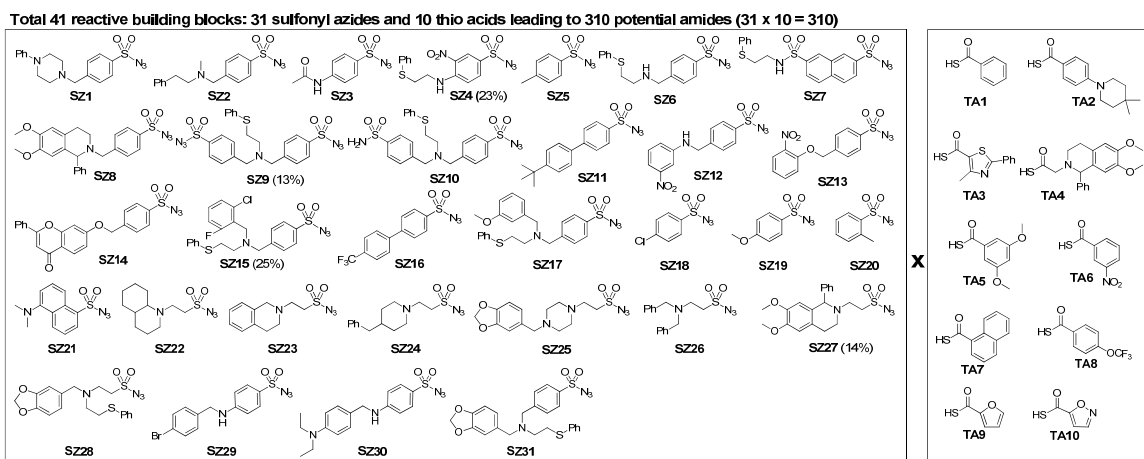


**Figure 3.4.** Library of sulfonyl azides and thio acids utilized for kinetic TGS screening against Mcl-1

Comparison of LC/MS-SIM data for samples in presence and absence of Mcl-1 revealed that, out of forty one fragments, only eleven fragments (**SZ9**, **SZ15**, **SZ17**, **SZ31**, **TA1**, **TA2**, **TA3**, **TA5**, **TA6**, **TA7**, and **TA8**) leading to fourteen combinations were templated by the protein, since elevated amounts of those acylsulfonamides were observed in the Mcl-1 containing samples (Figure 3.5). To investigate whether these fragments were templated at the binding site of Mcl-1, a control experiment incorporating wildtype pro-apoptotic Bim BH3 peptide along with the fragments in the presence of Mcl-1 was designed. Suppression of the product formation is observed if the fragments compete with Bim BH3 peptide for the binding site. On the contrary, if the product formation results from non-specific binding, addition of Bim BH3 peptide to the incubation sample would not have any effect and such fragment combinations can obviously be ruled out.

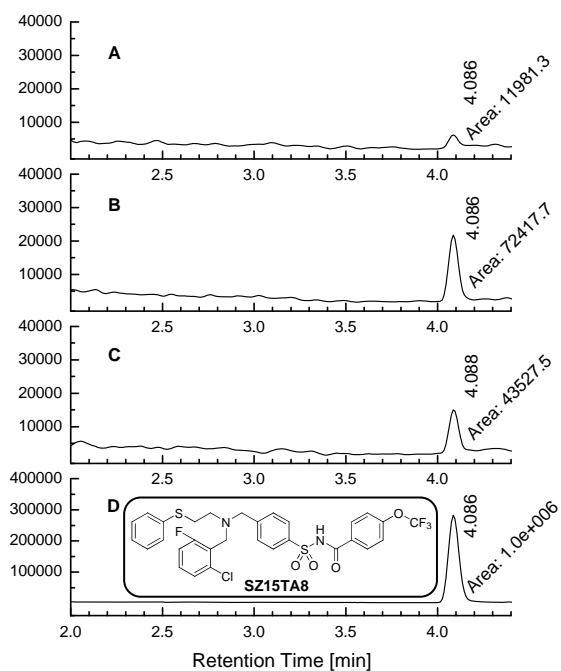


**Figure 3.5.** LC/MS-SIM analysis of kinetic TGS incubations with fragments **SZ15** and **TA8** targeting Mcl-1. The samples were incubated for six hours at 37 °C and subjected to the LC/MS-SIM analysis. (A) Incubation sample containing fragments **SZ15** and **TA8** in the absence of Mcl-1. (B) Incubation sample containing fragments **SZ15** and **TA8** in the presence of 10  $\mu$ M Mcl-1. (C) Incubation sample containing fragments **SZ15** and **TA8** in the presence of 10  $\mu$ M Mcl-1 and 20  $\mu$ M Bim BH3 peptide. (D) Synthetic **SZ15TA8** as the reference compound.

Consequently, some combinations (**SZ9TA3**, **SZ15TA2**, and **SZ31TA2**) could be abandoned based on the aforementioned control experiments, whereas other eleven combinations were confirmed as the kinetic TGS hits (Figure 3.6).

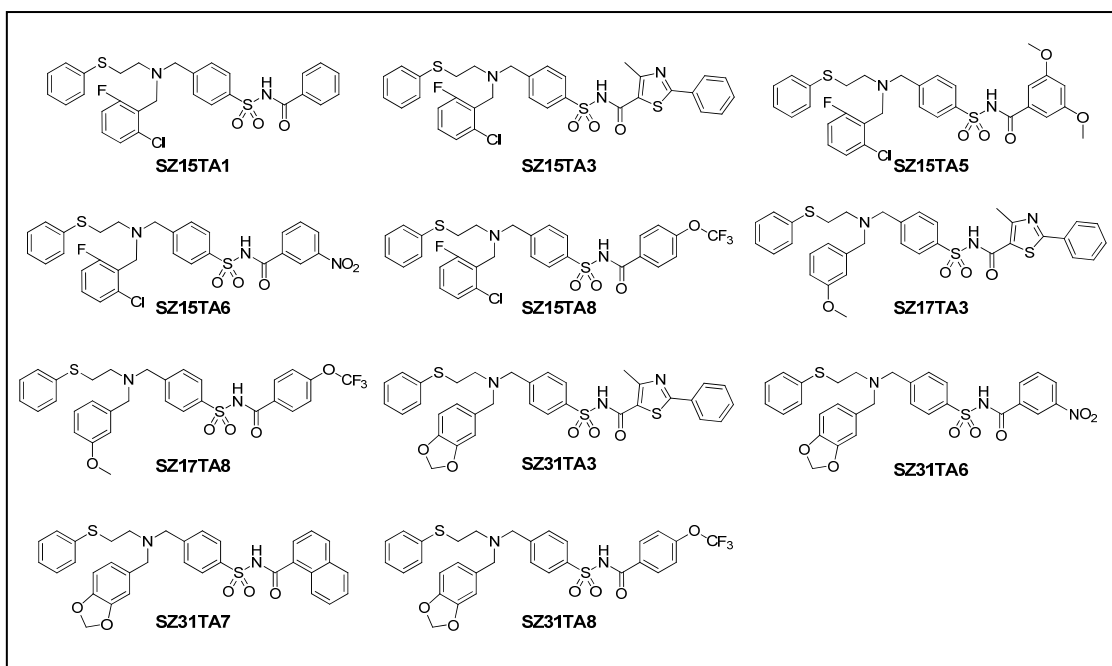


**Figure 3.6.** Acylsulfonamides confirmed as kinetic TGS hits against Mcl-1

### 3.2.3 Biological activity of the kinetic TGS hits

The acylsulfonamides confirmed as kinetic TGS hits were synthesized using synthetic procedures mentioned above and then tested for their ability to disrupt Mcl-1/BH3 interactions using conventional fluorescence polarization assay utilizing GST-Mcl-1 and fluorescein-labeled Bim BH3 peptide. Majority of these compounds displayed  $IC_{50}$  values in the single digit  $\mu M$  range when subjected to dose-response studies. Moreover, ligand efficiencies in the range of 0.16-0.18 were observed for these acylsulfonamides (Table 3.1). It is worth mentioning that, the ligand efficiencies between 0.16-0.24 are theoretically predicted to be optimal for PPIMs.<sup>18</sup> Interestingly, when all reactive fragments (**SZ1-SZ31** and **TA1-TA10**) were tested in the fluorescence polarization assay at 100  $\mu M$  concentration, less than 5% inhibition was detected except four sulfonyl azides: **SZ4** (23%), **SZ9** (13%), **SZ15** (25%), and **SZ27** (14%). These results are exciting since the high-quality inhibitors can be unambiguously identified

through the screening of fragments possessing weak binding affinities, remarkably reducing the synthetic efforts. To probe whether these molecules would display any biological activity against Bcl-X<sub>L</sub>, they were subjected to the fluorescence polarization assay designed using fluorescein-labeled GST-Bcl-X<sub>L</sub> and fluorescein-labeled Bak BH3 peptide. Strikingly, comparison of IC<sub>50</sub> values revealed that all of the compounds exhibited noticeable selectivity towards Mcl-1, evident from the selectivity indices ranging from 3 to 19 (Table 3.1).

**Table 3.1.** Biological activity of acylsulfonamides against Mcl-1 and Bcl-X<sub>L</sub>

Entry	Compound	MW (Da)	IC <sub>50</sub> Mcl-1 (μM)	LE Mcl-1 (kcal/mol/HA)	IC <sub>50</sub> Bcl-X <sub>L</sub> (μM)	SI Bcl-X <sub>L</sub> /Mcl-1
1	SZ15TA1	569.1	9.7	0.180	29.1	3.00
2	SZ15TA3	666.3	5.8	0.162	36.4	6.27
3	SZ15TA5	629.0	13.4	0.158	53.0	3.95
4	SZ15TA6	614.1	11.7	nd	71.6	6.12
5	SZ15TA8	653.1	7.6	0.162	47.0	6.18
6	SZ17TA3	643.8	8.6	0.157	50.0	5.81
7	SZ17TA8	630.7	8.4	0.161	76.0	9.05
8	SZ31TA3	657.8	9.4	0.152	84.0	8.94
9	SZ31TA6	605.7	6.2	0.169	20.4	3.29
10	SZ31TA7	610.7	10.6	0.158	56.7	5.35
11	SZ31TA8	644.7	5.9	0.162	111	18.81

### 3.2.4 Discussion

Recent advances in the field of fragment-based lead discovery have demonstrated that the PPIMs targeting the anti-apoptotic Bcl-2 family can be developed. Although highly potent molecules such as **ABT-737** and **ABT-263** were discovered as dual inhibitors of Bcl-2 and Bcl-X<sub>L</sub> through SAR by NMR approach, subsequent resistance developed by cancer cells has highlighted the role of Mcl-1 as another key regulator of apoptosis. Recently, the SAR by ILOEs approach was exploited leading to the identification of acylsulfonamides targeting Bcl-X<sub>L</sub> and Mcl-1 with binding affinities in the nanomolar range. Meanwhile, acylsulfonamides as PPIMs of Bcl-X<sub>L</sub> were also identified through the sulfo-click kinetic TGS, another fragment-based approach. Inspired by these results, we extended this approach for the identification of structurally diverse acylsulfonamides as Mcl-1 inhibitors. First, a library of thirty one sulfonyl azides and ten thio acids resulting in three hundred and ten acylsulfonamides was incubated as binary mixtures in the presence and absence of the target protein, Mcl-1. In an additional control experiment, Bim BH3 peptide was added to the incubation sample containing Mcl-1. Subsequent LC/MS-SIM analysis disclosed that only eleven acylsulfonamides were templated by the protein, designated as kinetic TGS hits. Also, the product formation through templation was suppressed by addition of Bim BH3 peptide suggesting that, the templation occurs at the binding site of Mcl-1. The kinetic TGS hits were synthesized and tested using fluorescence polarization assay. As expected, all the acylsulfonamides were found to possess respectable biological activity in the single digit micromolar range and also displayed optimal ligand efficiencies.

Careful observation of all the acylsulfonamides identified through kinetic TGS screening provided some useful structural information. For example, acylsulfonamides derived from sulfonyl azides with bis-benzylic tertiary amines (**SZ15**, **SZ17**, and **SZ31**) were found to be most active against Mcl-1. Surprisingly, none of the alkyl sulfonyl azides (**SZ22-SZ28**) led to the kinetic TGS hits. Moreover, other sulfonyl azides, being comparatively smaller in size, were also found to be not templated by the protein target. On the other hand, thio acids **TA3** and **TA8** were found to be favored during the kinetic TGS screening, although thio acids **TA1**, **TA5**, **TA6**, and **TA7** also featured in some of the PPIMs. Notably, structurally bulky (**TA2** and **TA4**) as well as heterocyclic (**TA9** and **TA10**) thio acids did not contribute to the kinetic TGS hits. It is noteworthy to mention that, the majority of the fragments showed less than 5% inhibition even at 100  $\mu$ M concentration. Importantly, these acylsulfonamides exhibited striking selectivity towards Mcl-1. These results are highly valuable since identification of Mcl-1-selective inhibitors still remains a challenging task and has met with limited success. Collectively, these results can be regarded as preliminary structure activity relationship studies and therefore serve as a foundation for the future endeavors towards hit-to-lead optimization.

### 3.3 Conclusions

Herein, we have demonstrated that the sulfo-click kinetic TGS approach can also be applied to discover acylsulfonamides with diversified scaffolds as inhibitors of Mcl-1. Based on our previous work on Bcl-X<sub>L</sub>, fragment libraries of sulfonyl azides and thio acids were screened against Mcl-1. Eleven acylsulfonamides were identified as kinetic TGS hits, which were confirmed using peptide control experiments. Interestingly, certain fragments from the library (**SZ15**, **SZ17**, **SZ31**, **TA3**, and **TA8**) were found to be

predominantly templated by the protein target. Furthermore, the kinetic TGS hits displayed IC<sub>50</sub> values in the single digit nanomolar range, underlining that the most potent compounds of the library were identified during the screening. Besides, these acylsulfonamides were found to be selective towards Mcl-1, presenting a route to generate Mcl-1-selective inhibitors. Based on these findings, this strategy can be envisioned to be applied to other challenging protein-protein interaction targets such as MDM2/p53, TNF/TNFR1 and IL-2/IL-2R $\alpha$ .

### 3.4 Experimental section

#### 3.4.1 General information

All reagents and solvents were purchased from commercial sources and used without further purification. All reactions were run under an Argon atmosphere unless otherwise indicated. Prior to use of solvents in reactions, they were purified by passing the degassed solvents through a column of activated alumina and transferred by an oven dried syringe or cannula. Thin layer chromatography was performed on Merck TLC plates (silica gel 60 F<sub>254</sub>). <sup>1</sup>H NMR and <sup>13</sup>C NMR were recorded on a Varian Inova 400 (400 MHz) or a Bruker Avance DPX 250 (250 MHz) instrument. The purification of designated compounds was carried out using reverse phase HPLC system (Waters Prep LC 4000 system with Waters 996 photo-diode array detector, Agilent column Eclipse XDB-C18, 5  $\mu$ m, 9.4 mm  $\times$  250 mm). The compounds were eluted using a gradient elution of A:B (80:20 to 0:100) over 40 min at a flow rate of 5.0 mL/min, where solvent A was H<sub>2</sub>O (0.05% TFA) and solvent B was CH<sub>3</sub>CN (0.05% TFA). The HRMS data were

measured on an Agilent 1100 Series MSD/TOF with electrospray ionization. The LC/MS data were measured on an Agilent 1100 LC/MSD-VL with electrospray ionization.

The gradient used for LC/MS-SIM analysis is shown below:

**Table 3.2.** Elution gradient system employed for the LC/MS-SIM analysis

Time	% B*	Flow rate	Time	% B*	Flow rate
0.00	10.0	2.0 mL min <sup>-1</sup>	4.60	100.0	3.0 mL min <sup>-1</sup>
0.60	10.0	2.0 mL min <sup>-1</sup>	4.61	100.0	2.0 mL min <sup>-1</sup>
4.09	100.0	2.0 mL min <sup>-1</sup>	4.62	10.0	2.0 mL min <sup>-1</sup>
4.10	100.0	3.0 mL min <sup>-1</sup>	5.20	10.0	2.0 mL min <sup>-1</sup>

\* eluent A: H<sub>2</sub>O (0.05% TFA); eluent B: CH<sub>3</sub>CN (0.05% TFA)

The sulfonyl azides<sup>14, 16</sup> **SZ1-SZ11**, **SZ16**, **SZ18**, **SZ19**, **SZ21**, **SZ23**, **SZ28** and the thioesters<sup>16</sup> **TE1-TE3**, **TE5**, **TE7**, and **TE8** have been previously reported.

### 3.4.2 General protocol for incubations of Mcl-1 with reactive fragments

In a 96-well plate, one thio acid building block (1  $\mu$ L of a 2 mM solution in methanol) and one sulfonyl azide building block (1  $\mu$ L of a 2 mM solution in methanol) were added to a solution of Mcl-1 (98  $\mu$ L of a 10  $\mu$ M Mcl-1 solution in buffer (58 mM Na<sub>2</sub>HPO<sub>4</sub>, 17 mM NaH<sub>2</sub>PO<sub>4</sub>, 68 mM NaCl, 1 mM NaN<sub>3</sub>, pH = 7.40)). The 96-well plate was sealed and incubated at 37 °C for six hours. The incubation samples were then subjected to Liquid Chromatography combined with mass spectrometry analysis in the Selected Ion Mode (LC/MS-SIM, Kinetex PFP preceded by a Phenomenex C18 guard column, electrospray ionization and mass spectrometric detection in the positive SIM, tuned to the expected molecular mass of the product). The TGS hit compound was identified by the mass and the retention time. As a control, identical building block

combinations were incubated in buffer without Mcl-1 and subjected to LC/MS-SIM analysis. Comparison of the LC/MS-SIM chromatograms of these control incubations with the chromatograms of the Mcl-1 containing incubations allows us to determine whether the protein is templating the corresponding amidation reaction. Furthermore, synthetically prepared acylsulfonamide was subjected to LC/MS-SIM analysis and the retention time was compared with the one identified in the Mcl-1 containing incubation.

### 3.4.3 General protocol for the control incubations of Mcl-1 with reactive fragments and Bim BH3 peptide

For the Mcl-1 containing incubation sample showing acylsulfonamide formation, control incubation with Bim peptide has been undertaken to demonstrate that the templation reaction occurs at the desired binding site. Thus, in a 96-well plate, one thio acid (1  $\mu$ L of a 2 mM solution in methanol) and one sulfonyl azide (1  $\mu$ L of a 2 mM solution in methanol) were added to a solution of Mcl-1 (97  $\mu$ L of a 10  $\mu$ M Mcl-1 solution in methanol) were added to a solution of Mcl-1 (97  $\mu$ L of a 10  $\mu$ M Mcl-1 solution in buffer). Finally, Bim BH3 peptide (1  $\mu$ L of a 2 mM solution in DMSO) was added and the incubation sample in a sealed 96-well plate was incubated at 37 °C for six hours. This incubation sample was then subjected to LC/MS-SIM analysis along with the Mcl-1 containing sample without the Bim BH3 peptide.

### 3.4.4 General procedure A for the synthesis of sulfonyl azides

A mixture of 4-(bromomethyl)benzenesulfonyl azide (276 mg, 1 mmol), corresponding amine (1 mmol), and potassium carbonate (276 mg, 2 mmol) in acetonitrile and water (9:1; 6 mL), was stirred at room temperature for 12 hours. After treating with ethyl acetate (20 mL) and water (20 mL), the system was extracted with

ethyl acetate (20 mL ×3). The combined organic layers were dried over anhydrous sodium sulfate and concentrated. The sulfonyl azide was then obtained by flash chromatography.

The sulfonyl azides **SZ12-SZ15**, **SZ17**, and **SZ31** were synthesized using this procedure. In case of **SZ12**, corresponding aniline was used, whereas corresponding phenol was used for the synthesis of **SZ13** and **SZ14**. Also, the reaction temperature was maintained at 66 °C for the sulfonyl azides **SZ12-SZ14**.

#### 3.4.5 General procedure B for the synthesis of sulfonyl azides

The sulfonyl azides were synthesized starting from corresponding amines, *in situ* generated 2-chloroethanesulfonyl azide and potassium carbonate, using a previously reported procedure.<sup>16</sup>

The sulfonyl azides **SZ22**, and **SZ24-SZ27** were synthesized using this procedure.

#### 3.4.6 General procedure C for the synthesis of sulfonyl azides

The sulfonyl azides were synthesized starting from corresponding sulfonamides using triflyl azide, a diazo transfer reagent, following the previously reported procedure.<sup>15</sup>

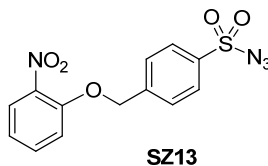
The synthesis of the sulfonamides used has been described later in this document.

The sulfonyl azides **SZ29-SZ30** have been synthesized using this procedure.

### 3.4.7 Synthesis of fragments



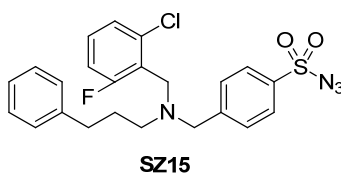
**Sulfonyl azide SZ12:** Yield = 67%.  $R_f = 0.35$  in hexanes : EtOAc = 3:1. <sup>1</sup>H NMR (400 MHz, CDCl<sub>3</sub>)  $\delta$ : <sup>1</sup>H NMR (600 MHz, CDCl<sub>3</sub>)  $\delta$  7.94 (d,  $J = 8.3$  Hz, 2H), 7.61 (d,  $J = 8.2$  Hz, 2H), 7.57 (dd,  $J = 8.1, 1.8$  Hz, 1H), 7.40 (t,  $J = 2.1$  Hz, 1H), 7.30 (t,  $J = 8.2$  Hz, 1H), 6.86 (dd,  $J = 8.2, 2.2$  Hz, 1H), 4.64 (s, 1H), 4.56 (s, 2H) ppm. <sup>13</sup>C NMR (101 MHz, CDCl<sub>3</sub>)  $\delta$ : 148.2, 146.4, 130.2, 128.4, 128.3, 128.2, 127.8, 118.9, 113.0, 106.9, 47.5 ppm. HRMS (ESI) calcd for C<sub>13</sub>H<sub>11</sub>N<sub>5</sub>O<sub>4</sub>S [M+K]<sup>+</sup>: 372.0163, found: 372.0145



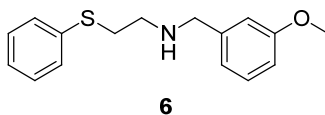
**Sulfonyl azide SZ13:** Yield = 40%.  $R_f = 0.44$  in hexanes : EtOAc = 3:1. <sup>1</sup>H NMR (400 MHz, CDCl<sub>3</sub>)  $\delta$ : 7.94 – 7.84 (m, 3H), 7.68 – 7.34 (m, 5H), 4.50 (s, 2H) ppm. <sup>13</sup>C NMR (101 MHz, CDCl<sub>3</sub>)  $\delta$ : 143.3, 141.2, 134.4, 134.2, 129.2, 128.7, 127.9, 126.0, 125.2, 53.8 ppm. HRMS (ESI) calcd for C<sub>13</sub>H<sub>10</sub>N<sub>4</sub>O<sub>5</sub>S [M+NH<sub>4</sub>]<sup>+</sup>: 352.0716, found: 352.0719



**Sulfonyl azide SZ14:** Yield = 45%.  $R_f$  = 0.21 in hexanes : EtOAc = 3:1.  $^1\text{H}$  NMR (400 MHz,  $\text{CDCl}_3$ )  $\delta$ : 8.10 (dd,  $J$  = 8.6, 3.4 Hz, 1H), 7.91 – 7.82 (m, 4H), 7.51 (d,  $J$  = 7.4 Hz, 5H), 7.38 (d,  $J$  = 2.1 Hz, 1H), 6.93 (dd,  $J$  = 8.7, 1.9 Hz, 1H), 6.77 (d,  $J$  = 3.8 Hz, 1H) 4.49 (s, 2H) ppm.  $^{13}\text{C}$  NMR (101 MHz,  $\text{CDCl}_3$ )  $\delta$ : 177.2, 163.9, 156.5, 152.9, 143.0, 134.6, 132.0, 131.2, 129.2, 129.0, 128.7, 127.6, 126.3, 122.8, 119.5, 112.2, 107.7, 53.8 ppm. HRMS (ESI) calcd for  $\text{C}_{22}\text{H}_{15}\text{N}_3\text{O}_5\text{S}$   $[\text{M}+\text{H}]^+$ : 434.0805, found: 434.0796



**Sulfonyl azide SZ15:** was synthesized starting from **SZ6** and 1-chloro-2-(chloromethyl)-3-fluorobenzene. Yield = 54%.  $R_f$  = 0.62 in hexanes : EtOAc = 5:1.  $^1\text{H}$  NMR (400 MHz,  $\text{CDCl}_3$ )  $\delta$ : 7.80 (d,  $J$  = 8.1 Hz, 2H), 7.54 (d,  $J$  = 8.1 Hz, 2H), 7.22 – 7.11 (m, 7H), 6.96 – 6.89 (m, 1H), 3.87 (s, 2H), 3.75 (s, 2H), 3.07 (t,  $J$  = 7.6 Hz, 2H), 2.79 (t,  $J$  = 7.6 Hz, 2H) ppm.  $^{13}\text{C}$  NMR (101 MHz,  $\text{CDCl}_3$ )  $\delta$ : 162.1 (d,  $J$  = 249.0 Hz), 147.9, 136.8, 136.5, 136.0, 129.6, 129.5, 129.1 (d,  $J$  = 26.0 Hz), 127.3, 126.1, 125.6, 124.2 (d,  $J$  = 16.8 Hz), 114.1 (d,  $J$  = 23.3 Hz), 58.0, 53.7, 49.6, 31.3 ppm. HRMS (ESI) calcd for  $\text{C}_{22}\text{H}_{20}\text{ClFN}_4\text{O}_2\text{S}_2$   $[\text{M}+\text{H}]^+$ : 491.0779, found: 491.0771

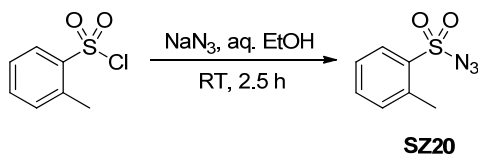


**Amine 6:** A mixture of 2-(phenylthio)ethanamine (500 mg, 3.3 mmol), 1-(chloromethyl)-3-methoxybenzene (517 mg, 3.3 mmol) and potassium carbonate (911 mg, 6.6 mmol) in acetonitrile and water (9:1, 20 mL), was stirred at room temperature for 12 hours. After

adding ethyl acetate (20 mL) and water (20 mL), the system was extracted with ethyl acetate (20 mL  $\times$ 3). The combined organic phase was dried over anhydrous sodium sulfate and concentrated. Intermediate **6** was obtained by flash chromatography in 37% yield.  $R_f = 0.2$  in hexanes : EtOAc = 1:1.  $^1\text{H NMR}$  (400 MHz,  $\text{CDCl}_3$ )  $\delta$ : 7.40 – 7.15 (m, 6H), 6.94 – 6.87 (m, 2H), 6.81 (d,  $J = 8.5$  Hz, 1H), 3.79 (s, 3H), 3.78 (s, 2H), 3.09 (t,  $J = 6.1$  Hz, 2H), 2.87 (t,  $J = 6.2$  Hz, 2H), 1.72 (s, 1H) ppm.  $^{13}\text{C NMR}$  (101 MHz,  $\text{CDCl}_3$ )  $\delta$ : 159.7, 141.7, 135.8, 129.4, 129.3, 128.8, 126.0, 120.2, 113.4, 112.4, 55.0, 53.2, 47.4, 34.1 ppm. HRMS (ESI) calcd for  $\text{C}_{16}\text{H}_{19}\text{NOS}$   $[\text{M}+\text{H}]^+$ : 274.1260, found: 274.1257



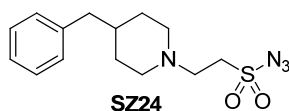
**Sulfonyl azide SZ17:** Yield = 82%.  $R_f = 0.43$  in hexanes : EtOAc = 4:1.  $^1\text{H NMR}$  (400 MHz,  $\text{CDCl}_3$ )  $\delta$ : 7.86 (d,  $J = 8.3$  Hz, 2H), 7.61 (d,  $J = 8.2$  Hz, 2H), 7.28 – 7.12 (m, 6H), 7.00 – 6.95 (m, 2H), 6.82 (dd,  $J = 8.1, 1.7$  Hz, 1H), 3.81 (s, 3H), 3.69 (s, 2H), 3.63 (s, 2H), 3.07 (t,  $J = 7.2$  Hz, 2H), 2.77 (t,  $J = 7.2$  Hz, 2H) ppm.  $^{13}\text{C NMR}$  (101 MHz,  $\text{CDCl}_3$ )  $\delta$ : 159.7, 147.8, 140.2, 136.7, 136.2, 129.6, 129.3, 128.8, 128.7, 127.4, 125.8, 121.0, 114.3, 112.5, 58.4, 57.7, 55.1, 52.8, 31.3 ppm. HRMS (ESI) calcd for  $\text{C}_{23}\text{H}_{24}\text{N}_4\text{O}_3\text{S}_2$   $[\text{M}+\text{H}]^+$ : 469.1368, found: 469.1378



**Sulfonyl azide SZ20:** To a solution of 2-methylbenzene-1-sulfonyl chloride (1 g, 5.24 mmol) in aqueous ethanol (24 mL) was added sodium azide (682 mg, 10.5 mmol) and the reaction mixture was stirred at room temperature for 2.5 hours. The reaction mixture was treated with water, extracted with ethyl acetate (30 mL  $\times$ 3). The combined organic phase was dried over anhydrous sodium sulfate and concentrated. The sulfonyl azide **SZ20** was obtained after flash column chromatography. Yield = 89%.  $R_f$  = 0.64 in hexanes : EtOAc = 4:1.  $^1\text{H}$  NMR (250 MHz,  $\text{CDCl}_3$ )  $\delta$  8.06 – 7.96 (m, 1H), 7.62 – 7.52 (m, 1H), 7.42 – 7.32 (m, 2H), 2.65 (s, 3H) ppm.  $^{13}\text{C}$  NMR (63 MHz,  $\text{CDCl}_3$ )  $\delta$ : 138.6, 136.9, 134.8, 133.2, 129.5, 126.6, 20.5 ppm.

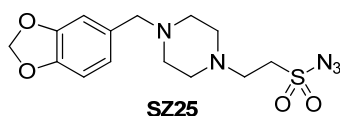


**Sulfonyl azide SZ22:** Yield = 18%.  $R_f$  = 0.63 in hexanes : EtOAc = 2:1 (stained with Ninhydrin).  $^1\text{H}$  NMR (400 MHz,  $\text{CDCl}_3$ )  $\delta$  3.56 – 3.47 (m, 1H), 3.43 – 3.25 (m, 2H), 2.96 – 2.83 (m, 2H), 2.22 – 2.13 (m, 1H), 2.04 – 1.98 (m, 1H), 1.84 – 1.68 (m, 2H), 1.67 – 1.53 (m, 5H), 1.28 – 1.06 (m, 4H), 1.03 – 0.89 (m, 2H) ppm.  $^{13}\text{C}$  NMR (101 MHz,  $\text{CDCl}_3$ )  $\delta$  66.2, 54.0, 52.7, 46.8, 42.0, 33.1, 32.4, 30.2, 25.9, 25.8, 25.7 ppm. HRMS (ESI) calcd for  $\text{C}_{11}\text{H}_{20}\text{N}_4\text{O}_2\text{S}$   $[\text{M}+\text{H}]^+$ : 273.1380, found: 273.1375



**Sulfonyl azide SZ24:** Yield = 38%.  $R_f$  = 0.73 in hexanes : EtOAc = 1:1.  $^1\text{H}$  NMR (400 MHz,  $\text{CDCl}_3$ )  $\delta$  7.32 – 7.11 (m, 5H), 3.47 (t,  $J$  = 6.3 Hz, 2H), 2.91 (d,  $J$  = 11.1 Hz, 2H),

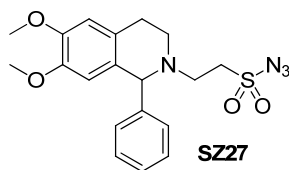
2.83 (t,  $J = 6.3$  Hz, 2H), 2.52 (d,  $J = 7.0$  Hz, 2H), 1.97 (m, 2H), 1.66 (d,  $J = 12.6$  Hz, 2H), 1.60 – 1.48 (m, 1H), 1.38 – 1.23 (m, 2H) ppm.  $^{13}\text{C}$  NMR (101 MHz,  $\text{CDCl}_3$ )  $\delta$  140.5, 129.2, 128.3, 126.0, 53.9, 53.8, 52.5, 43.2, 37.8, 32.2 ppm. HRMS (ESI) calcd for  $\text{C}_{14}\text{H}_{20}\text{N}_4\text{O}_2\text{S}$   $[\text{M}+\text{H}]^+$ : 309.1380, found: 309.1373



**Sulfonyl azide SZ25:** Yield = 42%.  $R_f = 0.45$  in hexanes : EtOAc = 1:4.  $^1\text{H}$  NMR (400 MHz,  $\text{CDCl}_3$ )  $\delta$  6.82 (s, 1H), 6.72 (m, 2H), 5.91 (s, 2H), 3.48 (t,  $J = 6.3$  Hz, 2H), 3.39 (s, 2H), 2.87 (t,  $J = 6.3$  Hz, 2H), 2.56 – 2.42 (m,  $J = 22.7$  Hz, 8H) ppm.  $^{13}\text{C}$  NMR (101 MHz,  $\text{CDCl}_3$ )  $\delta$  147.7, 146.7, 131.9, 122.2, 109.4, 107.9, 100.9, 62.6, 53.5, 53.0, 52.8, 52.2 ppm. HRMS (ESI) calcd for  $\text{C}_{14}\text{H}_{19}\text{N}_5\text{O}_4\text{S}$   $[\text{M}+\text{H}]^+$ : 354.1231, found: 354.1226



**Sulfonyl azide SZ26:** Yield = 60%.  $R_f = 0.54$  in hexanes : EtOAc = 4:1.  $^1\text{H}$  NMR (400 MHz,  $\text{CDCl}_3$ )  $\delta$  7.38 – 7.23 (m, 10H), 3.65 (s, 4H), 3.34 (dd,  $J = 8.3, 6.1$  Hz, 2H), 3.05 (dd,  $J = 8.3, 6.2$  Hz, 2H) ppm.  $^{13}\text{C}$  NMR (101 MHz,  $\text{CDCl}_3$ )  $\delta$  138.1, 129.0, 128.7, 127.7, 58.8, 53.8, 47.6 ppm. HRMS (ESI) calcd for  $\text{C}_{16}\text{H}_{18}\text{N}_4\text{O}_2\text{S}$   $[\text{M}+\text{H}]^+$ : 331.1223, found: 331.1218



**Sulfonyl azide SZ27:** Yield = 40%.  $R_f = 0.44$  in hexanes : EtOAc = 2:1.  $^1\text{H}$  NMR (400 MHz,  $\text{CDCl}_3$ )  $\delta$  7.35 – 7.21 (m, 5H), 6.61 (s, 1H), 6.18 (s, 1H), 4.61 (s, 1H), 3.85 (s, 3H), 3.61 (s, 3H), 3.49 – 3.40 (m, 1H), 3.39 – 3.30 (m, 1H), 3.18 – 2.94 (m, 4H), 2.89 – 2.72 (m, 2H) ppm.  $^{13}\text{C}$  NMR (101 MHz,  $\text{CDCl}_3$ )  $\delta$  147.9, 147.4, 142.5, 129.6, 129.1, 128.5, 127.9, 126.3, 111.6, 110.9, 67.7, 55.9, 55.9, 54.1, 48.8, 47.3, 28.0 ppm. HRMS (ESI) calcd for  $\text{C}_{19}\text{H}_{22}\text{N}_4\text{O}_4\text{S}$   $[\text{M}+\text{H}]^+$ : 403.1435, found: 403.1435

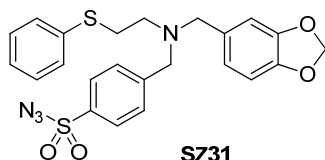


**Sulfonyl azide SZ29:** Yield = 35%.  $R_f = 0.51$  in hexanes : EtOAc = 4:1.  $^1\text{H}$  NMR (400 MHz,  $\text{CDCl}_3$ )  $\delta$  7.69 (d,  $J = 8.8$  Hz, 2H), 7.49 (d,  $J = 8.2$  Hz, 2H), 7.21 (d,  $J = 8.2$  Hz, 2H), 6.64 (d,  $J = 8.8$  Hz, 2H), 4.91 (t,  $J = 5.3$  Hz, 1H), 4.38 (d,  $J = 5.4$  Hz, 2H) ppm.  $^{13}\text{C}$  NMR (101 MHz,  $\text{CDCl}_3$ )  $\delta$  152.8, 136.6, 132.2, 130.0, 129.0, 125.2, 121.8, 112.3, 47.0 ppm.

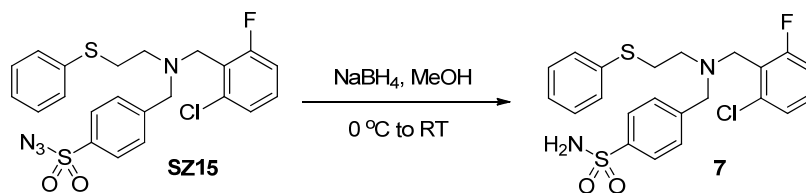


**Sulfonyl azide SZ30:** Yield = 50%.  $R_f = 0.48$  in hexanes : EtOAc = 4:1.  $^1\text{H}$  NMR (400 MHz,  $\text{CDCl}_3$ )  $\delta$  7.69 (d,  $J = 8.6$  Hz, 2H), 7.17 (d,  $J = 8.4$  Hz, 2H), 6.70 – 6.59 (m, 4H), 4.73 (s, 1H), 4.24 (d,  $J = 4.8$  Hz, 2H), 3.35 (q,  $J = 6.9$  Hz, 4H), 1.16 (t,  $J = 7.0$  Hz, 6H) ppm.  $^{13}\text{C}$  NMR (101 MHz,  $\text{CDCl}_3$ )  $\delta$  153.3, 147.7, 130.1, 129.1, 124.1, 123.6, 112.1,

112.1, 47.4, 44.6, 12.7 ppm. HRMS (ESI) calcd for  $C_{17}H_{21}N_5O_2S$   $[M+H]^+$ : 360.1489, found: 360.1490

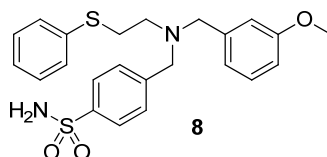


**Sulfonamide SZ31:** Yield = 81%.  $R_f$  = 0.64 in hexanes : EtOAc = 2:1.  $^1H$  NMR (400 MHz,  $CDCl_3$ )  $\delta$  7.87 (d,  $J$  = 8.3 Hz, 2H), 7.60 (d,  $J$  = 8.3 Hz, 2H), 7.22 (d,  $J$  = 4.3 Hz, 4H), 7.19 – 7.12 (m, 1H), 6.92 (s, 1H), 6.80 – 6.73 (m, 2H), 5.94 (s, 2H), 3.68 (s, 2H), 3.55 (s, 2H), 3.09 – 3.03 (m, 2H), 2.78 – 2.72 (m, 2H) ppm.  $^{13}C$  NMR (101 MHz,  $CDCl_3$ )  $\delta$  147.8, 147.8, 146.8, 136.8, 136.2, 132.4, 129.6, 128.8, 128.8, 127.4, 125.9, 121.9, 109.1, 107.9, 100.9, 58.3, 57.6, 52.6, 31.3 ppm. HRMS (ESI) calcd for  $C_{23}H_{22}N_4O_4S_2$   $[M+H]^+$ : 483.1155, found: 483.1159

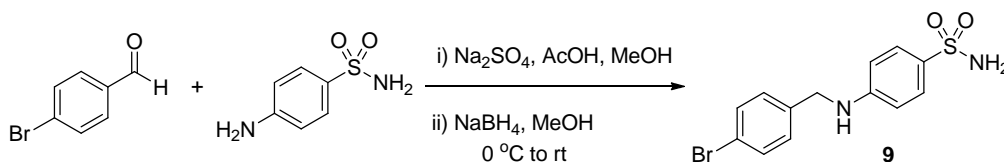


**Sulfonamide 7:** Sodium borohydride (60 mg, 1.5 mmol) was added slowly to the solution of sulfonamide SZ15 (540 mg, 1.1 mmol) in methanol at 0 °C. The system was stirred for 30 min at room temperature, quenched by solid  $NH_4Cl$  and the solvent was removed under reduced pressure to obtain crude product. The sulfonamide 7 (484 mg, 95%) was obtained by flash chromatography.  $R_f$  = 0.33 in hexanes : EtOAc = 2:1.  $^1H$  NMR (400 MHz,  $CDCl_3$ )  $\delta$ : 7.79 (d,  $J$  = 8.2 Hz, 2H), 7.42 (d,  $J$  = 8.1 Hz, 2H), 7.21 – 7.09 (m, 7H), 6.97 – 6.88 (m, 1H), 5.23 (bs, 2H), 3.83 (s, 2H), 3.68 (s, 2H), 3.06 – 2.99

(m, 2H), 2.78 – 2.71 (m, 2H) ppm.  $^{13}\text{C}$  NMR (101 MHz,  $\text{CDCl}_3$ )  $\delta$ : 162.1 (d,  $J = 248.2$  Hz), 145.1, 140.5, 136.5, 136.0, 129.5, 129.4, 129.2, 129.0, 128.9, 126.2, 126.0, 125.6, 124.4 (d,  $J = 17.2$  Hz), 114.1 (d,  $J = 23.4$  Hz), 58.0, 53.3, 49.5, 31.1 ppm. HRMS (ESI) calcd for  $\text{C}_{22}\text{H}_{22}\text{ClFN}_2\text{O}_2\text{S}_2$   $[\text{M}+\text{H}]^+$ : 465.0868, found: 465.0866

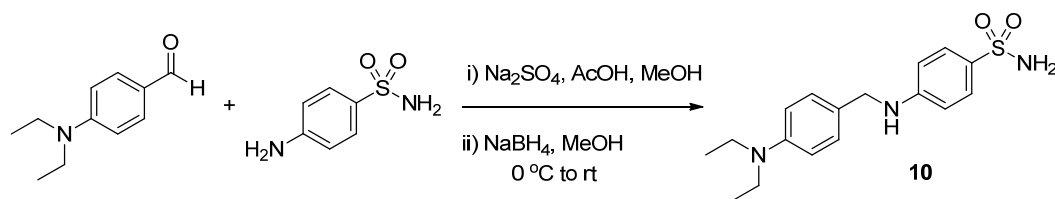


**Sulfonamide 8:** The sulfonamide **8** was obtained starting from the sulfonyl azide **SZ17** following the procedure described for the synthesis of sulfonamide **7** in 97% yield.  $R_f = 0.5$  in hexanes : EtOAc = 1:1.  $^1\text{H}$  NMR (400 MHz,  $\text{CDCl}_3$ )  $\delta$  7.85 (d,  $J = 8.4$  Hz, 2H), 7.51 (d,  $J = 8.3$  Hz, 2H), 7.24 – 7.10 (m, 6H), 6.96 – 6.91 (m, 2H), 6.80 (dd,  $J = 8.3, 2.5$  Hz, 1H), 5.08 (s, 2H), 3.81 (s, 3H), 3.65 (s, 2H), 3.60 (s, 2H), 3.07 – 3.01 (m, 2H), 2.78 – 2.72 (m, 2H) ppm.  $^{13}\text{C}$  NMR (101 MHz,  $\text{CDCl}_3$ )  $\delta$  159.8, 145.2, 140.6, 140.6, 136.4, 129.5, 129.4, 129.0, 128.9, 126.5, 126.0, 121.2, 114.5, 112.6, 58.5, 58.0, 55.3, 52.9, 31.5 ppm. HRMS (ESI) calcd for  $\text{C}_{23}\text{H}_{26}\text{N}_2\text{O}_3\text{S}_2$   $[\text{M}+\text{H}]^+$ : 443.1458, found: 443.1446

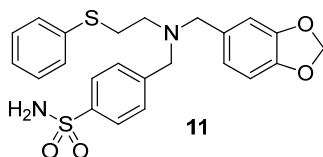


**Sulfonamide 9:** To a solution of 4-bromobenzaldehyde (200 mg, 1.08 mmol) and 4-aminobenzenesulfonamide (186 mg, 1.08 mmol) in MeOH (7 mL) was added sodium sulfate (1 g) and acetic acid (50  $\mu\text{L}$ ) and the resulting mixture was stirred at room temperature. After 3 hours, sodium sulfate was removed, reaction mixture was cooled to 0  $^\circ\text{C}$  and the sodium borohydride (123 mg, 3.24 mmol) was added carefully. The system

was stirred for 30 min at room temperature, quenched by solid  $\text{NH}_4\text{Cl}$  and the solvent was removed under reduced pressure. The sulfonamide **9** was obtained after flash chromatography in 45% yield.  $R_f = 0.59$  in  $\text{DCM} : \text{MeOH} = 10:1$ .  $^1\text{H}$  NMR (400 MHz,  $\text{DMSO-}d_6$ )  $\delta$  7.55 – 7.47 (m, 4H), 7.29 (d,  $J = 8.3$  Hz, 2H), 7.03 (t,  $J = 6.1$  Hz, 1H), 6.91 (s, 2H), 6.62 (d,  $J = 8.8$  Hz, 2H), 4.32 (d,  $J = 6.1$  Hz, 2H) ppm.  $^{13}\text{C}$  NMR (101 MHz,  $\text{DMSO-}d_6$ )  $\delta$  151.0, 139.0, 131.2, 130.5, 129.3, 127.3, 119.7, 111.2, 45.2 ppm. HRMS (ESI) calcd for  $\text{C}_{13}\text{H}_{13}\text{BrN}_2\text{O}_2\text{S}$   $[\text{M}+\text{Na}]^+$ : 362.9773, found: 362.9759



**Sulfonamide 10:** The sulfonamide **10** was obtained following the procedure described for the synthesis of sulfonamide **9** in 65% yield.  $R_f = 0.28$  in hexanes :  $\text{EtOAc} = 1:1$ .  $^1\text{H}$  NMR (400 MHz,  $\text{DMSO-}d_6$ )  $\delta$  7.49 (d,  $J = 8.8$  Hz, 2H), 7.13 (d,  $J = 8.6$  Hz, 2H), 6.88 (s, 2H), 6.79 (t,  $J = 5.6$  Hz, 1H), 6.66 – 6.60 (m, 4H), 4.16 (d,  $J = 5.6$  Hz, 2H), 3.29 (q,  $J = 6.9$  Hz, 4H), 1.06 (t,  $J = 7.0$  Hz, 6H) ppm.  $^{13}\text{C}$  NMR (101 MHz,  $\text{DMSO-}d_6$ )  $\delta$  151.4, 146.5, 129.9, 128.4, 127.2, 125.1, 111.6, 111.0, 45.6, 43.7, 12.4 ppm. HRMS (ESI) calcd for  $\text{C}_{17}\text{H}_{23}\text{N}_3\text{O}_2\text{S}$   $[\text{M}+\text{H}]^+$ : 334.1584, found: 334.1584

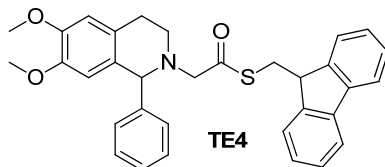


**Sulfonamide 11:** The sulfonamide **11** was obtained starting from sulfonyl azide **SZ31** following the procedure described for sulfonamide **7** in 92% yield.  $R_f = 0.2$  in hexanes :

EtOAc = 2:1.  $^1\text{H}$  NMR (400 MHz,  $\text{CDCl}_3$ )  $\delta$  7.84 (d,  $J = 8.3$  Hz, 2H), 7.48 (d,  $J = 8.3$  Hz, 2H), 7.23 – 7.10 (m, 5H), 6.89 – 6.87 (m, 1H), 6.75 – 6.72 (m, 2H), 5.92 (s, 2H), 5.23 (s, 2H), 3.62 (s, 2H), 3.50 (s, 2H), 3.04 – 2.99 (m, 2H), 2.73 – 2.69 (m, 2H) ppm.  $^{13}\text{C}$  NMR (101 MHz,  $\text{CDCl}_3$ )  $\delta$  147.7, 146.7, 145.0, 140.5, 136.2, 132.6, 129.2, 128.9, 128.8, 126.4, 125.8, 121.9, 109.1, 107.9, 100.9, 58.2, 57.7, 52.6, 31.3 ppm. HRMS (ESI) calcd for  $\text{C}_{23}\text{H}_{24}\text{N}_2\text{O}_4\text{S}_2$   $[\text{M}+\text{H}]^+$ : 457.1250, found: 457.1240

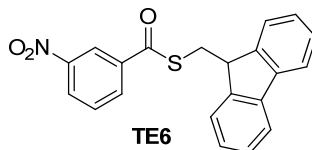
### 3.4.8 Synthesis of 9-fluorenylmethyl thioesters

All the 9-fluorenylmethyl thioesters were synthesized from the corresponding carboxylic acids following the reported procedure.<sup>16</sup> The carboxylic acids were commercially available, while 2-(6,7-dimethoxy-1-phenyl-3,4-dihydroisoquinolin-2(1H)-yl)acetic acid was synthesized as reported previously.<sup>14b</sup>

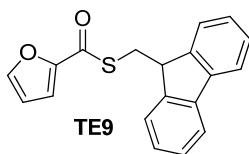


**Thioester TE4:** Yield = 51%.  $R_f = 0.2$  in hexanes : EtOAc = 10:1.  $^1\text{H}$  NMR (600 MHz,  $\text{CDCl}_3$ )  $\delta$  7.76 (t,  $J = 6.5$  Hz, 2H), 7.64 (dd,  $J = 7.3, 3.9$  Hz, 2H), 7.39 (t,  $J = 7.4$  Hz, 2H), 7.34 – 7.26 (m, 7H), 6.62 (s, 1H), 6.13 (s, 1H), 4.54 (s, 1H), 4.15 (t,  $J = 5.8$  Hz, 1H), 3.87 (s, 3H), 3.61 (s, 3H), 3.46 (d,  $J = 5.9$  Hz, 2H), 3.33 (d,  $J = 16.5$  Hz, 1H), 3.16 (d,  $J = 16.5$  Hz, 1H), 3.06 – 3.00 (m, 1H), 2.89 – 2.84 (m, 1H), 2.69 – 2.60 (m, 2H) ppm.  $^{13}\text{C}$  NMR (151 MHz,  $\text{CDCl}_3$ )  $\delta$  201.4, 147.6, 147.2, 145.9, 145.7, 143.0, 141.3, 129.7, 128.4, 127.7, 127.7, 127.6, 127.1, 126.5, 124.9, 124.9, 119.9, 119.8, 111.7, 111.0, 67.5, 63.9, 55.9,

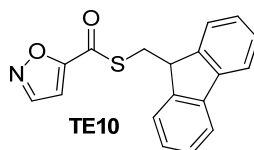
55.9, 49.2, 47.0, 31.4, 28.5 ppm. HRMS (ESI) calcd for  $C_{33}H_{31}NO_3S$   $[M+K]^+$ : 560.1656, found: 560.1656



**Thioester TE6:** Yield = 80%.  $R_f$  = 0.71 in hexanes : EtOAc = 3:1.  $^1H$  NMR (400 MHz,  $CDCl_3$ )  $\delta$  8.70 (t,  $J$  = 1.9 Hz, 1H), 8.36 (ddd,  $J$  = 8.2, 2.2, 1.0 Hz, 1H), 8.19 – 8.15 (m, 1H), 7.76 (d,  $J$  = 7.4 Hz, 2H), 7.71 (d,  $J$  = 7.5 Hz, 2H), 7.58 (t,  $J$  = 8.0 Hz, 1H), 7.41 (t,  $J$  = 7.2 Hz, 2H), 7.38 – 7.32 (m, 2H), 4.29 (t,  $J$  = 5.7 Hz, 1H), 3.78 (d,  $J$  = 5.8 Hz, 2H) ppm.  $^{13}C$  NMR (101 MHz,  $CDCl_3$ )  $\delta$  189.7, 148.3, 145.1, 141.2, 138.2, 132.7, 129.8, 128.0, 127.5, 127.3, 124.7, 122.2, 120.1, 46.5, 33.0 ppm. HRMS (ESI) calcd for  $C_{21}H_{15}NO_3S$   $[M+H]^+$ : 362.0845, found: 362.0848



**Thioester TE9:** Yield = 84%.  $R_f$  = 0.75 in hexanes : EtOAc = 2:1.  $^1H$  NMR (400 MHz,  $CDCl_3$ )  $\delta$  7.78 – 7.71 (m, 4H), 7.55 – 7.54 (m, 1H), 7.44 – 7.31 (m, 4H), 7.18 – 7.16 (m, 1H), 6.50 (dd,  $J$  = 3.6, 1.7 Hz, 1H), 4.26 (t,  $J$  = 6.0 Hz, 1H), 3.68 (d,  $J$  = 6.0 Hz, 2H) ppm.  $^{13}C$  NMR (101 MHz,  $CDCl_3$ )  $\delta$  180.3, 150.9, 146.3, 145.6, 141.2, 127.9, 127.3, 124.8, 120.0, 115.7, 112.3, 46.9, 31.7 ppm. HRMS (ESI) calcd for  $C_{19}H_{14}O_2S$   $[M+Na]^+$ : 329.0607, found: 329.0611



**Thioester TE10:** Yield = 75%.  $R_f = 0.63$  in hexanes : EtOAc = 3:1.  $^1\text{H NMR}$  (400 MHz,  $\text{CDCl}_3$ )  $\delta$  8.32 – 8.29 (m, 1H), 7.76 (d,  $J = 7.6$  Hz, 2H), 7.68 (d,  $J = 7.5$  Hz, 2H), 7.44 – 7.39 (m, 2H), 7.37 – 7.31 (m, 2H), 6.84 (m, 1H), 4.27 (t,  $J = 5.7$  Hz, 1H), 3.74 (d,  $J = 5.8$  Hz, 2H) ppm.  $^{13}\text{C NMR}$  (101 MHz,  $\text{CDCl}_3$ )  $\delta$  179.6, 164.4, 150.7, 144.9, 141.1, 128.0, 127.3, 124.6, 120.1, 105.9, 46.3, 32.2 ppm. HRMS (ESI) calcd for  $\text{C}_{18}\text{H}_{13}\text{NO}_2\text{S}$   $[\text{M}+\text{Na}]^+$ : 330.0559, found: 330.0558

### 3.4.9 General procedure A for the synthesis of acylsulfonamides

The acylsulfonamides were synthesized from corresponding sulfonamides, carboxylic acids in the presence of EDCI following a reported procedure.<sup>14b</sup>

The acylsulfonamides **SZ15TA1**, **SZ15TA3**, **SZ15TA5**, **SZ15TA6**, **SZ15TA8**, and **SZ17TA3** were synthesized using this procedure.

### 3.4.10 General procedure B for the synthesis of acylsulfonamides

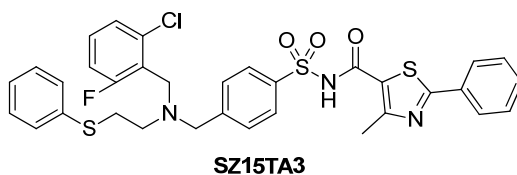
The acylsulfonamides were prepared according to a reported procedure wherein, the thioesters were first deprotected to generate corresponding thio acids *in situ*, followed by the addition of the sulfonyl azide.<sup>16</sup>

The acylsulfonamides **SZ17TA8**, **SZ31TA3**, **SZ31TA6**, **SZ31TA7**, and **SZ31TA8** were synthesized using this procedure.

### 3.4.11 Synthesis of acylsulfonamides



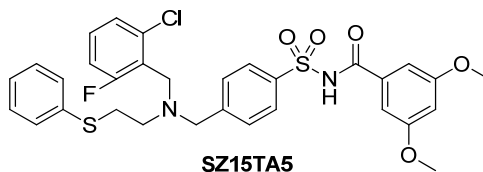
**Acylsulfonamide SZ15TA1:** Yield = 61%.  $R_f = 0.6$  in DCM : MeOH = 20:1.  $^1\text{H}$  NMR (600 MHz, DMSO)  $\delta$  7.88 – 7.84 (m, 4H), 7.56 (t,  $J = 7.3$  Hz, 1H), 7.49 (d,  $J = 8.1$  Hz, 2H), 7.44 (t,  $J = 7.7$  Hz, 2H), 7.32 – 7.26 (m, 2H), 7.15 (t,  $J = 7.8$  Hz, 3H), 7.09 (d,  $J = 7.4$  Hz, 2H), 7.01 (t,  $J = 7.2$  Hz, 1H), 3.80 (s, 2H), 3.72 (s, 2H), 3.11 – 3.06 (m, 2H), 2.66 – 2.62 (m, 2H) ppm.  $^{13}\text{C}$  NMR (101 MHz,  $\text{CD}_3\text{CN}$ )  $\delta$ : 166.3, 163.1 (d,  $J = 249.0$  Hz), 160.9, 160.5, 141.3, 138.0, 137.3, 134.5, 134.0, 133.7 (d,  $J = 10.0$  Hz), 132.4, 132.3, 131.0, 130.3, 129.7, 129.2, 128.1, 127.1, 115.7 (d,  $J = 22.5$  Hz), 58.2, 53.8, 49.8, 28.7 ppm. HRMS (ESI) calcd for  $\text{C}_{29}\text{H}_{26}\text{ClFN}_2\text{O}_3\text{S}_2$   $[\text{M}+\text{H}]^+$ : 569.1136, found: 569.1144



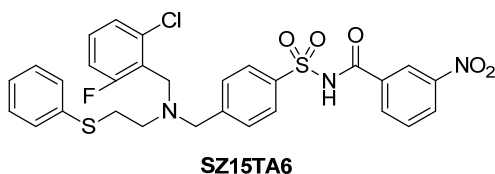
**Acylsulfonamide SZ15TA3:** Yield = 55%.  $R_f = 0.29$  in DCM : MeOH = 20:1.  $^1\text{H}$  NMR (600 MHz, DMSO)  $\delta$  7.88 – 7.84 (m, 2H), 7.71 (d,  $J = 8.0$  Hz, 2H), 7.45 – 7.40 (m, 3H), 7.32 – 7.25 (m, 4H), 7.17 – 7.10 (m, 3H), 7.03 – 6.95 (m, 3H), 3.76 (s, 2H), 3.63 (s, 2H), 3.04 – 2.98 (m, 2H), 2.60 – 2.55 (m, 2H), 2.52 (s, 3H) ppm.  $^{13}\text{C}$  NMR (63 MHz,  $\text{CDCl}_3$ )  $\delta$ : 169.9, 160.4 (d,  $J = 145.0$  Hz), 160.3, 140.0, 137.0 (d,  $J = 12.5$  Hz), 136.9, 133.0, 132.6 (d,  $J = 10.3$  Hz), 132.1, 131.8, 131.1, 130.9, 129.5, 129.4, 129.3, 127.7, 127.1,

126.4, 122.1, 117.2, 116.9, 115.0 (d,  $J = 22.5$  Hz), 57.6, 52.8, 49.0, 28.9, 17.8 ppm.

HRMS (ESI) calcd for  $C_{33}H_{29}ClFN_3O_3S_3$   $[M+H]^+$ : 666.1116, found: 666.1097

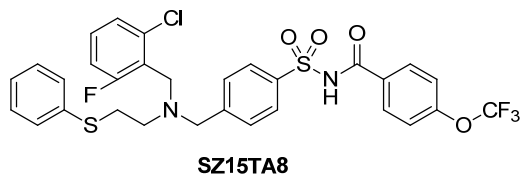


**Acylsulfonamide SZ15TA5:** Yield = 44%.  $R_f = 0.57$  in DCM : MeOH = 20:1.  $^1H$  NMR (600 MHz, DMSO)  $\delta$  7.72 (d,  $J = 8.0$  Hz, 2H), 7.45 – 7.39 (m, 1H), 7.33 – 7.22 (m, 4H), 7.16 – 7.10 (m, 3H), 7.05 – 7.00 (m, 4H), 6.98 (t,  $J = 7.4$  Hz, 1H), 6.45 (s, 1H), 3.75 (s, 2H), 3.68 (s, 6H), 3.62 (s, 2H), 3.04 – 2.98 (m, 2H), 2.61 – 2.55 (m, 2H) ppm.  $^{13}C$  NMR (101 MHz,  $CDCl_3$ )  $\delta$ : 165.0, 162.4 (d,  $J = 226.0$  Hz), 161.0, 140.2, 136.8, 136.1, 133.0, 132.9, 132.6, 131.2, 131.0, 129.5, 129.4, 127.8, 126.4, 116.3 (d,  $J = 17.0$  Hz), 115.0 (d,  $J = 22.7$  Hz), 106.3, 105.9, 57.6, 55.7, 52.8, 49.0, 28.6 ppm. HRMS (ESI) calcd for  $C_{31}H_{30}ClFN_2O_5S_2$   $[M+H]^+$ : 629.1342, found: 629.1343

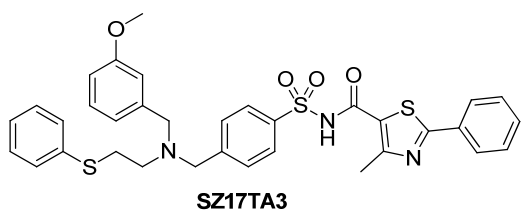


**Acylsulfonamide SZ15TA6:** Yield = 61%.  $R_f = 0.24$  in DCM : MeOH = 20:1.  $^1H$  NMR (600 MHz, DMSO)  $\delta$  8.63 (s, 1H), 8.24 (t,  $J = 6.3$  Hz, 2H), 7.78 – 7.72 (m, 2H), 7.61 (t,  $J = 7.9$  Hz, 1H), 7.45 – 7.38 (m, 2H), 7.34 – 7.22 (m, 5H), 7.15 – 7.09 (m, 3H), 7.04 – 6.94 (m, 1H), 3.75 (s, 2H), 3.64 (s, 2H), 3.04 – 2.99 (m, 2H), 2.62 – 2.55 (m, 2H) ppm.  $^{13}C$  NMR (101 MHz,  $CDCl_3$ )  $\delta$ : 163.7, 162.5 (d,  $J = 207.0$  Hz), 161.0, 148.2, 140.0, 136.8, 134.3, 133.2, 132.8, 131.3, 130.7, 130.1, 129.4, 127.7, 126.4, 123.6, 116.7 (d,  $J = 18.0$

Hz), 115.0 (d,  $J = 22.0$  Hz), 57.7, 52.8, 49.0, 28.7 ppm. HRMS (ESI) calcd for  $C_{29}H_{25}ClFN_3O_5S_2$   $[M+Na]^+$ : 636.0800, found: 636.0804

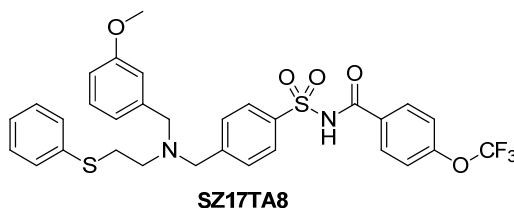


**Acylsulfonamide SZ15TA8:** Yield = 82%.  $R_f = 0.52$  in DCM : MeOH = 20:1.  $^1H$  NMR (400 MHz,  $CDCl_3$ )  $\delta$ :  $^1H$  NMR (400 MHz,  $CDCl_3$ )  $\delta$  8.00 (d,  $J = 8.8$  Hz, 2H), 7.94 (s, 2H), 7.84 (d,  $J = 8.3$  Hz, 2H), 7.19 (d,  $J = 8.3$  Hz, 2H), 7.10 – 7.04 (m, 4H), 7.04 – 7.00 (m, 2H), 6.98 – 6.90 (m, 3H), 6.89 – 6.82 (m, 1H), 3.75 (s,  $J = 1.2$  Hz, 2H), 3.53 (s, 2H), 2.95 – 2.88 (m, 2H), 2.68 – 2.60 (m, 2H) ppm.  $^{13}C$  NMR (101 MHz,  $CDCl_3$ )  $\delta$ : 164.3, 162.2 (d,  $J = 250.0$  Hz), 161.4 (d,  $J = 37.0$  Hz), 152.9, 139.8, 137.8, 136.8, 133.2, 132.3 (d,  $J = 9.5$  Hz), 131.0, 130.5, 129.6, 129.3, 129.2, 127.4, 126.2, 120.5, 120.3 (q,  $J = 259.25$  Hz), 117.6 (d,  $J = 16.1$  Hz), 114.8 (d,  $J = 22.6$  Hz), 57.4, 52.7, 48.8, 28.7 ppm. HRMS (ESI) calcd for  $C_{30}H_{25}ClF_4N_2O_4S_2$   $[M+H]^+$ : 653.0953, found: 653.0935

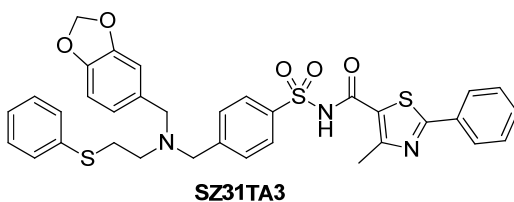


**Acylsulfonamide SZ17TA3:** Yield = 80%.  $R_f = 0.26$  in DCM : MeOH = 20:1.  $^1H$  NMR (600 MHz, DMSO)  $\delta$  7.88 – 7.84 (m, 2H), 7.75 (d,  $J = 7.8$  Hz, 2H), 7.44 – 7.41 (m, 3H), 7.36 (d,  $J = 7.8$  Hz, 2H), 7.21 – 7.12 (m, 3H), 7.09 (d,  $J = 8.0$  Hz, 2H), 7.01 (t,  $J = 7.2$  Hz, 1H), 6.94 – 6.88 (m, 2H), 6.76 (d,  $J = 7.9$  Hz, 1H), 3.70 (s, 3H), 3.59 (s, 2H), 3.55 (s, 2H), 3.12 – 3.06 (m, 2H), 2.61 – 2.55 (m, 2H), 2.53 (s, 3H) ppm.  $^{13}C$  NMR (101 MHz,

CD<sub>3</sub>OD)  $\delta$  170.7, 163.2, 161.7, 161.2, 143.3, 136.1, 134.1, 133.6, 132.8, 132.5, 132.1, 131.8, 131.6, 130.5, 130.3, 130.0, 128.8, 127.9, 125.6, 124.2, 117.4, 117.0, 59.3, 58.0, 56.0, 52.5, 28.8, 17.9 ppm. HRMS (ESI) calcd for C<sub>34</sub>H<sub>33</sub>N<sub>3</sub>O<sub>4</sub>S<sub>3</sub> [M+H]<sup>+</sup>: 644.1706, found: 644.1737

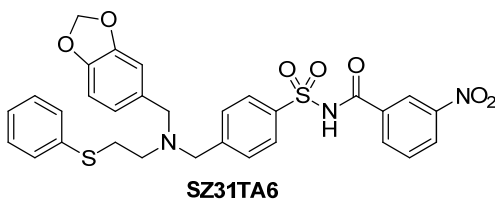


**Acylsulfonamide SZ17TA8:** Yield = 68%. R<sub>f</sub> = 0.46 in DCM : MeOH = 20:1. <sup>1</sup>H NMR (600 MHz, DMSO)  $\delta$  7.95 (d, *J* = 8.8 Hz, 2H), 7.81 (d, *J* = 8.2 Hz, 2H), 7.44 (d, *J* = 8.1 Hz, 2H), 7.31 (d, *J* = 8.3 Hz, 2H), 7.19 (t, *J* = 7.8 Hz, 1H), 7.14 – 7.07 (m, 4H), 6.98 (t, *J* = 7.2 Hz, 1H), 6.93 – 6.88 (m, 2H), 6.76 (d, *J* = 6.1 Hz, 1H), 3.70 (s, 3H), 3.62 (s, 2H), 3.57 (s, 2H), 3.12 – 3.06 (m, 2H), 2.61 – 2.55 (m, 2H) ppm. <sup>13</sup>C NMR (101 MHz, CDCl<sub>3</sub>)  $\delta$  164.5, 161.9, 161.5, 160.6, 153.1, 140.7, 134.7, 132.5, 131.7, 131.3, 130.8, 130.6, 129.6, 129.6, 128.1, 123.0, 120.6, 120.4 (q, *J* = 259.8 Hz), 116.6, 115.9, 58.2, 57.0, 55.4, 51.3, 28.3 ppm. HRMS (ESI) calcd for C<sub>31</sub>H<sub>29</sub>F<sub>3</sub>N<sub>2</sub>O<sub>5</sub>S<sub>2</sub> [M+H]<sup>+</sup>: 631.1543, found: 631.1534

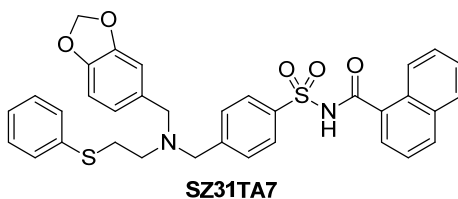


**Acylsulfonamide SZ31TA3:** Yield = 60%. R<sub>f</sub> = 0.4 in DCM : MeOH = 20:1. <sup>1</sup>H NMR (600 MHz, DMSO)  $\delta$  7.88 – 7.84 (m, 2H), 7.77 – 7.72 (m, 2H), 7.44 – 7.41 (m, 3H), 7.35

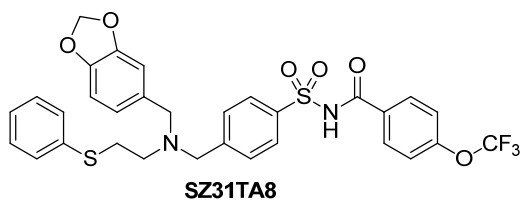
(d,  $J = 7.9$  Hz, 2H), 7.16 (t,  $J = 7.5$  Hz, 2H), 7.10 (d,  $J = 7.8$  Hz, 2H), 7.02 (t,  $J = 7.1$  Hz, 1H), 6.90 (s, 1H), 6.80 – 6.75 (m, 2H), 5.94 (s, 2H), 3.57 (s, 2H), 3.48 (s, 2H), 3.10 – 3.04 (m, 2H), 2.58 – 2.54 (m, 2H), 2.53 (s, 3H) ppm.  $^{13}\text{C}$  NMR (101 MHz,  $\text{CDCl}_3$ )  $\delta$  170.0, 161.5, 159.8, 149.6, 148.8, 140.8, 134.8, 132.6, 132.1, 131.8, 131.6, 131.5, 129.6, 129.6, 129.4, 128.2, 127.2, 125.6, 122.5, 121.2, 110.9, 109.1, 102.0, 58.1, 56.8, 50.8, 28.5, 17.9 ppm. HRMS (ESI) calcd for  $\text{C}_{34}\text{H}_{31}\text{N}_3\text{O}_5\text{S}_3$   $[\text{M}+\text{Na}]^+$ : 680.1318, found: 680.1344



**Acylsulfonamide SZ31TA6:** Yield = 65%.  $R_f = 0.27$  in DCM : MeOH = 20:1.  $^1\text{H}$  NMR (600 MHz, DMSO)  $\delta$  8.63 (s, 1H), 8.25 (d,  $J = 7.6$  Hz, 1H), 8.20 (d,  $J = 8.0$  Hz, 1H), 7.77 (t,  $J = 7.8$  Hz, 2H), 7.58 (t,  $J = 7.9$  Hz, 1H), 7.51 – 7.41 (m, 2H), 7.36 (d,  $J = 7.9$  Hz, 2H), 7.15 (t,  $J = 7.6$  Hz, 2H), 7.10 (d,  $J = 7.8$  Hz, 2H), 7.00 (t,  $J = 7.2$  Hz, 1H), 6.80 – 6.74 (m, 2H), 5.94 (s, 2H), 3.57 (s, 2H), 3.47 (s, 2H), 3.08 (d,  $J = 6.9$  Hz, 2H), 2.55 (d,  $J = 6.9$  Hz, 2H) ppm.  $^{13}\text{C}$  NMR (101 MHz,  $\text{CD}_3\text{OD}$ )  $\delta$  164.9, 149.4, 148.6, 148.3, 141.1, 135.4, 134.0, 132.8, 131.6, 131.0, 130.1, 129.3, 129.0, 127.6, 127.3, 125.5, 123.1, 122.2, 110.7, 108.6, 101.9, 58.1, 56.6, 50.9, 27.6 ppm. HRMS (ESI) calcd for  $\text{C}_{30}\text{H}_{27}\text{N}_3\text{O}_7\text{S}_2$   $[\text{M}+\text{H}]^+$ : 606.1363, found: 606.1360



**Acylsulfonamide SZ31TA7:** Yield = 50%.  $R_f = 0.54$  in DCM : MeOH = 20:1.  $^1\text{H}$  NMR (400 MHz,  $\text{CDCl}_3$ )  $\delta$  8.15 (d,  $J = 7.9$  Hz, 1H), 8.05 (d,  $J = 7.8$  Hz, 2H), 7.84 (d,  $J = 8.0$  Hz, 1H), 7.75 (d,  $J = 7.7$  Hz, 1H), 7.60 (d,  $J = 6.5$  Hz, 1H), 7.52 – 7.37 (m, 5H), 7.20 – 7.13 (m, 5H), 6.85 (s, 1H), 6.73 – 6.68 (m, 2H), 5.90 (s, 2H), 3.60 (s, 2H), 3.48 (s, 2H), 3.03 – 2.94 (m, 2H), 2.73 – 2.65 (m, 2H) ppm.  $^{13}\text{C}$  NMR (101 MHz,  $\text{CDCl}_3$ )  $\delta$  167.2, 147.9, 146.9, 146.6, 137.6, 136.4, 133.8, 132.7, 130.7, 130.2, 129.2, 129.1, 128.6, 128.0, 126.9, 126.1, 125.1, 124.6, 122.1, 109.3, 108.1, 101.1, 58.4, 57.9, 52.8, 31.6 ppm. HRMS (ESI) calcd for  $\text{C}_{34}\text{H}_{30}\text{N}_2\text{O}_5\text{S}_2$   $[\text{M}+\text{Na}]^+$ : 633.1488, found: 633.1506



**Acylsulfonamide SZ31TA8:** Yield = 62%.  $R_f = 0.57$  in DCM : MeOH = 20:1.  $^1\text{H}$  NMR (400 MHz, DMSO)  $\delta$  7.99 – 7.90 (m, 3H), 7.75 (d,  $J = 8.2$  Hz, 2H), 7.34 (d,  $J = 8.2$  Hz, 2H), 7.24 (d,  $J = 8.1$  Hz, 2H), 7.18 – 7.08 (m, 4H), 7.00 (t,  $J = 7.1$  Hz, 1H), 6.81 – 6.74 (m, 2H), 5.95 (s, 2H), 3.57 (s, 2H), 3.48 (s, 2H), 3.11 – 3.04 (m, 2H), 2.59 – 2.52 (m, 2H) ppm.  $^{13}\text{C}$  NMR (101 MHz,  $\text{CDCl}_3$ )  $\delta$  164.4, 153.1, 149.6, 148.8, 140.6, 134.9, 132.6, 131.6, 131.5, 130.6, 129.6, 129.6, 128.1, 125.6, 121.2, 120.6, 120.4 (q,  $J = 259.6$  Hz), 110.8, 109.1, 102.0, 58.1, 56.9, 50.8, 28.5 ppm. HRMS (ESI) calcd for  $\text{C}_{31}\text{H}_{27}\text{F}_3\text{N}_2\text{O}_6\text{S}_2$   $[\text{M}+\text{H}]^+$ : 645.1335, found: 645.1352

### 3.4.12 Peptide control experiments: LC/MS-SIM analysis

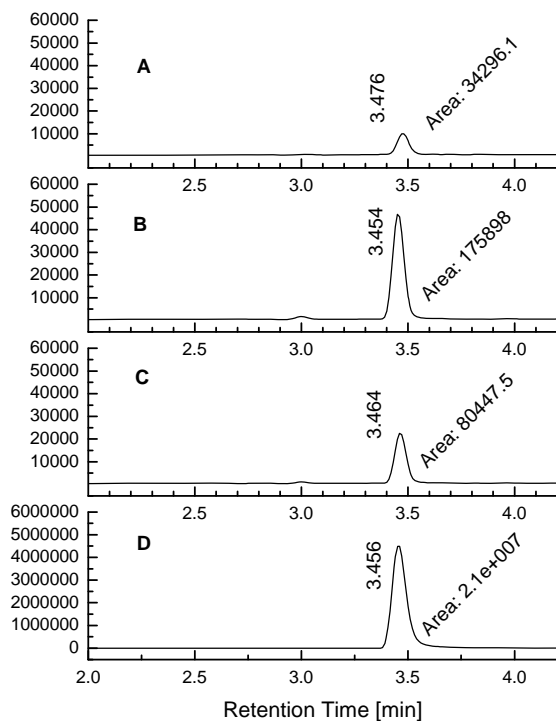


**Figure 3.7.** Incubation of **SZ15** and **TA1** and suppressing Mcl-1-templated incubations with Bim BH3 peptide. The samples were incubated for six hours at 37 °C and subjected to the LC/MS-SIM analysis. A) Incubation of **SZ15** and **TA1** without Mcl-1 B) Incubation of **SZ15** and **TA1** with 10  $\mu$ M Mcl-1 C) Incubation of **SZ15** and **TA1** with 10  $\mu$ M Mcl-1 and 20  $\mu$ M Bim D) Synthetic **SZ15TA1** as the reference.

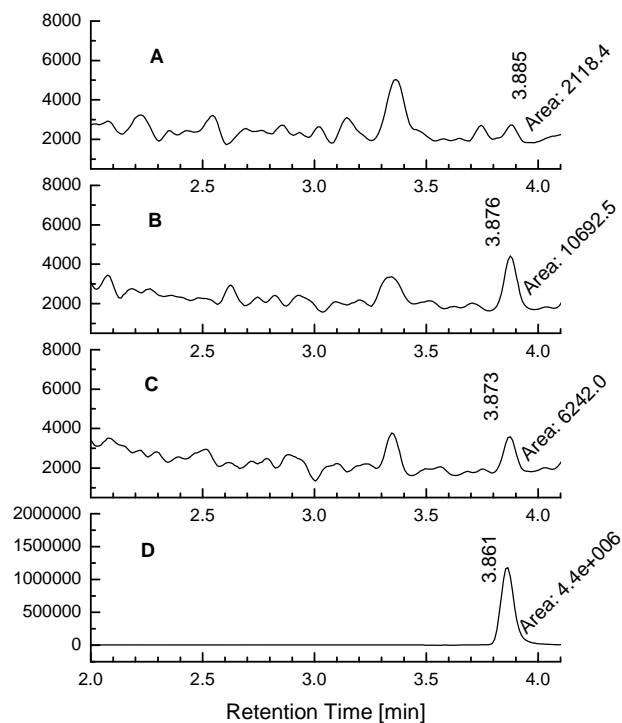


**Figure 3.8.** Incubation of **SZ15** and **TA3** and suppressing Mcl-1-templated incubations with Bim BH3 peptide. The samples were incubated for six hours at 37 °C and subjected to the LC/MS-SIM analysis. A) Incubation of **SZ15** and **TA3** without Mcl-1 B) Incubation of **SZ15** and **TA3** with 10  $\mu$ M Mcl-1 C) Incubation of **SZ15** and **TA3** with 10  $\mu$ M Mcl-1 and 20  $\mu$ M Bim D) Synthetic **SZ15TA3** as the reference.

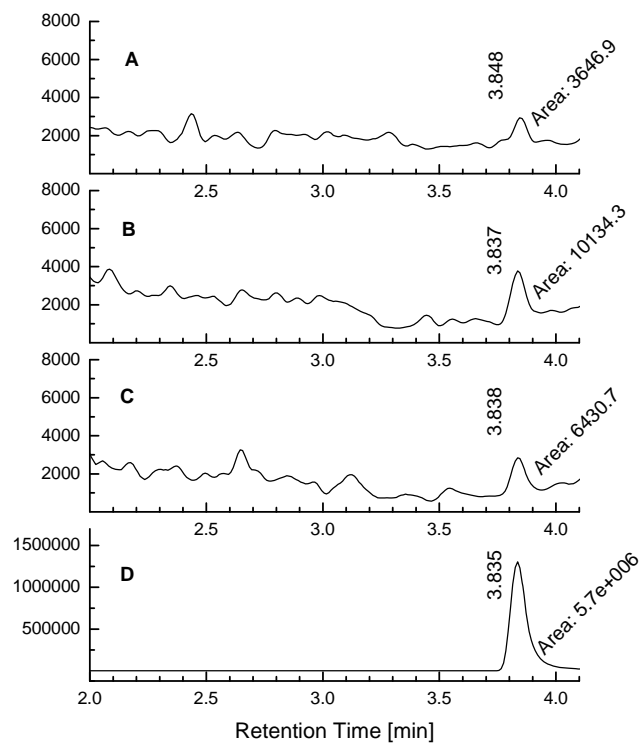


**Figure 3.9.** Incubation of **SZ15** and **TA5** and suppressing Mcl-1-templated incubations with Bim BH3 peptide. The samples were incubated for six hours at 37 °C and subjected to the LC/MS-SIM analysis. A) Incubation of **SZ15** and **TA5** without Mcl-1 B) Incubation of **SZ15** and **TA5** with 10  $\mu$ M Mcl-1 C) Incubation of **SZ15** and **TA5** with 10  $\mu$ M Mcl-1 and 20  $\mu$ M Bim D) Synthetic **SZ15TA5** as the reference.

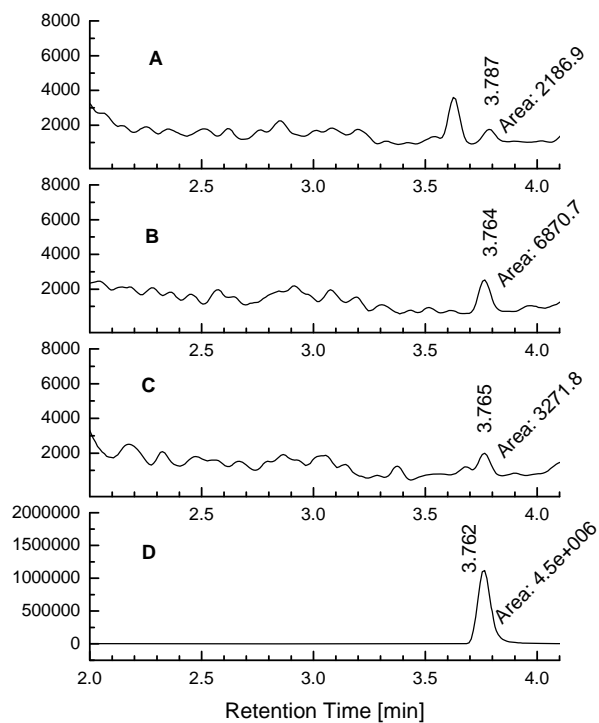


**Figure 3.10.** Incubation of **SZ15** and **TA6** and suppressing Mcl-1-templated incubations with Bim BH3 peptide. The samples were incubated for six hours at 37 °C and subjected to the LC/MS-SIM analysis. A) Incubation of **SZ15** and **TA6** without Mcl-1 B) Incubation of **SZ15** and **TA6** with 10  $\mu$ M Mcl-1 C) Incubation of **SZ15** and **TA6** with 10  $\mu$ M Mcl-1 and 20  $\mu$ M Bim D) Synthetic **SZ15TA6** as the reference.

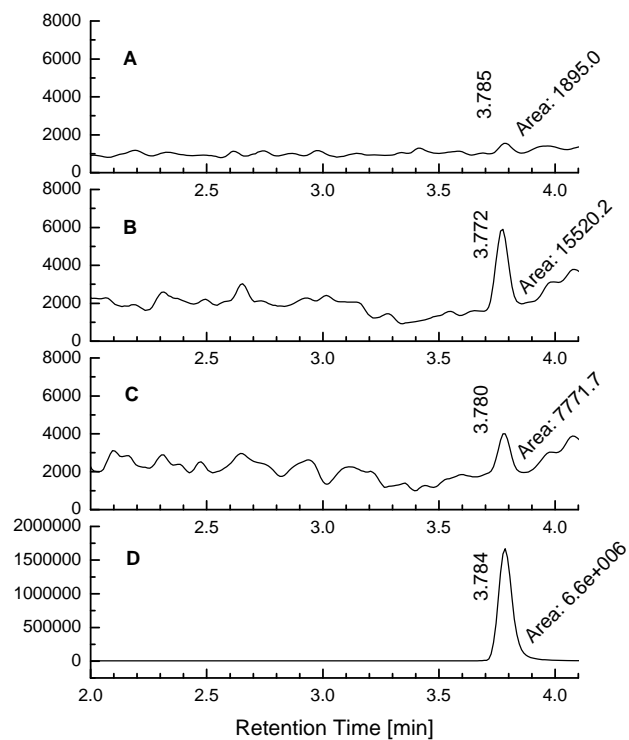


**Figure 3.11.** Incubation of **SZ17** and **TA3** and suppressing Mcl-1-templated incubations with Bim BH3 peptide. The samples were incubated for six hours at 37 °C and subjected to the LC/MS-SIM analysis. A) Incubation of **SZ17** and **TA3** without Mcl-1 B) Incubation of **SZ17** and **TA3** with 10  $\mu$ M Mcl-1 C) Incubation of **SZ17** and **TA3** with 10  $\mu$ M Mcl-1 and 20  $\mu$ M Bim D) Synthetic **SZ17TA3** as the reference.

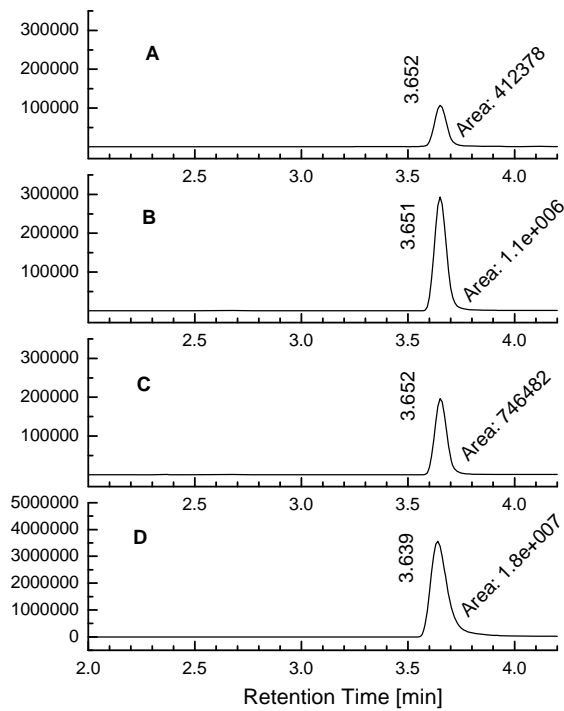


**Figure 3.12.** Incubation of **SZ17** and **TA8** and suppressing Mcl-1-templated incubations with Bim BH3 peptide. The samples were incubated for six hours at 37 °C and subjected to the LC/MS-SIM analysis. A) Incubation of **SZ17** and **TA8** without Mcl-1 B) Incubation of **SZ17** and **TA8** with 10  $\mu$ M Mcl-1 C) Incubation of **SZ17** and **TA8** with 10  $\mu$ M Mcl-1 and 20  $\mu$ M Bim D) Synthetic **SZ17TA8** as the reference.

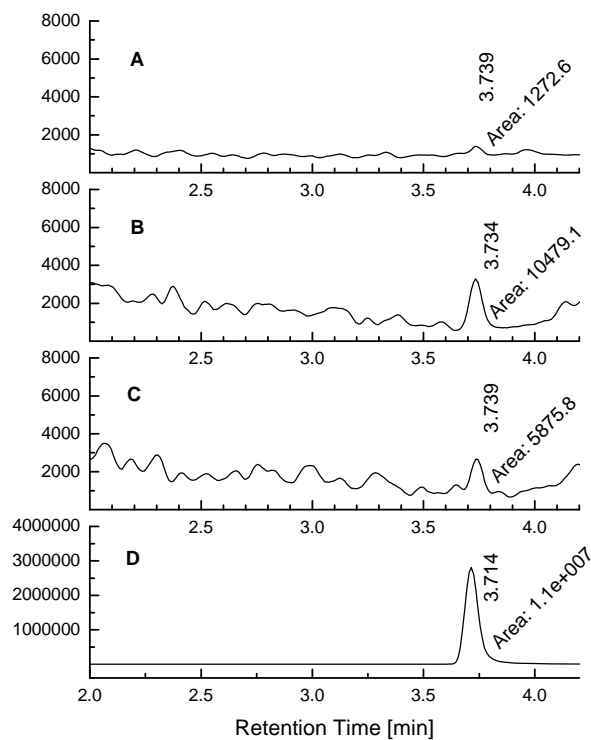


**Figure 3.13.** Incubation of **SZ31** and **TA3** and suppressing Mcl-1-templated incubations with Bim BH3 peptide. The samples were incubated for six hours at 37 °C and subjected to the LC/MS-SIM analysis. A) Incubation of **SZ31** and **TA3** without Mcl-1 B) Incubation of **SZ31** and **TA3** with 10  $\mu$ M Mcl-1 C) Incubation of **SZ31** and **TA3** with 10  $\mu$ M Mcl-1 and 20  $\mu$ M Bim D) Synthetic **SZ31TA3** as the reference.

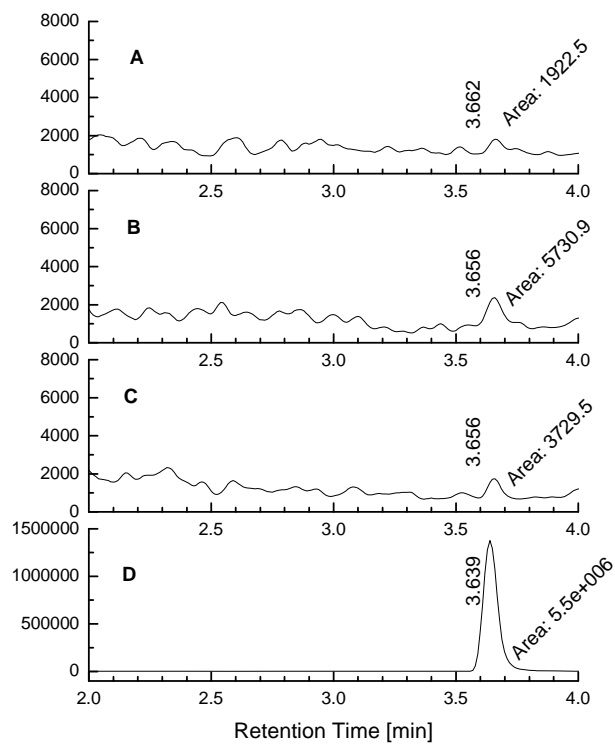


**Figure 3.14.** Incubation of **SZ31** and **TA6** and suppressing Mcl-1-templated incubations with Bim BH3 peptide. The samples were incubated for six hours at 37 °C and subjected to the LC/MS-SIM analysis. A) Incubation of **SZ31** and **TA6** without Mcl-1 B) Incubation of **SZ31** and **TA6** with 10  $\mu$ M Mcl-1 C) Incubation of **SZ31** and **TA6** with 10  $\mu$ M Mcl-1 and 20  $\mu$ M Bim D) Synthetic **SZ31TA6** as the reference.

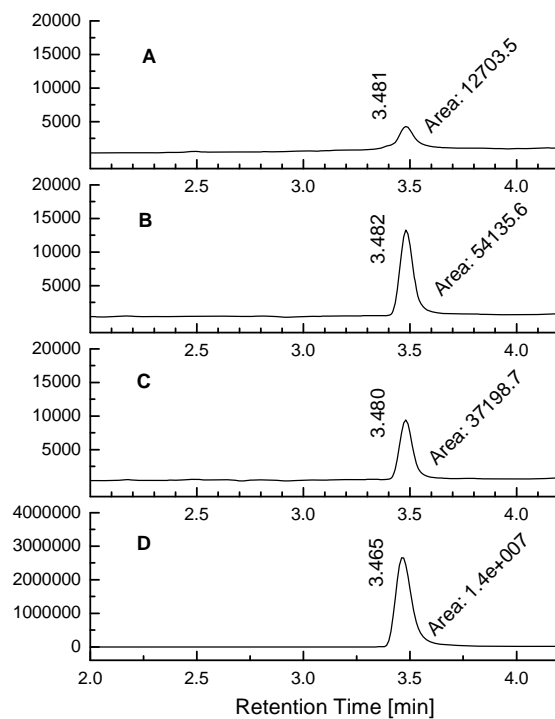


**Figure 3.15.** Incubation of **SZ31** and **TA7** and suppressing Mcl-1-templated incubations with Bim BH3 peptide. The samples were incubated for six hours at 37 °C and subjected to the LC/MS-SIM analysis. A) Incubation of **SZ31** and **TA7** without Mcl-1 B) Incubation of **SZ31** and **TA7** with 10  $\mu$ M Mcl-1 C) Incubation of **SZ31** and **TA7** with 10  $\mu$ M Mcl-1 and 20  $\mu$ M Bim D) Synthetic **SZ31TA7** as the reference.

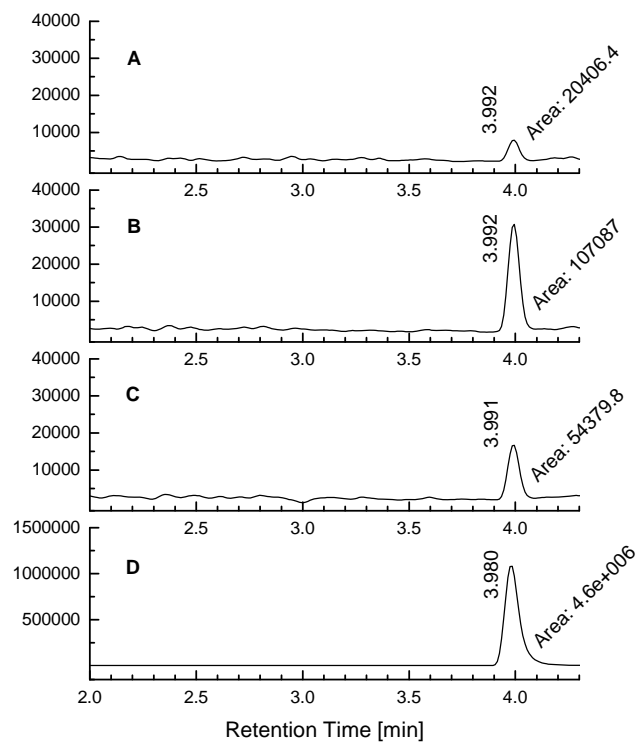


**Figure 3.16.** Incubation of **SZ31** and **TA8** and suppressing Mcl-1-templated incubations with Bim BH3 peptide. The samples were incubated for six hours at 37 °C and subjected to the LC/MS-SIM analysis. A) Incubation of **SZ31** and **TA8** without Mcl-1 B) Incubation of **SZ31** and **TA8** with 10  $\mu$ M Mcl-1 C) Incubation of **SZ31** and **TA8** with 10  $\mu$ M Mcl-1 and 20  $\mu$ M Bim D) Synthetic **SZ31TA8** as the reference.

### 3.5 References cited

1. (a) Tsujimoto, Y.; Cossman, J.; Jaffe, E.; Croce, C. M., Involvement of the Bcl-2 Gene in Human Follicular Lymphoma. *Science* **1985**, 228 (4706), 1440-1443; (b) Walensky, L. D., BCL-2 in the crosshairs: tipping the balance of life and death. *Cell Death Differ.* **2006**, 13 (8), 1339-1350.
2. (a) Youle, R. J.; Strasser, A., The BCL-2 protein family: opposing activities that mediate cell death. *Nat. Rev. Mol. Cell Biol.* **2008**, 9 (1), 47-59; (b) Green, D. R.; Evan, G. I., A matter of life and death. *Cancer Cell* **2002**, 1 (1), 19-30; (c) Green, D. R., At the gates of death. *Cancer Cell* **2006**, 9 (5), 328-330.
3. (a) Azmi, A. S.; Mohammad, R. M., Non-Peptidic Small Molecule Inhibitors Against Bcl-2 for Cancer Therapy. *J. Cell. Physiol.* **2009**, 218 (1), 13-21; (b) Wang, J. L.; Liu, D. X.; Zhang, Z. J.; Shan, S. M.; Han, X. B.; Srinivasula, S. M.; Croce, C. M.; Alnemri, E. S.; Huang, Z. W., Structure-based discovery of an organic compound that binds Bcl-2 protein and induces apoptosis of tumor cells. *Proc. Natl. Acad. Sci. U.S.A.* **2000**, 97 (13), 7124-7129; (c) Degterev, A.; Lugovskoy, A.; Cardone, M.; Mulley, B.; Wagner, G.; Mitchison, T.; Yuan, J. Y., Identification of small-molecule inhibitors of interaction between the BH3 domain and Bcl-x(L). *Nat. Cell Biol.* **2001**, 3 (2), 173-182; (d) Tzung, S. P.; Kim, K. M.; Basanez, G.; Giedt, C. D.; Simon, J.; Zimmerberg, J.; Zhang, K. Y. J.; Hockenbery, D. M., Antimycin A mimics a cell-death-inducing Bcl-2 homology domain 3. *Nat. Cell Biol.* **2001**, 3 (2), 183-191; (e) Enyedy, I. J.; Ling, Y.; Nacro, K.; Tomita, Y.; Wu, X. H.; Cao, Y. Y.; Guo, R. B.; Li, B. H.; Zhu, X. F.; Huang, Y.; Long, Y. Q.; Roller, P. P.; Yang, D. J.; Wang, S. M., Discovery of small-molecule inhibitors of bcl-2 through structure-based computer screening. *J. Med. Chem.* **2001**, 44

(25), 4313-4324; (f) Kutzki, O.; Park, H. S.; Ernst, J. T.; Orner, B. P.; Yin, H.; Hamilton, A. D., Development of a potent Bcl-x(L) antagonist based on alpha-helix mimicry. *J. Am. Chem. Soc.* **2002**, *124* (40), 11838-11839; (g) Zhou, H. B.; Aguilar, A.; Chen, J. F.; Bai, L. C.; Liu, L.; Meagher, J. L.; Yang, C. Y.; McEachern, D.; Cong, X.; Stuckey, J. A.; Wang, S. M., Structure-Based Design of Potent Bcl-2/Bcl-xL Inhibitors with Strong in Vivo Antitumor Activity. *J. Med. Chem.* **2012**, *55* (13), 6149-6161.

4. (a) Yip, K. W.; Reed, J. C., Bcl-2 family proteins and cancer. *Oncogene* **2008**, *27* (50), 6398-6406; (b) Vogler, M.; Dinsdale, D.; Dyer, M. J. S.; Cohen, G. M., Bcl-2 inhibitors: small molecules with a big impact on cancer therapy. *Cell Death Differ.* **2009**, *16* (3), 360-367; (c) Tse, C.; Shoemaker, A. R.; Adickes, J.; Anderson, M. G.; Chen, J.; Jin, S.; Johnson, E. F.; Marsh, K. C.; Mitten, M. J.; Nimmer, P.; Roberts, L.; Tahir, S. K.; Mao, Y.; Yang, X. F.; Zhang, H. C.; Fesik, S.; Rosenberg, S. H.; Elmore, S. W., ABT-263: A potent and orally bioavailable Bcl-2 family inhibitor. *Cancer Res.* **2008**, *68* (9), 3421-3428.

5. (a) Yecies, D.; Carlson, N. E.; Deng, J.; Letai, A., Acquired resistance to ABT-737 in lymphoma cells that up-regulate MCL-1 and BFL-1. *Blood* **2010**, *115* (16), 3304-3313; (b) Hikita, H.; Takehara, T.; Shimizu, S.; Kodama, T.; Shigekawa, M.; Iwase, K.; Hosui, A.; Miyagi, T.; Tatsumi, T.; Ishida, H.; Li, W.; Kanto, T.; Hiramatsu, N.; Hayashi, N., The Bcl-xL Inhibitor, ABT-737, Efficiently Induces Apoptosis and Suppresses Growth of Hepatoma Cells in Combination with Sorafenib. *Hepatology* **2010**, *52* (4), 1310-1321.

6. (a) Oltersdorf, T.; Elmore, S. W.; Shoemaker, A. R.; Armstrong, R. C.; Augeri, D. J.; Belli, B. A.; Bruncko, M.; Deckwerth, T. L.; Dinges, J.; Hajduk, P. J.; Joseph, M. K.;

Kitada, S.; Korsmeyer, S. J.; Kunzer, A. R.; Letai, A.; Li, C.; Mitten, M. J.; Nettesheim, D. G.; Ng, S.; Nimmer, P. M.; O'Connor, J. M.; Oleksijew, A.; Petros, A. M.; Reed, J. C.; Shen, W.; Tahir, S. K.; Thompson, C. B.; Tomaselli, K. J.; Wang, B. L.; Wendt, M. D.; Zhang, H. C.; Fesik, S. W.; Rosenberg, S. H., An inhibitor of Bcl-2 family proteins induces regression of solid tumours. *Nature* **2005**, *435* (7042), 677-681; (b) van Delft, M. F.; Wei, A. H.; Mason, K. D.; Vandenberg, C. J.; Chen, L.; Czabotar, P. E.; Willis, S. N.; Scott, C. L.; Day, C. L.; Cory, S.; Adams, J. M.; Roberts, A. W.; Huang, D. C. S., The BH3 mimetic ABT-737 targets selective Bcl-2 proteins and efficiently induces apoptosis via Bak/Bax if Mcl-1 is neutralized. *Cancer Cell* **2006**, *10* (5), 389-399; (c) Chen, S.; Dai, Y.; Harada, H.; Dent, P.; Grant, S., Mcl-1 down-regulation potentiates ABT-737 lethality by cooperatively inducing bak activation and bax translocation. *Cancer Res.* **2007**, *67* (2), 782-791; (d) Konopleva, M.; Contractor, R.; Tsao, T.; Samudio, I.; Ruvalo, P. P.; Kitada, S.; Deng, X. M.; Zhai, D. Y.; Shi, Y. X.; Sneed, T.; Verhaegen, M.; Soengas, M.; Ruvolo, V. R.; McQueen, T.; Schober, W. D.; Watt, J. C.; Jiffar, T.; Ling, X. Y.; Marini, F. C.; Harris, D.; Dietrich, M.; Estrov, Z.; McCubrey, J.; May, W. S.; Reed, J. C.; Andreeff, M., Mechanisms of apoptosis sensitivity and resistance to the BH3 mimetic ABT-737 in acute myeloid leukemia. *Cancer Cell* **2006**, *10* (5), 375-388; (e) Lin, X.; Morgan-Lappe, S.; Huang, X.; Li, L.; Zakula, D. M.; Verneti, L. A.; Fesik, S. W.; Shen, Y., 'Seed' analysis of off-target siRNAs reveals an essential role of Mcl-1 in resistance to the small-molecule Bcl-2/Bcl-X-L inhibitor ABT-737. *Oncogene* **2007**, *26* (27), 3972-3979; (f) Tahir, S. K.; Yang, X. F.; Anderson, M. G.; Morgan-Lappe, S. E.; Sarthy, A. V.; Chen, J.; Warner, R. B.; Ng, S. C.; Fesik, S. W.; Elmore, S. W.;

Rosenberg, S. H.; Tse, C., Influence of Bcl-2 family members on the cellular response of small-cell lung cancer cell lines to ABT-737. *Cancer Res.* **2007**, *67* (3), 1176-1183.

7. Willis, S. N.; Chen, L.; Dewson, G.; Wei, A.; Naik, E.; Fletcher, J. I.; Adams, J. M.; Huang, D. C. S., Proapoptotic Bak is sequestered by Mcl-1 and Bcl-x(L), but not Bcl-2, until displaced by BH3-only proteins. *Gene Dev* **2005**, *19* (11), 1294-1305.

8. Warr, M. R.; Shore, G. C., Unique biology of Mcl-1: therapeutic opportunities in cancer. *Curr. Mol. Med.* **2008**, *8* (2), 138-147.

9. Doi, K.; Li, R. S.; Sung, S. S.; Wu, H. W.; Liu, Y.; Manieri, W.; Krishnegowda, G.; Awwad, A.; Dewey, A.; Liu, X.; Amin, S.; Cheng, C. W.; Qin, Y.; Schonbrunn, E.; Daughdrill, G.; Loughran, T. P.; Sebti, S.; Wang, H. G., Discovery of Marinopyrrole A (Maritoclax) as a Selective Mcl-1 Antagonist that Overcomes ABT-737 Resistance by Binding to and Targeting Mcl-1 for Proteasomal Degradation. *J. Biol. Chem.* **2012**, *287* (13), 10224-10235.

10. (a) Wei, J.; Kitada, S.; Stebbins, J. L.; Placzek, W.; Zhai, D. Y.; Wu, B. N.; Rega, M. F.; Hang, Z. M.; Cellitti, J.; Yang, L.; Dahl, R.; Reed, J. C.; Pellecchia, M., Synthesis and Biological Evaluation of Apogossypolone Derivatives as Pan-active Inhibitors of Antiapoptotic B-Cell Lymphoma/Leukemia-2 (Bcl-2) Family Proteins. *J. Med. Chem.* **2010**, *53* (22), 8000-8011; (b) Wang, G. P.; Nikolovska-Coleska, Z.; Yang, C. Y.; Wang, R. X.; Tang, G. Z.; Guo, J.; Shangary, S.; Qiu, S.; Gao, W.; Yang, D. J.; Meagher, J.; Stuckey, J.; Krajewski, K.; Jiang, S.; Roller, P. P.; Abaan, H. O.; Tomita, Y.; Wang, S. M., Structure-based design of potent small-molecule inhibitors of anti-apoptotic Bcl-2 proteins. *J. Med. Chem.* **2006**, *49* (21), 6139-6142; (c) Tang, G. Z.; Ding, K.; Nikolovska-Coleska, Z.; Yang, C. Y.; Qiu, S.; Shangary, S.; Wang, R. X.; Guo, J.; Gao,

W.; Meagher, J.; Stuckey, J.; Krajewski, K.; Jiang, S.; Roller, P. P.; Wang, S. M., Structure-based design of flavonoid compounds as a new class of small-molecule inhibitors of the anti-apoptotic bcl-2 proteins. *J. Med. Chem.* **2007**, *50* (14), 3163-3166;

(d) Rega, M. F.; Wu, B. A.; Wei, J.; Zhang, Z. M.; Cellitti, J. F.; Pellecchia, M., SAR by Interligand Nuclear Overhauser Effects (ILOEs) Based Discovery of Acylsulfonamide Compounds Active against Bcl-x(L) and Mcl-1. *J. Med. Chem.* **2011**, *54* (17), 6000-6013;

(e) Tang, G. Z.; Yang, C. Y.; Nikolovska-Coleska, Z.; Guo, J.; Qiu, S.; Wang, R. X.; Gao, W.; Wang, G. P.; Stuckey, J.; Krajewski, K.; Jiang, S.; Roller, P. P.; Wang, S. M., Pyrogallol-based molecules as potent inhibitors of the antiapoptotic Bcl-2 proteins. *J. Med. Chem.* **2007**, *50* (8), 1723-1726;

(f) Zhang, C. Z.; Zhang, H. T.; Yun, J. P.; Chen, G. G.; Lai, P. B. S., Dihydroartemisinin exhibits antitumor activity toward hepatocellular carcinoma in vitro and in vivo. *Biochem. Pharmacol.* **2012**, *83* (9), 1278-1289;

(g) Prakesch, M.; Denisov, A. Y.; Naim, M.; Gehring, K.; Arya, P., The discovery of small molecule chemical probes of Bcl-X(L) and Mcl-1. *Bioorg. Med. Chem.* **2008**, *16* (15), 7443-7449;

(h) Feng, Y.; Ding, X.; Chen, T.; Chen, L. L.; Liu, F.; Jia, X.; Luo, X. M.; Shen, X.; Chen, K. X.; Jiang, H. L.; Wang, H.; Liu, H.; Liu, D. X., Design, Synthesis, and Interaction Study of Quinazoline-2(1H)-thione Derivatives as Novel Potential Bcl-x(L) Inhibitors. *J. Med. Chem.* **2010**, *53* (9), 3465-3479;

(i) Wei, J.; Stebbins, J. L.; Kitada, S.; Dash, R.; Placzek, W.; Rega, M. F.; Wu, B. N.; Cellitti, J.; Zhai, D. Y.; Yang, L.; Dahl, R.; Fisher, P. B.; Reed, J. C.; Pellecchia, M., BI-97C1, an Optically Pure Apogossypol Derivative as Pan-Active Inhibitor of Antiapoptotic B-Cell Lymphoma/Leukemia-2 (Bcl-2) Family Proteins. *J. Med. Chem.* **2010**, *53* (10), 4166-4176;

(j) Wei, J.; Kitada, S.; Rega, M. F.; Stebbins, J. L.; Zhai, D. Y.; Cellitti, J.; Yuan,

H. B.; Emdadi, A.; Dahl, R.; Zhang, Z. M.; Yang, L.; Reed, J. C.; Pellecchia, M., Apogossypol Derivatives as Pan-Active Inhibitors of Antiapoptotic B-Cell Lymphoma/Leukemia-2 (Bcl-2) Family Proteins. *J. Med. Chem.* **2009**, *52* (14), 4511-4523; (k) Tang, G. Z.; Nikolovska-Coleska, Z.; Qiu, S.; Yang, C. Y.; Guo, J.; Wang, S. M., Acylpyrogallols as inhibitors of antiapoptotic Bcl-2 proteins. *J. Med. Chem.* **2008**, *51* (4), 717-720; (l) Zhang, Z. C.; Wu, G. Y.; Xie, F. B.; Song, T.; Chang, X. L., 3-Thiomorpholin-8-oxo-8H-acenaphtho[1,2-b]pyrrole-9-carbonitrile (S1) Based Molecules as Potent, Dual Inhibitors of B-Cell Lymphoma 2 (Bcl-2) and Myeloid Cell Leukemia Sequence 1 (Mcl-1): Structure-Based Design and Structure-Activity Relationship Studies. *J. Med. Chem.* **2011**, *54* (4), 1101-1105.

11. (a) Stewart, M. L.; Fire, E.; Keating, A. E.; Walensky, L. D., The MCL-1 BH3 helix is an exclusive MCL-1 inhibitor and apoptosis sensitizer. *Nat. Chem. Biol.* **2010**, *6* (8), 595-601; (b) Bernardo, P. H.; Sivaraman, T.; Wan, K. F.; Xu, J.; Krishnamoorthy, J.; Song, C. M.; Tian, L. M.; Chin, J. S. F.; Lim, D. S. W.; Mok, H. Y. K.; Yu, V. C.; Tong, J. C.; Chai, C. L. L., Structural Insights into the Design of Small Molecule Inhibitors That Selectively Antagonize Mcl-1. *J. Med. Chem.* **2010**, *53* (5), 2314-2318; (c) Oh, H.; Jensen, P. R.; Murphy, B. T.; Fiorilla, C.; Sullivan, J. F.; Ramsey, T.; Fenical, W., Cryptosphaerolide, a Cytotoxic Mcl-1 Inhibitor from a Marine-Derived Ascomycete Related to the Genus *Cryptosphaeria*. *J. Nat. Prod.* **2010**, *73* (5), 998-1001; (d) Lee, E. F.; Czabotar, P. E.; Van Delft, M. F.; Michalak, E. M.; Boyle, M. J.; Willis, S. N.; Puthalakath, H.; Bouillet, P.; Colman, P. M.; Huang, D. C. S.; Fairlie, W. D., A novel BH3 ligand that selectively targets Mcl-1 reveals that apoptosis can proceed without Mcl-1 degradation. *J. Cell Biol.* **2008**, *180* (2), 341-355.

12. (a) Becattini, B.; Pellecchia, M., SAR by ILOEs: An NMIR-based approach to reverse chemical genetics. *Chem.-Eur. J.* **2006**, *12* (10), 2658-2662; (b) Becattini, B.; Sareth, S.; Zhai, D. Y.; Crowell, K. J.; Leone, M.; Reed, J. C.; Pellecchia, M., Targeting apoptosis via chemical design: Inhibition of bid-induced cell death by small organic molecules. *Chem. Biol.* **2004**, *11* (8), 1107-1117.
13. Petros, A. M.; Dinges, J.; Augeri, D. J.; Baumeister, S. A.; Betebenner, D. A.; Bures, M. G.; Elmore, S. W.; Hajduk, P. J.; Joseph, M. K.; Landis, S. K.; Nettlesheim, D. G.; Rosenberg, S. H.; Shen, W.; Thomas, S.; Wang, X. L.; Zanze, I.; Zhang, H. C.; Fesik, S. W., Discovery of a potent inhibitor of the antiapoptotic protein Bcl-x(L) from NMR and parallel synthesis. *J. Med. Chem.* **2006**, *49* (2), 656-663.
14. (a) Hu, X. D.; Sun, J. Z.; Wang, H. G.; Manetsch, R., Bcl-X-L-templated assembly of its own protein-protein interaction modulator from fragments decorated with thio acids and sulfonyl azides. *J. Am. Chem. Soc.* **2008**, *130* (42), 13820-13821; (b) Kulkarni, S. S.; Hu, X. D.; Doi, K.; Wang, H. G.; Manetsch, R., Screening of Protein-Protein Interaction Modulators via Sulfo-Click Kinetic Target-Guided Synthesis. *ACS Chem. Biol.* **2011**, *6* (7), 724-732.
15. Raushel, J.; Pitram, S. M.; Fokin, V. V., Efficient synthesis of sulfonyl azides from sulfonamides. *Org. Lett.* **2008**, *10* (16), 3385-3388.
16. Namelikonda, N. K.; Manetsch, R., Sulfo-click reaction via in situ generated thioacids and its application in kinetic target-guided synthesis. *Chem. Commun.* **2012**, *48* (10), 1526-1528.

17. Wu, X. H.; Hu, L. Q., Efficient amidation from carboxylic acids and azides via selenocarboxylates: Application to the coupling of amino acids and peptides with azides. *J. Org. Chem.* **2007**, *72* (3), 765-774.
18. (a) Hajduk, P. J., Fragment-based drug design: How big is too big? *J. Med. Chem.* **2006**, *49* (24), 6972-6976; (b) Hopkins, A. L.; Groom, C. R.; Alex, A., Ligand efficiency: a useful metric for lead selection. *Drug Discov. Today* **2004**, *9* (10), 430-431; (c) Abad-Zapatero, C.; Metz, J. T., Ligand efficiency indices as guideposts for drug discovery. *Drug Discov. Today* **2005**, *10* (7), 464-469; (d) Abad-Zapatero, C., Ligand efficiency indices for effective drug discovery. *Expert Opin. Drug Discovery* **2007**, *2* (4), 469-488.

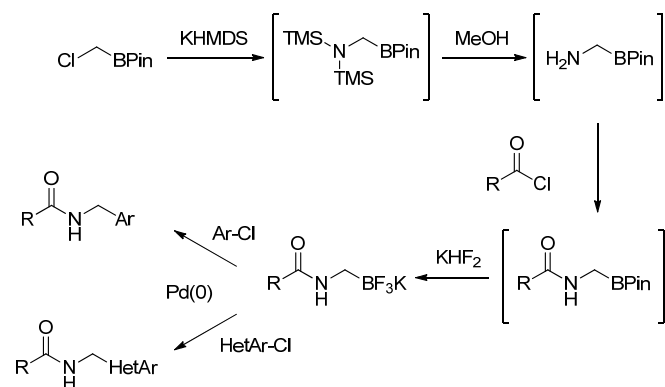
## Chapter 4

### A Simple Base-Mediated Amidation of Aldehydes with Azides

#### 4.1 Introduction

The amide bond serves as one of the nature's most fundamental functional groups. Indeed, it is an integral component of a large number of organic and biological molecules such as pharmaceuticals, natural products, peptides, and proteins. Traditionally, the amide functionality is incorporated through a reaction of an amine with either an activated carboxylic acid (generally acid halides or anhydrides) or by an activation using carbodiimide coupling reagents. However, several innovative approaches have been developed in the past decade, which include the Staudinger reaction,<sup>1</sup> the  $\alpha$ -bromo nitroalkane-amine coupling,<sup>2</sup> the native chemical ligation,<sup>3</sup> the thio acid-azide amidation,<sup>4</sup> the alkyne-sulfonyl azide coupling,<sup>5</sup> the coupling of acyltrifluoroborates with hydroxylamines<sup>6</sup> or azides,<sup>7</sup> the Au/DNA-catalyzed amidation from alcohols and amines,<sup>8</sup> the aminocarbonylation of aryl halides,<sup>9</sup> and the Pd catalyzed coupling of aryl halides with isocyanides.<sup>10</sup> Additionally, numerous one-pot oxidative amidation methods have been reported wherein, aldehydes,<sup>11</sup> alcohols<sup>12</sup> or alkynes<sup>13</sup> are oxidized using transition metal catalysts and treated with amines yielding corresponding amides. Meanwhile, some environmentally benign metal-free amidation procedures employing silyl reagents<sup>14</sup> or oxidants like sodium chlorite,<sup>15</sup> peroxide<sup>16</sup> have also been exploited.

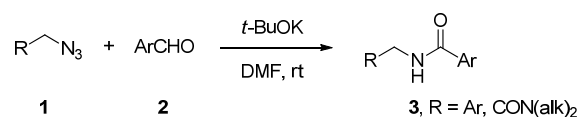
Another important approach to amides is the Schmidt reaction,<sup>17</sup> involving ketones and hydrazoic acid. Aube and co-workers have reported an intramolecular Schmidt reaction of cyclic ketones to construct *N*-substituted lactams in which hydrazoic acid was replaced by an alkyl azide.<sup>18</sup> An interesting extension of this reaction, known as the Boyer reaction,<sup>19</sup> was first reported<sup>19a</sup> in 1950s, wherein, two aromatic aldehydes were reacted with  $\beta$ -phenylethyl azide under harsh acidic conditions generating the corresponding amides in moderate yields. Strikingly, this reaction failed to afford the desired amide when benzyl or *n*-butyl azide was used. The reaction of benzyl azide is of particular interest since it leads to amidomethylarenes. In fact, a variety of therapeutic agents such as Picotamide,<sup>20</sup> Raltegravir<sup>21</sup> and others<sup>22</sup> are comprised of an amidomethylarene moiety. Recently, Molander *et al.* reported a synthetic route to generate these types of molecules via a C-C bond forming reaction between amidomethyltrifluoroborates and aryl or heteroaryl chlorides (Scheme 4.1).<sup>22c</sup>



**Scheme 4.1.** Synthesis of amidomethylarenes

Implementing a one-pot approach, a series of reactions were performed starting from 2-(chloromethyl)-4,4,5,5-tetramethyl-1,3,2-dioxaborolane and various acid chlorides to obtain the corresponding amidomethyltrifluoroborates, which were

subsequently treated with the aryl or heteroaryl chlorides under standard Pd catalyzed cross-coupling conditions leading to the amidomethylarenes. Although a wide range of substrates were tolerated under the reported reaction conditions, a tedious 4-step sequence to access amidomethyltrifluoroborates demanding long reaction times, high temperatures and the Pd catalyst required in the following C-C bond formation are the drawbacks associated with this approach. Therefore, a simple, convenient method deprived of the aforementioned disadvantages would be of great interest. We herein unveil a straightforward protocol starting from azides and aromatic aldehydes to synthesize amidomethylarenes under mild basic conditions (Scheme 4.2).



**Scheme 4.2.** Reaction between azides and aromatic aldehydes yielding amides

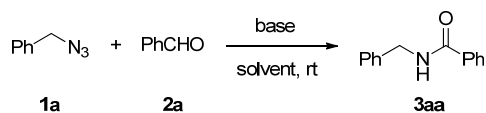
## 4.2 Results and discussion

### 4.2.1 Optimization of the reaction conditions

Initially, the reaction conditions were screened using benzyl azide and benzaldehyde as the model substrates. The summary of these results is presented in Table 4.1. Surprisingly, among the non-nucleophilic bases tested, *t*-BuOK alone produced the desired amide. From the set of the solvents explored, polar aprotic solvents such as THF, DMF, and DMSO proved to be suitable for this transformation, DMF offering the best results. In the course of further optimization, increasing the amount of *t*-BuOK to 2 eq was found to significantly improve the yield of the product. Furthermore, the reaction

was completed in 15 min at room temperature making it a highly efficient and practical synthetic route.

**Table 4.1.** Optimization of the reaction conditions<sup>a</sup>



Entry	Base	Solvent	Yield (%) <sup>b</sup>
1	DIPEA	DMF	-
2	Cs <sub>2</sub> CO <sub>3</sub>	DMF	-
3	DBU	DMF	-
4	<i>t</i> -BuOK	DMF	50
5	<i>t</i> -BuOK	THF	40
6	<i>t</i> -BuOK	DMSO	23
7	<i>t</i> -BuOK <sup>c</sup>	DMF	72

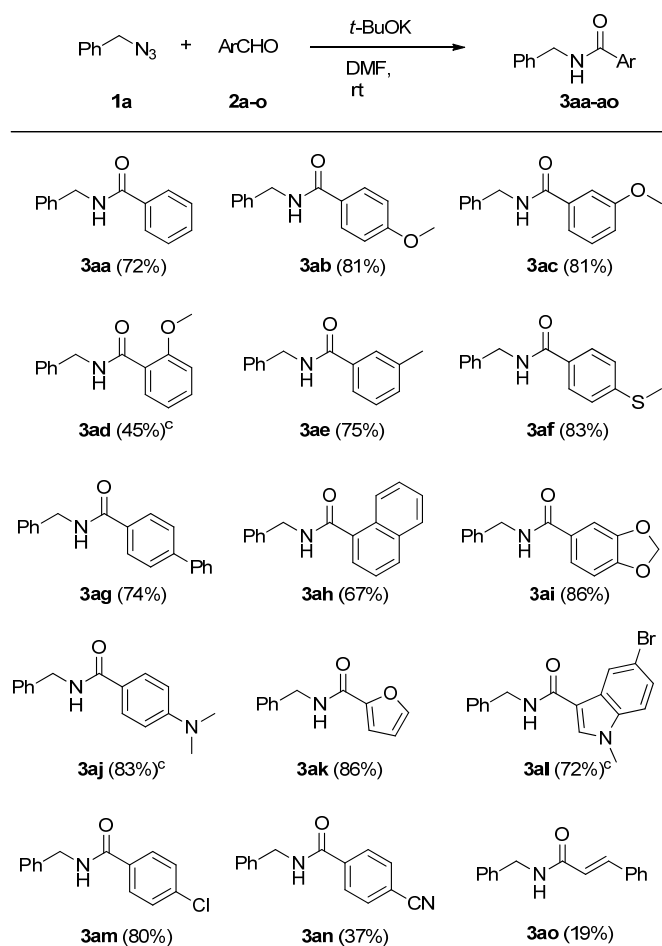
<sup>a</sup> General reaction conditions: **1a** (0.5 mmol), **2a** (0.6 mmol), base (0.75 mmol), solvent (2.5 mL), 15 min; <sup>b</sup> Isolated yield based on **1a**; <sup>c</sup> *t*-BuOK (1.0 mmol).

#### 4.2.2 Scope of the reaction regarding the aldehydes

Having the reaction conditions optimized, the scope of the reaction involving benzyl azide and a diverse array of aldehydes was first examined (Table 4.2). Aromatic aldehydes bearing electron-donating groups afforded excellent yields although an excess amount of the base was required in some cases (**3ad**, **3aj**, and **3al**). Changing the position of methoxy substituent on the aromatic ring from *para* to *meta* did not affect the yield (**3ab** and **3ac**). However, the amidation reaction with the sterically challenging 2-methoxybenzaldehyde offered a moderate amount of the product (**3ad**). Substrates such as 3-methylbenzaldehyde, 4-(methylthio)benzaldehyde, [1,1'-biphenyl]-4-carbaldehyde and 1-naphthaldehyde led to the formation of desired products **3ae-3ah** in good to

excellent yields. Functional moieties like 1,3-dioxolane (**3ai**) and *N,N*-dimethylamine (**3aj**) were well tolerated as well. Heterocyclic substrates such as furan and indole derivatives provided excellent results (**3ak** and **3al**).

**Table 4.2.** Reaction of benzyl azide with various aromatic aldehydes<sup>a,b</sup>



<sup>a</sup> Reaction conditions: **1a** (0.5 mmol), **2** (0.6 mmol), *t*-BuOK (1.0 mmol), DMF (2.5 mL), 15 min; <sup>b</sup> Isolated yields based on **1a**; <sup>c</sup> *t*-BuOK (2.0 mmol).

Among aldehydes with electron-withdrawing substituents, 4-chlorobenzaldehyde exhibited great compatibility (**3am**) whereas, lower yield was obtained when 4-cyanobenzaldehyde was used (**3an**). Cinnamaldehyde, despite being a Michael acceptor, did undergo the reaction (**3ao**) albeit with poor yield. Unfortunately, the

aliphatic aldehydes are not appropriate starting materials under these reaction conditions due to the presence of a more acidic  $\alpha$ -proton.

#### 4.2.3 Scope of the reaction regarding the azides

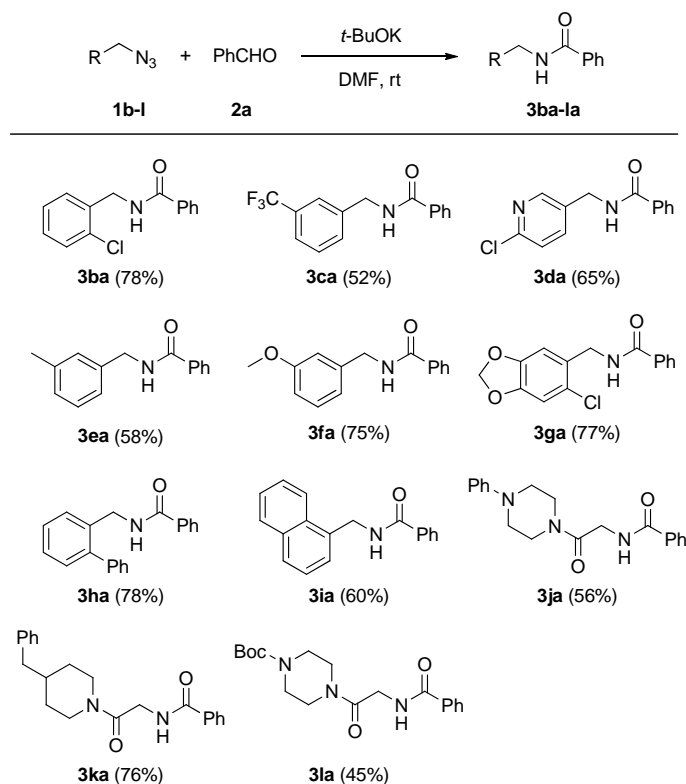
These encouraging results prompted us to expand the scope of this reaction with respect to the azides (Table 4.3). Benzyl azides consisting of electron-withdrawing substituents were successfully converted to the amides **3ba**, **3ca**, and **3da** in moderate to substantial yields. Especially, the reaction of an azide incorporated on a heteroaryl moiety proceeded smoothly resulting in amide **3da**. Benzyl azides containing electron-donating substituents were found to be suitable substrates for this reaction (**3ea** and **3fa**). It is noteworthy to mention that an azide with both electron-donating and withdrawing functionalities furnished the amide **3ga** in 77% yield. Substrates with sterical hindrance participated well under these reaction conditions (**3ha** and **3ia**). In pursuit of substrates other than the substituted benzyl azides, we discovered that the  $\alpha$ -azido amides also take part in this reaction efficiently providing moderate yields for the corresponding diamides **3ja**, **3ka**, and **3la**. An acid labile Boc group was obviously unaffected (**3la**) under these conditions, offering an advantage over the Boyer reaction. Aromatic and other aliphatic azides failed to generate corresponding amides under the reaction conditions described herein.

#### 4.2.4 Control experiments and the plausible mechanism

Intrigued by the outcome of this study, we decided to delve into the mechanistic details of this reaction. A control experiment was designed wherein *t*-BuOK was added to

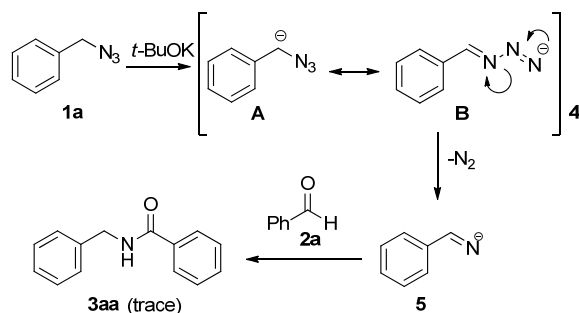
a solution of azide **1a** in DMF resulting in a deprotonation followed by the loss of molecular nitrogen leading to benzylideneamide **5** (Scheme 4.3).

**Table 4.3.** Reaction of various azides with benzaldehyde<sup>a,b</sup>



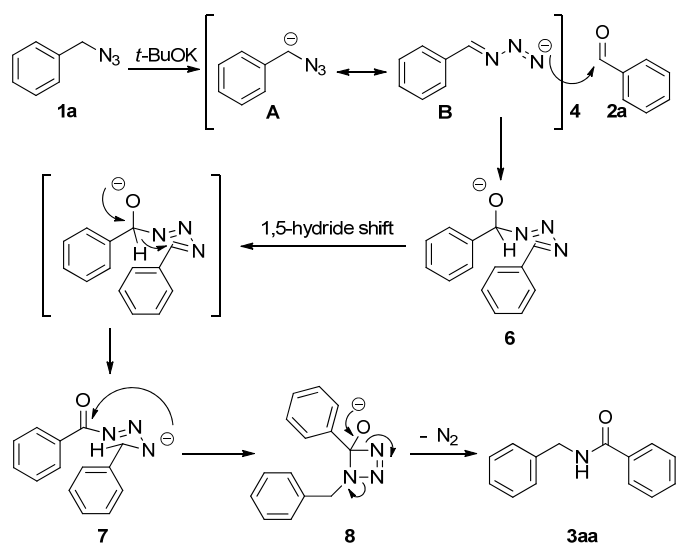
<sup>a</sup> Reaction conditions: **1** (0.5 mmol), **2a** (0.6 mmol), *t*-BuOK (1.0 mmol), DMF (2.5 mL), 15 min; <sup>b</sup> Isolated yields based on **1**.

After 10 minutes of stirring, aldehyde **2a** was added to the reaction mixture. Interestingly, the desired amide **3aa** was formed only in trace amounts. On the contrary, when a mixture of azide **1a** and aldehyde **2a** in DMF was treated with *t*-BuOK, amide **3aa** was obtained in 72% yield (Table 4.2).



**Scheme 4.3.** Control experiments to investigate the reaction mechanism. Reaction conditions: **1a** (0.5 mmol), **2a** (0.6 mmol), *t*-BuOK (1.0 mmol), DMF (2.5 mL), 15 min.

This implies that the intermediate benzyldeneamide **5** loses its reactivity towards aldehyde, failing to generate an amide. Whereas, if the reactive species **4** formed by addition of *t*-BuOK reacts with the aldehyde prior to the elimination of molecular nitrogen, an amide is obtained suggesting that, the nucleophilic attack of outermost nitrogen atom in species **4** on the carbonyl carbon of aldehyde is crucial for the reaction to proceed. Based on these results, a plausible mechanism is proposed in the Scheme 4.4. The first step would involve a deprotonation of benzyl azide, generating a highly reactive species **4**. One of the resonance forms of species **4** (**4-B**) can readily react with the benzaldehyde **2a** leading to an intermediate **6** followed by a 1,5-hydride shift resulting in triazenide **7**. An intramolecular nucleophilic attack on the carbonyl carbon would produce **8**, which would be converted to the amide **3aa** through retro [2+2] cycloaddition or stepwise loss of molecular nitrogen.



**Scheme 4.4.** Plausible reaction mechanism of amidation

#### 4.2.5 Discussion

Although a lot of synthetic methods to access amides are available, the amide bond formation starting from azide and aldehydes seems to be surprisingly less explored. For instance, the Boyer reaction was reported in 1950s wherein, two aromatic aldehydes reacted with alkyl azides under harsh acidic conditions yielding amides. While exploring various reactions for a different application, we serendipitously discovered a reaction between a set of alkyl azides (substituted benzyl azides and  $\alpha$ -azido amides) and aromatic aldehydes under mild basic conditions which resulted in the formation of corresponding amides. Among various bases investigated, only potassium tert-butoxide (*t*-BuOK) was suitable to carry out the desired transformation, whereas DMF was the solvent of choice. A wide range of electronically and sterically diverse aromatic aldehydes were tolerated and the corresponding amides were obtained in good to excellent yields. Unfortunately, aliphatic aldehydes are not suitable under these conditions due to the presence of a more acidic  $\alpha$ -proton. With these encouraging results, scope of the reaction with respect to

azides was then investigated. In addition to various substituted benzyl azides,  $\alpha$ -azido amides were found to undergo the reaction as well. Aromatic and other aliphatic azides however, did not take part in the reaction. This implies that an electron-stabilizing group on the azides is required for this reaction to proceed.

Mechanistically, the initial step involves deprotonation of benzyl azide, followed by the nucleophilic attack of the terminal nitrogen on the carbonyl carbon of aldehyde. Other key steps include 1,5-hydride shift resulting in a triazenide intermediate, intramolecular nucleophilic attack on the carbonyl carbon and loss of molecular nitrogen finally leading to the amide. Experiments to gain additional mechanistic insights are currently in progress.

#### 4.3 Conclusion

In summary, a simple, yet highly efficient methodology has been developed for the synthesis of amides starting from benzyl azides or  $\alpha$ -azido amides and aromatic aldehydes. A wide variety of substrates were shown to deliver the desired product in moderate to excellent yields, demonstrating the scope of this reaction. Besides, innocuous by-products (molecular nitrogen and *t*-BuOH), short reaction time, ambient temperature and easily accessible starting materials make it an attractive alternative to the contemporary synthetic routes. Notably, biologically valuable amidomethylarenes could be easily synthesized using this method.

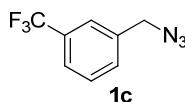
## 4.4 Experimental section

### 4.4.1 General information

All reagents and solvents were purchased from commercial sources and used without further purification. All reactions were run under an Argon atmosphere unless otherwise indicated. Prior to use of solvents in reactions, they were purified by passing the degassed solvents through a column of activated alumina and transferred by an oven-dried syringe or cannula. Thin layer chromatography was performed on Merck TLC plates (silica gel 60 F<sub>254</sub>). <sup>1</sup>H NMR and <sup>13</sup>C NMR were recorded on a Varian Inova 400 (400 MHz) or a Bruker Avance DPX-250 (250 MHz) instrument. The HRMS data were measured on an Agilent 1100 Series MSD/TOF with electrospray ionization.

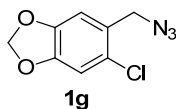
The azides **1a**,<sup>23</sup> **1b**,<sup>24</sup> **1d**,<sup>25</sup> **1e**,<sup>26</sup> **1f**,<sup>27</sup> **1i**,<sup>28</sup> **1j**,<sup>29</sup> **1l**,<sup>30</sup> and an aldehyde **2n**<sup>31</sup> were synthesized as previously reported in the literature.

### 4.4.2 Synthesis of azides

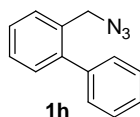


**1-(azidomethyl)-3-(trifluoromethyl)benzene (1c):** To a solution of 1-(bromomethyl)-3-(trifluoromethyl)benzene (1.0 g, 4.18 mmol) in DMSO (15 mL), was added sodium azide (326 mg, 5.0 mmol, 1.2 eq) and the resulting reaction mixture was stirred overnight at 70 °C. The reaction was then treated with H<sub>2</sub>O (40 mL) and extracted with EtOAc (30 mL × 2). The combined organic layers were washed with brine (30 mL × 3), dried with Na<sub>2</sub>SO<sub>4</sub> and concentrated under reduced pressure. The azide **1c** was then obtained by flash

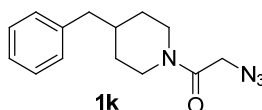
chromatography. Yield = 76%.  $R_f$  = 0.31 in hexanes.  $^1\text{H}$  NMR (400 MHz,  $\text{CDCl}_3$ )  $\delta$  7.61 – 7.55 (m, 2H), 7.51 – 7.48 (m, 2H), 4.42 (s, 2H) ppm.  $^{13}\text{C}$  NMR (101 MHz,  $\text{CDCl}_3$ )  $\delta$  136.74, 131.48, 131.42 (q,  $J$  = 32.5 Hz), 129.53, 125.25 (q,  $J$  = 3.7 Hz), 124.94 (q,  $J$  = 3.7 Hz), 124.12 (q,  $J$  = 272.4 Hz), 54.31 ppm.



**5-(azidomethyl)-6-chlorobenzo[*d*][1,3]dioxole (1g):** The azide **1g** was prepared following the procedure described for the synthesis of azide **1c**. Yield = 73%.  $R_f$  = 0.62 in hexanes : EtOAc = 5:1.  $^1\text{H}$  NMR (400 MHz,  $\text{CDCl}_3$ )  $\delta$  6.86 (s, 1H), 6.82 (s, 1H), 5.98 (s, 2H), 4.36 (s, 2H) ppm.  $^{13}\text{C}$  NMR (101 MHz,  $\text{CDCl}_3$ )  $\delta$  148.47, 147.14, 126.41, 126.12, 110.29, 109.85, 102.22, 52.35 ppm.



**2-(azidomethyl)-1,1'-biphenyl (1h):** The azide **1h** was synthesized following the procedure described for the synthesis of azide **1c**. Yield = 83%.  $R_f$  = 0.22 in hexanes.  $^1\text{H}$  NMR (400 MHz,  $\text{CDCl}_3$ )  $\delta$  7.47 – 7.43 (m, 2H), 7.42 – 7.37 (m, 4H), 7.36 – 7.30 (m, 3H), 4.28 (s, 2H) ppm.  $^{13}\text{C}$  NMR (101 MHz,  $\text{CDCl}_3$ )  $\delta$  142.42, 140.45, 132.99, 130.64, 129.76, 129.39, 128.53, 127.99, 127.65, 52.80 ppm.

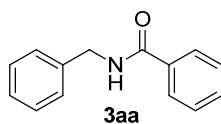


**2-azido-1-(4-benzylpiperidin-1-yl)ethanone (1k):** The azide **1k** was prepared following the procedure described for the synthesis of azide **1c**, starting from 1-(4-benzylpiperidin-1-yl)-2-chloroethanone.<sup>32</sup> Yield = 54%.  $R_f = 0.3$  in hexanes : EtOAc = 2:1.  $^1\text{H NMR}$  (250 MHz,  $\text{CDCl}_3$ )  $\delta$  7.36 – 7.09 (m, 5H), 4.58 (d,  $J = 13.3$  Hz, 1H), 3.92 (s, 2H), 3.61 (d,  $J = 13.7$  Hz, 1H), 3.05 – 2.87 (m, 1H), 2.67 – 2.47 (m, 3H), 1.90 – 1.65 (m, 3H), 1.19 (q,  $J = 11.8$  Hz, 2H) ppm.  $^{13}\text{C NMR}$  (63 MHz,  $\text{CDCl}_3$ )  $\delta$  165.20, 139.61, 128.95, 128.20, 125.98, 50.47, 45.11, 42.66, 42.31, 37.83, 32.18, 31.43 ppm. HRMS (ESI) calcd for  $\text{C}_{14}\text{H}_{18}\text{N}_4\text{O}$   $[\text{M}+\text{H}]^+$ : 259.1553, found: 259.1557

#### 4.4.3 General procedure for the synthesis of amides

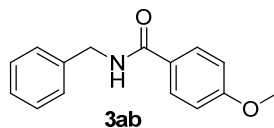
To a mixture of the azide (0.5 mmol) and an aldehyde (0.6 mmol, 1.2 eq) in DMF (2.5 mL) at room temperature, *t*-BuOK (1.0 or 2.0 mmol, 2 or 4 eq) was carefully added and bubbling was observed immediately. After the completion of reaction, (monitored by TLC) water (10 mL) was added and the pH was adjusted to 7.0 using saturated  $\text{NH}_4\text{Cl}$  solution. The reaction mixture was extracted with EtOAc (20 mL  $\times$  2) and the combined organic layers were washed with brine (30 mL  $\times$  3), dried with  $\text{Na}_2\text{SO}_4$  and concentrated under reduced pressure. The product was purified by flash chromatography.

#### 4.4.4 Synthesis of amides

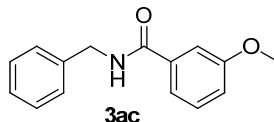


***N*-benzylbenzamide (3aa):** Yield = 72%.  $R_f = 0.41$  in hexanes : EtOAc = 2:1.  $^1\text{H NMR}$  (400 MHz,  $\text{CDCl}_3$ )  $\delta$  7.78 (d,  $J = 7.6$  Hz, 2H), 7.46 – 7.37 (m, 2H), 7.31 (t,  $J = 7.6$  Hz,

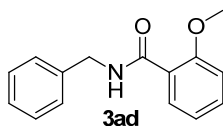
2H), 7.28 – 7.20 (m, 4H), 4.52 (d,  $J = 5.8$  Hz, 2H) ppm.  $^{13}\text{C}$  NMR (101 MHz,  $\text{CDCl}_3$ )  $\delta$  167.68, 138.49, 134.37, 131.39, 128.59, 128.43, 127.68, 127.30, 127.16, 43.87 ppm. HRMS (ESI) calcd for  $\text{C}_{14}\text{H}_{13}\text{NO}$   $[\text{M}+\text{H}]^+$ : 212.1070, found: 212.1068



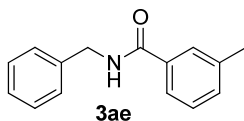
***N*-benzyl-4-methoxybenzamide (3ab):** Yield = 81%.  $R_f = 0.31$  in hexanes : EtOAc = 2:1.  $^1\text{H}$  NMR (400 MHz,  $\text{CDCl}_3$ )  $\delta$  7.74 (d,  $J = 8.7$  Hz, 2H), 7.35 – 7.18 (m, 5H), 7.07 (s, 1H), 6.84 – 6.77 (m, 2H), 4.52 (d,  $J = 5.8$  Hz, 2H), 3.76 (s, 3H) ppm.  $^{13}\text{C}$  NMR (101 MHz,  $\text{CDCl}_3$ )  $\delta$  167.16, 162.19, 138.74, 128.99, 128.65, 127.79, 127.35, 126.75, 113.71, 55.41, 43.94 ppm. HRMS (ESI) calcd for  $\text{C}_{15}\text{H}_{15}\text{NO}_2$   $[\text{M}+\text{H}]^+$ : 242.1176, found: 242.1172



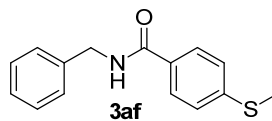
***N*-benzyl-3-methoxybenzamide (3ac):** Yield = 81%.  $R_f = 0.35$  in hexanes : EtOAc = 2:1.  $^1\text{H}$  NMR (400 MHz,  $\text{CDCl}_3$ )  $\delta$  7.38 – 7.36 (m, 1H), 7.32 (d,  $J = 0.5$  Hz, 1H), 7.32 – 7.29 (m, 3H), 7.29 – 7.28 (m, 1H), 7.28 – 7.24 (m, 2H), 7.03 – 6.97 (m, 1H), 6.61 (s, 1H), 4.59 (d,  $J = 5.7$  Hz, 2H), 3.80 (s, 3H) ppm.  $^{13}\text{C}$  NMR (101 MHz,  $\text{CDCl}_3$ )  $\delta$  167.42, 159.99, 138.35, 136.02, 129.71, 128.91, 128.03, 127.74, 118.89, 117.92, 112.57, 55.59, 44.29 ppm. HRMS (ESI) calcd for  $\text{C}_{15}\text{H}_{15}\text{NO}_2$   $[\text{M}+\text{H}]^+$ : 242.1176, found: 242.1175



***N*-benzyl-2-methoxybenzamide (3ad):** Yield = 45%.  $R_f = 0.39$  in hexanes : EtOAc = 2:1.  $^1\text{H}$  NMR (400 MHz,  $\text{CDCl}_3$ )  $\delta$  8.22 (dd,  $J = 7.8, 1.8$  Hz, 2H), 7.43 – 7.37 (m, 1H), 7.36 – 7.28 (m, 4H), 7.27 – 7.21 (m, 1H), 7.04 (t,  $J = 7.5$  Hz, 1H), 6.91 (d,  $J = 8.4$  Hz, 1H), 4.66 (d,  $J = 5.7$  Hz, 2H), 3.83 (s, 3H) ppm.  $^{13}\text{C}$  NMR (101 MHz,  $\text{CDCl}_3$ )  $\delta$  165.33, 157.48, 138.77, 132.79, 132.20, 128.57, 127.42, 127.16, 121.19, 111.37, 55.87, 43.66 ppm. HRMS (ESI) calcd for  $\text{C}_{15}\text{H}_{15}\text{NO}_2$   $[\text{M}+\text{H}]^+$ : 242.1176, found: 242.1177



***N*-benzyl-3-methylbenzamide (3ae):** Yield = 75%.  $R_f = 0.51$  in hexanes : EtOAc = 2:1.  $^1\text{H}$  NMR (400 MHz,  $\text{CDCl}_3$ )  $\delta$  7.67 – 7.56 (m, 3H), 7.29 – 7.16 (m, 7H), 4.51 (d,  $J = 5.9$  Hz, 2H), 2.28 (s, 3H) ppm.  $^{13}\text{C}$  NMR (101 MHz,  $\text{CDCl}_3$ )  $\delta$  167.84, 138.57, 138.06, 134.31, 132.01, 128.43, 128.19, 127.86, 127.55, 127.11, 124.14, 43.71, 21.17 ppm. HRMS (ESI) calcd for  $\text{C}_{15}\text{H}_{15}\text{NO}$   $[\text{M}+\text{H}]^+$ : 226.1226, found: 226.1230

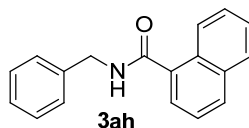


***N*-benzyl-4-(methylthio)benzamide (3af):** Yield = 83%.  $R_f = 0.37$  in hexanes : EtOAc = 2:1.  $^1\text{H}$  NMR (400 MHz,  $\text{CDCl}_3$ )  $\delta$  7.71 – 7.67 (m, 2H), 7.34 – 7.25 (m, 5H), 7.23 – 7.20 (m, 2H), 6.42 (s, 1H), 4.61 (d,  $J = 5.7$  Hz, 2H), 2.48 (s, 3H) ppm.  $^{13}\text{C}$  NMR (101 MHz,  $\text{CDCl}_3$ )  $\delta$  167.00, 143.65, 138.44, 130.63, 128.92, 128.05, 127.74, 127.57, 125.58, 44.25, 15.21 ppm. HRMS (ESI) calcd for  $\text{C}_{15}\text{H}_{15}\text{NOS}$   $[\text{M}+\text{H}]^+$ : 258.0947, found: 258.0951

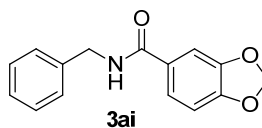


***N*-benzyl-[1,1'-biphenyl]-4-carboxamide (3ag):** Yield = 74%.  $R_f$  = 0.49 in hexanes : EtOAc = 2:1.  $^1\text{H}$  NMR (400 MHz,  $\text{CDCl}_3$ )  $\delta$  7.86 (d,  $J$  = 7.1 Hz, 2H), 7.58 (t,  $J$  = 6.5 Hz, 4H), 7.44 (t,  $J$  = 6.4 Hz, 2H), 7.41 – 7.22 (m, 6H), 6.96 (s, 1H), 4.62 (d,  $J$  = 4.5 Hz, 2H) ppm.  $^{13}\text{C}$  NMR (101 MHz,  $\text{CDCl}_3$ )  $\delta$  167.34, 144.40, 140.11, 138.48, 133.18, 129.04, 128.87, 128.47, 128.12, 127.99, 127.73, 127.31, 44.23 ppm. HRMS (ESI) calcd for  $\text{C}_{20}\text{H}_{17}\text{NO}$   $[\text{M}+\text{H}]^+$ : 288.1383, found: 288.1384

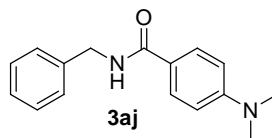
***N*-benzyl-1-naphthamide (3ah):**



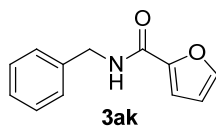
Yield = 67%.  $R_f$  = 0.49 in hexanes : EtOAc = 2:1.  $^1\text{H}$  NMR (400 MHz,  $\text{CDCl}_3$ )  $\delta$  8.24 (d,  $J$  = 7.7 Hz, 1H), 7.80 (d,  $J$  = 8.1 Hz, 2H), 7.51 – 7.40 (m, 3H), 7.34 – 7.21 (m, 6H), 6.85 (s, 1H), 4.52 (d,  $J$  = 5.8 Hz, 2H) ppm.  $^{13}\text{C}$  NMR (101 MHz,  $\text{CDCl}_3$ )  $\delta$  169.49, 138.34, 134.19, 133.62, 130.51, 130.18, 128.68, 128.26, 127.75, 127.43, 126.99, 126.33, 125.46, 125.00, 124.62, 43.85 ppm. HRMS (ESI) calcd for  $\text{C}_{18}\text{H}_{15}\text{NO}$   $[\text{M}+\text{H}]^+$ : 262.1226, found: 262.1224



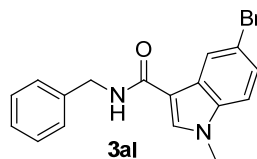
***N*-benzylbenzo[*d*][1,3]dioxole-5-carboxamide (3ai):** Yield = 86%.  $R_f$  = 0.32 in hexanes : EtOAc = 2:1.  $^1\text{H}$  NMR (400 MHz,  $\text{CDCl}_3$ )  $\delta$  7.32 – 7.26 (m, 7H), 6.76 (dd,  $J$  = 8.0, 0.5 Hz, 1H), 6.52 (s, 1H), 5.97 (s, 2H), 4.56 (d,  $J$  = 5.7 Hz, 2H) ppm.  $^{13}\text{C}$  NMR (101 MHz,  $\text{CDCl}_3$ )  $\delta$  166.84, 150.49, 148.11, 138.48, 128.89, 128.76, 128.01, 127.69, 121.76, 108.12, 107.86, 101.83, 44.28 ppm. HRMS (ESI) calcd for  $\text{C}_{15}\text{H}_{13}\text{NO}_3$   $[\text{M}+\text{H}]^+$ : 256.0968, found: 256.0966



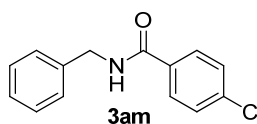
***N*-benzyl-4-(dimethylamino)benzamide (3aj):** Yield = 83%.  $R_f$  = 0.26 in hexanes : EtOAc = 2:1.  $^1\text{H}$  NMR (400 MHz,  $\text{CDCl}_3$ )  $\delta$  7.68 (d,  $J$  = 9.0 Hz, 2H), 7.35 – 7.25 (m, 5H), 6.64 (d,  $J$  = 9.0 Hz, 2H), 6.26 (s, 1H), 4.61 (d,  $J$  = 5.7 Hz, 2H), 2.99 (s, 6H) ppm.  $^{13}\text{C}$  NMR (101 MHz,  $\text{CDCl}_3$ )  $\delta$  167.44, 152.63, 139.05, 128.81, 128.63, 128.01, 127.49, 121.25, 111.21, 44.04, 40.27 ppm. HRMS (ESI) calcd for  $\text{C}_{16}\text{H}_{18}\text{N}_2\text{O}$   $[\text{M}+\text{H}]^+$ : 255.1492, found: 255.1500



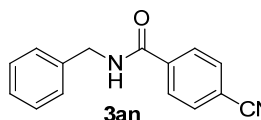
***N*-benzylfuran-2-carboxamide (3ak):** Yield = 86%.  $R_f$  = 0.48 in hexanes : EtOAc = 1:1.  $^1\text{H}$  NMR (400 MHz,  $\text{CDCl}_3$ )  $\delta$  7.33 (s, 1H), 7.30 – 7.18 (m, 4H), 7.06 (d,  $J$  = 3.2 Hz, 2H), 6.43 – 6.37 (m, 1H), 4.53 (d,  $J$  = 5.9 Hz, 2H) ppm.  $^{13}\text{C}$  NMR (101 MHz,  $\text{CDCl}_3$ )  $\delta$  158.39, 147.89, 143.96, 138.17, 128.58, 127.73, 127.39, 114.18, 111.99, 42.99 ppm. HRMS (ESI) calcd for  $\text{C}_{12}\text{H}_{11}\text{NO}_2$   $[\text{M}+\text{H}]^+$ : 202.0863, found: 202.0862



***N*-benzyl-5-bromo-1-methyl-1*H*-indole-3-carboxamide (3al):** Yield = 72%.  $R_f$  = 0.25 in hexanes : EtOAc = 1:1.  $^1\text{H}$  NMR (400 MHz,  $\text{CDCl}_3$ )  $\delta$  8.19 – 8.16 (m, 1H), 7.51 (s, 1H), 7.36 – 7.25 (m, 6H), 7.16 – 7.13 (m, 1H), 6.22 (s, 1H), 4.63 (d,  $J$  = 5.8 Hz, 2H), 3.71 (s, 3H) ppm.  $^{13}\text{C}$  NMR (101 MHz,  $\text{CDCl}_3$ )  $\delta$  164.69, 138.99, 136.00, 132.47, 128.90, 127.97, 127.60, 127.56, 125.78, 123.53, 115.27, 111.51, 110.43, 43.65, 33.59 ppm. HRMS (ESI) calcd for  $\text{C}_{17}\text{H}_{15}\text{BrN}_2\text{O}$   $[\text{M}+\text{H}]^+$ : 343.0441, found: 343.0440



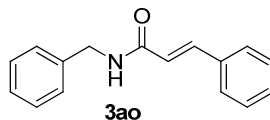
***N*-benzyl-4-chlorobenzamide (3am):** Yield = 80%.  $R_f$  = 0.55 in hexanes : EtOAc = 2:1.  $^1\text{H}$  NMR (400 MHz,  $\text{CDCl}_3$ )  $\delta$  7.70 (d,  $J$  = 8.5 Hz, 2H), 7.38 – 7.25 (m, 7H), 6.54 (s, 1H), 4.59 (d,  $J$  = 5.7 Hz, 2H) ppm.  $^{13}\text{C}$  NMR (101 MHz,  $\text{CDCl}_3$ )  $\delta$  166.53, 138.17, 137.98, 132.95, 129.02, 128.63, 128.10, 127.90, 44.41 ppm. HRMS (ESI) calcd for  $\text{C}_{14}\text{H}_{12}\text{ClNO}$   $[\text{M}+\text{H}]^+$ : 246.0680, found: 246.0678



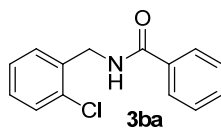
***N*-benzyl-4-cyanobenzamide (3an):** Yield = 37%.  $R_f$  = 0.35 in hexanes : EtOAc = 2:1.  $^1\text{H}$  NMR (400 MHz,  $\text{CDCl}_3$ )  $\delta$  7.83 (d,  $J$  = 8.4 Hz, 2H), 7.62 (d,  $J$  = 8.4 Hz, 2H), 7.33 – 7.25 (m, 5H), 7.00 (s, 1H), 4.56 (d,  $J$  = 5.7 Hz, 2H) ppm.  $^{13}\text{C}$  NMR (101 MHz,  $\text{CDCl}_3$ )  $\delta$

165.85, 138.36, 137.75, 132.49, 128.95, 127.93, 127.91, 118.14, 115.10, 44.37 ppm.

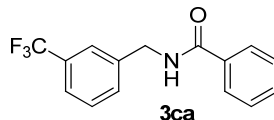
HRMS (ESI) calcd for  $C_{15}H_{12}N_2O$   $[M+H]^+$ : 237.1022, found: 237.1023



***N*-benzylcinnamamide (3ao)**: Yield = 19%.  $R_f$  = 0.38 in hexanes : EtOAc = 2:1.  $^1H$  NMR (400 MHz,  $CDCl_3$ )  $\delta$  7.63 (d,  $J$  = 15.6 Hz, 1H), 7.43 (dd,  $J$  = 6.4, 2.8 Hz, 2H), 7.35 – 7.22 (m, 8H), 6.52 (s, 1H), 6.47 (d,  $J$  = 15.6 Hz, 1H), 4.50 (d,  $J$  = 5.8 Hz, 2H) ppm.  $^{13}C$  NMR (101 MHz,  $CDCl_3$ )  $\delta$  166.14, 141.36, 138.40, 134.97, 129.79, 128.92, 128.83, 128.16, 127.95, 127.62, 120.80, 43.93 ppm. HRMS (ESI) calcd for  $C_{16}H_{15}NO$   $[M+H]^+$ : 238.1226, found: 238.1223

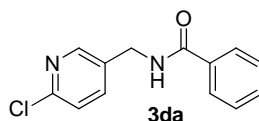


***N*-(2-chlorobenzyl)benzamide (3ba)**: Yield = 78%.  $R_f$  = 0.5 in hexanes : EtOAc = 2:1.  $^1H$  NMR (400 MHz,  $CDCl_3$ )  $\delta$  7.78 – 7.74 (m, 2H), 7.49 – 7.33 (m, 5H), 7.23 – 7.18 (m, 2H), 6.75 (s, 1H), 4.69 (d,  $J$  = 6.0 Hz, 2H) ppm.  $^{13}C$  NMR (101 MHz,  $CDCl_3$ )  $\delta$  167.55, 135.79, 134.42, 133.84, 131.76, 130.48, 129.73, 129.17, 128.75, 127.32, 127.17, 42.20 ppm. HRMS (ESI) calcd for  $C_{14}H_{12}ClNO$   $[M+H]^+$ : 246.0680, found: 246.0677

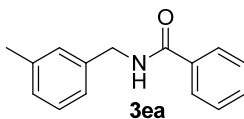


***N*-(3-(trifluoromethyl)benzyl)benzamide (3ca)**: Yield = 52%.  $R_f$  = 0.37 in hexanes : EtOAc = 2:1.  $^1H$  NMR (400 MHz,  $CDCl_3$ )  $\delta$  7.80 – 7.75 (m, 2H), 7.57 – 7.46 (m, 4H),

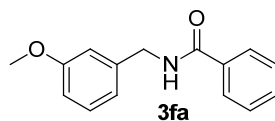
7.45 – 7.37 (m, 3H), 6.75 (s, 1H), 4.65 (d,  $J = 5.9$  Hz, 2H) ppm.  $^{13}\text{C}$  NMR (101 MHz,  $\text{CDCl}_3$ )  $\delta$  167.79, 139.56, 134.21, 131.96, 131.37 (q,  $J = 1.3$  Hz), 131.22 (q,  $J = 32.2$  Hz), 129.42, 128.85, 127.19, 124.70 – 124.50 (m, two quartets being merged,  $J = 3.8$  Hz), 124.20 (q,  $J = 272.4$  Hz), 43.73 ppm. HRMS (ESI) calcd for  $\text{C}_{15}\text{H}_{12}\text{F}_3\text{NO}$   $[\text{M}+\text{H}]^+$ : 280.0944, found: 280.0949



***N*-((6-chloropyridin-3-yl)methyl)benzamide (3da):** Yield = 65%.  $R_f = 0.33$  in hexanes : EtOAc = 1:1.  $^1\text{H}$  NMR (400 MHz,  $\text{CDCl}_3$ )  $\delta$  8.24 (s, 1H), 7.77 – 7.72 (m, 2H), 7.61 (dd,  $J = 8.2, 2.4$  Hz, 1H), 7.49 – 7.43 (m, 1H), 7.40 – 7.34 (m, 2H), 7.21 (d,  $J = 8.2$  Hz, 1H), 7.08 (s, 1H), 4.53 (d,  $J = 6.0$  Hz, 2H) ppm.  $^{13}\text{C}$  NMR (101 MHz,  $\text{CDCl}_3$ )  $\delta$  167.96, 150.68, 149.07, 138.83, 133.88, 133.37, 132.06, 128.82, 127.19, 124.48, 40.85 ppm. HRMS (ESI) calcd for  $\text{C}_{13}\text{H}_{11}\text{ClN}_2\text{O}$   $[\text{M}+\text{H}]^+$ : 247.0633, found: 247.0635



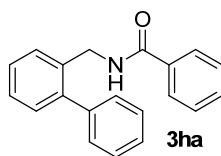
***N*-(3-methylbenzyl)benzamide (3ea):** Yield = 58%.  $R_f = 0.45$  in hexanes : EtOAc = 2:1.  $^1\text{H}$  NMR (400 MHz,  $\text{CDCl}_3$ )  $\delta$  7.80 – 7.76 (m, 2H), 7.50 – 7.44 (m, 1H), 7.42 – 7.36 (m, 2H), 7.24 – 7.19 (m, 1H), 7.15 – 7.06 (m, 3H), 6.58 (s, 1H), 4.57 (d,  $J = 5.7$  Hz, 2H), 2.32 (s, 3H) ppm.  $^{13}\text{C}$  NMR (101 MHz,  $\text{CDCl}_3$ )  $\delta$  167.49, 138.63, 138.30, 134.59, 131.65, 128.83, 128.83, 128.71, 128.49, 127.16, 125.10, 44.27, 21.55 ppm. HRMS (ESI) calcd for  $\text{C}_{15}\text{H}_{15}\text{NO}$   $[\text{M}+\text{H}]^+$ : 226.1226, found: 226.1231



***N*-(3-methoxybenzyl)benzamide (3fa):** Yield = 75%.  $R_f = 0.32$  in hexanes : EtOAc = 2:1.  $^1\text{H NMR}$  (400 MHz,  $\text{CDCl}_3$ )  $\delta$  7.80 – 7.75 (m, 2H), 7.51 – 7.44 (m, 1H), 7.42 – 7.36 (m, 2H), 7.27 – 7.22 (m, 1H), 6.93 – 6.86 (m, 2H), 6.81 (dd,  $J = 8.2, 2.5$  Hz, 1H), 6.60 (s, 1H), 4.58 (d,  $J = 5.7$  Hz, 2H), 3.77 (s, 3H) ppm.  $^{13}\text{C NMR}$  (101 MHz,  $\text{CDCl}_3$ )  $\delta$  167.56, 160.09, 139.98, 134.53, 131.70, 129.97, 128.74, 127.15, 120.26, 113.65, 113.17, 55.41, 44.23 ppm. HRMS (ESI) calcd for  $\text{C}_{15}\text{H}_{15}\text{NO}_2$   $[\text{M}+\text{H}]^+$ : 242.1176, found: 242.1179

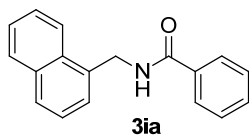


***N*-((6-chlorobenzo[*d*][1,3]dioxol-5-yl)methyl)benzamide (3ga):** Yield = 77%.  $R_f = 0.4$  in hexanes : EtOAc = 2:1.  $^1\text{H NMR}$  (400 MHz,  $\text{CDCl}_3$ )  $\delta$  7.77 – 7.73 (m, 2H), 7.49 – 7.43 (m, 1H), 7.41 – 7.35 (m, 2H), 6.91 (s, 1H), 6.80 (s, 1H), 6.70 (s, 1H), 5.92 (s, 2H), 4.57 (d,  $J = 6.0$  Hz, 2H) ppm.  $^{13}\text{C NMR}$  (101 MHz,  $\text{CDCl}_3$ )  $\delta$  167.56, 147.91, 147.04, 134.39, 131.77, 129.03, 128.75, 127.16, 125.61, 110.30, 110.03, 102.03, 42.08 ppm. HRMS (ESI) calcd for  $\text{C}_{15}\text{H}_{12}\text{ClNO}_3$   $[\text{M}+\text{H}]^+$ : 290.0578, found: 290.0583

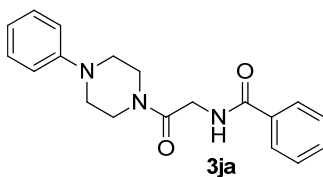


***N*-([1,1'-biphenyl]-2-ylmethyl)benzamide (3ha):** Yield = 78%.  $R_f = 0.53$  in hexanes : EtOAc = 2:1.  $^1\text{H NMR}$  (400 MHz,  $\text{CDCl}_3$ )  $\delta$  7.63 – 7.60 (m, 2H), 7.49 – 7.40 (m, 4H), 7.38 – 7.32 (m, 7H), 7.29 – 7.26 (m, 1H), 6.26 (s, 1H), 4.61 (d,  $J = 5.6$  Hz, 2H) ppm.  $^{13}\text{C}$

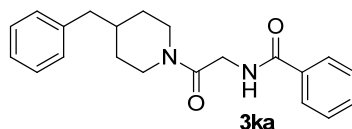
NMR (101 MHz, CDCl<sub>3</sub>)  $\delta$  167.20, 141.89, 140.95, 135.61, 134.51, 131.57, 130.44, 129.15, 129.03, 128.67, 128.65, 128.03, 127.73, 127.58, 127.02, 42.27 ppm. HRMS (ESI) calcd for C<sub>20</sub>H<sub>17</sub>NO [M+H]<sup>+</sup>: 288.1383, found: 288.1383



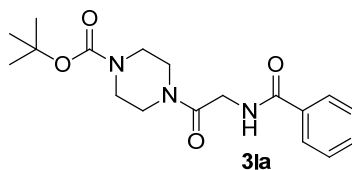
**N-(naphthalen-1-ylmethyl)benzamide (3ia):** Yield = 60%. R<sub>f</sub> = 0.47 in hexanes : EtOAc = 2:1. <sup>1</sup>H NMR (400 MHz, CDCl<sub>3</sub>)  $\delta$  8.07 – 8.04 (m, 1H), 7.89 – 7.85 (m, 1H), 7.81 (d, *J* = 8.1 Hz, 1H), 7.75 – 7.71 (m, 2H), 7.55 – 7.45 (m, 3H), 7.45 – 7.39 (m, 2H), 7.38 – 7.32 (m, 2H), 6.48 (s, 1H), 5.05 (d, *J* = 5.3 Hz, 2H) ppm. <sup>13</sup>C NMR (101 MHz, CDCl<sub>3</sub>)  $\delta$  167.36, 134.46, 134.09, 133.58, 131.68, 131.66, 128.98, 128.91, 128.71, 127.15, 127.04, 126.91, 126.22, 125.59, 123.68, 42.54 ppm. HRMS (ESI) calcd for C<sub>18</sub>H<sub>15</sub>NO [M+H]<sup>+</sup>: 262.1226, found: 262.1225



**N-(2-oxo-2-(4-phenylpiperazin-1-yl)ethyl)benzamide (3ja):** Yield = 56%. R<sub>f</sub> = 0.17 in hexanes : EtOAc = 1:1. <sup>1</sup>H NMR (400 MHz, CDCl<sub>3</sub>)  $\delta$  7.86 – 7.81 (m, 2H), 7.52 – 7.46 (m, 1H), 7.45 – 7.39 (m, 2H), 7.35 (s, 1H), 7.30 – 7.25 (m, 2H), 6.93 – 6.88 (m, 3H), 4.28 (d, *J* = 4.0 Hz, 2H), 3.83 – 3.79 (m, 2H), 3.62 – 3.58 (m, 2H), 3.21 – 3.15 (m, 4H) ppm. <sup>13</sup>C NMR (101 MHz, CDCl<sub>3</sub>)  $\delta$  167.38, 166.74, 150.89, 134.05, 131.85, 129.47, 128.74, 127.26, 121.02, 116.99, 49.77, 49.53, 44.58, 42.22, 41.90 ppm. HRMS (ESI) calcd for C<sub>19</sub>H<sub>21</sub>N<sub>3</sub>O<sub>2</sub> [M+H]<sup>+</sup>: 324.1707, found: 324.1716



***N*-(2-(4-benzylpiperidin-1-yl)-2-oxoethyl)benzamide (3ka):** Yield = 76%.  $R_f$  = 0.14 in hexanes : EtOAc = 2:1.  $^1\text{H}$  NMR (400 MHz,  $\text{CDCl}_3$ )  $\delta$  7.86 – 7.81 (m, 2H), 7.51 – 7.46 (m, 1H), 7.45 – 7.37 (m, 3H), 7.31 – 7.24 (m, 2H), 7.23 – 7.17 (m, 1H), 7.14 – 7.10 (m, 2H), 4.62 – 4.52 (m, 1H), 4.29 – 4.12 (m, 2H), 3.80 – 3.70 (m, 1H), 2.96 (tt,  $J$  = 15.6, 8.0 Hz, 1H), 2.65 – 2.52 (m, 3H), 1.84 – 1.67 (m, 3H), 1.26 – 1.11 (m, 2H) ppm.  $^{13}\text{C}$  NMR (101 MHz,  $\text{CDCl}_3$ )  $\delta$  167.30, 166.26, 139.79, 134.13, 131.73, 129.20, 128.67, 128.51, 127.22, 126.31, 44.85, 42.97, 42.69, 41.85, 38.24, 32.36, 31.73 ppm. HRMS (ESI) calcd for  $\text{C}_{21}\text{H}_{24}\text{N}_2\text{O}_2$   $[\text{M}+\text{H}]^+$ : 337.1911, found: 337.1904



***tert*-butyl 4-(2-benzamidoacetyl)piperazine-1-carboxylate (3la):** Yield = 45%.  $R_f$  = 0.12 in hexanes : EtOAc = 1:1.  $^1\text{H}$  NMR (400 MHz,  $\text{CDCl}_3$ )  $\delta$  7.83 – 7.76 (m, 2H), 7.46 (ddd,  $J$  = 6.4, 3.7, 1.3 Hz, 1H), 7.42 – 7.37 (m, 2H), 7.31 (s, 1H), 4.22 (d,  $J$  = 4.0 Hz, 2H), 3.63 – 3.56 (m, 2H), 3.48 – 3.37 (m, 6H), 1.43 (s, 9H) ppm.  $^{13}\text{C}$  NMR (101 MHz,  $\text{CDCl}_3$ )  $\delta$  167.39, 166.95, 154.55, 133.94, 131.85, 128.71, 127.23, 80.70, 44.45, 42.05, 41.89, 28.50 ppm. HRMS (ESI) calcd for  $\text{C}_{18}\text{H}_{25}\text{N}_3\text{O}_4$   $[\text{M}+\text{Na}]^+$ : 370.1737, found: 370.1738

#### 4.5 References cited

1. (a) Saxon, E.; Bertozzi, C. R., Cell surface engineering by a modified Staudinger reaction. *Science* **2000**, *287* (5460), 2007-2010; (b) Saxon, E.; Armstrong, J. I.; Bertozzi, C. R., A "traceless" Staudinger ligation for the chemoselective synthesis of amide bonds. *Org. Lett.* **2000**, *2* (14), 2141-2143; (c) Nilsson, B. L.; Kiessling, L. L.; Raines, R. T., Staudinger ligation: A peptide from a thioester and azide. *Org. Lett.* **2000**, *2* (13), 1939-1941; (d) Saxon, E.; Luchansky, S. J.; Hang, H. C.; Yu, C.; Lee, S. C.; Bertozzi, C. R., Investigating cellular metabolism of synthetic azidosugars with the Staudinger ligation. *J. Am. Chem. Soc.* **2002**, *124* (50), 14893-14902; (e) Kohn, M.; Breinbauer, R., The Staudinger ligation - A gift to chemical biology'. *Angew. Chem., Int. Ed.* **2004**, *43* (24), 3106-3116.
2. Shen, B.; Makley, D. M.; Johnston, J. N., Umpolung reactivity in amide and peptide synthesis. *Nature* **2010**, *465* (7301), 1027-1033.
3. Dawson, P. E.; Muir, T. W.; Clarklewis, I.; Kent, S. B. H., Synthesis of Proteins by Native Chemical Ligation. *Science* **1994**, *266* (5186), 776-779.
4. (a) Shangguan, N.; Katukojvala, S.; Greenburg, R.; Williams, L. J., The reaction of thio acids with azides: A new mechanism and new synthetic applications. *J. Am. Chem. Soc.* **2003**, *125* (26), 7754-7755; (b) Kolakowski, R. V.; Shangguan, N.; Sauers, R. R.; Williams, L. J., Mechanism of thio acid/azide amidation. *J. Am. Chem. Soc.* **2006**, *128* (17), 5695-5702; (c) Namelikonda, N. K.; Manetsch, R., Sulfo-click reaction via in situ generated thioacids and its application in kinetic target-guided synthesis. *Chem. Commun.* **2012**, *48* (10), 1526-1528.

5. (a) Cho, S. H.; Yoo, E. J.; Bae, L.; Chang, S., Copper-catalyzed hydrative amide synthesis with terminal alkyne, sulfonyl azide, and water. *J. Am. Chem. Soc.* **2005**, *127* (46), 16046-16047; (b) Cassidy, M. P.; Raushel, J.; Fokin, V. V., Practical synthesis of amides from in situ generated copper(I) acetylides and sulfonyl azides. *Angew. Chem., Int. Ed.* **2006**, *45* (19), 3154-3157.
6. Dumas, A. M.; Molander, G. A.; Bode, J. W., Amide-Forming Ligation of Acyltrifluoroborates and Hydroxylamines in Water. *Angew. Chem., Int. Ed.* **2012**, *51* (23), 5683-5686.
7. Molander, G. A.; Raushel, J.; Ellis, N. M., Synthesis of an Acyltrifluoroborate and Its Fusion with Azides To Form Amides. *J. Org. Chem.* **2010**, *75* (12), 4304-4306.
8. Wang, Y.; Zhu, D. P.; Tang, L.; Wang, S. J.; Wang, Z. Y., Highly Efficient Amide Synthesis from Alcohols and Amines by Virtue of a Water-Soluble Gold/DNA Catalyst. *Angew. Chem., Int. Ed.* **2011**, *50* (38), 8917-8921.
9. (a) Martinelli, J. R.; Clark, T. P.; Watson, D. A.; Munday, R. H.; Buchwald, S. L., Palladium-catalyzed aminocarbonylation of aryl chlorides at atmospheric pressure: The dual role of sodium phenoxide. *Angew. Chem., Int. Ed.* **2007**, *46* (44), 8460-8463; (b) Brennfuhrer, A.; Neumann, H.; Beller, M., Palladium-Catalyzed Carbonylation Reactions of Aryl Halides and Related Compounds. *Angew. Chem., Int. Ed.* **2009**, *48* (23), 4114-4133; (c) Wu, X. F.; Neumann, H.; Beller, M., Selective Palladium-Catalyzed Aminocarbonylation of Aryl Halides with CO and Ammonia. *Chem.-Eur. J.* **2010**, *16* (32), 9750-9753.

10. Jiang, H. F.; Liu, B. F.; Li, Y. B.; Wang, A. Z.; Huang, H. W., Synthesis of Amides via Palladium-Catalyzed Amidation of Aryl Halides. *Org. Lett.* **2011**, *13* (5), 1028-1031.
11. (a) Yoo, W. J.; Li, C. J., Highly efficient oxidative amidation of aldehydes with amine hydrochloride salts. *J. Am. Chem. Soc.* **2006**, *128* (40), 13064-13065; (b) De Sarkar, S.; Studer, A., Oxidative Amidation and Azidation of Aldehydes by NHC Catalysis. *Org. Lett.* **2010**, *12* (9), 1992-1995; (c) Ekoue-Kovi, K.; Wolf, C., One-Pot Oxidative Esterification and Amidation of Aldehydes. *Chem.-Eur. J.* **2008**, *14* (31), 6302-6315.
12. (a) Gunanathan, C.; Ben-David, Y.; Milstein, D., Direct synthesis of amides from alcohols and amines with liberation of H<sub>2</sub>. *Science* **2007**, *317* (5839), 790-792; (b) Nordstrom, L. U.; Vogt, H.; Madsen, R., Amide Synthesis from Alcohols and Amines by the Extrusion of Dihydrogen. *J. Am. Chem. Soc.* **2008**, *130* (52), 17672-17673; (c) Chen, C.; Zhang, Y.; Hong, S. H., N-Heterocyclic Carbene Based Ruthenium-Catalyzed Direct Amide Synthesis from Alcohols and Secondary Amines: Involvement of Esters. *J. Org. Chem.* **2011**, *76* (24), 10005-10010.
13. (a) Chan, W. K.; Ho, C. M.; Wong, M. K.; Che, C. M., Oxidative amide synthesis and N-terminal alpha-amino group ligation of peptides in aqueous medium. *J. Am. Chem. Soc.* **2006**, *128* (46), 14796-14797; (b) Park, J. H.; Kim, S. Y.; Kim, S. M.; Chung, Y. K., Cobalt-rhodium heterobimetallic nanoparticle-catalyzed synthesis of alpha,beta-unsaturated amides from internal alkynes, amines, and carbon monoxide. *Org. Lett.* **2007**, *9* (13), 2465-2468; (c) Mak, X. Y.; Ciccolini, R. P.; Robinson, J. M.; Tester, J. W.; Danheiser, R. L., Synthesis of Amides and Lactams in Supercritical Carbon Dioxide. *J.*

- Org. Chem.* **2009**, *74* (24), 9381-9387; (d) Wei, W.; Hu, X.-Y.; Yan, X.-W.; Zhang, Q.; Cheng, M.; Ji, J.-X., Direct use of dioxygen as an oxygen source: catalytic oxidative synthesis of amides. *Chem. Commun.* **2012**, *48* (2), 305-307.
14. Chen, H.; He, M. M.; Wang, Y. Y.; Zhai, L. H.; Cui, Y. B.; Li, Y. Y.; Li, Y.; Zhou, H. B.; Hong, X. C.; Deng, Z. X., Metal-free direct amidation of peptidyl thiol esters with alpha-amino acid esters. *Green Chem.* **2011**, *13* (10), 2723-2726.
15. Goh, K. S.; Tan, C. H., Metal-free pinick-type oxidative amidation of aldehydes. *RSC Adv.* **2012**, *2* (13), 5536-5538.
16. Xiao, F. H.; Liu, Y.; Tang, C. L.; Deng, G. J., Peroxide-Mediated Transition-Metal-Free Direct Amidation of Alcohols with Nitroarenes. *Org. Lett.* **2012**, *14* (4), 984-987.
17. (a) Wolff, H., Schmidt reaction. *Org. React.* **1946**, *3*, 307-336; (b) Smith, P. A. S., Rearrangements involving migration to an electron-deficient nitrogen or oxygen. *Molecular Rearrangements* **1963**, *1*, 457-591; (c) Koldobskii, G. I.; Tereshchenko, G. F.; Gerasimova, E. S.; Bagal, L. I., Schmidt reaction with ketones. *Usp. Khim.* **1971**, *40* (10), 1790-813.
18. (a) Aube, J.; Milligan, G. L., Intramolecular Schmidt Reaction of Alkyl Azides. *J. Am. Chem. Soc.* **1991**, *113* (23), 8965-8966; (b) Gracias, V.; Milligan, G. L.; Aube, J., Efficient Nitrogen Ring-Expansion Process Facilitated by in-Situ Hemiketal Formation - an Asymmetric Schmidt Reaction. *J. Am. Chem. Soc.* **1995**, *117* (30), 8047-8048; (c) Milligan, G. L.; Mossman, C. J.; Aube, J., Intramolecular Schmidt Reactions of Alkyl Azides with Ketones - Scope and Stereochemical Studies. *J. Am. Chem. Soc.* **1995**, *117* (42), 10449-10459; (d) Gracias, V.; Frank, K. E.; Milligan, G. L.; Aube, J., Ring

expansion by in situ tethering of hydroxy azides to ketones: The Boyer reaction. *Tetrahedron* **1997**, 53 (48), 16241-16252; (e) Sahasrabudhe, K.; Gracias, V.; Furness, K.; Smith, B. T.; Katz, C. E.; Reddy, D. S.; Aube, J., Asymmetric Schmidt reaction of hydroxyalkyl azides with ketones. *J. Am. Chem. Soc.* **2003**, 125 (26), 7914-7922; (f) Yao, L.; Aube, J., Cation-pi control of regiochemistry of intramolecular Schmidt reactions en route to bridged bicyclic lactams. *J. Am. Chem. Soc.* **2007**, 129 (10), 2766-2767.

19. (a) Boyer, J. H.; Hamer, J., The Acid-Catalyzed Reaction of Alkyl Azides Upon Carbonyl Compounds. *J. Am. Chem. Soc.* **1955**, 77 (4), 951-954; (b) Boyer, J. H.; Canter, F. C.; Hamer, J.; Putney, R. K., Acid-Catalyzed Reactions of Aliphatic Azides. *J. Am. Chem. Soc.* **1956**, 78 (2), 325-327; (c) Chakraborty, R.; Franz, V.; Bez, G.; Vasadia, D.; Popuri, C.; Zhao, C. G., Some new aspects of the Boyer reaction. *Org. Lett.* **2005**, 7 (19), 4145-4148; (d) Lee, H. L.; Aube, J., Intramolecular and intermolecular Schmidt reactions of alkyl azides with aldehydes. *Tetrahedron* **2007**, 63 (36), 9007-9015.

20. Ratti, S.; Quarato, P.; Casagrande, C.; Fumagalli, R.; Corsini, A., Picotamide, an antithromboxane agent, inhibits the migration and proliferation of arterial myocytes. *Eur. J. Pharmacol.* **1998**, 355 (1), 77-83.

21. Belyk, K. M.; Morrison, H. G.; Jones, P.; Summa, V. Preparation of N-(4-fluorobenzyl)-5-hydroxy-1-methyl-2-(1-methyl-1-[(5-methyl-1,3,4-oxadiazol-2-yl)carbonyl]amino}ethyl)-6-oxo-1,6-dihydropyrimidine-4-carboxamide potassium salts as HIV integrase inhibitors. WO 2006060712, 20051202, 2006.

22. (a) French, K. J.; Zhuang, Y.; Maines, L. W.; Gao, P.; Wang, W.; Beljanski, V.; Upson, J. J.; Green, C. L.; Keller, S. N.; Smith, C. D., Pharmacology and antitumor activity of ABC294640, a selective inhibitor of sphingosine kinase-2. *J. Pharmacol. Exp.*

- Ther.* **2010**, 333 (1), 129-39; (b) McIntyre, J. A.; Castaner, J.; Martin, L., Lacosamide - Antiepileptic drug treatment of neuropathic pain NMDA glycine-site antagonist. *Drug Future* **2004**, 29 (10), 992-997; (c) Molander, G. A.; Hiebel, M. A., Synthesis of Amidomethyltrifluoroborates and Their Use in Cross-Coupling Reactions. *Org. Lett.* **2010**, 12 (21), 4876-4879.
23. Alvarez, S. G.; Alvarez, M. T., A practical procedure for the synthesis of alkyl azides at ambient temperature in dimethyl sulfoxide in high purity and yield. *Synthesis* **1997**, (4), 413-414.
24. Chakraborty, A.; Dey, S.; Sawoo, S.; Adarsh, N. N.; Sarkar, A., Regioselective 1,3-Dipolar Cycloaddition Reaction of Azides with Alkoxy Alkynyl Fischer Carbene Complexes. *Organometallics* **2010**, 29 (23), 6619-6622.
25. Tang, W.; Shi, D. Q., Synthesis and Herbicidal Activity of O,O-Dialkyl(Phenyl)-N-{1-[(6-Chloropyridin-3-Yl)methyl]-4-Cyano-1h-1,2,3-Triazol-5-Yl}-1-Amino-1-Substitutedbenzyl-Phosphonates. *Phosphorus, Sulfur Silicon Relat. Elem.* **2011**, 186 (3), 496-502.
26. Wang, X. L.; Wan, K.; Zhou, C. H., Synthesis of novel sulfanilamide-derived 1,2,3-triazoles and their evaluation for antibacterial and antifungal activities. *Eur. J. Med. Chem.* **2010**, 45 (10), 4631-4639.
27. Stefely, J. A.; Palchadhuri, R.; Miller, P. A.; Peterson, R. J.; Moraski, G. C.; Hergenrother, P. J.; Miller, M. J., N-((1-Benzyl-1H-1,2,3-triazol-4-yl)methyl)arylamide as a New Scaffold that Provides Rapid Access to Antimicrotubule Agents: Synthesis and Evaluation of Antiproliferative Activity Against Select Cancer Cell Lines. *J. Med. Chem.* **2010**, 53 (8), 3389-3395.

28. Suzuki, T.; Ota, Y.; Kasuya, Y.; Mutsuga, M.; Kawamura, Y.; Tsumoto, H.; Nakagawa, H.; Finn, M. G.; Miyata, N., An Unexpected Example of Protein-Templated Click Chemistry. *Angew. Chem., Int. Ed.* **2010**, *49* (38), 6817-6820.
29. Zhang, X. R.; Yang, X. H.; Zhang, S. S., Synthesis of Triazole-Linked Glycoconjugates by Copper(I)-Catalyzed Regiospecific Cycloaddition of Alkynes and Azides. *Synth. Commun.* **2009**, *39* (5), 830-844.
30. Angell, Y.; Chen, D.; Brahim, F.; Saragovi, H. U.; Burgess, K., A combinatorial method for solution-phase synthesis of labeled bivalent beta-turn mimics. *J. Am. Chem. Soc.* **2008**, *130* (2), 556-565.
31. Chakrabarty, M.; Basak, R.; Harigaya, Y.; Takayanagi, H., Reaction of 3/2-formylindoles with TOSMIC: formation of indolyloxazoles and stable indolyl primary enamines (vol 61, pg 1793, 2005). *Tetrahedron* **2005**, *61* (16), 4173-4173.
32. Contreras, J. M.; Parrot, I.; Sippl, W.; Rival, Y. M.; Wermuth, C. G., Design, synthesis, and structure-activity relationships of a series of 3-[2-(1-benzylpiperidin-4-yl)ethylamino]pyridazine derivatives as acetylcholinesterase inhibitors. *J. Med. Chem.* **2001**, *44* (17), 2707-2718.

## **Appendices**

## Appendix 1

### Copyright Permission

9/6/12 Rightslink® by Copyright Clearance Center

 **Copyright Clearance Center**

 **RightsLink®**

[Home](#) [Create Account](#) [Help](#)

 **ACS Publications** High quality. High impact.

**Title:** Screening of Protein-Protein Interaction Modulators via Sulfo-Click Kinetic Target-Guided Synthesis

**Author:** Sameer S. Kulkarni, Xiangdong Hu, Kenichiro Doi, Hong-Gang Wang, and Roman Manetsch

**Publication:** ACS Chemical Biology

**Publisher:** American Chemical Society

**Date:** Jul 1, 2011

Copyright © 2011, American Chemical Society

User ID

Password

Enable Auto Login

**LOGIN**

[Forgot Password/User ID?](#)

If you're a **copyright.com** user, you can login to RightsLink using your copyright.com credentials. Already a **RightsLink** user or want to [learn more?](#)

#### PERMISSION/LICENSE IS GRANTED FOR YOUR ORDER AT NO CHARGE

This type of permission/license, instead of the standard Terms & Conditions, is sent to you because no fee is being charged for your order. Please note the following:

- Permission is granted for your request in both print and electronic formats, and translations.
- If figures and/or tables were requested, they may be adapted or used in part.
- Please print this page for your records and send a copy of it to your publisher/graduate school.
- Appropriate credit for the requested material should be given as follows: "Reprinted (adapted) with permission from (COMPLETE REFERENCE CITATION). Copyright (YEAR) American Chemical Society." Insert appropriate information in place of the capitalized words.
- One-time permission is granted only for the use specified in your request. No additional uses are granted (such as derivative works or other editions). For any other uses, please submit a new request.

**BACK**

**CLOSE WINDOW**

Copyright © 2012 [Copyright Clearance Center, Inc.](#) All Rights Reserved. [Privacy statement.](#)  
Comments? We would like to hear from you. E-mail us at [customercare@copyright.com](mailto:customercare@copyright.com)